



University of **HUDDERSFIELD**

University of Huddersfield Repository

Afzal, Mohammad Suhail

The Influence of Salt Formation on Physicochemical and Electrostatic Properties of Carboxylic Acid Drugs

Original Citation

Afzal, Mohammad Suhail (2020) The Influence of Salt Formation on Physicochemical and Electrostatic Properties of Carboxylic Acid Drugs. Doctoral thesis, University of Huddersfield.

This version is available at <http://eprints.hud.ac.uk/id/eprint/35321/>

The University Repository is a digital collection of the research output of the University, available on Open Access. Copyright and Moral Rights for the items on this site are retained by the individual author and/or other copyright owners. Users may access full items free of charge; copies of full text items generally can be reproduced, displayed or performed and given to third parties in any format or medium for personal research or study, educational or not-for-profit purposes without prior permission or charge, provided:

- The authors, title and full bibliographic details is credited in any copy;
- A hyperlink and/or URL is included for the original metadata page; and
- The content is not changed in any way.

For more information, including our policy and submission procedure, please contact the Repository Team at: E.mailbox@hud.ac.uk.

<http://eprints.hud.ac.uk/>

Doctoral Thesis

The Influence of Salt Formation on Physicochemical and Electrostatic Properties of Carboxylic Acid Drugs

A thesis submitted in partial fulfilment of the requirements
for a degree of Doctor of Philosophy

Department of Chemical Sciences
Applied Sciences
University of Huddersfield

Mohammad Suhail Afzal

February 2020

Copyright Statement

- i. The author of this thesis (including any appendices and/ or schedules to this thesis) owns any copyright in it (the "Copyright") and s/he has given The University of Huddersfield the right to use such Copyright for any administrative, promotional, educational and/or teaching purposes.
- ii. Copies of this thesis, either in full or in extracts, may be made only in accordance with the regulations of the University Library. Details of these regulations may be obtained from the Librarian. Details of these regulations may be obtained from the Librarian. This page must form part of any such copies made.
- iii. The ownership of any patents, designs, trademarks and any and all other intellectual property rights except for the Copyright (the "Intellectual Property Rights") and any reproductions of copyright works, for example graphs and tables ("Reproductions"), which may be described in this thesis, may not be owned by the author and may be owned by third parties. Such Intellectual Property Rights and Reproductions cannot and must not be made available for use without permission of the owner(s) of the relevant Intellectual Property Rights and/or Reproductions.

Acknowledgements

I would firstly like to thank my supervisors, Dr Enes Šupuk and Professor Barbara Conway, for all their time, support and guidance throughout my PhD, and without whom; completion would not have been possible.

Gratitude is given to Professor Peter Timmins who has acted as a third supervisor, providing his endless knowledge, stimulating discussions, ideas and advice. I am grateful for the inspiration and support provided by the three supervisors.

I would like to thank the technical staff at the University for their assistance and source of knowledge, as well as Dr Kofi Asare-Addo for his support and contributions. I acknowledge the valuable insights shared by Professor Carl Schwalbe for his crucial contribution to the crystallography. His advice was much appreciated, and he will be missed by the pharmaceutical materials research community. Many thanks to Vivienne Gray from Bristol-Myers Squibb for her contribution in undertaking the experimental work for the compaction properties, and Dr Robert Faulkner for his guidance in interpreting the NMR results.

To my friends who have been an endless source of laughter and support, I owe particular thanks to Kamran, Omar, João , Jade and Claire.

Lastly, I would like to thank my parents; Amir and Rifat, and siblings; Raeal, Zulekha and Aysha for their love, support and encouragement.

Abstract

Salification of an active pharmaceutical ingredient (API) is an approach effectively utilised to modify physicochemical properties of acidic and basic drugs, including solubility, dissolution rate, stability and hygroscopicity. It is commonly reported that approximately 50% of drugs are administered in the salt form, and this continued frequency of salt formation supports the need for sustained research to discover entities with the greatest physicochemical and material handling properties to help reduce the cost of manufacturing. However, little work has been carried out to determine the effects of salt formation upon the tribo-electrification propensity of the resulting material. Tribo-electrification can influence material handling properties, whereby powder handling operations can induce a charge upon the particles, resulting in an increase in tendency of particles to adhere to themselves and the walls of the processing equipment, leading to blockages in pipes. In industries such as pharmaceutical this can extend to segregation of material, resulting in poorer content uniformity.

The aim of this study was to investigate the influences of solvent selection and ratio of counterion to active pharmaceutical ingredient were investigated to determine the effects upon the final form in terms of crystal habit and tribo-electrification propensity as a result of solvent selection, the experimental results show the magnitude of ratio selection and solvent selection upon the crystal habit, and the solvent selection upon the tribo-electrification propensity. The discovery of the 2:1 flurbiprofen: cyclopropylamine salt cocrystal was utilised to scrutinise the mechanical, physicochemical and tribo-electrification properties in comparison to the salt form, to determine any increased benefits over the salt form. The experimental data showed that both strategies had their merits. Previous research has shown the influences of counterion selection upon tribo-electrification propensity. For the purpose of this study three different carboxylic acid drugs were used, flurbiprofen, felbinac and biphenyl-4-carboxylic acid, due to their similar structures. Also three counterions; cyclopropylamine cyclobutylamine and cyclopentylamine were selected. This allowed for a comparison of the influences of counterion selection as well as active pharmaceutical ingredient to be made. From the results it is evident that significant differences were observed in physicochemical properties such as a reduction in solubility as the carbon chain length of the counterion increased, as well as the extremely low charging propensity of

biphenyl-4-carboxylic acid, potentially improving powder handling properties. As well as this, the current trends in salt formation between the Orange book database to reflect north American activity and the British National Formulary (BNF) were established; to reflect European territories, in order to ascertain the popularity of counterion selection during a the latest 12 year period. Salt formation is still a very popular method for forming dosage forms, Sodium and Chloride were found to be the most popular choice in counterion selection.

This work clearly demonstrates the potential of investigating the drug salt physicochemical-tribo-electrification property relationship in pharmaceutical materials.

Contents

Acknowledgements.....	I
Abstract.....	II
Contents.....	IV
List of Tables.....	VIII
List of Figures	IX
Abbreviations List.....	XII
1. Introduction.....	1
1.1 Background	1
1.2 Project Aims & Objectives	2
1.3 Structure of Thesis	4
2 Literature Review	6
2.1 Drug Discovery Process	6
2.1.1 Clinical Trials	7
2.2 Dosage Forms.....	8
2.3 Drug Solubility	9
2.3.1 Solubility Improvement Strategies	10
2.3.1.1 Salt Formation.....	10
2.3.1.2 Particle Size Reduction	10
2.3.1.3 Crystal Engineering	11
2.3.1.4 Cosolvency	11
2.3.1.5 pH Adjustment	12
2.3.1.6 Inclusion complex formation	12
2.3.2 Biopharmaceutics Classification System.....	13
2.3.2.1 Class I	13
2.3.2.2 Class II	14
2.3.2.3 Class III	14
2.3.2.4 Class IV	14
2.4 Salt Selection Process.....	14
2.5 Salt Selection Strategies	15
2.6 Salt Formation	15
2.6.1 Crystal Engineering	16
2.6.2 Crystallisation Mechanism.....	17
2.6.3 Effect of Crystal Habit upon Pharmaceutical Material	17
2.7 Cocrystal Formation	18
2.7.1 Traditional Methods	18
2.7.1.1 Solvent Evaporation	18
2.7.1.2 Slurry/Grinding Method	18

2.7.2	Novel Methods	19
2.7.2.1	Heat Induced CocrySTALLISATION.....	19
2.7.2.2	Spray Drying	19
2.7.2.3	Supercritical Fluid Technology	19
2.7.2.4	Laser Irradiation	19
2.8	Powder Flow Background.....	20
2.8.1	Powder Flow - Schulze Shear Cell	20
2.9	Tribo-Electrification Background.....	23
2.9.1	Tribo-electrification	23
2.9.2	Factors Affecting Tribo-electrification	25
2.9.2.1	Fundamental Properties	25
2.9.2.1.1	Work Function.....	25
2.9.2.1.2	Tribo-electric series.....	26
2.9.2.1.3	Contact Potential Difference (CPD).....	27
2.9.2.1.4	Image Charge	28
2.9.2.1.5	Space Charge	28
2.9.2.1.6	Induced Charge	29
2.9.2.2	Physiochemical Properties	29
2.9.2.2.1	Particle Shape.....	29
2.9.2.2.2	Particle Size	30
2.9.2.2.3	Particle Surface Area (Contact Area).....	31
2.9.2.2.4	Functional Groups	31
2.9.2.2.5	Surface Contamination.....	32
2.9.2.3	Environmental Conditions.....	33
2.9.2.3.1	Temperature or Humidity	33
2.9.2.4	Physical Parameters	33
2.9.2.4.1	Frequency.....	33
2.9.2.4.2	Number of Collisions	34
2.9.2.5	Charge to Mass Measurement.....	34
2.10	Conclusions	35
3	Materials and Methods	37
3.1	Materials	37
3.1.1	Model Drugs	37
3.1.2	Carboxylic Acid Drugs	37
3.1.2.1	Flurbiprofen	37
3.1.2.2	Felbinac.....	38
3.1.2.3	Biphenyl-4-Carboxylic Acid.....	38
3.2	Counterion Selection.....	39
3.2.1	Cyclic Compounds.....	39
3.3	Methods	40
3.3.1	Salt Preparation	40
3.3.2	Salt Recrystallisation.....	41
3.3.3	Salt Cocystal formation	42
3.3.4	Single crystal X-ray diffractometry	42

3.3.5	Salt formation confirmation	42
3.3.5.1	Fourier Transform Infrared Spectroscopy (FTIR).....	42
3.3.5.2	Powder X-ray diffraction (PXRD)	43
3.3.5.3	Nuclear Magnetic Resonance (NMR)	44
3.3.6	Thermal Methods	45
3.3.6.1	Thermogravimetric analysis (TGA)	45
3.3.6.2	Differential Scanning Calorimetry (DSC)	45
3.3.7	Dissolution and solubility studies	46
3.3.7.1	Solubility.....	46
3.3.7.2	High Pressure Liquid Chromatography (HPLC).....	48
3.3.7.3	Intrinsic Dissolution Rate (IDR)	50
3.3.8	Powder properties	53
3.3.8.1	Fractionization of API salts	53
3.3.8.2	Scanning Electron Microscopy (SEM).....	54
3.3.8.3	Powder Compaction.....	55
3.3.8.4	Schulze shear cell	56
3.3.8.5	Brunauer–Emmett–Teller (BET)	58
3.3.8.6	True Density	59
3.3.8.7	Tribo electrification	60
3.3.8.7.1	Powder adhesion.....	60
3.4	Conclusions	61
4	<i>Salts of active pharmaceutical ingredients; recent selection trends and developments.....</i>	62
	Background	62
4.1	Study Strategy	65
4.2	Results and Discussion	65
4.3	Conclusion	84
5	<i>The influences of varying salt former ratios and solvent selection upon physicochemical properties of the resulting material.....</i>	85
	Background	85
5.1	Results and Discussion	86
5.1.1	Fourier Transform Infra-Red Spectroscopy (FT-IR)	86
5.1.2	Powder X-ray analysis (PXRD).....	87
5.1.3	Thermal Analysis (DSC & HSM)	90
5.1.4	Scanning Electron Microscopy (SEM)	94
5.1.5	Tribo-electrification	97
5.2	Conclusion	102
6	<i>Properties comparison of flurbiprofen cyclopropyl-ammonium salt with the salt cocrystal and flurbiprofen active ingredient</i>	103
	Background	103
6.1	Results and Discussion	104

6.1.1	Single Crystal X-ray Crystallography	104
6.1.2	Solid state characterisation	110
6.1.3	Solubility	113
6.1.4	Mechanical Properties	113
6.1.5	Tribo-electrification and adhesion behaviour	116
6.2	Conclusion	118
7	<i>The influence of counterion selection on physico-chemical and electrostatic properties of analogous carboxylic acid salts.....</i>	119
	Background	119
7.1	Results and Discussion	121
7.1.1	Solid State Characterisation.....	121
7.2	Saturated Solubility and Intrinsic Dissolution	131
7.3	Particle Shape Analysis.....	133
7.4	Powder Flow.....	134
7.5	Brunauer–Emmett–Teller (BET) analysis.....	137
7.6	Tribo-electrification and adhesion behaviour	138
7.7	Conclusion	155
8	<i>Conclusions</i>	157
8.1	Analogous Carboxylic Acid Salts	157
8.2	Flurbiprofen, Flurbiprofen Cyclopropyl-ammonium Salt and Salt Cocrystal	158
8.3	Salt Former Ratios	159
8.4	Salt Trends.....	159
9	<i>Future Work</i>	161
	References.....	162
10	<i>Appendices</i>	173

List of Tables

Table 2-1 Tribo-electric series [84]	27
Table 4-1 Distribution of Anions Used in APIs of Class 1	69
Table 4-2 Distribution of Cations Used in APIs of Class 2	72
Table 4-3 Distribution of Anions Used in Oral Dosage Forms.....	74
Table 4-4 Distribution of Cations Used in Oral Dosage Forms.....	75
Table 4-5 Distribution of Anions Used in Injectable Dosage Forms	77
Table 4-6 Distribution of Cations Used in Injectable Dosage Forms.....	78
Table 4-7 Distribution of Anions Used in New Chemical Entities of Class 1:	79
Table 4-8 Anions Used in for salt formation in the BNF	80
Table 4-9 Cations Used in for salt formation in the BNF	81
Table 4-10 Comparison of data from Berge, Monkhouse and Bighley (1974 and 1993) with data from the orange book database (2006 and 2018) and the BNF. Adapted with permission from [16]. Copyright (2007) American Chemical Society*	82
Table 6-1 Crystallographic data for flurbiprofen, flurbiprofen cyclopropylamine (1:1) salt and flurbiprofen cyclopropylamine (2:1) salt cocrystal.....	105
Table 6-2: Selected hydrogen bond geometries for flurbiprofen, flurbiprofen cyclopropylamine (1:1) salt and flurbiprofen cyclopropylamine (2:1) salt cocrystal.....	109
Table 6-3: Physical properties for flurbiprofen, flurbiprofen cyclopropylamine (1:1) salt and flurbiprofen cyclopropylamine (2:1) salt cocrystal*	110
Table 6-4: Mechanical Properties of FBP, salt and salt cocrystal flurbiprofen, flurbiprofen cyclopropylamine (1:1) salt and flurbiprofen cyclopropylamine (2:1) salt cocrystal.....	114
Table 7-1 Parent Drugs and Counter-ion Structures	121
Table 7-2: Melting onset and endset for the parent compounds and salts	130
Table 7-3: Solubility data for the parent compounds and the salts	132
Table 7-4: IDR data for the parent compounds and the salts.....	133
Table 7-5 BET surface area data for parent compounds and salts	138
 Table A.1 Distribution of Cations Used in New Chemical Entities of Class 2:	 173
Table A.2 Number and Distribution of Anions Used in the Variety of Dosage Forms for New Chemical Entities:	174
Table A.3 Number and Distribution of Cations Used in the Different of Dosage Forms for New Chemical Entities:	175

List of Figures

Figure 2.1 Drug Development process (adapted from SRUK.org.uk)	7
Figure 2.2 Uniaxial Compression Test [70]	21
Figure 2.3 Measurement of Unconfined Yield Strength [70].....	22
Figure 2.4 Powder Flow Function	22
Figure 2.5 Electron Potential Energy at a Metal - Metal Contact [82].....	26
Figure 2.6 Potential difference caused by the image charge effect [87].....	28
Figure 2.7 Electric field generated by space charge [87]	29
Figure 2.8 Left: The effect of contamination of lactose particles on charge of lactose size fractions, 90-125um following tribo-electrification. Right: The effect of surface cleaning upon charge for size fractions 125-150um following tribo-electrification. [95].....	32
Figure 2.9 Faraday Cup Schematic [101]	34
Figure 3.1 Structure of a carboxylic acid	37
Figure 3.2 Chemical structure of Flurbiprofen	38
Figure 3.3 Chemical structure of Felbinac	38
Figure 3.4 Chemical structure of Biphenyl-4-carboxylic acid	38
Figure 3.5 Structures of Selected Counterions	39
Figure 3.6 pH solubility profile of a free acid and its salt. Adapted from [31].....	47
Figure 3.7 Diffusion layer model for drug dissolution. Adapted from [93]	50
Figure 3.8 Danckwert's Model. Adapted from [93]	51
Figure 3.9 Schematic of IDR equipment	52
Figure 3.10 Cut-away view of shear cell depicting the key components, adapted from http://www.dietmar-schulze.com/leafxse.pdf	58
Figure 4.1 Salt formation process diagram.....	62
Figure 4.2: Distribution of API form in the Orange book database per class according to charge type and route of administration	67
Figure 5.1 FT-IR spectrum for flurbiprofen, and the 1:1, 1:2 and 2:1 FBP-cyclo-propylamine salts.....	86
Figure 5.2: XRD data for FBP, FBP cyclo-propylamine 1:1, 1:2 & 2:1(A-D)	89
Figure 5.3: DSC data for FBP, FBP cyclo-propylamine 1:1, 1:2 & 2:1 (A-D).....	92
Figure 5.4: HSM for FBP 1:1 cyclo-propylamine at (A) 90°C (prior to melting), (B) 95°C and (C) 104°C	93
Figure 5.5: HSM for FBP 1:2 cyclo-propylamine at (A) 86.5°C (prior to melting), (B) 95°C and (C) 110°C.....	93
Figure 5.6: HSM for FBP 2:1 cyclo-propylamine at (A) 83.5°C (prior to melting), (B) 95°C and (C) 108°C.....	94
Figure 5.7: SEM Images of FBP cyclo-propylamine (A) 1:1, (B) 1:2 & (C) 2:1 AT X100 magnification.....	94
Figure 5.8: SEM Images of the resulting crystals of FBP cyclo-propylamine using various solvents, (A) Absolute Ethanol, (B) Acetonitrile, (C) DCM, (D) Diethyl Ether	96
Figure 5.9: SEM Images of the resulting crystals of FBP cyclo-propylamine when adjusting the ratio	96
Figure 5.10: Tribo-electrification and percentage adhesion of the original salt form ratios..	98
Figure 5.11: Tribo-electrification and percentage adhesion for recrystallised salts	99
Figure 5.12: Tribo-electrification and percentage adhesion for recrystallised salts at varying ratios.....	100

Figure 5.13: Tribo-electrification and percentage adhesion for recrystallised salts made from original salt of varying ratios	101
Figure 6.1 Hydrogen bonded ladders built from alternating R ₄ ² (8) and R ₄ ⁴ (12) rings in the cyclopropylammonium salt of flurbiprofen with atom labelling. Hydrogen atoms not involved in hydrogen bonding and disordered alternative sites with lower occupancy have been omitted for clarity.....	106
Figure 6.2: CABP arrangement within asymmetric unit for flurbiprofen cyclopropylamine 2:1 salt cocrystal.....	107
Figure 6.3: Partial structure of arrangement of flurbiprofen and cyclopropylamine within the 2:1 co-crystal to show the three different sorts of intermolecular interaction.	108
Figure 6.4: Powder XRD data for flurbiprofen (a), flurbiprofen cyclopropylamine (1:1) salt (b) and flurbiprofen: cyclopropylamine (2:1) co-crystal (c)	111
Figure 6.5: SEM images of (a) flurbiprofen (b) salt of flurbiprofen using cyclopropylamine (c) flurbiprofen cyclopropylamine salt cocrystal 2:1 ratio, Depicted at x100 and x500 magnifications.	112
Figure 6.6: Packing diagrams for salt projecting down the b axis (a)) and salt cocrystal projecting down the b axis (b). Arrows indicate position of potential slip planes.	115
Figure 6.7: Tribo-electrification (a) and adhesion data (b) of flurbiprofen, flurbiprofen cyclopropylamine (1:1) salt and flurbiprofen: cyclopropylamine (2:1) salt co-crystal	117
Figure 7.1 FT-IR data for FBP and its salts	122
Figure 7.2 XRD data for FBP and its salts.....	123
Figure 7.3: NMR Scan for Flurbiprofen	124
Figure 7.4: NMR Scan for the Salts of Flurbiprofen	125
Figure 7.5: NMR Scan for Felbinac.....	126
Figure 7.6: NMR Scan for the Salts of Felbinac.....	127
Figure 7.7: NMR Scan for Biphenyl-4-carboxylic acid	128
Figure 7.8: NMR Scan for the Salts of Biphenyl-4-carboxylic acid	129
Figure 7.9 TGA data for FBP and its salts.....	131
Figure 7.10: SEM images of, A) FBP, B) Felbi and C) B4CA depicted at 100x and 500x magnifications.	134
Figure 7.11: Shear cell data for parent compounds and salt forms	136
Figure 7.12: Tribo-electrification and adhesion data for the parent compounds	139
Figure 7.13: Tribo-electrification and adhesion data for FBP CBA at (A) 0.5 and (B) 2 mins	141
Figure 7.14: Tribo-electrification and adhesion data for Felbi CBA at (A) 0.5 and (B) 2 mins	143
Figure 7.15: Tribo-electrification and adhesion data for B4CA CBA at (A) 0.5 and (B) 2 mins	145
Figure 7.16: Tribo-electrification and adhesion data for FBP C-prop at (A) 0.5 and (B) 2 mins	147
Figure 7.17: Tribo-electrification and adhesion data for Felbi C-prop at (A) 0.5 and (B) 2 mins	149
Figure 7.18: Tribo-electrification and adhesion data for FBP CPA at (A) 0.5 and (B) 2 mins	151
Figure 7.19: Tribo-electrification and adhesion data for Felbi CPA at (A) 0.5 and (B) 2 mins	153
Figure 7.20: Tribo-electrification and adhesion data for B4CA CPA at (A) 0.5 and (B) 2 mins	155

Figure A.1 FT-IR spectrum for the 1:1 salt after recrystallisation from various solvents	176
Figure A.2 FT-IR spectrum for the 1:1 salt with excess of either drug or counter-ion	176
Figure A.3 FT-IR spectrum for 1:2 and 2:1 salts recrystallised form various solvents	177
Figure A.4 FT-IR data for flurbiprofen, flurbiprofen cyclopropylamine (1:1) salt and flurbiprofen: cyclopropylamine (2:1) salt cocrystal.....	178
Figure A.5 Packing diagrams for salt projecting down the b axis (A) and salt cocrystal the a axis (B). Arrows indicate position of potential slip planes.....	179
Figure A.6 FT-IR data for felbinac, B4CA and the subsequent salts.....	180
Figure A.7 XRD data for felbinac, B4CA and the salts.....	180
Figure A.8 TGA data for felbinac, B4CA and the subsequent salts	181
Figure A.9 SEM images of A) FBP CBA, B) FBP CPA, C) FBP C-prop, D) Felbi CBA, E) Felbi CPA, F) Felbi C-prop G) B4CA CBA and H) B4CA CPA depicted at 100x and 500x magnifications.	182
Figure A.10 Tribo-electrification and adhesion data for FBP CBA at 5 and 10 mins.....	183
Figure A.11 Tribo-electrification and adhesion data for Felbi CBA at 5 and 10 mins	183
Figure A.12 Tribo-electrification and adhesion data for B4CA CBA at 5 and 10 mins	184
Figure A.13 Tribo-electrification and adhesion data for FBP C-Prop at 5 and 10 mins	184
Figure A.14 Tribo-electrification and adhesion data for Felbi C-Prop at 5 and 10 mins.....	185
Figure A.15 Tribo-electrification and adhesion data for FBP CPA at 5 and 10 mins	185
Figure A. 16 Tribo-electrification and adhesion data for Felbi CPA at 5 and 10 mins	186
Figure A. 17 Tribo-electrification and adhesion data for B4CA CPA at 5 and 10 mins	186

Abbreviations List

ACN	Acetonitrile
API	Active Pharmaceutical Ingredient
B4CA	Biphenyl-4-carboxylic acid
BCS	Biopharmaceutical Classification System
BET	Brunauer-Emmett-Teller
BNF	British National Formulary
C-But	Cyclobutylamine
CC	Salt Cocystal
CPD	Contact Potential Difference
C-Pent	Cyclopentylamine
C-Prop	Cyclopropylamine
DSC	Differential Scanning Calorimetry
FBP	Flurbiprofen
FDA	Food and Drug Administration
Felbi	Felbinac
FTIR	Fourier-Transform Infrared Spectroscopy
HPLC	High Performance Liquid Chromatography
IDR	Intrinsic Dissolution Rate
NMR	Nuclear Magnetic Resonance
(P)XRD	Powder X-Ray Diffraction
nC	Nanocoulombs
nC/g	Mass to Charge Ratio
Q	Charge
RH	Relative Humidity
SCL	Saturated Charge Level
SEM	Scanning Electron Microscope
TGA	Thermogravimetric Analysis
NCE	New Chemical Entities

1. Introduction

1.1 Background

Salt formation of an active pharmaceutical ingredient (API) is an efficient method employed to adapt physicochemical properties of acidic and basic drugs, such as solubility, stability, dissolution rate as well as hygroscopicity [1-5]. Some of the most beneficial properties usually considered are high dissolution rate or solubility, as well as by stability and crystallinity, also in some instances, improving the material handling properties which are beneficial for formulation and manufacturing [6]. The choice of salt form is largely dependent upon the acidity/basicity of the ionisable group contained on the API, also the route of administration, dosage form and safety of counterion, influence the selection process as these affect the solid-state properties of crystalline salts.

Solubility is defined as the greatest quantity of solute that can be dissolved in a set volume of solvent. This definition can be qualitative as well as quantitative; quantitatively speaking it refers to the concentration of solute in a saturated solution at a given temperature, however in qualitative terms, solubility is outlined as an interface of two or more constituents to form a homogeneous dispersion. A saturated solution is one which the solute and solvent are in equilibrium [7]. Poor solubility is a growing problem and plays a substantial contribution to the failing of compounds during drug development, increasing the difficulty when planning a suitable formulation for oral drug delivery.

For successful salt formation, the pK_a value is one of the key components which need to be considered as it is used to determine the degree of ionisation, where a lower value denotes a stronger acid. The pK_a rule states that for successful salt formation to occur, there must be a difference of at least two or three units between the acid and the base [8]. This difference in pK_a ensures that there is a strong affinity of the two species to bind, hence will not disproportionate back into the individual species when not required.

Cocrystals can be utilised instead of salt forms as they are multicomponent structures containing at least two molecules, one consisting of the drug (API), and the other a coformer, held by hydrogen bonding. The coformer can be a second active pharmaceutical ingredient (API) or an excipient [9, 10]. The development of cocrystals has gained significant interest due to their ability to often present enhanced physicochemical properties for the API by modifying the structure without affecting the pharmacological properties of the drug [11-14]. The impact of cocrystal formation is not limited to absorption and has the ability to significantly modify the drug's pharmacokinetics and solubility profile [15]. It can be used as an alternate method to salt formation in order to amend the undesirable properties possessed by APIs.

As salt/co-crystal formation can influence the properties of the resulting material, one of the properties which can be affected is tribo-electrification. The electrification of particles is a phenomenon which occurs in many powder handling industries such as flour mills and pharmaceuticals, a source of ignition may easily cause an explosion [16]. Particle electrification, commonly known as tribo-electric charging or tribo-electrification occurs when particles come into contact with one other as well as the surface of the manufacturing equipment resulting in production of electrical charge, due to electron or ion exchange taking place as a result of impact, shearing and friction forces acting upon the material [17], hence contacting materials are left with equal but opposite charge after the separation process. This enables the particles to behave differently whereby they may adhere to each other or repel other charged materials. This can result in a number of complications such as particle segregation where the charged particles form agglomerates, resulting in variable particle size, unpredictable dosage masses and process delays. In the pharmaceutical industry, the most commonly used powders can be classified as insulators, and segregation is problematic as it leads to reduced content uniformity of a product, as well as increasing adhesion and reducing flowability [18]

1.2 Project Aims & Objectives

The main aim of this study was to develop an understanding of triboelectrification propensity and powder handling properties of Active Pharmaceutical Ingredients (API) and their salt forms. The ability to control the tribo-electrification propensity of a material is essential in

improving the quality of the finished product, by minimising the powder loss and deposition of powder in the manufacturing equipment.

In this work, the formation of amine salts from a series of counterions, with a series of similar structured carboxylic acid parent compounds were used, to explore the relationships between physicochemical and triboelectric charging properties of the resulting material in comparison to the parent compounds. As well as to establish salt trends by scrutinising counterion selection for salt formation in the North American in comparison to European territories.

The more specific objectives of the thesis were to:

- Form salts of the carboxylic acid drugs with the amine counterions.
- Investigate the effects of varying the ratio of counterion to active ingredient during salt formation upon the resulting product.
- Investigate the physicochemical properties of the salts and parent compounds using a variety of analytical techniques.
- Determine the effects of counterion selection upon the solubility and dissolution of the carboxylic acid drugs.
- Investigate the mechanical properties of the parent compounds and the salt forms by consolidating the powder and determining the flowability.
- Examine the effects of counterion selection upon particle morphology.
- Scrutinise the physicochemical properties of co crystal formation in comparison to the salt.
- Investigate the differences in tribo-electrification propensity of a material as a result of counterion or parent drug selection.
- Determine salt form and routes of administration trends between the orange book database and the BNF to establish territorial trends during the previous 12 years.

1.3 Structure of Thesis

A detailed outline of the thesis, comprising of eight main chapters is described as follows:

Chapter 2 is a literature review of topics that are relevant to this research project. An overview of the drug discovery process has been considered, the effects of salt formation upon the physicochemical properties, such as solubility are then reviewed, as well as co-crystal formation. Tribo-electrification and flowability of powders using the Schulze shear cell are then discussed.

In chapter 3 the three materials tested in this work; flurbiprofen, felbinac and biphenyl-4-carboxylic acid are characterised by various methods including differential scanning calorimetry, X-ray diffraction, sieving, and infrared spectroscopy. The tribo-electrification and powder flow methods that were used were then described.

Chapter 4 comprises of a study of API salt selection trends for small molecules, based on analysis of the Orange Book database, and the British National Formulary to reflect territorial trends, evaluating the occurrence of a range of counterions utilised in salt formation in order to better understand the key developments in salt formation over time, and to ascertain whether territorial influences promote certain choices in counterion selection. Also the influences upon routes of administration and the emergence of new molecular entities such as biologics, upon the salt trends, the data was compared with previous studies.

Chapter 5 consists of the influences of varying the ratio of API to counterion upon the resulting material, as well as the effects of changing the recrystallisation solvent upon the properties of the final material.

Chapter 6 includes the salt cocrystal formation and the data collected to ascertain the advantages of co-crystal formation in comparison to the salt form.

Chapter 7 includes the salts formed by the three similar structured APIs with the three cyclic amine counterions which varied by one carbon chain length, the physicochemical properties were compared

Chapter 8 then includes the conclusions drawn from this research project

The future work that may contribute to the development of this research work to understand the links between salt formation and tribo-electrification is outlined in Chapter 9.

2 Literature Review

2.1 Drug Discovery Process

Drug discovery has progressed vastly from the nineteenth century where serendipity of medicinal chemists played a major role in the emergence of new drugs. Whereas in the early twentieth century; the discovery of new structures contributed to the rise in antibiotics. With the advances in technology for new and powerful techniques including molecular modelling/informatics and high throughput screening, playing a part in the rapid advancement of drug discovery towards the end of the century, this has continued to progress in the twenty first century, with a drive to find new chemical entities (NCE's).

High-throughput screening is utilised to determine a 'hit' molecule which targets the biological markers of interest, the properties of the molecule are studied to evaluate the absorption, distribution, metabolism and excretion (ADME) and other interactions of the drug. These studies relate to desirability of the molecule relating to the physicochemical properties, solubility, lipophilicity, permeability and stability [19]. Drugs can fail for one of two reasons, for not being safe for patient use or that they do not work for the intended purpose. For a drug to be successful it is required to elicit a biological response which can be measure in vitro and in vivo.

Drug development is an expensive and rigorous process, with a median cost of developing a single cancer drug to be \$648 million [20] although previously this cost has been estimated to be as high as \$2.6 billion [21], with increasing failure rates contributing to the increase in development costs. From research and development to the drug entering the market takes up to 12-15 years, as many as 10,000 compounds may be considered for drug development and are filtered out till approximately 200-250 remain which could potentially provide therapeutic effect, these enter the pre-clinical stage to ensure safety, where 5-10 compounds remain which will then be used in the clinical trials, which once again are filtered during the trials if they fail, where one compound will be presented to the government authorities for licensing and permission to market the drug (figure 2.1)

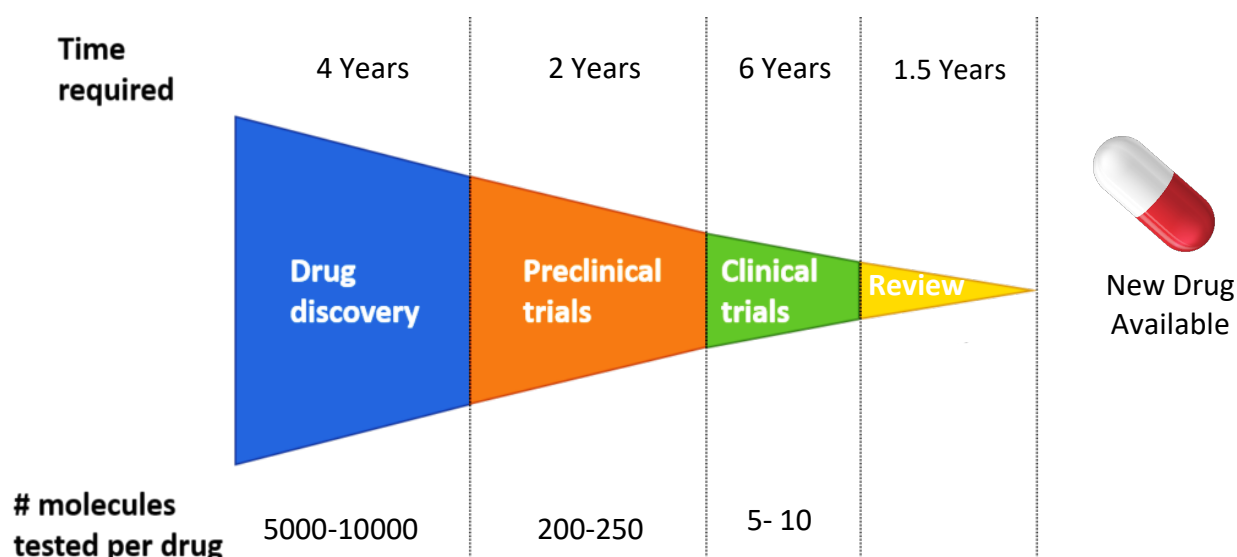


Figure 2.1 Drug Development process (adapted from SRUK.org.uk)

2.1.1 Clinical Trials

After preclinical research, potential drug molecules go through a set of clinical trials which can comprise of Phase 0, Phase I, Phase II, Phase III and Phase IV. The number of volunteers increases as the phase increases, due to the drive in new chemical entities, there are a large number of companies undertaking clinical trials for pharmaceutical industries.

- Phase 0 trials: are the first time the drug is tested on people, with an aim to understand how the drug is processed in the body and any effects it has upon the body. This trial involves a sample size of 10-15 people and a very small dose of the drug is administered.
- Phase I trials: are undertaken with an aim to find the best dose of drug for the people with the least number of side effects. Once again the trials are carried out on a small group of people, generally about 20-80 patients. Very low doses are given to some of the patients whilst others are administered higher doses up until the side effects become too severe or the desired effect is obtained. Phase I is mainly used to screen a drug's safety, those which pass are allowed to continue to Phase II clinical trial.
- Phase II trials: assesses safety further as well as determines if the drug actually works, by testing on people suffering from the ailment which the drug is designed to help

treat. Phase II trials are carried out on a larger number of volunteers than phase I, usually up to 500 people if the drug is found to work, it can be further tested in phase III of the trial.

- Phase III trials: comprise of a much larger number of volunteers, usually a few thousand and are done to compare the new drug to the existing medication used to treat the same condition. Mostly these trials are randomised, where the people are put into treatment groups, to ensure that the people in each group are alike, the trials are usually double-blind to help eliminate bias. Phase III trials are required by the FDA prior to approving a new medication.
- Phase IV trials: are usually carried out on approximately 25-30% of new medications, this phase is carried out after the medication has been approved and includes many thousands of people in the trial over a number of years, investigators use this phase to get more information for the medication about the long term safety, effectiveness and any other benefits.

2.2 Dosage Forms

A broad range of formulation delivery platforms are available to administer the novel pharmaceutical dosage form to the site of action, this can be in the form of tablets, suspensions, inhalers, capsules, parenteral dosage forms, sustained release dosage forms, and transdermal dosage forms. The selection of the route of administration and the particular dosage form largely depends on the drug characteristics and the clinical circumstances, the oral route of administration is one of the most popular routes used, due to its convenience, high patient compliance, ease of production, cost effectiveness and flexibility in the dosage form design [22]. Of the well-defined APIs listed in the orange book database, 62% of these were administered orally, in comparison to 35% used for injectables [23]. All routes of administration have their pros and cons with the oral delivery providing to be limiting when a patient is uncooperative, as well as the slow absorption of the drug, or unpredictable absorption due to degradation of the tablet by enzymes or stomach acid. In comparison to intravenous where the entire dose reaches systematic circulation immediately, providing

reproducible effects, however is more expensive and labour intensive than other routes of administration and requires a cannula, requiring patient compliance. The inhalation route provides rapid adsorption due to a large surface area of the respiratory system, and inhaled steroids and bronchodilators can be targeted to the lungs, the main issue with the inhaled route is inhaler technique by the patient. [24]

2.3 Drug Solubility

Solubility is defined as the maximum amount of solute that can be dissolved in a set amount of solvent under specified conditions of temperature and pressure. This definition can be made both qualitatively and quantitatively; quantitatively it is the concentration of solute in a saturated solution at a certain temperature, whereas in qualitative terms, solubility is defined as an interaction of two or more substances to form a homogeneous dispersion. A saturated solution is one which the solute and solvent are in equilibrium [7].

Poor solubility is becoming an increasing problem and is one of the contributors to failing compounds during the development pipeline, making it increasingly difficult when designing a suitable formulation or oral drug delivery. A study containing the top two hundred oral medications in the US, Great Britain, Spain and Japan revealed that approximately 37% of drugs has a solubility of less than 0.1 mg/ml in water which is defined as practically insoluble, one explanation may be that the drugs are highly potent at low doses, however this still indicates the challenges in drug discovery and finding suitable molecule with a good solubility profile. For a drug to be classed as soluble it is required to fit the range from 33-100 mg/ml, if greater than this, the drug would fit the profile for either freely soluble (100-1000 mg/ml) or very soluble (≥ 1000 mg/ml) [25]. Furthermore, due to the increase in high throughput screening for identifying new chemical entities, there has been a substantial decrease in the solubility of new molecules, whereby intrinsic solubilities of less than 1 $\mu\text{g/ml}$ are a lot more common [26]. According to Serajuddin (2007), approximately one third of newly synthesized compounds have an aqueous solubility of less than 10 $\mu\text{g/ml}$, with another third possessing a solubility from 10 – 100 $\mu\text{g/ml}$, and the remaining third is > 100 $\mu\text{g/ml}$, in comparison to pre 1980s where less than 20 $\mu\text{g/ml}$ was unusual [1].

Currently there is a rise in research to predict the solubility of molecules to aid drug development, in some cases by predicting the biorelevant solubility in media which mimics

the human intestinal fluids rather than the solubility in pure water [27-29], providing new approaches to predict solubility more accurately, as well as; providing a deeper understanding of the molecular interactions and processes occurring during the dissolution and solubilisation process.

2.3.1 Solubility Improvement Strategies

A number of techniques can be utilised to enhance solubility, these can be categorised into three categories, physical modifications, chemical modifications and miscellaneous methods [30]. One frequently used method to enhance solubility is salt formation [1].

Some of the commonly used strategies include:

2.3.1.1 Salt Formation

Salt formation is one of the most common techniques utilised in increasing the dissolution rate and solubility of basic and acidic drugs. Salt formation allows for improved physicochemical properties without affecting the pharmacological properties of the drug. In the case of a weak acid formulated as a salt, its solubility and dissolution rate will increase in the stomach (pH ~1.5), the salt will result in an increase in the pH of the drugs microenvironment, leading to higher dissolution rate for an acidic drug. However, in the case of a drug which is a weak base, an increase in solubility and dissolution will occur in the intestine (pH ~7.0), as a result of buffering action of the salt, upon dissolution of the salt, an increase in protons being released to the environment which will, decreasing the pH and resulting in an increase in dissolution of a basic drug [2, 31].

2.3.1.2 Particle Size Reduction

Particle size reduction is one of the oldest strategies employed in improving solubility of a drug, solubility of drugs is intrinsically associated to the particle size of the drug. The reduction in particle size results in a larger surface area, thus increasing the surface area to volume ratio, therefore resulting in an increase in the surface area available for solvation. Particle size reduction techniques are therefore regularly used to increase the bioavailability of poorly soluble drugs [32]. A few commonly used techniques include, mechanical micronization, jet milling, ball milling and high pressure homogenisation. Although these techniques are

convenient and simple, they are at times unfavourable depending on the type of drug material, as they are limited in controlling particle size, shape, morphology electrostatic charge, or even lead to agglomerated particles at the end [33]. Particle engineering has been developed in order to control the particle size and properties, these methods include, cryogenic spray processes and crystal engineering to produce nanosized particles in an attempt to reduce particle size to enhance solubility and dissolution, in turn the bioavailability of the drug [34].

2.3.1.3 Crystal Engineering

Cocrystals are made up of an API and a coformer connected by a hydrogen bond [35]. Cocrystallisation is a technique that can improve the physicochemical properties of an API, however, the technique is more versatile than salt formation as it can be applied to neutral, acidic alkaline and ionic compounds. Cocrystals are becoming an important class in pharmaceuticals as they can improve the dissolution and solubility of an API by forming a complex crystal [36]. As well as this, the surface area for drug dissolution to occur is dependent upon particle size, which is influenced by crystallisation conditions, particle size reduction techniques can also be utilised, however, this may result in charged and cohesive materials which may be problematic downstream. Hence, controlled crystallisation is favourable as it produces high purity product with well-defined crystal habit, surface energy, particle size distribution, by manipulating the crystallisation conditions e.g. changing the solvent, may result in a different packing arrangement, resulting in a polymorph which can exhibit improved physicochemical properties including solubility.

2.3.1.4 Cosolvency

Cosolvency is one of the most popular methods used for improving the solubility of poorly aqueous soluble drugs in liquid formulations [37]. Cosolvents are often comprised of a mixture of miscible solvents aiding in improving the solubility of poorly soluble drugs [38]. They work by reducing the interfacial tension between the hydrophobic solute and aqueous solution. Most cosolvents have hydrogen bond donor/ acceptor groups in addition to small hydrocarbon regions. These hydrophilic hydrogen-bonding groups increase water miscibility, whereas the hydrophobic hydrocarbon regions inhibit the waters hydrogen bonding network,

decreasing the intermolecular attraction of water. By disturbing the water's self-association, cosolvents reduce water's capacity to push out nonpolar, hydrophobic compounds, thus increasing solubility [39]. The advantage of cosolvent technology improving drug solubility in a liquid formulation includes [40] convenience, safety and cost. The most frequently used low-toxicity cosolvents are propylene glycol, ethanol, glycerine, polyethylene glycol (PEG), dimethyl sulfoxide (DMSO), and dimethylacetamide (DMA) [41-45].

2.3.1.5 pH Adjustment

pH adjustment is a technique which can be utilised to improve the solubility of a compound as molecules which can be protonated (bases) or deprotonated (acids) can often exhibit a greater solubility as a result of pH adjustment using HCl, NaOH or by using a buffer [46]. This approach is a good technique to evaluate the dissolution behaviour of a poorly soluble drug due to its simplicity.

2.3.1.6 Inclusion complex formation

Inclusion complex formation technique has shown to have been employed more precisely in improving dissolution rate, bioavailability and solubility of poorly water soluble drugs. The formation of inclusion complexes involves the insertion of a non-polar region of one molecule into the cavity of a separate molecule, the most popular choice of host molecules are cyclodextrins (CDs) [30]. CDs are cyclic oligosaccharides formed by either 6 (α), 7 (β), 8 (γ) or more α -1,4 D-glucopyranose units. Due to the chair structure of the glucopyranose unit, the molecule forms a cone shape, allowing the CD to possess a hydrophilic outer surface and a slightly lipophilic inner cavity. The most common complex in dilute aqueous solutions is a 1:1 drug :CD [47]. In pharmaceuticals CDs are versatile as they have the ability to provide multiple benefits including improved solubility, stability, bioavailability, prevent gastrointestinal irritation and mask the taste and smell of a drug [34, 48]. Previous research has shown the successful inclusion of β -cyclodextrin with felbinac, whereby higher drug plasma concentrations were achieved as well as a greater anti-inflammatory activity [49]. However, complexation has a number of disadvantages which include, the method of preparation can be laborious and expensive, the difficulties faced in incorporating into the dosage forms, stability issues in some cases as well as in scale up [50].

2.3.2 Biopharmaceutics Classification System

The Biopharmaceutical Classification System (BCS) is based upon the work of Amidon and colleagues [51]. It is not only useful in providing in vivo bioequivalence studies, but also for decision making during drug development for new chemical entities [52]. The BCS is a scientific framework used for classifying a drug based upon its solubility and intestinal permeability [51], when combined with dissolution characteristics (in vitro) of the drug, the BCS considers three major factors; dissolution rate, intestinal permeability and solubility, all of which are instrumental in governing the rate and extent of solid oral dosage forms; due to this the BCS has been adopted by the FDA [53]. The BCS classifies drugs into four classes according to their solubility across the gastrointestinal mucosa.

The solubility of a drug according to the BCS is based upon the highest dose strength of an immediate release drug, whereby a substance is classified as highly soluble when the highest dose is soluble in 250 mL or less of aqueous media over a pH range of 1.0 – 7.5, if this is not met then the drug substance is classified as poor solubility. The criteria has to fulfil 250 mL due to the volume concurring with that estimated to be in the stomach of a fasted person with a glass of water [54].

The permeability is based upon the magnitude of intestinal absorption of a drug in a human, whereby a highly permeable drug is considered when the extent of absorption surpasses 90% of the administered dosage [54].

The four classes of the BCS are:

- Class I : High Solubility/ High Permeability
- Class II : Low Solubility/ High Permeability
- Class III : High Solubility/ Low Permeability
- Class IV : Low Solubility/ Low Permeability

2.3.2.1 Class I

These drugs behave like an oral solution, possessing fast dissolution as well as bioavailability, drugs which fall into this classification are good candidates for controlled drug delivery

providing they qualify pharmacodynamically and pharmacokinetically for their intended purpose. Gastric emptying is usually the rate governing step. Examples of class I drugs include; Verapamil, Metoprolol, Propranolol and Diltiazem [55].

2.3.2.2 Class II

Due to the low solubility and high permeability of drugs in this class, the dissolution rate is the determining step for bioavailability, these drugs require enhancement in solubility (Section 2.3.1) for increased bioavailability, however, these drugs make good candidates for controlled release purposes. Examples of class II drugs comprise of Nicardapine, Ketoconazole, Nifedipine and Flurbiprofen [55].

2.3.2.3 Class III

Permeation of the drug through the intestinal membrane is the rate determining step for class III drugs. These drugs exhibit low bioavailability and permeability enhancement is usually required, these drugs are not suitable for control release. Some examples include; Alendronate, Enalaprilate, Captopril and Acyclovir [55].

2.3.2.4 Class IV

Drugs in this class exhibit poor bioavailability as several factors dictate the overall bioavailability, such as gastric emptying, intestinal permeability and rate of dissolution. These drugs are not appropriate for oral drug delivery, alternative routes of administration can be considered or alternative drug delivery methods such as nanosuspensions will aid in improving absorption into systemic circulation. Class IV drugs include; Tobramycin, Cefuroxime and Clorthiazide [55].

2.4 Salt Selection Process

The physicochemical properties of a new chemical entity are investigated once an active compound has been identified. Where salts are concerned, the pK_a value is one of the primary pieces of information obtained. It is used to determine the degree of ionisation, whereby a lower value indicates a stronger acid. The pK_a rule states that for a successful salt formation to occur, there must be a difference between a base and an acid of at least two or three [8]. This difference in pK_a ensures that there is a strong affinity to bind of the two species and will

not disproportionate back into the individual species when not required. Upon selection of relevant counterions, further studies are required to determine the overall physicochemical properties of the material such as solubility which is seen as one of the important parameters of a drug [30], as well as the crystallinity or amorphicity to determine if there are possible polymorphs, which can be discovered using X-ray Diffraction (XRD). The formation of solvates/ hydrates is also a possibility which can be investigated using thermogravimetric analysis (TGA). Also, tribo-electrification propensity of a material can be problematic during powder handling [56]. Therefore salt selection is paramount as it influences each of these properties differently.

2.5 Salt Selection Strategies

Due to the emergence of combinatorial chemistry and high throughput screening (HTS) during the past 10-15 years, the pharmaceutical industry has been going through a revolutionary technique in the way new drugs have been discovered and developed.

2.6 Salt Formation

Salification is a simple and effective method of improving undesirable properties of acidic and basic drugs, including solubility, hygroscopicity, stability and dissolution rate due to their ability to be ionised [1], with the most sought after properties being high dissolution rate and solubility, followed by stability and crystallinity, and finally ease of formulation and manufacturing [6]. Approximately 50% of drugs are administered in a salt form [23].

Salt formation occurs when a compound is ionised in solution and a strong ionic interaction is produced between an oppositely charged counterion, resulting in the formation of a precipitate. Intermolecular columbic forces are utilised to produce interactions which in turn affect the potential energy, leading to an increase in interactions between the polar solvent and the charged active pharmaceutical ingredient. Therefore, enhancing dissolution rate and increasing solubility, in turn producing greater drug delivery. The solubility of a salt is dependent upon a number of properties, such as its size, lipophilicity, polarity, and ionisation potential, as the solvent is required to overcome the lattice energy of the solid and create space for the solute.

There are a number of advantages and disadvantages to salt formation, some of the advantages include improved thermal stability, reduced hygroscopicity, improved drug efficacy and improved compactibility. The disadvantages include, decreased percentage of active ingredient in the formulation, increased formation of polymorphs and hydrates resulting in greater variability of pharmaceutical properties, corrosiveness of the salt; potentially causing tableting problems and the additional step in synthesis resulting in increased manufacturing time and costs.

Although there are an abundance of counterions available, a few are used recurrently, such as Chloride (46%) and Sodium (67.5%) being the most commonly used counterions for basic and acidic drugs, respectively (Chapter 4). However, there is an increase in percentage incidences of some of the lesser used counterions; promoting diversity.

2.6.1 Crystal Engineering

Recently there has been an increasing interest for engineering the morphology of pharmaceutical APIs in order to form the desirable size, shape and surface of materials. One technique widely used for improving the physiochemical properties of an API whilst maintaining the activity of the drug is salt formation. This technique is especially popular in the pharmaceutical industry for improving solubility or stability, as well as overcoming some undesirable characteristics exhibited by the parent drug [57], popularity stems from the ability to modify the undesirable characteristics whilst maintaining therapeutic effect. The internal packing dictates whether the material is crystalline, defined as when the crystal structure is packed in a defined order, amorphous, in which it possesses no long-range 3D order, or even polymorphic; whereby there is a different repeating packing arrangement, or include solvent (hydrates/solvates). These variations in the internal packing result in alterations to the bulk properties such as mechanical and physico-chemical [58].

For a crystalline material, it is possible to manipulate the crystal habit which affects the shape of the crystal as a result of the rate of growth of crystal faces. The shape of crystal is dependent upon the solute-solvent interaction as some crystal faces may possess a high number of exposed non-polar groups where as others may be polar. Therefore, the polarity of the solvent used to undertake the recrystallization process needs to be selected carefully as it influences the orientation and packing geometry of the molecules into the lattice [59].

As a result, it is possible to contrive changes in the crystal habit by controlling the rate of growth of the faces of the crystals.

2.6.2 Crystallisation Mechanism

Crystallisation of a material may be initiated by inducing a change from the liquid to solid state, when crystallising from solution, the process is as follows

- I. Supersaturation of the solution
- II. Formation of the crystal nuclei
- III. Crystal development around the nuclei

The supersaturation process involves a solution with an excess of dissolved solid than feasibly possible under saturation conditions for a given temperature. As supersaturated solutions are not thermodynamically stable, hence the system will equilibrate to its true solubility and result in precipitation of the excess solute within the solution [59].

There are three types of nucleation possible for supersaturated solutions. One is primary homogeneous nucleation in which a very high concentration of material is required [60]. Primary heterogeneous nucleation is initiated by the presence of a foreign solid phase [61]. Secondary heterogeneous nucleation is the most common and it involves the addition of solid phase solute particle be added to the solution. The benefit to this type of nucleation includes its versatility to initiate within the metastable zone [60].

The crystal development process consists of a number of stages for growth. The growth is dependent upon the interaction between the molecules and the layers of pre-formed crystal hence influencing the change in morphology of the resulting crystal [62]

2.6.3 Effect of Crystal Habit upon Pharmaceutical Material

Changes in the crystal habit of materials are of great interest due to the direct link to changes in the physicochemical properties [59], such as material dissolution, stability, solubility due to an array of shapes resulting in changes in surface area, density and tribo-electrification, which in itself has been shown to affect the powder flowability and compressibility, flowability of a material extends to particle shapes, for example, needle crystals increase handling complications in comparison to equidimensional particles [63].

2.7 Cocystal Formation

Pharmaceutical cocrystals are multicomponent structures consisting of at least two molecules, one being the drug (API), and the other a coformer being held by hydrogen bonding and the coformer can be another active pharmaceutical ingredient (API) or an excipient [9, 10]. The formation of cocrystals has gained substantial interest due to their ability to often exhibit better physicochemical properties for the API by altering the structure without affecting the pharmacological properties of the drug [11-14]. The impact of cocrystal formation is not limited to absorption and has the ability to drastically alter the drug's pharmacokinetics and solubility [15]. It can be used as an alternative to salt formation to amend the undesirable properties possessed by APIs.

A number of methods can be utilised in cocrystal formation as described in Sections 2.7.1-2.7.8.

2.7.1 Traditional Methods

2.7.1.1 Solvent Evaporation

The solvent evaporation method is one of the most common techniques used for cocrystal formation. Where the drug and coformer are dissolved in a specific solvent, stirred at constant conditions to initiate molecular interactions between the drug and the conformer. The solvent is then allowed to evaporate under controlled conditions and the cocrystal forms a solid substance. This is a three step process comprising of supersaturation, nucleation and crystal growth [64].

2.7.1.2 Slurry/Grinding Method

The slurry method is an alternative method to the solvent evaporation and involves a small amount of solvent to be added to a mixture of drug and coformer. The slurry suspension is stirred until the cocrystallisation process has completed. This technique can be coupled with grinding whereby a dry physical mixture of drug and coformer is ground together using a mortar or a ball mill, or a wet method which includes small drop of solvent, the solvent acts as a catalyst, either as a factor which promotes a multi component framework or by facilitating molecular diffusion [65].

2.7.2 Novel Methods

2.7.2.1 Heat Induced CocrySTALLISATION

CocrySTALLISATION using heat is a method which can be utilised as it has several advantages in comparison to solvent evaporation, as it does not require a solvent, the drug and coformer solubility does not require any consideration. Hot melt extrusion is a technique which combines cocrySTALLISATION and drug formulation, providing an easier way for drug manufacturing [66].

2.7.2.2 Spray Drying

Spray drying is a quick and continuous process in producing a dry powder from a suspension or solution with the aid of a hot air stream. For a drug and coformer which cannot produce cocrySTALS using the solvent evaporation method, the spray drying technique can be used as an alternative. Carbamazepine-glutaric acid and caffeine-glutaric acid are examples of incongruent systems which cannot form a pure cocrySTAL through solvent evaporation, hence other techniques are required [65].

2.7.2.3 Supercritical Fluid Technology

The solid state and solution cocrySTALLISATION usually present several disadvantages which can be overcome using supercritical methods. The benefits of utilising supercritical CO₂ include, a low environmental impact, relatively low temperature hence reduced API degradation as well as the production of solvent free pharmaceuticals. There are various methods of supercritical CO₂ to produce cocrySTALS, a few of these include, rapid expansion of supercritical solutions where CO₂ is a solvent, cocrySTALLISATION with supercritical solvent where CO₂ as solvent and molecular mobility enhancer, supercritical antisolvent crystallization where CO₂ acts as an antisolvent [67].

2.7.2.4 Laser Irradiation

A recently reported method for cocrySTALLISATION by Titapiwatanakun *et al.* which utilises a CO₂ laser to produce a 2:1 caffeine-oxalic acid and a 2:1 caffeine-malonic acid cocrySTAL. The energy produced by the laser results in a rapid rise in temperature of the sample in a small space of time, generating a melting of the crystalline material, which subsequently mixes,

followed by rapid recrystallisation upon cooling, one condition must be met whereby the coformer must be sublimable, in order for the nucleation process to occur during the vapour phase [68].

2.8 Powder Flow Background

As salt formation is an effective method to alter the physicochemical properties of a drug, in most cases good solubility and dissolution are considered highly important, with other advantages such as improved stability to extend shelf life, better taste, or even improved drug effectiveness. However, salt formation can alter some of the physical properties which include flowability of the powder, this is influenced by a change in particle size and/or particle shape of the resulting material as needle and rod shaped material can result in poor powder flow. Although the particle morphology can be influenced by crystallisation conditions, some forms can have a persistence to crystallise in specific morphologies. Increased powder flow can improve powder handling properties as well as influence the tribo-electrification (Section 2.9) propensity of a material.

2.8.1 Powder Flow - Schulze Shear Cell

Powder flow properties are extremely important to consider, as poor flow can result in a number of complications such as flooding, flow obstructions, irregular flow, segregation and even tribo-electrification of material. Flow of bulk materials is required in order to determine the effects of flow agents or other excipients upon flow behaviour of a powder. A number of parameters influence the flow properties: particle size, particle shape, tribo-electrification propensity of a material, moisture and temperature.

Due to the complexities, it is not possible to determine the flow behaviour of bulk materials while considering all these parameters, appropriate testing devices are available to test the powder flow properties.

The flowability of a bulk material is dependent upon the adhesive forces between individual particles. The adhesive forces can come about from various mechanisms however electrostatic force plays a major role. As the particle size decreases the impact of the adhesive forces increases, hence a material will present poorer flow properties as particle size is reduced [69].

If an external force is introduced and the particles are compressed, large stresses are induced upon the particle contact points and in turn results in adhesive forces. A good flowing material does not consolidate much and will flow out of a storage vessel or hopper without any external influences or flow promoting devices and under the forces of gravity alone, whereas a poor flowing material will consolidate easier during storage or transport [70].

As the shear cell works on a process including consolidation, the flow properties are considered from a bulk solid with an external load acting upon it, i.e. the failure of a consolidated bulk material, the degree of load required for flow to initiate is known as flowability. A uniaxial compression test is carried out by filling a cylinder with a bulk solid (figure 2.2), a consolidation stress (σ_1) is induced upon the material, in the vertical direction, the greater reduction in volume the greater consolidation of the bulk solid. After consolidation the bulk solid is released of the consolidation stress (σ_1) and the cylinder removed. The cylindrical bulk is then subjected to compressive stress in the vertical plane and the compact will fail at a certain strength. The failure is known as the unconfined yield strength (σ_c) and indicates an onset of the incipient flow has been attained. Since the bulk material only fails at a sufficient vertical stress, which is equal to the compressive strength, a yield limit must exist for the bulk material, once this limit has been achieved, only then the bulk material will flow [70].

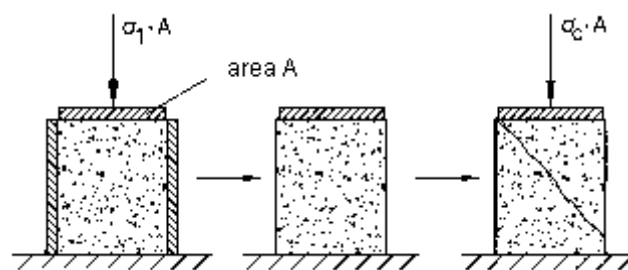


Figure 2.2 Uniaxial Compression Test [70]

The state of stress expressed upon a bulk solid can be represented by a Mohr stress circle. The Mohr circle A (figure 2.3) describes the stresses acting upon the bulk solid when subjected to consolidation, during the increase in vertical load in the second step of the experiment, the circles increase with diameter due to the stress states at different loads (B_1 , B_2 , B_3). The Mohr circle B_3 represents the failure of the specimen, indicating that incipient flow has been reached. However, if during the experiment, a constant horizontal stress was applied, as well

as a vertical stress, a yield limit would be achieved hence indicating failure of the bulk solid (stress circle C) [70].

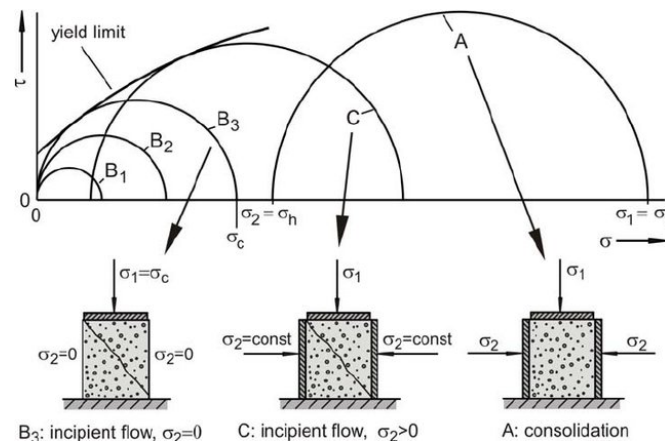


Figure 2.3 Measurement of Unconfined Yield Strength [70]

Flow ability is based upon the ratio ff_c of consolidation stress to unconfined yield strength to provide a numerical value (Equation 2.1).

$$ffc = \sigma_1 / \sigma_c \quad \text{Equation 2.1}$$

The greater the ff_c is, the smaller the ratio between unconfined yield strength to consolidation stress, and the better flow exhibited by the bulk material (figure 2.4) [70].

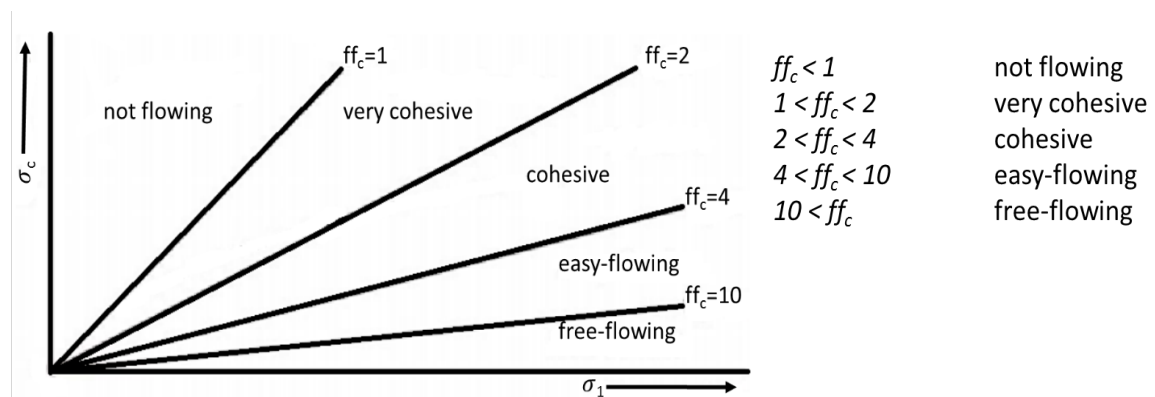


Figure 2.4 Powder Flow Function

2.9 Tribo-Electrification Background

The physicochemical properties of new salt forms are comprehensively characterised for the early stages of drug development, these usually include, flow properties, particle size, particle shape, particle habit etc. Though little work has been reported on the tribo-electrification of salt forms, no previous research has scrutinised the effects on the tribo-electrification propensity of salts formed using a counter-ion and similar structured APIs. As well as establishing the effects of the counter-ion selection, whereby a linear series of counter-ion allowed for the consequences of increasing the bulk of the counter-ion for salt formation upon the tribo-electrification propensity of the resulting material to be better understood. As tribo-electrification is dependent upon physical contacts, surface modifications as a result of salt formation are likely to alter the charge transfer process. Tribo-electrification can be influenced by the powder flow properties of a material as both powder flow (section 2.8) and tribo-electrification are influenced by similar properties such as particle shape, size, surface area etc.

2.9.1 Tribo-electrification

Tribo-electrification occurs as a result of particles coming into contact with each other as well as the surface of the equipment resulting in generation of electrical charge, due to electron or ion exchange taking place as a result of sliding and friction forces acting upon the material [17], hence contacting materials are left with equal but opposite charge after the separation process. If no lateral motion occurs then the process is known as contact electrification. However, the term tribo-electrification has parted from the original understanding of predominantly associating with the rubbing of particles, more recently a wider definition has been attributed to tribo-electrification, which includes a broad range of particle movements and collisions [71].

Charging is a phenomenon which occurs between all materials which come into contact. When two conductive materials make contact, the charge transfer is dependent upon the work function of the materials, and a lesser charging propensity is seen in comparison to insulator materials due to a grounding effect. In the case of insulators, the charge is trapped as the electron movement is restricted, this can lead to greater material handling problems.

A number of possible charge transfer mechanisms are identified in order to explain the tribo-electrification process, these comprise of *electron*, *ion* and *material* transfer [72]. It is well known that charge transfer is initiated by the energy required to offset the differentiation in work function between the two materials [72]. A theory has been proposed in order to explain the mechanics behind insulator-insulator contacts, which states that the electron states are presumed to be located on the materials surface whereby the exchange of charge propagates the offset in the effective work function across the contacting area of the materials [73]. Work function is defined as the minimum quantity of energy which is required to remove an electron to infinity from the surface of a given solid, usually a metal [74].

Mixing is one of the most essential stages in powder processing, this unit operation brings about complications when particle-particle interactions take place, as well as when the particles interact with the surface of the equipment during the manufacturing process.

As the powders are in contact with each other or with the surfaces of the processing equipment, electron exchange may occur due to a difference in surface potential between the two materials [75]. The potential difference may be influenced by the surface roughness, particle size and shape of the powder [76]

Examples of the complications due to tribo-electrification include particle segregation whereby the charged particles form agglomerates, leading to inconsistent particle size, varying dosage masses and process delays. In the pharmaceutical industry, the most commonly used powders can be classified as insulators and segregation is problematic as it plays a role in reducing content uniformity of a product, as well as increasing adhesion and reducing flowability [18]. The quantity of Active Pharmaceutical Ingredient (API) has to be within limits for a randomly selected sample in a batch. Failure to comply leads to rejected products, increasing costs and manufacturing times. Tribo-electrification is challenging within the pharmaceutical industry, as well as powder handling plants in the food industry such as flour mills which are vulnerable to dust explosions due to the high concentration of fine particles suspended in air. A source of ignition may easily cause an explosion [16].

Previous studies have shown that electrostatic charge is generated when an insulating material is brought into contact with another material and subsequently separated [77]. An electrically conductive material has the ability to dissipate the charge instantaneously, when the surface is grounded, thus proving to be an effective method of neutralising the charge on

a conductor. Pharmaceutical powders however are insulators and are usually comprised of fine particles that do not allow charge to travel through the body of the powder hence grounding is usually an ineffective method to neutralise a charged powder. Finer materials in general have been shown to be more cohesive, due to their large surface area available for charge transfer to take place as well as free moisture that can form capillary bonds between the particles which results in an increase in particle to particle adhesion [78]. Furthermore, gravitational forces acting upon the finer materials are smaller as the particles have low mass. The insulating properties reduce the tendency of electrostatic charge dissipation, resulting in difficulties in dealing with the charge imbalance

Electrostatic charge has been utilised to provide benefits in a variety of applications, charge control additives (CCA) are popular in the electrophotography industry [79], used in photo copiers and laser printers [79]. Other applications include, electrostatic precipitator [80], and electrostatic spray painting [81]. Utilising the electrostatic charging in a positive way is possible due to the ability to charge the particles which allows for the concept of opposite charges attracting, to enable the deposition of the particles to be controlled. For the pharmaceutical industry, exploiting the benefits of charging is limited to certain chemicals which are suitable for medical applications.

2.9.2 Factors Affecting Tribo-electrification

2.9.2.1 Fundamental Properties

2.9.2.1.1 Work Function

Electrification occurs when two dissimilar materials make contact with each other by friction or impaction and subsequently separate, resulting in a charge imbalance of both materials. The extent of charging is dependent upon the properties of the materials. The degree of tribo-electrification of the particle is highly dependent upon the work function. Work function is defined as the minimum thermodynamic work required to remove an electron to infinity from the surface of a solid [74]. During the contact of the material, electrons are transferred across the contact points, the extent of electron transfer is dependent upon the difference in work function of the two materials [82]. A material which possesses a high work function tends to

act as electron acceptors, hence charging negatively, whereas materials with a low work function possess donor properties and have a net positive charge.

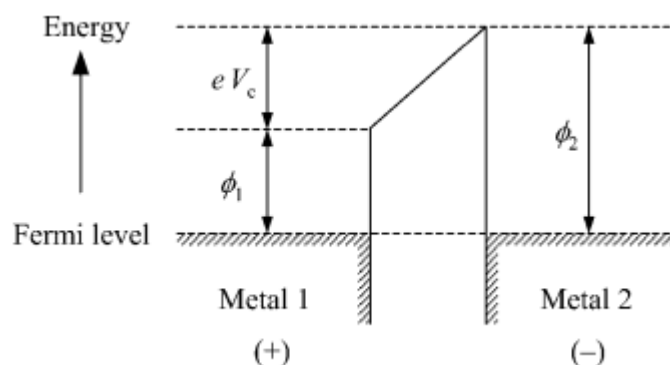


Figure 2.5 Electron Potential Energy at a Metal - Metal Contact [82]

In the case of metals the energy levels (figure 2.5) are readily understood however insulators do not possess energy levels of a similar nature to metals. Metal-insulator charging was found to be linearly proportional (with exception) to that of the metal work function upon testing with an insulator [83]. This brought about the theory of “effective” work function when considering polymers. Whereby the electron transfer is undertaken between the Fermi level of the metal, compared to localised energy levels in the band gap of the insulator. However, there are complications in this theory as the electrons in insulators are not found in a single energy level as they are in conductive metals [83].

2.9.2.1.2 Tribo-electric series

The charging tendency of insulators can be estimated by taking the tribo-electric series into account, whereby the insulators at the top of the ranking will obtain a net positive charge when placed in contact with a material lower in the series.

The drawback to the series prevents charge to be predicted by considering the position of the insulator on the series, due to influencing factors such as surface contamination which can effect insulator charging. Hence requiring charge studies to determine the effects of such materials used within industrial applications upon the powder during processing. An example of the series is shown in table 2.1 [84].

Table 2-1 Tribo-electric series [84]

Glass	⊕
Nylon	↑ Acquire positive charge (lower work function)
Wool	
Lead	
Silk	
Aluminium	
Paper	Zero
Cotton	
Steel	
Nickel and Copper	
Silver	
Gold and Platinum	
Sulphur	
Polyester	
Polyethylene	
Silicone rubber	↓ Acquire negative charge (higher work function) ⊖

2.9.2.1.3 Contact Potential Difference (CPD)

If two metals of varying work functions are placed in close proximity to one another, but not touching, and are electrically connected, a potential difference is induced due to the Fermi levels of the two metals coinciding. Resulting in a flow of electrons from the metal with the lower work function to the metal with the higher work function. This establishes a contact potential difference between the two metals [85].

CPD can be measured, whereby a reference electrode is placed in parallel, the metal under investigation and vibrated. This caused a displacement of the electrodes which results in a change in capacitance causing a charge flow to be detected. Studies have used gold as a reference due to its known contact potential difference to measure the charge densities of other metals.

Further studies have found that equilibrium charge is in fact related to the contact potential difference of the powders under investigation [86].

2.9.2.1.4 Image Charge

The image charge effect has an influence upon the net charge distribution, as the charge upon a particle is equal to the total charge (q) at the centre of the particle. To maintain an isopotential environment, an equal but opposite charge ($-q$) is induced upon the metal surface. The image effect is illustrated in figure 2.6 depicting the effect of a spherical particle near a conductive wall [87].

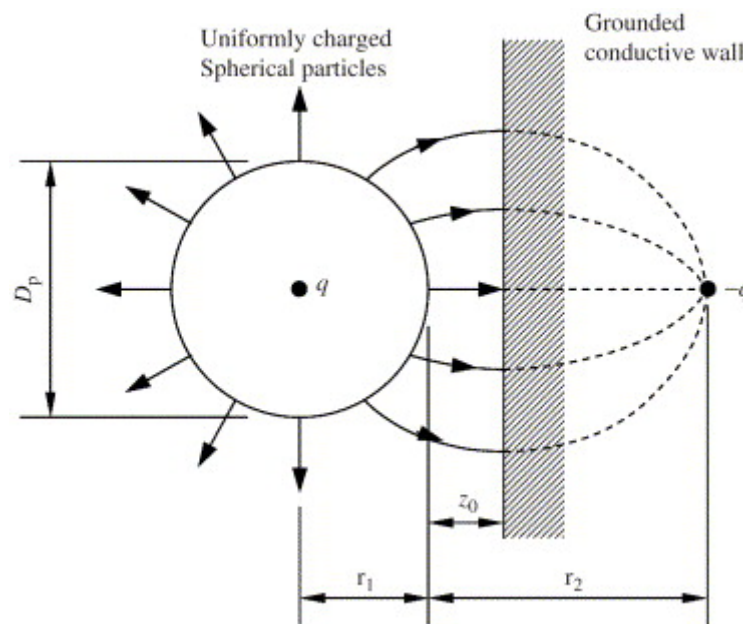


Figure 2.6 Potential difference caused by the image charge effect [87]

2.9.2.1.5 Space Charge

In tribo-electrification, space charge (figure 2.7) is a concept in which the excess charge acts as a continuum charge distribution over a region of area (cloud). Opposed to just charging at the points of the particle. The charge can either be of positive or negative polarity, due to it occurring as a result of an electric field, it is commonly found in insulating environments, conducting environments will allow for the charge to be neutralised rapidly [87].

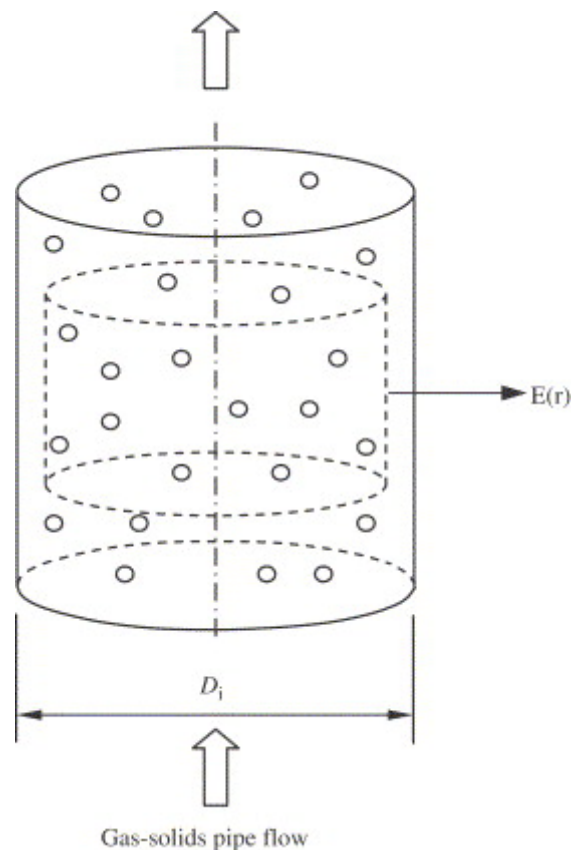


Figure 2.7 Electric field generated by space charge [87]

2.9.2.1.6 Induced Charge

Another fundamental charge transfer mechanism is via induction, whereby a charged particle within close proximity to a neutral conducting object causes there to be a movement of electrons within the conductor, resulting in an imbalance of charge on the opposite ends of the conductor. This can result in a permanent charge imbalance left upon the particle/object. Induction causes the charge receiver to remain in a state of opposite polarity to the object initiating the charge induction.

2.9.2.2 Physiochemical Properties

2.9.2.2.1 Particle Shape

The process of tribo-charging is complex and many factors are involved, with particle shape playing a fairly major role, Watanabe *et al*, have shown that impact charging of spherical glass

and sugar particles possess a strong linear relation between initial charge and impact charge, in comparison to aspirin and α -lactose, whereby a plethora of scattered results were obtained [86]. This may be down to the particle shape of the samples, as aspirin and a lactose have oblong and prismoidal particle shapes, respectively [88]. The contact area between the material and target for non-spherical particles is heavily dependent upon the orientation of the particle upon impaction, it can be assumed that a larger contact surface results in a greater charge transfer, this is in line with the work by Matsuyama 1995 [89]. As asymmetrical particles will retain regions of increased curvature than a sphere, this corresponds to greater surface charge densities ensuing redistribution of charge across the surface of the particle. Also during contact the surface may deform, resulting in varying results of charge generation. [90]

In reality, surface asperities of powder particles are the norm, the area of the points of contact between the materials is known as the effective distance. The flatter the contacting surfaces of the powder are, the smaller the effective distance. [91]

2.9.2.2.2 Particle Size

For many years there has been an interest in the effects of particle size on the degree of tribo-electrification of pharmaceutical powders. Previous studies have shown inconsistent results regarding the extent of charge. [92]

A study undertaken by Rowley[93] demonstrated the effect of the particle size of α -lactose on charge generation, when carrying out tribo-electrification against a stainless steel container, a net negative charge was obtained. The charge obtained is inversely proportional to the particle size. Particle adhesion of powder to the contact surface was insignificant, the tribo-charging was a direct result of the interaction between the metal surface and powder[93]. The smaller particles gained a higher charge due to an increase in probability of particle to metal interactions. The findings showed that when the α -lactose was subjected to a PVC contact surface, a net positive charge was produced. Also the relationship between charge and particle size becomes increasingly complicated when the particle size in question is below 90 μ m, this is due to an increase in probability for particles adhering to the walls of the PVC contact surface, in turn altering the charge mechanism from particle/wall interactions to particle/particle interactions as well.

2.9.2.2.3 Particle Surface Area (Contact Area)

The charging capacity of a particle is influenced by the surface roughness of the particle; increasing the roughness can increase the surface area, however the area available for contact reduces. This coupled with varying modes of contacts e.g. rolling, bouncing and sliding influences the charging behaviour of particles. The duration of contact and the area of contact influence the charging tendencies. A study by Ireland confirmed that the duration of particle contact with the surface was an important factor in charge transfer [94]. The presence or absence of a particles bouncing is directly linked to contact time, hence this was taken into account. It was concluded that the distinction between fixed orientation contact and rolling was critical to the charge transfer process. As a particle rolls, the entire surface is available for charging in comparison to a fixed orientation particle, where only a small area is available for charging. For a non-spherical particle the most stable contact surface will be the one which presents the least curvature therefore providing a relatively larger average contact area for charge transfer. This charging behaviour is also seen when comparing rough and smooth particles due to the different contact area to surface area ratio.

2.9.2.2.4 Functional Groups

In many cases the physical properties of an active pharmaceutical ingredient requires modification in order to provide greater processing characteristics required for formulation. One method of modifying physical aspects of a pharmaceutical ingredient includes the formation of salts. This enables enhancements to the stability and solubility, as well as diminishing undesirable properties of the original parent drug. Flurbiprofen is a hydrophobic crystalline drug, commonly known to have poor adhesion and mechanical properties. Factors indicative of high propensity for tribo-charging as studied by Afzal et.al. [95] Various counter ions are available to form a range of salts. A study by Šupuk *et al.* states that the type of counter ion used has a significant impact on the particle morphology hence influencing the work function of the material, and in turn effecting the electrostatic behaviour of the material [56]. The salt form results in an altering of the crystallinity which has shown to greatly transform the electrostatic properties as a result of the different arrangement of atoms. Different counter ions present a range of results for tribo-electrification when used to form a

salt of the same parent drug, highlighting the importance of counter ion selection for the influence on electrostatic behaviour.

2.9.2.2.5 Surface Contamination

Eilbeck *et al* investigated the effect of contamination of pharmaceutical equipment on powder tribo-electrification with a stainless steel surface. The results show that when the powder was fed into the cyclone apparatus, after the run the equipment was not cleaned, this caused for an increase in the powder adhesion to the walls after each run, the contamination lead to a decrease in charge at different gas velocities, this was more evident for the smaller size fractions (figure 2.8 - left)[96]. Cleaning methods were investigated to determine the effect on material charging. One technique included washing with 40°C water and rinsing with acetone to flash dry at ambient conditions. The alternate method involved cleaning the cyclone within an ultrasonic bath containing dilute ammonia solution and drying under a vacuum. The results (figure 2.8 - right) display that there is an increase in charge when the cyclone was cleaned using the ultrasonic bath technique when compared to the acetone method, the level of charging was greater than when the apparatus was not cleaned between the runs [96].

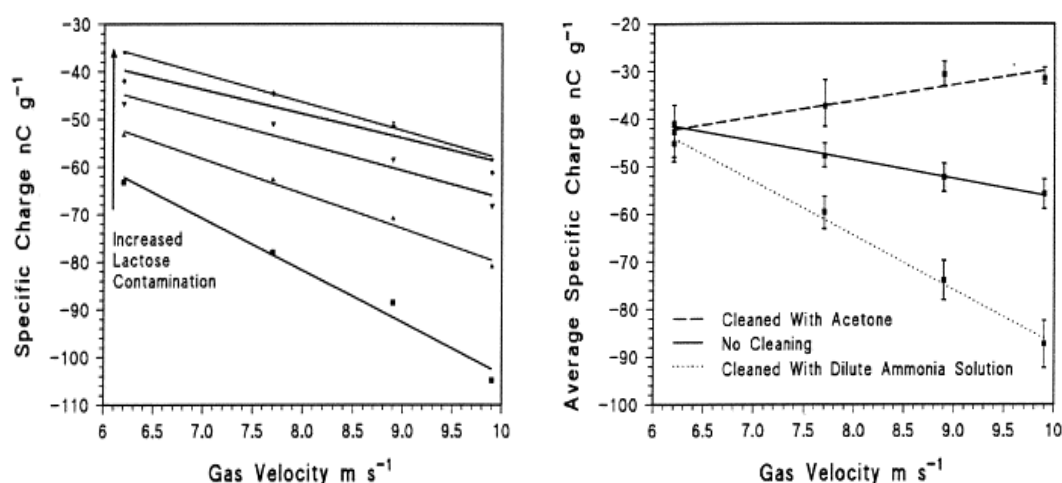


Figure 2.8 Left: The effect of contamination of lactose particles on charge of lactose size fractions, 90-125μm following tribo-electrification. Right: The effect of surface cleaning upon charge for size fractions 125-150μm following tribo-electrification. [95]

It is believed that the contamination is responsible for the reduced charge due to a decrease in powder-steel interactions [93].

2.9.2.3 Environmental Conditions

2.9.2.3.1 Temperature or Humidity

The surface chemistry of a pharmaceutical powder is affected by relative humidity (RH) as water adsorption in powders impacts upon the capillary forces, [97] as the electrical conductivity of a particles surface is influenced by RH, moisture levels may affect the charging process of pharmaceutical powders; however this is a controversial area as there is disagreement within the literature. Rowley and Machin (2003) undertook an experiment considering relative humidity, the conclusion drawn stated that as the relative humidity increased, the level of charge decreased. Two charging mechanisms are used to explain the results, firstly the surface conductivity of the powder is increased due to the increase in adsorbed water resulting in a backflow of charge, and secondly the higher moisture content within the air increases the conductivity of the air hence enforcing gas discharge. [98] The impact of humidity upon the electrostatic charge of pharmaceutical powders is not fully understood, as a correlation is not present. [99] Although little work has been done to determine the effects of temperature on tribo-electrification of a pharmaceutical powder. Ausburger and Hoag state that the temperature may influence the cohesive properties of a material, whereby heating may cause softening of the particles increasing the cohesive tendencies, resulting in the formation of agglomerates or even sticking to the surface of the processing equipment reducing flow. [100]

2.9.2.4 Physical Parameters

2.9.2.4.1 Frequency

When a particle is induced to a horizontal motion, the degree of charge generated upon the particles is dependent upon the frequency and shaking time. Upon shaking, a particle reaches a maximum charge, known as the saturated charge level (SCL). [101] Increasing the frequency or time does not influence the saturated charge of a particle. The time taken to reach the SCL is related to the factors mentioned above. Increasing the shaking frequency shows a decrease

in shaking time. This is as expected due to a rise in the frequency resulting in an increase in particle-particle and particle-wall collisions, also reducing the charge relaxation time between impacts. [101] As well as increasing the particle impact velocity, forming a larger surface area for the charge transfer process.

2.9.2.4.2 Number of Collisions

The effect of the number of collisions on tribo-electrification is closely linked to the frequency. Increasing the frequency increases the number of collisions each particle is induced to in a given time. For each particle contact, charge transfer can occur hence influencing the charge behaviour of a sample. Also effecting probability of particle to particle and particle to wall collisions hence effecting the charging tendency of a particle. [102]

2.9.2.5 Charge to Mass Measurement

The degree of tribo-electrification can be quantified by determining the charge to mass ratio of the powder. The most popular device for charge measurement is the Faraday cup connected to an electrometer (figure 2.9). [71, 103] There is a commercially available Faraday cup, for the purpose of these experiments a self-adapted cup modified by Šupuk is used.

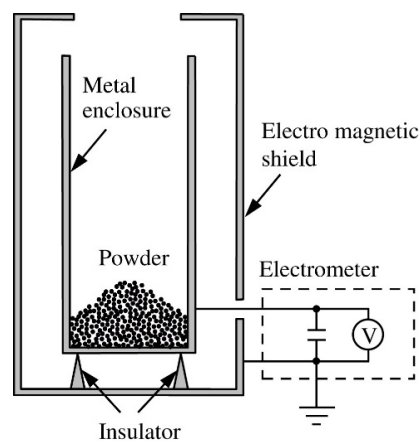


Figure 2.9 Faraday Cup Schematic [101]

The principle of operation for a Faraday cup electrometer, involves the charge inducing an image on the conducting surface. A Faraday cup is composed of two conducting cups with an opening at the top via which the powder under investigation is poured. An insulating spacer is used to isolate the inner cup from the outer. The role of the outer cup is to prevent external

charges from being measured, which may potentially affect the net charge value of the powder of interest. When a negatively charged particle enters the cup, it results in an induced positive charge distribution over the internal surface of the inner cup and a negative charge over the outer surface, providing a potential difference which can be quantified. [104]

The potential, $V = q/C$ is generated due to the capacitance (C) between the two cups. This is generated via the electrometer which provides a charge (Q) value in nanocoulombs (nC). To obtain the mass to charge ratio (nC/g), the net charge value is divided by mass of the sample used for the testing. As temperature and humidity may influence the charge levels. These need to be recorded prior to testing.

2.10 Conclusions

It is evident that salt formation is a well-known technique utilised for improving the physicochemical properties of pharmaceutical APIs; such as solubility, stability, dissolution rate as well as hygroscopicity. Approximately 50% of the drugs approvals are in a salt form, although there are a number of advantages and disadvantages to salification, some pros include improved thermal stability, reduced hygroscopicity, improved drug efficacy and improved compactibility. The cons consist of, reduced percentage of active ingredient in the final formulation, increased formation of polymorphs and hydrates resulting in greater variability of pharmaceutical properties, corrosiveness of the salt; potentially resulting in tableting complications as well as an additional step in synthesis, resulting in increased manufacturing time and costs.

Tribo-electrification is regarded as an electron transfer occurring between contacting materials resulting in an electron exchange. The driving force behind the charge transfer is the work function (the minimum thermodynamic work required to remove an electron to infinity from the surface of a solid). A number of factors which effect the measurement of charge-to-mass ratio include: particle size, shape, surface material, humidity, and contaminants. These have to be considered when characterising tribo- electrification.

This review revealed that there is a lack of information regarding the influence of salt formation on physicochemical and electrostatic properties of carboxylic acid drugs. Work

undertaken by Šupuk *et al* investigates the influence of salt formation on electrostatic properties of flurbiprofen salts [56], utilising an assortment of counterions. However this study investigates the salts from a series of counterions with a series of similar structured carboxylic acid parent compounds, to explore the relationships between physicochemical and triboelectric charging properties of the resulting material in comparison to the parent compounds. With an aim to develop a greater understanding of the effects of parent drug and counterion selection, upon the physicochemical properties and triboelectrification propensity of the resulting material.

3 Materials and Methods

3.1 Materials

3.1.1 Model Drugs

Three chemically similar molecules were selected as possible salt formers for this study. The drugs flurbiprofen, felbinac and biphenyl-4-carboxylic acid were selected. Felbinac and biphenyl-4-carboxylic acid were chosen due to similarities in structure to flurbiprofen, as well as this; all three are readily available in their raw form.

3.1.2 Carboxylic Acid Drugs

Carboxylic acids are weak acids and commonly have a dissociation constant, pK_a of approximately 4.5. Carboxylic acids make ideal salt formers, the functional group comprises of a carbon double bonded to an oxygen as well as an oxygen attached to a hydrogen (figure 3.1)

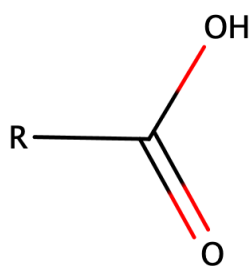


Figure 3.1 Structure of a carboxylic acid

3.1.2.1 Flurbiprofen

Flurbiprofen is a propionic acid derivative, used as a nonsteroidal anti-inflammatory agent with analgesic and antipyretic activity. It is practically insoluble in water and freely soluble in chloroform, ether and acetone and soluble in acetonitrile. Its chemical name is 2-(2-fluorobiphenyl-4-yl) propanoic acid, and it has a molecular weight of 244.261. The structure of flurbiprofen is shown in figure 3.2.

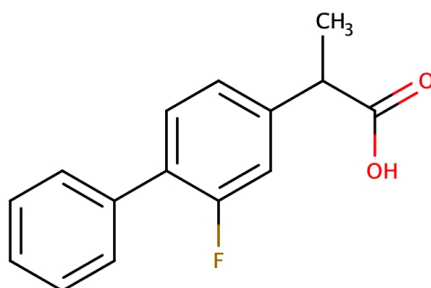


Figure 3.2 Chemical structure of Flurbiprofen

3.1.2.2 Felbinac

Felbinac is also a nonsteroidal anti-inflammatory agent with analgesic and antipyretic activity. It is poorly soluble in water and slightly soluble in methanol, it has a molecular mass of 212.244. The structure of felbinac is shown in figure 3.3.

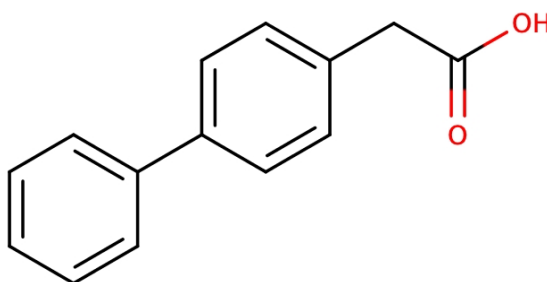


Figure 3.3 Chemical structure of Felbinac

3.1.2.3 Biphenyl-4-Carboxylic Acid

Biphenyl-4-carboxylic acid is similar in structure to felbinac and flurbiprofen. It is soluble in ethanol, ether, benzene, hot methanol, and partly soluble in water. It has a molecular mass of 198.22. It's structure is shown in figure 3.4.

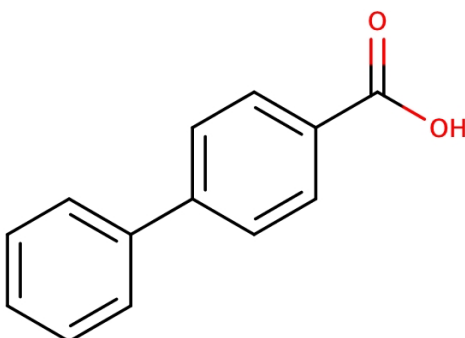


Figure 3.4 Chemical structure of Biphenyl-4-carboxylic acid

3.2 Counterion Selection

The specific salts of API's are often formed to overcome undesirable properties of the parent compound. The suitability of the candidate for salt selection is determined by the physical and chemical properties of the active ingredient. Different counterions may be utilised to overcome any shortcomings of the parent drug, conventional counterions such as Potassium, Sodium and Calcium have been the popular choice to improve solubility and dissolution properties.

3.2.1 Cyclic Compounds

A series of cyclic counterions were selected with increasing carbon atom in their cyclic structure. The effect of the chain length on salt formation and physicochemical properties was investigated using cyclopropylamine (C3), cyclobutylamine (C4) and cyclopentylamine (C5) (figure 3.5). The compounds are liquid at room temperature and insoluble in water.

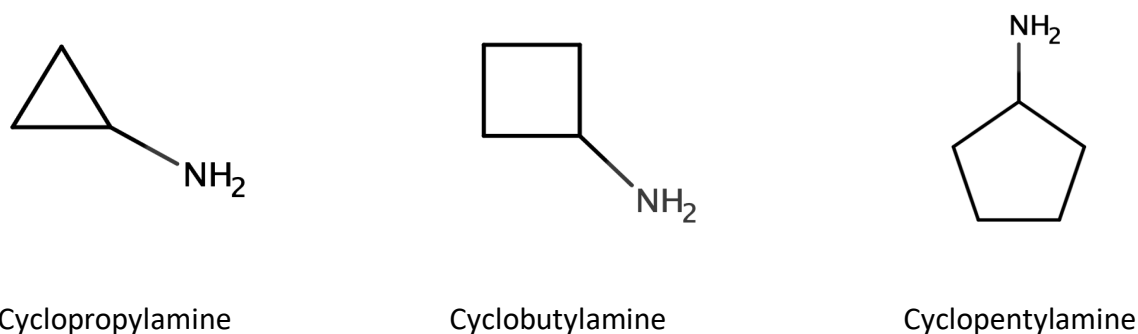


Figure 3.5 Structures of Selected Counterions

Salts were prepared using flurbiprofen, felbinac and biphenyl-4-carboxylic acid. Flurbiprofen was obtained from Discovery Fine Chemicals (Dorset, United Kingdom). Felbinac was purchased from Tokyo Chemical Industry (Oxford, United Kingdom), and biphenyl-4-carboxylic acid was obtained from Alfa Aesar (Lancashire, United Kingdom). Cyclopropylamine and cyclopentylamine were purchased from Sigma Aldrich (Dorset, United Kingdom), while cyclobutylamine was obtained from Fluorochem (Derbyshire United Kingdom). All materials purchased were of pharmaceutical grade. HPLC grade Acetonitrile and methanol were supplied by Fisher Scientific (Loughborough, United Kingdom) as well as absolute ethanol, dichloromethane, diethyl ether and acetonitrile.

3.3 Methods

3.3.1 Salt Preparation

Flurbiprofen cyclopropylamine, flurbiprofen cyclobutylamine and flurbiprofen cyclopentylamine salts were prepared by combining equimolar ratios (0.01 mol) of flurbiprofen dissolved in 50 mL acetonitrile, and the counterion base mixed in 50 mL of acetonitrile (ACN) [56]. The solutions were combined whilst stirring (250 rpm) and a precipitate formed immediately. The precipitate was recovered via vacuum filtration; then oven dried under vacuum at 300 mbar and 40 °C for four hours. Carboxylic acids are able to form salts with bases to form carboxylate salts, in which the hydrogen on hydroxyl group (-OH) of the carboxylic acid is replaced with a cation. In the case of amines, they contain a nitrogen, which accepts a hydrogen ion to the lone pair on the nitrogen and forms a positive ion. This is attracted to the negative charge of the carboxyl group.

The salt was then recrystallised from methanol solution through the slow evaporation of the solvent at room temperature (18-22 °C). The resulting material was dried and stored in a sealed container until use.

The felbinac cyclopropylamine, felbinac cyclobutylamine and felbinac cyclopentylamine salts were prepared by combining equimolar ratios (0.01 mol) of felbinac dissolved in 250 mL acetonitrile and the counterion base mixed in 50 mL of ACN. The solutions were combined whilst stirring at 250 rpm and a precipitate formed immediately, which was recovered via vacuum filtration, then oven dried under vacuum at 300 mbar and 40 °C for four hours. The salt was then recrystallised from methanol solution through the slow evaporation of the solvent at room temperature (18-22 °C). The resulting material was dried and stored in a sealed container until use.

The biphenyl-4-carboxylic acid cyclobutylamine and biphenyl-4-carboxylic acid cyclopentylamine salts were prepared by combining equimolar ratios (0.01 mol) of biphenyl-4-carboxylic acid dissolved in 500 mL acetonitrile with the aid of heating to approximately 50 °C and the counterion base mixed in 50 mL of ACN. The solutions were combined whilst stirring at 250 rpm. The precipitate formed immediately, which was recovered via vacuum filtration, then oven dried under vacuum at 300 mbar and 40 °C for four hours. The salts were then recrystallised from methanol solution through the evaporation of the solvent at room temperature (18-22 °C). The resulting material was dried and stored in a sealed container

until use. For the biphenyl-4-carboxylic acid cyclopropylamine salt, no precipitate formed upon addition of counterion, upon cooling a precipitation formed, consisting of a mixture of the salt and pure compound, hence was omitted from further studies.

3.3.2 Salt Recrystallisation

To determine the effect of solvent selection upon the crystal structure and properties of the final product, a range of solvents were selected and different ratios were utilised to investigate the effects of these changes upon the crystal structure and subsequent thermal properties (Chapter 5). The cyclo-propylamine salts were recrystallized from absolute ethanol, diethyl-ether, acetonitrile, and dichloromethane. A 400mg quantity of equimolar salt was dissolved in 25ml solvent. The solution was then heated to 50°C, and the salt was fully soluble in solution for all solvents except diethyl-ether. The solution was then removed from the heat and filtered using a syringe and a filter (17mm, 0.45µm). Solutions were placed in a cupboard at room temperature to allow crystals to form by slow solvent evaporation, the resulting material was dried and stored in a sealed container until use.

The samples named as 1:2 and 2:1 recrystallised, were produced from the salts formed from varying ratios. In the case of the 1:2 recrystallised salt, 0.01 mol of flurbiprofen was combined with 0.02 mol cyclopropylamine in acetonitrile and the precipitate was then filtered. The 2:1 recrystallised was formed using 0.02 mol of flurbiprofen combined with 0.01 mol cyclopropylamine in acetonitrile. The resulting material was then recrystallised using the same solvents and methodology as the equimolar salt recrystallisation.

For the salts labelled 1:2 and 2:1, they were formed by recrystallising the material obtained in section 3.3.1, by utilising the (1:1) equimolar salt, however for the 1:2 salt; during the recrystallisation process, an extra quantity of 0.01 mol of cyclo-propylamine was added to the recrystallisation solvent, therefore resulting in a 1 part flurbiprofen to a 2 part cyclopropylamine mixture. The 2:1 ratio involved the addition of 0.01 mol of flurbiprofen to the solvent containing the equimolar salt produced in section 3.3.1. Hence these ratios were adjusted post salt formation by utilising the equimolar salt and adding one part of either component, in comparison to the 1:2 and 2:1 recrystallised which were manufactured using the specified ratios of raw material.

3.3.3 Salt Cocrystal formation

The salt cocrystal (CC) was prepared by adding 1 g of flurbiprofen cyclopropylamine salt (Section 3.3.1) to 5 mL of methanol. The salt-containing solution was heated to 50 °C, then the beaker was placed in ice for 30 s. The solution was then passed through a 17 mm diameter, 0.45 µm pore size syringe filter. The beaker was covered with parafilm in which five pinholes were pierced. This was then left at room temperature (18-22 °C) to allow for crystal growth to occur through slow solvent evaporation, the resulting crystal was obtained from the solution using tweezers.

3.3.4 Single crystal X-ray diffractometry

Single-crystal X-ray diffraction data on the flurbiprofen, flurbiprofen cyclopropylammonium salt and the flurbiprofen cyclopropylamine 2:1 salt cocrystal were collected at the National Crystallography Service, Southampton, UK. Diffraction maxima with MoK α (λ = 0.71073 Å) radiation produced by a rotating anode generator were collected with an area detector to a maximum ϑ of approximately 27.5°. Additional single-crystal X-ray diffraction data on the flurbiprofen cyclopropylamine 2:1 salt cocrystal were collected on a Bruker D8 Venture diffractometer equipped with a graphite monochromated MoK α (λ = 0.71073 Å) radiation source and a cold stream of nitrogen gas.

Multi-scan absorption corrections were applied with SADABS [105]. Structures were solved by direct methods with SHELXS, revealing all non-hydrogen atoms. Non-hydrogen atom positions and anisotropic displacement parameters were refined with SHELXL2014/7 [106]. Hydrogen atoms were assumed to ride on their attached atom, primary ammonium and methyl groups being allowed to rotate. Crystallographic Information Files for the cyclopropylammonium salt and the flurbiprofen cyclopropylamine salt cocrystal have been deposited with the Cambridge Crystallographic Data Centre.

3.3.5 Salt formation confirmation

3.3.5.1 Fourier Transform Infrared Spectroscopy (FTIR)

FTIR was used to confirm the formation of a carboxylate salt from the carboxylic acid parent compound. It is a technique used to obtain an infrared spectrum, relying on the concept of most molecules absorb light in the infra-red region of the electromagnetic spectrum. The

resultant spectrum from the vibration frequencies denote the existence of specific functional groups and chemical bonds, these functional groups present characteristic vibrational frequencies in the infra-red region.

The carboxyl group is known for its two characteristic infrared stretch absorptions, carboxylic acids are present as hydrogen bonded dimers in condensed phases, producing a very strong O-H stretch usually located between 2500-3300 cm⁻¹. The carbonyl stretching dimer is present at around 1690-1750 cm⁻¹, upon deprotonation the carboxylate asymmetric band is produced at a lower energy, 1540-1650 cm⁻¹. In the case of the carboxylate salt, the stretching is found at a lower wavelength due to the emergence of resonance hence resulting in electron delocalisation and producing a greater single bond characterisation.

3.3.5.1.1 Equipment/ Method

A Nicolet 380 FT-IR was used to analyse the samples to confirm salt formation. Omnic spectroscopic software was used to interpret the results. The powder (approx. 5–10 mg) was placed on an Attenuated Total Reflection (ATR) plate and compressed and the sample was then analysed using FT-IR spectroscopy. Salt confirmation was analysed by measuring the transmittance of infrared wavelengths of the electromagnetic spectrum of the sample in the range of 400–4000 cm⁻¹.

3.3.5.2 Powder X-ray diffraction (PXRD)

Powder X-ray diffraction (PXRD) is a quick analytical techniques used in the identification of degree in crystallinity or amorphicity of materials. It is based on interference of a monochromatic X-ray and sample with some degree of crystallinity. A cathode ray tube is used to generate the radiation, concentrated to form a collimated beam towards the sample. The interface between the rays and the sample produces constructive interference (and a diffracted ray) when conditions satisfy Bragg's Law (Equation 3.1).

$$n\lambda = 2d \sin \theta \quad \text{Equation 3.1}$$

where:

λ is the wavelength of the x-ray,

d is the spacing of the crystal layers,

θ is the incident angle (the angle between the scatter plane and incident ray), and

n is an integer

The law reports the diffraction angle (θ) and the lattice spacing to the wavelength (λ) of the radiation in the sample. Producing an X-ray diffraction pattern which in turn is like a 'fingerprint' for the crystals present in the sample for analysis, allowing for comparison to reference standard in order to identify the crystal form of the sample. PXRD is instrumental in determining the crystallinity of a material, presence of polymorphs and the sample purity.

3.3.5.2.1 Equipment/ Method

PXRD patterns were obtained using a Bruker D2 Phaser XRD diffractometer, the Diffrac.commander software was used to set up the experiment. A silicon low background holder was used to load the sample. The samples were scanned from 5° to 60° 2 θ at 11°/min, the experiments were undertaken at room temperature (22-25°C).

3.3.5.3 Nuclear Magnetic Resonance (NMR)

NMR analysis was used to confirm salt formation as well as the expected proton count of a 1:1 salt. NMR works on the basis of many nuclei containing spin and all nuclei possessing an electrical charge, when an external magnetic field is applied, an energy transfer is possible from the base energy level to a higher energy level. The energy transfer occurs at a wavelength that corresponds to radio frequencies, when the spin returns back to its base level, this results in emitting of energy at the same frequency. This signal is processed in order to produce an NMR spectrum.

3.3.5.3.1 Equipment/ Method

The ^1H NMR were obtained using a Bruker Ascend 400 Mhz spectrometer. A small quantity of drug/salt sample was dissolved in dimethyl sulfoxide (DMSO) and 16 scans were performed.

3.3.6 Thermal Methods

3.3.6.1 Thermogravimetric analysis (TGA)

Thermogravimetric (TG) is a branch of thermal analysis techniques working on the principle of examining the mass change as a function of temperature for a given sample, primarily used in determining the composition of a material and to predict its thermal stability. In pharmaceutical industry, it is used to characterise hydrates, and to determine decomposition, vaporisation or sublimation temperatures. TGA is useful in identifying solvates or hydrates which occurs as a result of crystallisation solvent molecule inclusion within the crystal lattice. This can have an effect on the physical aspect of the drug, including, solubility, stability, crystallinity and hygroscopicity. Upon heating, the solvent is usually released at a set temperature, allowing for a stoichiometric weight loss of the solvent to be calculated.

3.3.6.1.1 Equipment/ Method

Thermogravimetric analysis (TGA) was performed using Mettler Toledo TGA. A Mettler AT261 balance was used to weigh the sample mass.

The TGA was calibrated prior to use to ensure accuracy of results. Samples between 5 and 10 mg were placed inside a 40 µl aluminium crucible (Mettler Toledo) and a lid was pressed in place. The experiment was run over the temperature range 25–250 °C with nitrogen as a purge gas flowing at 50 ml/min.

Data analysis was undertaken using the STARe Software.

3.3.6.2 Differential Scanning Calorimetry (DSC)

Differential scanning calorimetry (DSC) is a thermal analysis technique used to measure the difference in heat required to increase the temperature of a sample against a reference as a function of temperature. In a heat flux DSC; an empty reference pan and sample pan are placed on a thermoelectric disc within a furnace and the furnace is heated using a linear heating rate. Due to the heat capacity of the sample, there is a temperature difference between the sample and reference pan, this difference is measured by thermocouples. The heat flow is determined by the thermal counterpart of Ohms law (Equation 3.2).

$$q = \Delta T/R \quad \text{Equation 3.2}$$

Where q is the heat flow of the sample

ΔT is the temperature difference between the reference pan and sample pan.

R is the resistance of the thermoelectric disc.

There are various applications for DSC, these include melting point, percentage crystallinity, glass transitions, solid-solid transitions, dehydration and sublimation. One other application is the ability to measure degree of crystallisation of a material, in pharmaceuticals, formulation of crystalline drugs may result in some material forming an amorphous form during processing, in turn effecting the physical and chemical stability of the dosage form. DSC is instrumental as it provides the quantity of energy released upon crystallisation, which is related to lattice energy of the material, hence DSC can be utilised to obtain the percentage crystallinity of a pharmaceutical compound.

3.3.6.2.1 Equipment/Method

Differential scanning calorimetry (DSC) was performed using Mettler Toledo DSC. The equipment was calibrated for temperature and heat flow using indium as a standard. A Mettler AT261 balance was used to weigh the sample mass.

The DSC was calibrated prior to use to ensure accuracy of results. Samples were weighed on a balance, approximately 5 – 10 mg of sample was placed directly into a pre-tared 40 μ l aluminium crucible (Mettler Toledo) with a vented lid, which was pressed in place. The experiment was carried out at a temperature range of 25–250 °C at 10 °C min⁻¹ heating rate, under a nitrogen gas purge. All experiments were performed in triplicate.

Data analysis was undertaken using the STARe Software.

3.3.7 Dissolution and solubility studies

3.3.7.1 Solubility

For a drug to form a suitable salt; the aqueous solubility needs to be considered, solubility is a function of pH and this can be used to determine the appropriate counterions, as well as understand how easily the salt may dissociate to the free acid or base form. Additionally, how

a drug may behave during dissolution in various GI pH conditions, also the influence of common ions upon the solubility and dissolution rate of a drug.

When a drug salt is added to water, it can result in an acidic, basic or neutral environment. The interaction between the ions of the water and the ions of the drug salt is known as hydrolysis.

For this research, forming salts from weak acids and moderate bases, the salts ionise in aqueous solution, resulting in a basic solution by a hydrolysis reaction.

Acid strength is generally explained using a pK_a value; it is a negative logarithmic of K_a and has important implications in successful salt formation. It is usually the value above which a weak acid gets ionised and below which a weak base is ionised.

Figure 3.6 depicts the schematic diagram for the pH interrelationship between the salt form and its free acid, this can be expressed as two separate curves. One illustrates the free acid as an equilibrium species at a pH below pH_{max} , the other represents the salt at a pH greater than the pH_{max} . The free acid can only be converted to the salt form, if the pH is raised above pH_{max} , this can be achieved by adding extra counterion or sufficient amount of alkali. To form a salt of a weak base, if the counterion is weak; the pH cannot achieve pH_{max} then salt formation will not occur [31].

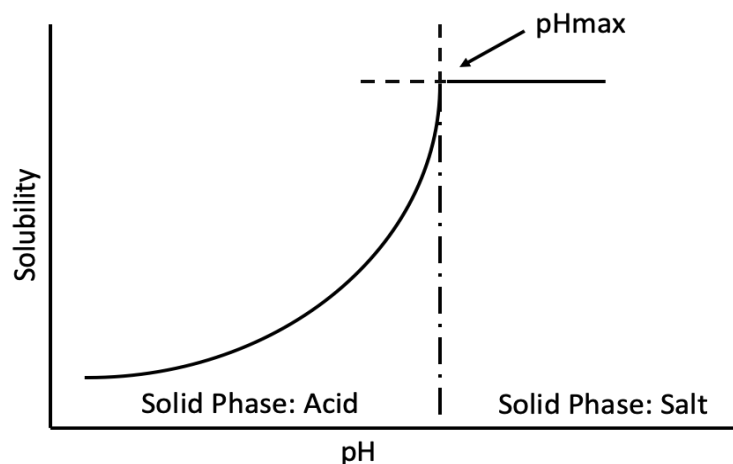


Figure 3.6 pH solubility profile of a free acid and its salt. Adapted from [31]

Due to these interdependencies between the pH, magnitude of ionization and successful salt formation, it is a general rule of thumb that for salt formation to occur is to achieve a difference of at least 2-3 units between the pK_a of the drug and the counterion. This ensures that the proton transfer is more energetically favourable. When a difference in 2-3 units is

not achieved, a complex may form but result in rapid dissociation in an aqueous environment. Nonetheless simply selecting a counterion with a 2 unit difference does not guarantee salt formation. Although pH-dependant solubility screening is a criterion for salt formation, the salt formation process is complex and reliant on a number of factors which can affect nucleation and crystallisation of the salt form.

3.3.7.1.1 Equipment/ Method

A GLS Aqua 12 plus shaking water bath was used at a linear shaking rate of 100 strokes/min. Saturated aqueous solubilities were determined at 37 °C, and excess powder was added to 10 ml of water that was agitated for 48 hours. The experiment was performed in triplicate and 5 ml of solution was extracted with a syringe and the pH measured. The sample was filtered through a 17mm, 0.45 µm PTFE syringe filter and diluted with water. Samples were analysed by HPLC (Section 2.3.2).

3.3.7.2 High Pressure Liquid Chromatography (HPLC)

HPLC was used to identify and quantify the compounds for the study. HPLC is a form of column chromatography used to pump a sample mixture in a solvent mobile phase under a high pressure through a packing material within a column, known as the stationary phase. The sample retention time is dependent upon its interactions with the stationary phase, the sample molecules or even the solvent used. The interaction between the mobile phase and stationary phase is at a different rate due to the polarities of the analytes. Whereby analytes with the least amount of interaction with the stationary phase, in turn more interaction with the mobile phase will exit the column at a quicker rate.

Retention time is the duration a compound may take to reach the detector from the time it was injected, there are a number of factors affecting retention time, and these include the compound, column, flow rate, column pressure and temperature.

Once the compound has reached the detector, Ultra-violet (UV) absorption is a very common technique used to detect the substance, due to compounds absorbing light at different wavelengths and the quantity of light absorbed is proportional to the amount of sample present.

3.3.7.2.1 Equipment/ Method

A Shimadzu LC-20AT series chromatographic system connected to a SIL-20A auto sampler and a SPD-20AV UV Vis detector was used with a XBridge C₁₈ (250 x 4.6 mm x 5 µm) column.

The HPLC was controlled by the Shimadzu LCSolution software.

Sample dilutions for the calibration were made using a solvent mixture comprising of 65:35 acetonitrile: water for all compounds used. Linear regression analysis was performed on a plot of the concentration against peak area and the equation of the line was used to calculate the concentration of the sample response of the unknown. The standards produced were serial dilutions of a stock solution over a range of 0.001 – 15mg/ml. The chromatographic conditions for the 3 APIs were the same with an injection volume of 1 µl, mobile phase comprising of 65:35 Acetonitrile: water, flow rate of 1 ml/min and the XBridge C₁₈ Column. The wavelength however did differ, for flurbiprofen 247 nm was used, for felbinac 254 nm and biphenyl-4-carboxylic acid 264 nm.

The main things to consider when producing a calibration curve is the limit of quantification (LOQ) which is the concentration at which the analyte can be quantitated with a linear response, and the limit of detection (LOD) is the smallest concentration of analyte that can be detected with no guarantee about the bias or imprecision of the result by an assay. They can be calculated using the residual standard deviation of the regression line (SD) and the slope of the calibration curve (S), using the following equations (Equation 3.3/3.4).

$$LOQ = \frac{10SD}{S} \quad \text{Equation 3.3}$$

Whereas

$$LOD = \frac{3SD}{S} \quad \text{Equation 3.4}$$

3.3.7.3 Intrinsic Dissolution Rate (IDR)

Intrinsic dissolution is defined as the dissolution rate of a substance under constant surface area conditions whereby only one face of the compact is subjected to the dissolution media.

Several theories to explain the dissolution of drugs have been proposed, some of the important ones include;

- Film theory / Diffusion layer model
- Danckwert's model / Penetration or Surface renewal theory
- Interfacial barrier model / Double barrier or Limited solvation theory

The diffusion layer model [107] figure 3.7 is the simplest and most common theory to describe dissolution. It consists of a two-step process, firstly; solution of solid to form a stagnant film or diffusive layer which is saturated with the drug, this step is usually rapid. Secondly, the diffusion of the soluble solute from the stagnant layer to the bulk of the solution, this step is usually a lot slower so is considered the rate determining step.

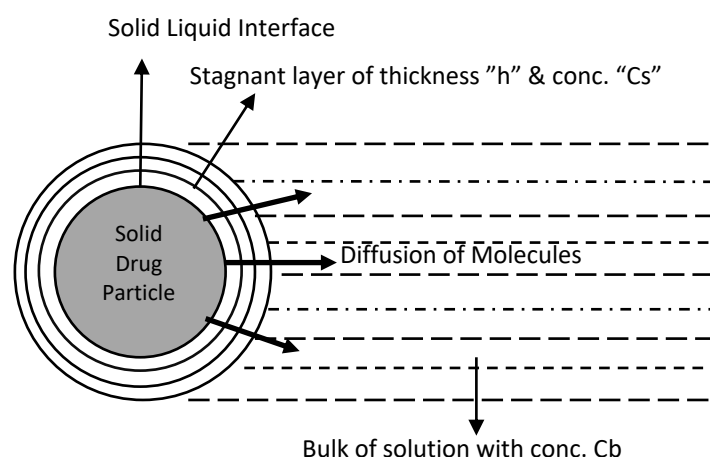


*Figure 3.7 Diffusion layer model for drug dissolution.
Adapted from [93]*

Danckwert's model (figure 3.8) proposes the formation of packets or eddies that are present in the agitated fluid which interact with the solid/liquid interface and absorb the solute by diffusion and carry the solute into the bulk of the solution. As these packets are replaced

continuously by new ones and expose a new solid surface, the theory is called 'surface renewal theory'

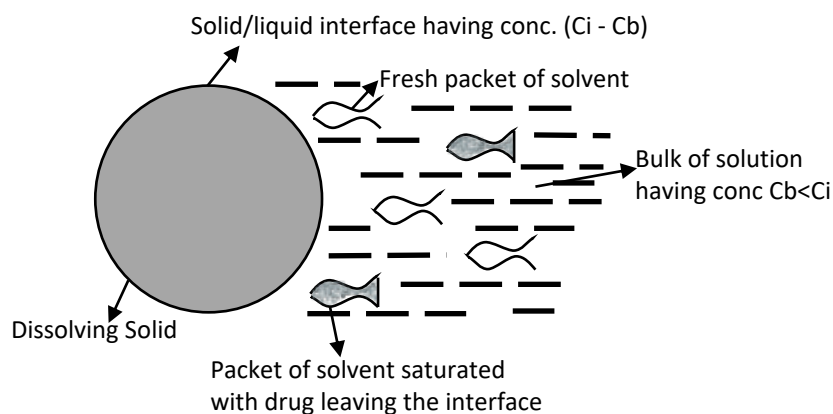


Figure 3.8 Danckwert's Model. Adapted from [93]

These two theories are based on two assumptions; firstly, the rate determining step controls dissolution of the mass transport, and secondly the solid-solution equilibrium is achieved at the solid/liquid interface.

The interfacial barrier model however, states that an intermediate concentration can exist at the interface as a result of solvation mechanism and is a function of solubility opposed to diffusion. When taking a crystal into consideration, each face will possess a different interfacial barrier.

Commercially available intrinsic dissolution apparatus consist of a die in which a cylindrical compact can be prepared in situ, with one face left exposed for dissolution to occur (figure 3.9).

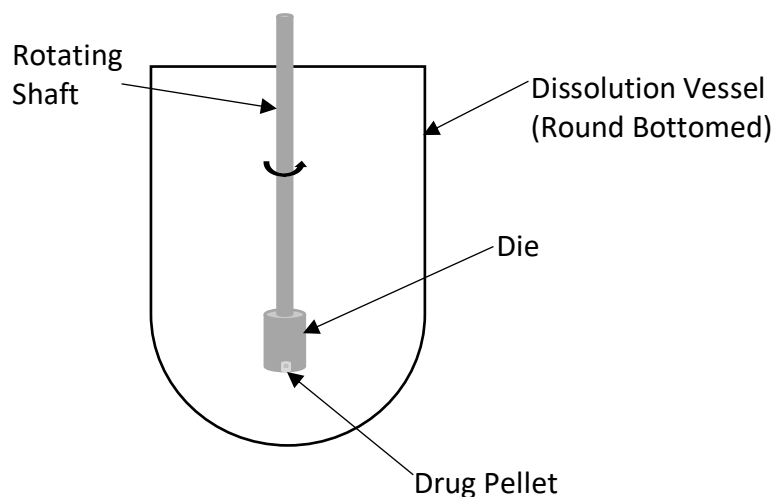


Figure 3.9 Schematic of IDR equipment

3.3.7.3.1 Equipment/ Method

A PharmaTest DT70 dissolution test equipment with 1L round bottomed vessels and IDR holders was used, auto sampling was carried out using a peristaltic pump and the concentration of drug was determined using a Unicam UV/Vis spectrophotometer (UV2). Using a stainless-steel cylindrical die and a press, each powder was compressed into a pellet (4.5 mm in diameter) against a stainless-steel support plate. The dissolution equipment was controlled using the IDIS EE software.

Sodium phosphate tribasic was obtained from Sigma-Aldrich (Dorset, United Kingdom) and hydrochloric acid was purchased from Fisher Scientific (Loughborough, United Kingdom). pH 6.8 phosphate buffer was prepared by mixing 0.1 N HCL with 0.20 M sodium phosphate tribasic (3:1) and adjusting if necessary to produce a solution of pH 6.8 ± 0.05 .

The compact was made in situ using a cylindrical die and a press under a pressure of 2 tonne with a 1 min dwell time, at least 3 replicates were made of each compound. The die assembly was attached to the rotating shaft and was immersed in 900 ml of phosphate buffer at pH 6.8 and at 37 ± 0.5 °C with a rotation speed of 50 rpm. Samples were withdrawn at specified time point (1.5 min intervals) using a peristaltic pump and the concentration of the compound was detected using a Unicam UV/Vis spectrophotometer (UV2). Intrinsic dissolution rate ($n=3$) was calculated using the slope of the initial linear region of the dissolution curve and the surface area of pellet exposed to the dissolution solution.

3.3.8 Powder properties

3.3.8.1 Fractionization of API salts

To characterise bulk materials consisting of different forms and sizes, knowledge of the size distribution is vital. The particle size distribution, i.e. the quantity of particles of varying sizes can play a role in the physical and chemical properties of a material, these include the solubility, tribo-electrification propensity and flowability. In many industries, sieve analysis is the standard for controlling size distribution of granules and powders.

To ensure a high degree of reliability and reproducibility, the sieve shakers and sieves have to adhere to the guidelines of national and international standards, ensuring that the equipment is calibrated.

There are a number of sieving methods for sieve analysis. The sample is subjected to vertical or horizontal movements when subjected to the sieving process. The probability of a particle passing through the mesh is determined by a number of factors, such as the number of encounters between the particle and the mesh, the particle orientation during the encounters and the ratio of particle size to the sieve mesh size.

During vibratory sieving, the sample is projected upwards due to the vibrations and rotate freely, then descent down statistically orientated due to the gravitational forces acting upon the particles. Due to this, the sample is spread evenly across the sieve area.

Horizontal sieving induces a sieve to move in horizontal circles in a plane, however due to the single plane motion, limited particles change their orientation on the sieve.

A tap sieve shaker combines the circular motion movement with a vertical motion imposed by a tapping impulse. However this induces a greater impulse upon the material resulting in lighter materials such as powders to remain suspended in the air, resulting in a lower fine particle fraction.

Another method is air jet sieving, which uses a single sieve which remains stationary throughout the process, the material itself is moved on the sieve surface by a rotating jet of air a vacuum is generated inside the sieve chamber, thus the finer materials are passed through the sieve mesh and collected.

3.3.8.1.1 Equipment/ Method

A mechanical sieve shaker (Endecotts UK) was used with Endecotts sieves consisting of the following sieve fraction, 250-300 μm (Chapter 5), 150-250 μm (Chapter 6) and a range of sieve fractions for chapter 7 are as follows, 125-150 μm , 150-180 μm , 180-250 μm , 250-300 μm , 300-355 μm , 355-425 μm , 425-500 μm and 500-600 μm for the purpose of a controlled study. The particles were induced to mechanical sieving using a nested column of sieves, becoming progressively smaller in mesh size. A mass of the powder added was taken using OHAUS Pioneer PA2102 precision balance and the particles were subjected to the shaking motion till a consistent mass was achieved. The sieve fractions were stored at ambient temperature (18-25 °C) and humidity (RH 33%-41%) before any further investigations.

3.3.8.2 Scanning Electron Microscopy (SEM).

The fundamental principles of a SEM rely on accelerated electrons which possess a significant quantity of kinetic energy. This energy is dissipated due to the sample-electron interaction producing a range of signals as the incident electrons are decelerated in the sample. These signals include secondary electrons are responsible for producing SEM images, backscatter electrons and diffracted backscatter electrons are used to determine orientation of material, photons for elemental analysis, visible light and heat. The backscatter and secondary electrons are most commonly used to produce images of samples, whereby high energy backscattered electrons are instrumental in illustrating contrast in a sample, whereas the low energy secondary electrons provide the topography and morphology of the particle. X-ray generation is created by inelastic collisions of the incident beam electrons with the electrons in the orbitals of atoms in the sample, the process of the excited electron returning to a lower energy state produces an X-ray at a fixed wavelength relating to the difference in energy level of electrons in the different shells for a given sample. Due to a very narrow electron beam, SEM are capable of a having a large depth of field, resulting in 3-dimensional images, as well as the ability to provide a wide range of magnifications, from as low as X20 to more than X500,000.

3.3.8.2.1 Equipment/ Method

A Quorum SC7620 Sputter coater was used to coat the samples with an ultra-thin layer coating of gold/palladium (80:20) for 60 seconds. A FEI Quanta FEG 250 (Thermo Fisher UK) was used for image acquisition

A layer of sample was placed on carbon tape and the sample coated with gold/palladium, image acquisition was undertaken at varying magnifications under a vacuum.

3.3.8.3 Powder Compaction

The Heckel equation is one of the most useful equations for describing the compaction properties of pharmaceutical powders. As one of the most common routes of administration is the tablet form, as they are easy to manufacture, good patient compliance and accurate for dosing. However, there are many critical factors to the tableting process, which include flowability and compressibility. There have been a number of equations proposed for characterising the compression process, which include the Heckel equation; it has been widely used to relate a powder bed's relative density during the compression by applied pressure (Equation 3.5).

$$\ln\left(\frac{1}{1-D}\right) = kP + A \quad \text{Equation 3.5}$$

Where:

D is the relative density of the tablet, hence $(1 - D)$ is the porosity

P is the applied pressure

K is a constant

A is a constant

3.3.8.3.1 Equipment/ Method

Compaction characterization was performed using a Stylcam 100R compression replicator (Medelpharm, France) fitted with coupling plate 5 and an 11.28 mm diameter round, flat faced tooling. The die was hand filled with 400 mg of powder of the drug, salt or salt cocrystal and the pressure adjusted to achieve a target compact thickness (all in-die measurements corrected for machine and punch deformation by the software) and hence a

target solid fraction of 0.85. Data was generated at 5 rpm and ~ 49 ms dwell time using the direct cam profile. Yield pressure (MPa) at the target solid fraction was determined using the in-die Stylcam data to determine tablet relative density (D) and recorded applied pressure (P) from the Heckel equation. Elastic recovery was measured by calculating the % difference from the in-die thickness (corrected for machine deformation by the software) and the measured thickness with callipers out of die, immediately after ejection.

The Heckel parameter K was obtained by linear regression on the linear portion of the curve and its reciprocal, the mean yield pressure, was calculated.

The weight, thickness (CA17 micrometer, Mitutoyo, Japan) and hardness, i.e. crushing strength (HT1 hardness tester, Sotax, Switzerland) of compacts were measured immediately after ejection. Tensile strength of compacts was calculated from the thickness and hardness data (Equation 3.6)

$$\text{Tensile Strength} = \frac{2h}{\pi dt} \quad \text{Equation 3.6}$$

Where:

h is crushing strength (N)

d is tablet diameter (mm)

t is tablet thickness (mm).

Elastic recovery (%) was determined from the difference of the in-die thickness and the thickness immediately after ejection.

3.3.8.4 Schulze shear cell

Powder flow properties are extremely important to consider, as poor flow can result in complications including, flooding, flow obstructions, irregular flow and even segregation of material. Flow of bulk materials is required in order to determine the effects of flow agents or other excipients upon flow behaviour of a powder. A number of parameters influence the flow properties:-

- Particle shape
- Particle size

- Moisture
- Temperature
- Chemical composition of the particles

3.3.8.4.1 Equipment/ Method

A Ring Shear Tester (RST-XS, Dietmar Schulze, Germany) was used alongside with a small volume cell.

A Ring Shear Tester was used for measuring the flow properties of the APIs and the salts. Key components of the shear cell are depicted in figure 3.10. The small volume cell was overfilled with the relevant powder, excess material was scraped off so that the surface was flush with the upper edge of the cell, ensuring that no force is applied to the powder bed. The filled cell was weighed and placed on the base of the ring shear tester, this was followed by placement of the lid on top of the powder surface, a loading rod was then inserted, (used for applying a normal stress to the powder bed). Two tie rods (for applying shear stress) were placed in the lid and two load cells. As the base rotated, the lid was held fixed in position by the tie rod, producing shear stresses to the powder. A two-step process occurred: pre-shear and shear. The powder was pre-sheared under a consolidation stress until a steady state was reached. The pre-sheared powder then underwent a shear test under normal stresses below the pre-shear consolidation stress. Powder bed failure was identified by a sudden drop in shear stress. In this study, the procedure was conducted in triplicate using a pre-shear consolidation stress of 10 KPa and 3 normal shear stresses correspondingly spaced between zero and the pre-shear consolidation stress. All experiments were performed at 20.9- 23.3°C and 28.1- 34.7 % relative humidity.

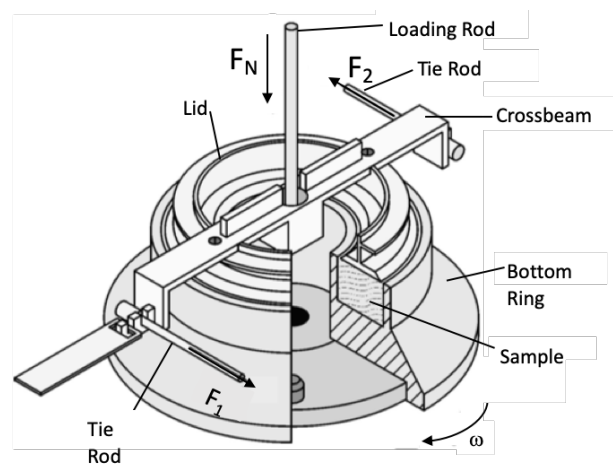


Figure 3.10 Cut-away view of shear cell depicting the key components, adapted from <http://www.dietmar-schulze.com/leaf/xse.pdf>

3.3.8.5 Brunauer–Emmett–Teller (BET)

The BET instrument determines the specific surface area (m^2/g) of a sample. To aid drying of the sample, it is purged with nitrogen or at a vacuum with raised temperatures. The experiment is carried out at 77K and the volume of gas adsorbed at the surface of the sample is measured. The quantity of adsorbed gas directly correlates to the total surface area of the sample including the pores in the surface. The calculation is based upon the BET theory, the data is treated according to the BET adsorption isotherm equation (Equation 3.7).

$$\frac{1}{\left[V_a \left(\frac{P_0}{P} - 1\right)\right]} = \frac{C-1}{V_m C} \times \frac{P}{P_0} + \frac{1}{V_m C} \quad \text{Equation 3.7}$$

P = Partial vapour pressure of adsorbate gas in equilibrium with the surface at 77.4 K (b.p. of liquid nitrogen), in pascals.

P_0 = Saturated pressure of adsorbate gas, in pascals.

V_a = Volume of gas adsorbed at standard temperature and pressure (STP) [273.15 K and atmospheric pressure ($1.013 \times 10^5 \text{ Pa}$)], in millilitres.

V_m = Volume of gas adsorbed at STP to produce an apparent monolayer on the sample surface, in millilitres

C = Dimensionless constant that is related to the enthalpy of adsorption of the adsorbate gas on the powder sample.

From the resulting linear plot, the slope, which is equal to $\frac{C-1}{V_m C}$, and the intercept, which is equal to $\frac{1}{V_m C}$ are assessed by linear regression analysis. From these values, V_m is calculated as $1/(\text{slope} + \text{intercept})$, while C is calculated as $(\text{slope}/\text{intercept}) + 1$. Once V_m has been determined, the specific surface area, S , in $\text{m}^2 \cdot \text{g}^{-1}$, is calculated by the following equation:

$$S = \frac{V_m N_a}{M \times 2400} \quad \text{Equation 3.8}$$

V_m = Determined above (eq 3.7)

N = Avogadro constant ($6.022 \times 10^{23} \text{ mol}^{-1}$)

a = Effective cross-sectional area of one adsorbate molecule, in square metres (0.162 nm² for nitrogen)

m = Mass of test powder, in grams

22400 = volume occupied by 1 mole of the adsorbate gas at STP allowing for minor departures from the ideal, in millilitres.

3.3.8.5.1 Equipment/ Method

The Micromeritics ASAP 2020 equipment was used to carry out the surface area analysis. Surface area analysis was undertaken using the Micromeritics ASAP 2020 apparatus. The study was carried out at 77 K, prior to analysis the samples were de-gassed under vacuum at 50 °C for 3 h. The surface area of the sample was calculated using Brunauer–Emmett–Teller (BET) equation from the adsorption data

3.3.8.6 True Density

Gas pycnometry is a method used to quantify the density of powder particles. A sample of known mass is placed within one of the two chambers of a known volume, which are maintained at constant temperature. The system is then purged with helium, the resulting equilibrium pressures are used to determine the density of the particles using the ideal gas law.

3.3.8.6.1 Equipment/ Method

The true densities of the drug, salt and salt cocrystal powders were measured in triplicate using a Helium Pycnometer (Micrometrics, UK).

3.3.8.7 Tribo electrification

Tribo-electrification occurs as a result of particles coming into contact with each other resulting in generation of electrical charge, due to electron or ion exchange taking place as a result of sliding and friction forces acting upon the material, hence contacting materials are left with equal but opposite charge after the separation process.

3.3.8.7.0.1 Equipment/ Method

A shaker concept developed by Supuk *et. al.* [101] was used whereby a Retsch MM 400 shaker was modified and the charge was measured using a Faraday cup attached to an electrometer (Keithley model 6514). Stainless steel shakers and a measuring cup was used to maintain material consistency.

The shaker concept device was utilised to induce a charge upon the particles and then the charge-to-mass ratio of the samples was determined. Approximately 100 mg of sample was placed within a stainless steel shaker container (10 mL), which was then subjected to a horizontal motion at a vibration frequency of 20 Hz for 0.5, 2, 5 and 10 mins. The net charge produced by the powder particles was measured using a Faraday cup attached to an electrometer.

The tribo-electrification of material was determined in triplicate, ensuring to clean the shaking container between each test using isopropyl alcohol, rinsing with water and drying with compressed air. Studies were undertaken at ambient temperature (18-24 °C) and humidity (30.4-36.2 % RH). Charge acquisition data is presented as a charge to mass ratio ($n = 3$).

3.3.8.7.1 Powder adhesion

Powder adhesion studies were carried out to establish the adhesion tendency to the stainless-steel container due to the shaking motion from section 3.3.8.5.1. The percentage adhesion was calculated by subtracting the final mass of recovered material after shaking and removing

from the Faraday cup by tapping, from the initial sample mass loaded in the shaker. The ratio of the difference between the initial amount of sample loaded and the amount recovered as a percentage represents the percent powder adhesion.

3.4 Conclusions

A number of techniques were utilised in order to confirm salt formation as well as to investigate the physicochemical properties of the salt forms in comparison to the parent compounds. These techniques includes FT-IR, DSC, NMR, Intrinsic dissolution and solubility studies.

For tribo-electrification and powder flow studies undertaken for the salts formed using similar structured pure compounds and the amine counterion series, the material was sieved into the following mesh sizes; 125-150 μm , 150-180 μm , 180-250 μm , 250-300 μm , 300-355 μm , 355-425 μm , 425-500 μm and 500-600 μm for the purpose of investigating the effect of particle size upon the powder flow and tribo-electrification properties.

4 Salts of active pharmaceutical ingredients; recent selection trends and developments

Background

Salification of an active pharmaceutical ingredient (API) is an effective approach utilised to modify physicochemical properties of acidic and basic drugs, including solubility, hygroscopicity, stability and dissolution rate [1-5], and in some cases improve handling properties beneficial for formulation and manufacturing [6]. The resulting salt is mainly governed by the acidity/basicity of the ionisable group of the API but the route of administration, dosage form and safety of counterion play a role in drug and coformer selection as these influence the solid-state properties of crystalline salts. For weakly basic drugs; inorganic acids, sulphonic acids and carboxylic acids could be considered for salt formation [108, 109]. For acidic drugs; salts of Sodium, Potassium and Calcium could be utilised [110], or alternatively salts of organic amines such as tromethamine or erbumine (t-butylamine) and basic amino acids such as arginine or lysine can be employed .

Salt formation involves the combination of a parent drug molecule with an appropriate counterion. The drug must possess ionisable functional groups which allow adequate ionic interaction between the counterion and the drug itself. These groups on the drug and counterion possess a charge which forms an attraction via ionic intermolecular forces, upon achieving favourable thermodynamic conditions, a crystallised salt precipitate is formed (Figure 4.1)

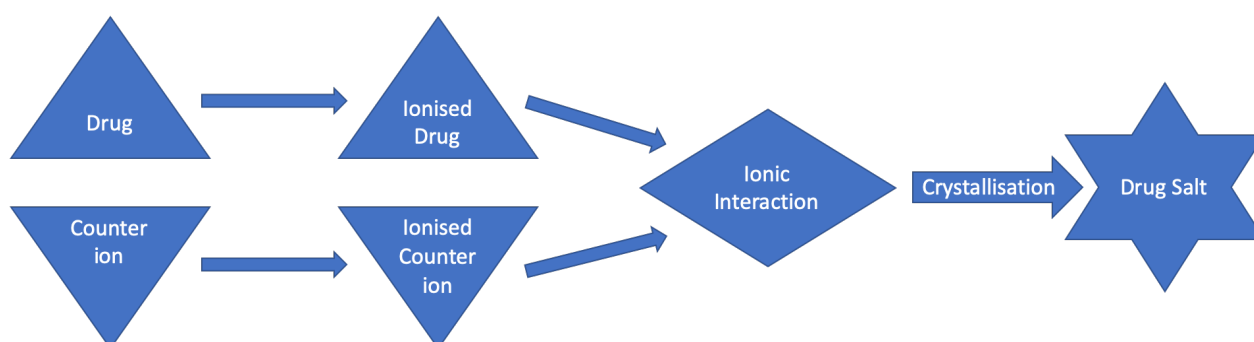


Figure 4.1 Salt formation process diagram

A number of criteria influence the salt former choice, which include dosage type; as for oral and injectable forms, highly soluble counterions such as Mesylate and hydrochloride can be used. Whereas for suspension dosage forms, tosylate may be utilised as it is relatively insoluble. The degree of ionisation is a key parameter as the pK_a values of both the drug and counterion indicate the efficacious salt formation. For salt formation of an acidic drug the pK_a of the counterion is required to be at least two units higher than the pK_a of the drug, whereas for a basic drug the pK_a of the counterion is required to be at least two pK_a units lower than the pK_a of the drug. The difference in pK_a of the ionisable groups is to ensure energetically favourable conditions for proton transfer. When a salt is formed from ionisable groups with a small difference in pK_a value, a salt may form, however, it can easily dissociate back into the drug and counterion components when placed in an aqueous environment.

Counterion selection is based upon a number of factors including, crystallisation and final isolation process, physical attributes of the isolated form that affect handling and storage (e.g. hygroscopicity), and acidity/basicity and intended use of the dosage form. The cost of raw materials and yield are major factors in the salt selection process. These multiple drivers and the need for simplicity explain the popularity of the hydrochloride salt form for basic drugs and, where salt formation is employed, the Sodium salt for acidic drugs. As it is unrealistic to screen all possible counterions, a range of guidelines can be employed to streamline the selection process, including the charge of the counterion as well as ensuring a difference of at least two units between the pK_a value of the acid and base on most occasions [111]. For non-ionisable drugs, or compounds with pK_a values of such where salt formation is likely to be unsuccessful, formation of a cocrystal may be an alternative approach [112]. However, a simple modification such as salt formation is the most popular technique utilised in changing physicochemical properties without changing the active ingredient as drugs are often formed from a weak base or a weak acid. The original form does not always provide optimal dissolution or absorption properties. Poor absorption results in reduced therapeutic effect, hence salt formation is utilised to increase a drug's uptake into the bloodstream, improving its effectiveness [113].

The importance of salt formation is exemplified in a research case involving Rucaparib drug that was initially formed as a phosphate salt during the early trials for intravenous delivery, however, this form had a propensity to hydrate and an alternative form was required for oral

dosage formulation[114]. A number of alternative salt forms were prepared which comprised of three anhydrous (*S*) – camphorsulfonate salt polymorphs, one anhydrous (*R*) - camphorsulfonate salt form, mixtures of (*S*)- and (*R*) - camphorsulfonate salts, two anhydrous maleate salt polymorphs and a HCl trihydrate. Due to the ability for the maleate and camphorsulfonic acid salts to be easily prepared as well as being less hygroscopic than the other salts, they were evaluated for tablet formation. The approach led to the discovery of camphorsulfonic acid salt to be highly compressible allowing for tablet formation. The (*S*) - camphorsulfonate salt was selected for the final dosage form [114].

There are several publications investigating salt selection and the effects on physicochemical properties of the resulting form, [56, 115-117], however very few publications provide an overview of the approved salt forms [2, 23, 118] with a view to identify trends associated with changing regulatory backgrounds and pharmaceutical industry dynamics. In the most recent of these analyses, it was speculated that there would be a trend towards a greater diversity in pharmaceutical salts as more challenging potential APIs enter preclinical development [23].

This study aims to update earlier work to determine if there any emerging trends in newer chemical entities that might reflect a response to those evolving physicochemical properties. Previous research has examined the trends in active pharmaceutical ingredient for salt selection from the ~1950s up until 2006 [5, 23, 118]. The study undertaken here examines the trend in counterion selection from 2007 – 2018, considering any regulatory changes and industry changes that may have an impact on salt selection. Recent activity in the selection of counterions used in salt formation was scrutinised by evaluating the approved drug products (Orange Book) [119] data published by the U.S. Food and Drug Administration (FDA) to reflect North American activity and the British National Formulary (BNF) [120] to reflect European territories. A large majority of products recently approved for prescribing in the UK are also approved in many European countries as a consequence of the European medicines agency (EMA) Centralised Procedure. The Orange Book database includes the date of approval, hence an analysis of frequency of counterion usage with time is possible. These data were compared to the overall incidence of counterion in salt selection using the BNF from the year 2013/14 (BNF 66) in comparison to the latest version (76) to determine if any recent salt form choices are apparent and that geographical differences occur.

4.1 Study Strategy

The FDA Orange Book database [119] was used to compile a study of the occurrence of counterions used in pharmaceutical salt formulations over a 12 year range from 2007 to 2018. The study omitted any dosage forms containing hormones, antibodies, enzymes, proteins, polymeric salt forms, metal complexes and inorganic APIs. From a database, 1531 chemical entities were extracted from a list of 35,841 approved products with slight variations in stoichiometry (such as hydrochloride and dihydrochloride which are included together within the Chloride subset). The data was assorted into classifications as follows:

- a) Class 1 comprised salts formed from basic molecules
- b) Class 2 includes salts from acidic species
- c) Class 3 consisting of non-salt forms (including both non-ionisable and free acids and bases)

The salt forms were filtered by date of approval into two categories consisting of 6-year blocks, from 2007-2012 and 2013-2018 (inclusive). The number of new chemical entities (NCE's) were also categorised in these time intervals. The initial assessment included those delivered by all routes of administration, a second assessment of the data was undertaken consisting of oral and injectable dosage forms. The BNF was used to compare the percentage incidences of the number of salts in the formulary during September 2013 – March 2014 [121] in comparison to the latest version to provide a reflection on the trends in salt formation between the two time intervals.

4.2 Results and Discussion

Of the 1,534 chemical entities identified in The Orange Book database, 539 (35.1 %) of these were salts formed from basic compounds (Class 1), 157 (10.2 %) were from acidic APIs (Class 2), and 838 (54.7 %) were in non-salt form (Class 3). Over the past 12 years there is a reduction in the number of different anions and cations used in comparison to pre-2006 [23]. The reduction is likely to be due to a large number of anions and cations occurring only during the pre-1982 subset which accounted for less than 1% of the incidence. Presently, 27 different anions and 10 cations are in use for salt formation; 14 anions being used on 3 or less occasions

during the last 6 years. This trend is similar to the 2007-2012 subset, indicating that there have not been any great changes in the low incidences of these salts.

During the two time intervals there have been a total of 246 NCE's approved, of these 41 were used for salt formation during 2007-2012 and 70 during the 2013-2018 time interval. Therefore, approximately 45% of the new chemical entities in these periods are utilised for salt formation.

Figure 4.2 depicts the distribution of APIs per class of the Orange Book Database, and compares with the route of administration. Oral and injectables were only considered due to their abundance so provided a clear comparison of the salt former choice and route of administration. However salts are used for other routes of administration, which included topical, nasal and ophthalmic. The number of bases increase when comparing 2007-2012 to 2013-2018 period, with the number of acids and non-salts showing a slight overall decline during the latter time interval. In the case of injectables, the number of non-salt and basic drugs show an increase between the two time intervals while a slight reduction in the number of acidic entities is seen in the latter time interval. In comparison to the previous data [23], an increase in the overall percentage incidence is evident for non-salt form and a decrease in the number of salts formed using acidic and basic entities. During the last 12 years, 45.4% of drugs were approved in the salt form, a slight reduction from the 51.4% reported for pre-2006 [23] but in part this can be accountable to the reduction in the small molecule salts formulated as injectables. It is commonly reported that approximately 50% of drugs are administered in the salt form [122, 123], this still stands true as 45.4% of the drugs were approved in the salt form based on this study. This sustained popularity of salt formation is due to the salt form's ability to reduce a number of unfavourable properties of the pure API, as well as improving physicochemical behaviour in comparison to the pure API.

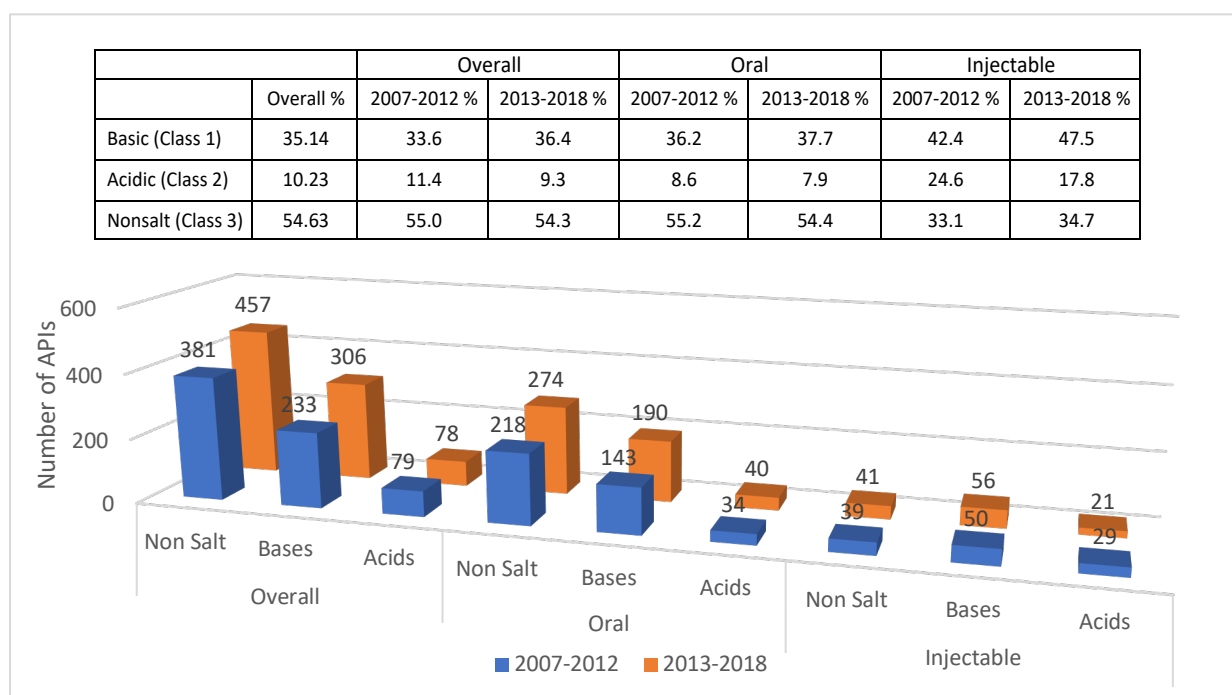


Figure 4.2: Distribution of API form in the Orange book database per class according to charge type and route of administration

In the case of injectable dosage forms there is a slight reduction in all three, non-salt, base and acid categories in comparison to the pre-2006 study, with the pre-1982 subset comprising a considerable proportion of the number of APIs [23]. The limited number of new APIs approved for use in injectables may be due to difficulties in developing formulations of acceptable solubility, osmolarity, as well as, low patient usability and acceptability. Furthermore, the proportion of biologics-based approvals has increased since the 1980s and 1990s, and represented one third of all new molecular entities (NMEs) during 2009-2010 [124]. It is evident that there have been an increase in the number of APIs approved during this study in comparison to the previous study, which investigated a longer time period. However, apart from the injectable dosage forms, the trends for number of APIs for each class compared to route of administration is virtually matching to that presented previously [23].

Table 4.1 shows the overall incidences of approval for anions approved during the time interval with the Chloride ion (49.7%) being the most popular choice by almost 6-fold. It is an endogenous counterion and its popularity stems from its simplicity, cost, availability and significant experience of use in the past [125]. However, its incidence is slightly reduced from 51.1% (2007-2012) to 48.7% (2013-2018); this may be due to an increase in the number of

occasions of other anions being used, such as Mesylate and Sulfate, as the total number of salts increased from 233 for 2007-2012 to 306 for 2013-2018, with Chloride increasing from 119 to 149 instances, respectively. Table 4.7 illustrates the NCE's approved during the two time intervals, during 2007-2012, the Chloride anion accounted for 51.4%, followed by Mesylate with a percentage incidence of 11.4 %, closely followed by Maleate and Fumarate; presenting 8.6% of the new chemical entities. However, during the 2013- 2018 subset for NCE's, Chloride appears to have reduced popularity in formation of new entities. Although the number of incidences were 15 compared to 18 during 2007-2012, this reduction is exacerbated due to a larger number of NCE's being approved during the latter time interval with a greater diversity of anions in comparison to the previous time interval.

The second most popular anion is Sulfate, accounting for a mere 8% of the basic molecules. The Sulfate subset includes any Bisulfate/ Hydrogen Sulfate salts which may produce salts with better solubility for weakly basic drugs due to resulting in an acidic solution, potentially explaining the increase in popularity of Sulfate as a salt form. Other counterions encountered include Mesylate (5.2%), Acetate (4.5%) Tartrate (4.1%), and Bromide showing a slight decrease from 4.6% to 3.7%. It is evident that there is a reduction in the number of different anions used for pharmaceutical salt formation in recent times compared to pre-2006, this may be due to 13 of the 16 anions being used only once in the pre-1982 subset. In the former Orange Book Database study [23], Nitrate accounted for 8% of anionic counterions during 1982-1986, however an average use of just 1.3% in this study. This discrepancy is exacerbated by the small number of salts (50) in the previous study time interval, compared to 200+ salts over the time intervals in this study. The anionic counterion selection is fairly constant during the two time intervals with one of the largest difference seen for the counterion Tosylate. Over the two time intervals, only 3 counterions presented an overall occurrence of >5%, these being Chloride, Sulfate and Mesylate. Aside from these, the only other counterion to have an incidence of greater than 5% was Acetate during 2007-2012. This is due to the increase in the number of salts approved during the last 12 years, as well as the constantly high percentage occurrence of the Chloride ion being used. In the previous study [23] over 50% of the percentage incidences reported during the pre-1982 – 2006 period are accounted for in the pre-1982 subset. With the subsequent time intervals accounting for only between 35 and 60 salts per subset [23].

Table 4-1 Distribution of Anions Used in APIs of Class 1

	Overall (%)	2007-2012 (%)	2013-2018 (%)
Acetate	4.5	5.2	3.9
Benzoate	0.6	0.4	0.7
Besylate	1.1	1.3	1.0
Bromide	3.7	3.4	3.9
Butyrate	0.4	0.4	0.3
Camsylate	0.2	0.0	0.3
Chloride	49.7	51.1	48.7
Citrate	2.8	3.0	2.6
Esylate	0.2	0.0	0.3
Fumarate	3.3	3.9	2.9
Gluconate	0.7	0.9	0.7
Hippurate	0.2	0.0	0.3
Iodide	0.6	0.9	0.3
Isethionate	0.2	0.0	0.3
Lactate	0.9	0.9	1.0
Malate	0.7	0.9	0.7
Maleate	3.5	3.0	3.9
Mesylate	5.2	4.3	5.9
Methylsulfate	0.4	0.4	0.3
Nitrate	1.3	1.7	1.0
Oxalate	0.6	0.4	0.7
Pamoate	1.3	1.3	1.3
Phosphate	2.2	2.1	2.3
Succinate	2.0	1.7	2.3
Sulfate	8.5	8.6	8.5
Tartrate	4.1	3.9	4.2
Tosylate	1.1	0.4	1.6
Total Number of Salts	539	233	306

One interesting trend to note is the incidence of the Mesylate salt during the time period of 1997-2018 [23] due to concerns of Mesylate esters of short chain alcohols ($n = 1-3$) showing to be reactive, genotoxic and potentially carcinogenic alkylating agents. In the year 2000 a communication in the Pharmeuropa surfaced [126], proposing the requirement for tests to limit alkyl Mesylates in Mesylate salts. A monograph for Mesylate salt production introduced in 2004 as a part of the European Pharmacopeia (Ph. Eur.) states: *“The production method must be evaluated to determine the potential for formation of alkyl mesylates, which is particularly likely to occur if the reaction medium contains lower alcohol. Where necessary, the production method is validated to demonstrate that alkyl mesylates are not detectable in the final product.”* [127]. Although set specific limits haven’t been imposed by Ph.Eur. the production method still required validation to confirm that alkyl Mesylates are not present within the final product. This communication may have influenced the decrease in Mesylate salt incidence between the time periods, 1997-2001 and 2002-2006. A large decrease is apparent, from 13.8% to 8.3% respectively, in comparison to the data presented in Table 4.1, where the incidence rate for Mesylate has decreased further to 4.3% during 2007-2012 period, during a marginally longer time period in comparison to that of the salts trends in the prior study [23]. For the period of 2013-2018, interestingly, an increase is seen (5.9%). From Table 4.7 it is evident that Mesylate was the second most popular anion utilised for NCE’s, with 4 and 6 incidences during 2007-2012 and 2013-2018, respectively. This may be due to the avoidance of Mesylate salts initially, as a result of the communication by the Pharmeuropa. The pharmaceutical industry may have addressed the issue, implementing steps for appropriate controls during formulation development and manufacturing. As well as applying improved methodologies available for detection of compounds below 1ppm as per the threshold of toxicological concern, requiring very low limits of detection and quantification [128-130]. This in turn allowing for easier progression through the approval process. This is indicative as the percentage incidence remained constant during the latest time period.

Table 4.2 consists of a list of all cationic counterions approved, displaying the respective incidences of each counterion for both time intervals. It is evident that Sodium is still the most used counterion, this is potentially due to Sodium providing an alternative to the parent drug with increased solubility and stability with a track record for forming a viable salt form. It

presented an overall incidence of 67.5%, although there is a reduction in Sodium's dominance from 74.7% during 2007-2012 to 60.3% throughout 2013-18, the decline in its use is likely to be due to the increase in popularity of Calcium and to some extent Magnesium and Potassium cations. Calcium and Potassium were the joint second most popular option with an overall incidence of 10.8%. Sodium presents a slightly lower overall of 67.5% in comparison to 75.3% in the previous study [23], however the use of Calcium and Potassium has increased from 6.9% to 10.8% and 6.3% to 10.8%, respectively [23]. Although Lysine had only been introduced approximately 20 years ago, its incidence has remained relatively low, with no approved drug during 2007-2012 and just one incidence for 2013-2018. There has been an addition of a couple of counterions; Erbumine and Arginine with the former being used within the 2007-2012 subset and the latter in the 2013-2018. Surprisingly, the Erbumine counterion is not as popular as it could be despite research showing it to consistently produce a crystalline product with a high melting point, as well as a modest improvement in solubility, hence potentially improving many undesirable characteristics [6]. The Magnesium cation, presented a relatively low incidence in the previous study of 1.2%; its popularity has increased during the last 12 years, presenting a total of 7 instances. The route of administration was found to influence cation/anion selection with Esomeprazole Magnesium the choice for oral dosage form in contrast to Esomeprazole Sodium for injectable. This is due to the Magnesium form being slightly soluble in water, compared to the more soluble Sodium form, which lends itself better to an injectable formulation. Tromethamine has not been used since 1996, however it was used in both recent time intervals. It is evident that there has been a major drive for the use of salt forms as the previous study present 174 cationic salts during a period of over 25 years, however during the previous 12 years there have been 157 approved, once again the majority of data presented in the previous study is accountable by the pre-1982 subset. From Table A1 (Appendix) it is evident that the drive for NCE's using cations was limited during 2007-2012 as only 6 new entities were approved. Potassium presenting the most popular with 33.3% of the incidences, in comparison to the 2013-2018 interval whereby Sodium was utilised for 75.0% of the NCE's, as well as Meglumine, Magnesium and Strontium.

Table 4-2 Distribution of Cations Used in APIs of Class 2

	Overall (%)	2007-2012 (%)	2013-2018 (%)
Arginine	0.6	0	1.3
Calcium	10.8	7.6	14.1
Erbumine	0.6	1.3	0.0
Lysine	0.6	0.0	1.3
Magnesium	4.5	3.8	5.1
Meglumine	2.5	1.3	3.8
Potassium	10.8	10.1	11.5
Sodium	67.5	74.7	60.3
Strontium	0.6	0.0	1.3
Tromethamine	1.3	1.3	1.3
Total Number of Salts	157	79	78

It is evident from Table 4.1 and 4.2 that the most popular anion and cation, Chloride and Sodium, have reduced in popularity over the most recent time intervals in comparison to 2007 – 2012 period. Counterions are an effective way to enhance the physicochemical properties of an API, in particular, solubility. However, the properties can differ from one salt form to another depending on the counterion used. By selecting the best matching counterion, the drug properties may be optimised.

Recently salt screening has increased in popularity, typically 50-100mg of free acid or base is utilised and multiple experiments can be carried out concurrently. Once the potential salt forms have been identified, further experimental work can be undertaken to confirm viability and stoichiometry. Salt screening may have led to the growth in diversity of alternative salt formers for ionisable drugs as opposed to relying on Chloride and Sodium.

Pharmaceutical Salts Utilised for Oral Formulations. Out of the 1,534 chemically-defined and approved APIs in the Orange Book Database, 899 were classified for use in the oral drug

delivery. From these, 492 (54.7%) of them were non-salts (Class 3), the salts of bases (Class 1) accounted for 333 (37.1%) and 74 (8.2%) of them were salts from acidic molecules (Class 2). Twenty-four different anions were listed for oral formulations, of which, Lactate, Hippurate, Camsylate and Esylate are used on a single occasion. Only nine cations were used for salt formation of oral formulations.

Anionic Counterions Used in Oral Formulations of Salts. The overall percentage incidence of all anionic counterions used in oral formulations is presented in Table 4.3. Chloride is the most frequently used anion, accounting for approximately 50% of the occurrences, like Sodium, its popularity can be accounted to its track record in producing a form with increased solubility and stability. Although Chloride's percentage incidence decreased from 57.3% during 2007-2012 to 46.8% between 2013 and 2018, there was an increase in frequency from 82 to 89 occurrences, respectively. The second most popular anion was Sulfate, accounting for 7.5% of anions used. A growth in popularity is especially evident for Maleate, increasing in percentage incidence from 2.1% to 5.3% in the 2013-2018 subset, with a substantial increase from 3 incidences to 10 in the 2013-2018 subset. This trend is interesting as it is vastly different to the injectable form presenting no incidences in the same time period, therefore indicating that the counterion selection is influenced by the intended route of administration. Mesylate also showed a similar increase, from 4.1 to 6.7%, although both showed an increase in incidence, the overall incidence is reverse to previous findings, with maleate showing to be more popular of the two [23]. The trend for the new chemical entities is similar to that presented in Table 4.1 whereby during 2007-2012, Chloride dominated in choice for salt selection with a percentage incidence of 55.2. However, during 2013-2018 the percentage incidence reduced to 26.7, although the number of incidences are not vastly different; 16 and 12 for the time intervals 2007-2012 and 2013-2018, respectively. This is accountable to the increase in popularity of other anions such as Tosylate, also Bromide and Acetate which were not used in the former time interval.

Table 4-3 Distribution of Anions Used in Oral Dosage Forms

	Overall (%)	2007-2012 (%)	2013-2018 (%)
Acetate	2.7	2.8	2.6
Benzoate	0.9	0.7	1.1
Besylate	0.6	0.7	0.5
Bromide	3.3	2.8	3.7
Butyrate	0.6	0.7	0.5
Camsylate	0.3	0.0	0.5
Chloride	51.4	57.3	46.8
Citrate	2.7	2.8	2.6
Esylate	0.3	0.0	0.5
Fumarate	4.2	4.2	4.2
Hippurate	0.3	0.0	0.5
Iodide	0.6	1.4	0.0
Lactate	0.3	0.0	0.5
Malate	1.2	1.4	1.1
Maleate	3.9	2.1	5.3
Mesylate	5.7	4.2	6.8
Nitrate	0.9	1.4	0.5
Oxalate	0.9	0.7	1.1
Pamoate	0.9	0.7	1.1
Phosphate	2.7	2.8	2.6
Succinate	2.7	2.1	3.2
Sulfate	7.5	7.7	7.4
Tartrate	3.9	2.8	4.7
Tosylate	1.5	0.7	2.1
Total Number of Salts	333	143	190

Cationic Counterions Used in Oral Formulations of Salts. Sodium is the most popular cation used (Table 4.4), accounting for an average of 50.0% of cations for oral formulations although the percentage incidence reduced from 55.9% during 2007-2012 to 45.0% between 2013 and 2018, due to an increase in other counterion during the time interval, such as Calcium and Magnesium. The next most popular cations were Potassium and Calcium, accounting for 20.3% and 16.2% respectively. During the 2007-2012 interval, there were only 4 newly approved chemical entities hence indicating that Potassium was the most popular choice for forming a new entity during the time period. However, the popularity of Sodium is evident during the 2013-2018 time interval, accounting for 70% of the new chemical entities for oral dosage forms.

Table 4-4 Distribution of Cations Used in Oral Dosage Forms

	Overall (%)	2007-2012 (%)	2013-2018 (%)
Arginine	1.4	0.0	2.5
Calcium	16.2	14.7	17.5
Erbumine	1.4	2.9	0.0
Magnesium	6.8	5.9	7.5
Meglumine	1.4	0.0	2.5
Potassium	20.3	20.6	20.0
Sodium	50.0	55.9	45.0
Strontium	1.4	0.0	2.5
Tromethamine	1.4	0.0	2.5
Total Number of salts	74	34	40

Pharmaceutical Salts Used in Injectable Formulations.

Out of the 236 approved APIs used in injectable form, consisted of 80 (33.9%) non-salts, 106 (45.0%) API salts from basic entities and 50 (21.1%) were salts from acidic molecules. The percentage of non-salts decreased in comparison to the oral form accounting for over 50%, with the basic molecules accounting for approximately half the number of approvals in injectables, indicating a significant role for salification to ensure solubility of injectables. A

total of 14 anions and 7 cations have been approved as suitable counterions for injectables during the two time intervals.

Anionic Counterions Used in Injectable Formulations of Salts. Similar to the oral dosage form, the most popular counterion remains Chloride (Table 4.5), accounting for an average of 51.9%. An increase to 53.6% was seen between the years 2013 and 2018 compared to 50.0% during 2007-2012. The second most used was Sulfate, representing 10.4% of the anions as injectables, remaining consistent over the two time intervals, Tartrate follows in third with an average of 6.6%, closely followed by Acetate, presenting a percentage interval of 5.7%. Citrate, Fumarate, Isethionate and Gluconate have presented just a single incidence. However, a number of the counterions showed an increase in percentage incidence during 2013-2018, indicating a potential increase in the diversity of counterion choice for injectable forms. This is further acknowledged as there is a considerable increase in new chemical entities from just four approvals in 2007-2012 to nine new entities during 2013-2018. Although Chloride was the most popular choice for the formation of the new entities for the injectable form.

Table 4-5 Distribution of Anions Used in Injectable Dosage Forms

	Overall (%)	2007-2012 (%)	2013-2018 (%)
Acetate	5.7	4.0	7.1
Besylate	3.8	4.0	3.6
Bromide	3.8	4.0	3.6
Chloride	51.9	50.0	53.6
Citrate	0.9	2.0	0.0
Fumarate	0.9	2.0	0.0
Gluconate	0.9	2.0	0.0
Isethionate	0.9	0.0	1.8
Lactate	3.8	4.0	3.6
Maleate	0.9	2.0	0.0
Mesylate	6.6	6.0	7.1
Phosphate	2.8	2.0	3.6
Sulfate	10.4	10.0	10.7
Tartrate	6.6	8.0	5.4
Total Number of Salts	106	50	56

Cationic Counterions Used in Injectable Formulations of Salts. The most prevalent counterion used in injectable dosage forms is Sodium, accounting for 82%, as summarised in Table 4.6. This is followed by Potassium, Meglumine and Tromethamine, with 2 instances each, in comparison to 41 by Sodium, although Tromethamine was last used between 1987 and 1991, its emergence indicting an increase in diversity. Calcium, Magnesium and Lysine had one instance each. A substantial reduction for Sodium is seen from 25 instances between 2007 and 2012 to 16 in the interval 2013-2018. However, there was an overall reduction in the number of salts approved during the latter time interval. It is evident that there were limited number of new chemical entities for injectables, with just 4 being approved between both time intervals, 50% of those accounted for by Sodium.

Table 4-6 Distribution of Cations Used in Injectable Dosage Forms

	Overall (%)	2007-2012 (%)	2013-2018 (%)
Calcium	2.0	0.0	4.8
Lysine	2.0	0.0	4.8
Magnesium	2.0	3.4	0.0
Meglumine	4.0	3.4	4.8
Potassium	4.0	3.4	4.8
Sodium	82.0	86.2	76.2
Tromethamine	4.0	3.4	4.8
Total Number of Salts	50	29	21

Trends in Routes of administration of New Chemical Entities (NCE).

The new chemical entities that were extracted from the FDA [131] approved drug database opposed to the Orange Book Database as the Orange Book Database included generic drug products which were introduced during the time intervals of interest. This in turn would have likely resulted in unreliable data and trends which did not provide a true representation of the trends for the actual new chemical entities. Table 4.7 illustrates the distribution of anions used in NCE. It is evident that the drive for Chloride salts is still strong; accounting for an overall 36.7%, followed by Mesylate at 11.1%. In comparison to table A1 which shows the distribution of the NCE cations, with Sodium dominating at 55.6% incidence; Potassium and Meglumine at a mere 11.1%. From Table A2 it is evident that the new chemical entities have been utilised in a range of routes of administration, with the oral route being the most popular with an overall incidence of ~80%, followed by parenteral, pulmonary and topical ophthalmic. Chloride appeared to be the most popular for the oral and parenteral route. For the cations (Table A3), the only routes of administration for the new entities were oral and parenteral. The oral route presented to be the most popular of the two, with an overall of approximately 80%. During 2007-2012, Potassium was the most popular for the oral route and Meglumine for the parenteral route, and for 2013-2018 Sodium was the most popular for both routes.

Table 4-7 Distribution of Anions Used in New Chemical Entities of Class 1:

	Overall %	2007-2012 %	2013-2018 %
Acetate	2.2	0.0	3.6
Benzoate	1.1	0.0	1.8
Besylate	1.1	2.9	0.0
Bromide	3.3	5.7	1.8
Camsylate	1.1	0.0	1.8
Chloride	36.7	51.4	27.3
Citrate	2.2	2.9	1.8
Esylate	1.1	0.0	1.8
Fumarate	4.4	8.6	1.8
Hippurate	1.1	0.0	1.8
Lactate	1.1	0.0	1.8
Malate	5.6	0.0	9.1
Maleate	3.3	8.6	0.0
Mesylate	11.1	11.4	10.9
Oxalate	1.1	0.0	1.8
Phosphate	4.4	2.9	5.5
Succinate	4.4	2.9	5.5
Sulfate	5.6	0.0	9.1
Tartrate	2.2	0.0	3.6
Tosylate	6.7	2.9	9.1
Total number of salts	90	35	55

Comparison with analysis of data from the British National Formulary (BNF). A total of 1,596 products are listed in the BNF. As the BNF does not provide date of approval for the salts, a comparison of the overall number of instances present in the BNF 66 (Sep 2013- Mar 14) was made with the number of instances in the BNF 76 (Sep 2018- Mar 19). The study omitted any dosage forms containing hormones, antibodies, enzymes, proteins, polymeric salt forms, metal complexes and inorganic APIs. The basic entities account for 185 instances in the BNF 66 and 185 in the BNF 76 whereas the cations presented 72 incidences during the 2013-14 period and 73 during the 2018-19 subset.

All anions encountered as counterions for API salts in the BNF are presented in Table 4.8. In comparison to the data from the Orange Book Database, the most popular anion in the BNF is the Chloride counterion accounting for 58.9% during 2013 -14 and 60.5% in 2018 -19, an

increase in contrast to the Orange Book which presented on overall of 49.7%. Furthermore, the subsequent most popular anion is the same as the Orange Book Database; Sulfate presenting very similar overall instances of 8.6% in the BNF, compared to 8.5% Orange Book. However, the third most popular in the BNF is the bromide counterion with an overall instance of approximately 6.2% in comparison to 3.2% in the Orange Book Database over the last 12 years. However, the total number of incidences of bromide are similar as there is an increase seen in the Orange Book Database during 2013-2018. Overall, it is apparent that the most popular anions are identical; with similar overall incidences and the remainder also presented similar frequency.

Table 4-8 Anions Used in for salt formation in the BNF

	BNF 2013-14 (%)	BNF 2018-19 (%)
Acetate	2.7	2.7
Benzoate	0.5	0.5
Bromide	6.5	5.9
Butyrate	0.5	0.5
Chloride	58.9	60.5
Citrate	3.2	2.2
Fumarate	2.2	2.2
Gluconate	2.2	1.6
Hippurate	0.5	0.5
Lactate	1.1	0.5
Maleate	2.7	2.7
Mesylate	1.6	1.6
Nitrate	2.7	3.2
Oxalate	0.5	0.5
Phosphate	1.1	1.6
Succinate	0.5	0.5
Sulfate	8.6	8.6
Tartrate	3.8	3.8
Total number of salts	185	185

Table 4.9 consists of a list of all cationic counterions, presented in the BNF; Sodium is still the most commonly used counterion, accounting for an overall incidence of ~71%. Calcium presents the second most popular option with an overall of 11.7%, once again a very similar trend to the Orange Book Database. The third most popular is Magnesium, presenting an overall incidence of approximately 7.6% followed by Potassium at approximately 6.9%. This is a reverse of the data presented in the Orange Book Database study with Potassium presenting to be more than twice as popular than Magnesium as a counterion.

It is evident that during the two time intervals there have not been any vast changes to the choice of counterion for salt formation according to the BNF with each counterion presenting similar percentage incidences for both subsets as well as the number of salts formed with the anions and cations presenting to be very similar also.

Table 4-9 Cations Used in for salt formation in the BNF

	BNF 2013-14 (%)	BNF 2018-19 (%)
Arginine	1.4	1.4
Calcium	11.1	12.3
Erbumine	1.4	1.4
Magnesium	6.9	8.2
Potassium	6.9	6.8
Sodium	72.2	69.9
Total number of salts	72	73

Comparison with other analyses of pre-2006 data.

A review article published by Berge, Bailey and Monkhouse in 1977, investigated the distribution of counterions using the Martindale - “The Extra Pharmacopeia” (26th edition) published in 1974 [118] and Martindale - “The Extra Pharmacopeia” (30th edition) in 1993 [5]. Presented in Table 4.10 is the distribution of some important counterions compared with the Orange Book Database in 2006 and 2018 [23] as well as the BNF. The distribution of anions is relatively consistent throughout the time periods. There are some limitations with direct

comparisons as the method of counting the salts varies between the data sets as the data present in the Orange Book is from a database and provides the year of approval of the salts, hence an analysis of each year was undertaken and subsets formed, whereas for the BNF, two different versions were compared. Furthermore, the Martindale - “The Extra Pharmacopeia” consists of drugs from all over the world in contrast to the Orange Book Database which only contains drugs approved in the U.S. and the BNF in UK.

*Table 4-10 Comparison of data from Berge, Monkhouse and Bighley (1974 and 1993) with data from the orange book database (2006 and 2018) and the BNF. Adapted with permission from [16]. Copyright (2007) American Chemical Society**

	Martindale, 1974 (%)*	Martindale, 1993 (%)*	Orange book, 2006 (%)*	Orange book, 2018 (%)	BNF, 2018 (%)
Bromide	7.6	5.7	4.6	3.7	6.2
Chloride	47.7	48.9	53.4	49.7	59.7
Maleate	3	3.1	4.2	3.5	2.7
Mesylate	2	3.2	4.2	4.8	1.6
Sulfate	7.8	6.1	7.5	8.5	8.6
Calcium	10.5	12.2	6.9	10.8	11.7
Potassium	10.8	9.8	6.3	10.8	6.9
Sodium	62	57.7	75.3	67.5	71.0

One evident trend is the consistently low percentage incidence of the Maleate counterion, presenting an increase from 3.0% in 1974 to 4.2% in 2006, and a reduction to 3.5 % in 2018 from the Orange Book and 2.7% in the BNF (Table 4.8). The reason for this is thought to be due to the ability of acidic or basic counterions to alter the pH of an environment in liquid forms, in turn can affect the reactivity of an API with excipients, resulting in either improved stability or degradation of the material, consequently increasing the probability of potential impurities. The emergence of a major degradation product has been reported in several pharmaceutical formulations, for example, Wong *et al* (2006) reported that the combination of Chlorpheniramine Maleate and Acetaminophen produces a small quantity of degradant [132]. Also, Amlodipine is a free base, capable of forming a Maleate salt, however the presence of maleic acid altered the environment of the product, leading to a Michael addition

forming an aspartic acid derivative, possessing a different biological activity to the Maleate salt, therefore emphasising the importance of counterion selection to obtain optimum drug stability [133].

One interesting note which was evident when comparing the datasets from this study to the previous study [23]. For the pre-2006 subsets over half (272) of the anions are accounted for in the pre-1982 subset. Such as Iodide which was present in the pre-1982 as well as the 1982-1986 subset, with a percentage incidence of 2% during 1982- 1986. However, from 1987 onward the iodide counterion was not used for salt formation at all; until 2007 where it reappeared in this present study and continued to do so in the 2013-2018. This trend was also evident for some of the cations, such as Calcium showed no incidences in three of the subsets, as well as presenting an overall incidence of 6.9%, in comparison to this study at 10.8%. This increase and decrease in popularity of counterion selection is evident pre-2006, however in this study a far greater diversity of counterion selection is evident, with some counterions which have not been used for many years having reappeared, such as hippurate and isethionate. This growth in counterion selection diversity is likely due to an interest for engineering solid form properties through salt formation over the recent years, [6, 56, 134-138] resulting in the formation of new chemical entities. As a result a rise in the number of anion salts is evident from 523 during pre-1982- 2006 to 539 during the 12 year period in this study. The increasing engagement in drug product development scientists as partners in API considerations and the collaborative screening to enable developability of a drug [139] may be in part responsible for the current diversity of alternative salt formers for approved drugs. Furthermore, the trends associated with changing regulatory backgrounds and pharmaceutical industry dynamics are noteworthy, as the communication in the Pharmeuropa surfaced in 2000 potentially influenced the reduction in the percentage incidence of the Mesylate anion for salt formation, increasing in popularity from 2013 onwards, possibly due to industries having addressed the issue by implementing steps for appropriate manufacturing and formulation.

4.3 Conclusion

This present study provided the trends in active pharmaceutical ingredient salt selection based on analysis of the Orange Book Database and compared with the overall incidence in the BNF and previous data. From the dataset it is apparent that the trend towards utilising a broad variety of counter ions for salt formation is still strong and there are a number of counterions such as Chloride, Calcium and Sodium which have maintained a high frequency throughout this study relative to findings for earlier study years. It is evident from the analysis undertaken, comparing the oral and injectable dosage forms that the choice of counterion selection is largely influenced by the route of administration. The comparison with the BNF, although the study does not compare time intervals, the overall percentage incidence of the counterion selection is comparable to the average values from the Orange Book Database. It is interesting to note that a trend is also apparent from Table 4.9, as a comparison of some of the important counterions yielded very similar incidence of counterions selection throughout the previous 44 year time period. However more recently the diversity of counterions selection for salt formation has grown, as is evident from the new chemical entities presenting incidences for a range of anions and cations. Although low in percentage in comparison to Chloride and Sodium, yet still demonstrating diversity in drug discovery, as the interest for engineering solid form properties through salt formation has surged. Due to this popularity and diversity in salt forms; it provides scope for their continued use, therefore stipulating rationale for the use of salt forms, in order to investigate the effect on the triboelectrification propensity in comparison to the parent material.

5 The influences of varying salt former ratios and solvent selection upon physicochemical properties of the resulting material

Background

Engineering the morphology of pharmaceutical APIs in order to form desirable size, shape and surface of materials has been of interest recently [140]. One method widely utilised for improving the physiochemical properties of an API is salt formation. Salt formation is popular in the pharmaceutical industry for improving solubility or stability, as well as overcoming undesirable characteristics exhibited by the parent drug [57]. The internal packing dictates whether the material is amorphous, polymorphic or crystalline. These variations in the internal packing result in alterations to the bulk properties such as mechanical and physico-chemical [58].

A crystalline material provides the ability to manipulate the crystal habit which affects the shape of the crystal, influenced by the rate of growth of the different faces. The crystal shape is determined by the solute-solvent interaction as some crystal faces may occupy a large number of exposed non-polar groups whereas others may be polar. The polarity of the solvent used for the recrystallization process needs to be chosen carefully as it plays a role in the orientation and packing geometry of the molecules into the lattice [59]. Therefore, it is possible to engineer changes in the crystal habit by controlling the rate of growth of the faces of the crystals.

For this chapter the original salt formation was carried out as specified in section 3.3.1, however the samples prepared by recrystallisation, named 1:2 and 2:1 were formed as described in section 3.3.2.

5.1 Results and Discussion

5.1.1 Fourier Transform Infra-Red Spectroscopy (FT-IR)

Salt formation was confirmed by FT-IR analysis. The patterns of the parent drug were compared to those produced by the salt. Flurbiprofen possesses a peak at 1215 cm^{-1} which signifies the C-F stretch. A characteristic broad peak is also present at $2500\text{--}3300\text{ cm}^{-1}$ due to hydrogen bonding. A signature C=O stretching of the carboxylic acid group present at 1695 cm^{-1} , this signature peak was not present in the salts. Indicative of successful salt formation is the presence of stretching in the $1440\text{--}1335\text{ cm}^{-1}$ region which are characteristic of carboxylic salts (Figure 5.1) (Figure A1, A2 & A3 (Appendix)). FT-IR also confirmed the occurrence of some recrystallised material, which disassociated back to the pure drug form, and as a result was disregarded for further analysis.

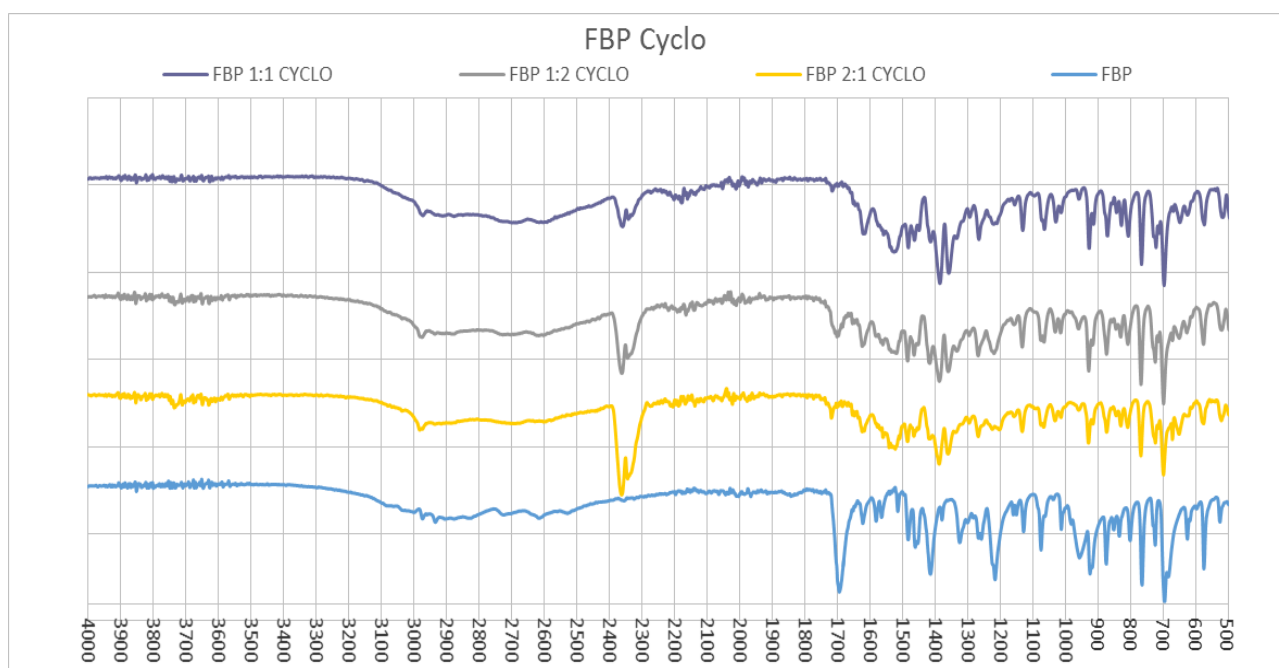


Figure 5.1 FT-IR spectrum for flurbiprofen, and the 1:1, 1:2 and 2:1 FBP-cyclo-propylamine salts

5.1.2 Powder X-ray analysis (PXRD)

The results from X-ray diffraction analysis are presented in figure 5.2. Salt formation was indicated due to differences in the $2\theta^\circ$ angle of 5° - 60° in the X-ray diffraction patterns between the parent drug and the salt forms. Prominent differences in the XRD data pattern for the salts compared to flurbiprofen are observed, from figure 5.2A it is clear that the intensity and locality of some peaks are characteristic as a result of altering the ratio of either component. Figure 5.2B shows the x-ray powder pattern has distinctive variations in location and intensity of the peaks, signifying different crystal structures of the FBP cyclo-propylamine 1:1 salt form as a result of solvent selection. The polarity of the solvent is an imperative aspect that can influence the crystal growth habit. As a change in dipole moment between the crystallisation material and the solvent may change the final habit of the crystal under formation [141]

From figure 5.2C & 5.2D it is clear that the effects of solvent selection, as well as the drug to counter-ion ratio utilised in producing the salt form, has an influence upon the crystal structure of the final product. For example, the material formed from 1:1 salt with an excess of counter-ion added during the recrystallisation process using absolute ethanol (shown as FBP 1:2 C ABS ETOH) is significantly different, when compared to the recrystallisation of the original salt, formed by varying ratios. This signifies that the variations are independent of solvent and original ratio of material. The peaks do display the retention of crystallinity when compared to FBP, however a loss of distinct peaks is evident when comparing the 1:1, 1:2 and the 2:1 ratios of the original salt, and the recrystallised material from the 1:2 and 2:1 salt to the parent drug.

The variation found as a result of solvent selection and the ratio of drug to counter-ion will benefit from single crystal X-ray diffraction to provide more detailed information on the crystal structure. This in turn will provide further information as to the result from the changes to the X-ray patterns of the same materials as a result of interacting with an assortment of solvents [141]

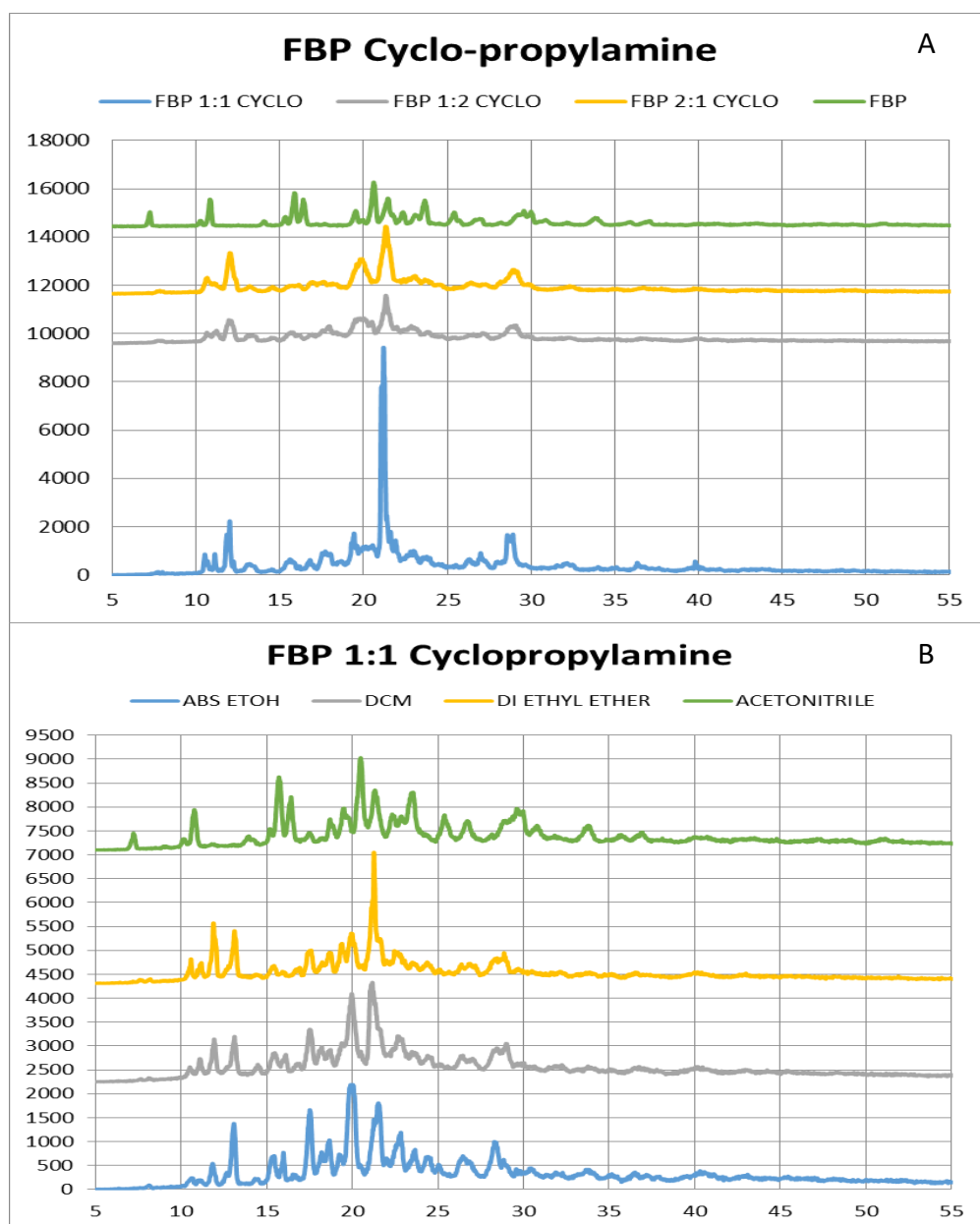


Figure 5.2: XRD data for FBP, FBP cyclo-propylamine 1:1, 1:2 & 2:1 (A-D)

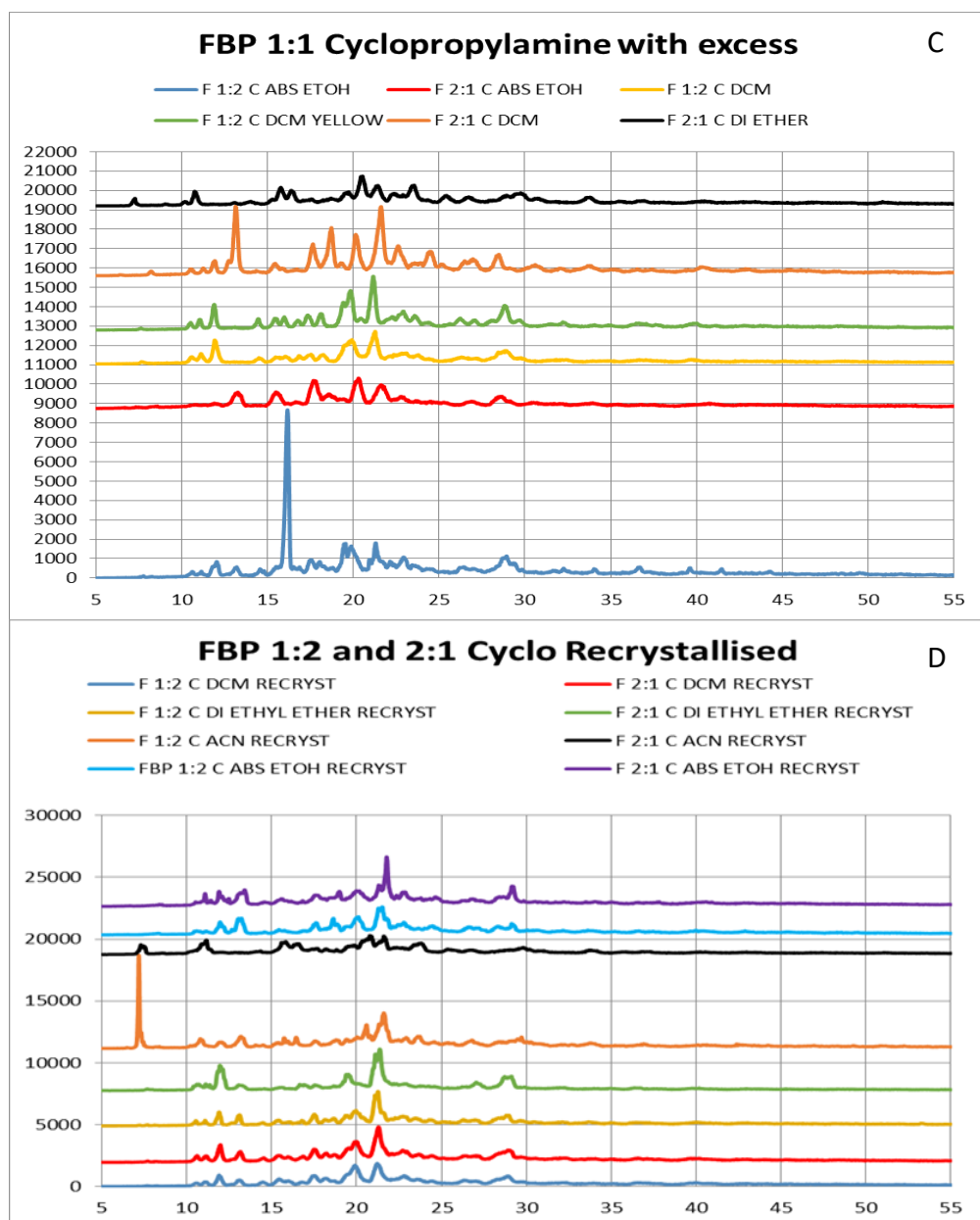


Figure 5.2: XRD data for FBP, FBP cyclo-propylamine 1:1, 1:2 & 2:1(A-D)

5.1.3 Thermal Analysis (DSC & HSM)

Figure 5.3 illustrates an array of melting endotherms, with two clearly observed at approximately 93 °C and 120 °C. From figure 5.3B it is apparent that the solvent selection results in a significant variation in the intensity of the two melting events in comparison to the original 1:1 salt form. FBP Cyclo Acn, FBP Cyclo 2:1 Acn recryst and FBP Cyclo 2:1 Diethyl ether have all shown to result in crystallisation back to the parent drug. The presence of the two melting endotherms is potentially indicative of a polymorph. Previous data published by Supuk *et al* has specified that for a range of salt forms produced from flurbiprofen [56], a single endothermic event materialised, at a different position to the one produced by the pure drug, indicative of salt formation. These two specific melting endotherms are visible under the HSM as two separate events (Figure 5.4, 5.5 & 5.6). This signifies a mixture of material formed as a result of the salt formation process of flurbiprofen and cyclo-propylamine. Additionally, figure 5.3A – 5.3D show the effects of solvent selection, as well as the ratio of original material upon the final product. Figure 5.3A displays the original material was predominantly the second melting endotherm (~120°C), however, the recrystallisation process directs the new material to form primarily the 93°C in most cases. The use of ratios allowed for the influence of starting material upon the mixture to be explored. In cases where the solvent was kept the consistent and the proportion of drug to counter-ion was changed, sizable variances in the melting endotherms are apparent, such as FBP 1:2 C Abs EtOH which produced a melting endotherm at predominantly 120°C, whereas for the FBP 2:1 C Abs EtOH the main endotherm is observed at 95°C. A similar trend is present for the salts recrystallised using DCM also. This behaviour is not as evident for the salts produced from the original 1:2 and 2:1 salt material. Indicating the role of excess flurbiprofen in directing the final material towards the 95°C form. Displaying not only the importance of solvent selection during crystallisation, the ratio of material must be kept consistent as variations during manufacturing can influence the final form for counter ions such as cyclo-propylamine.

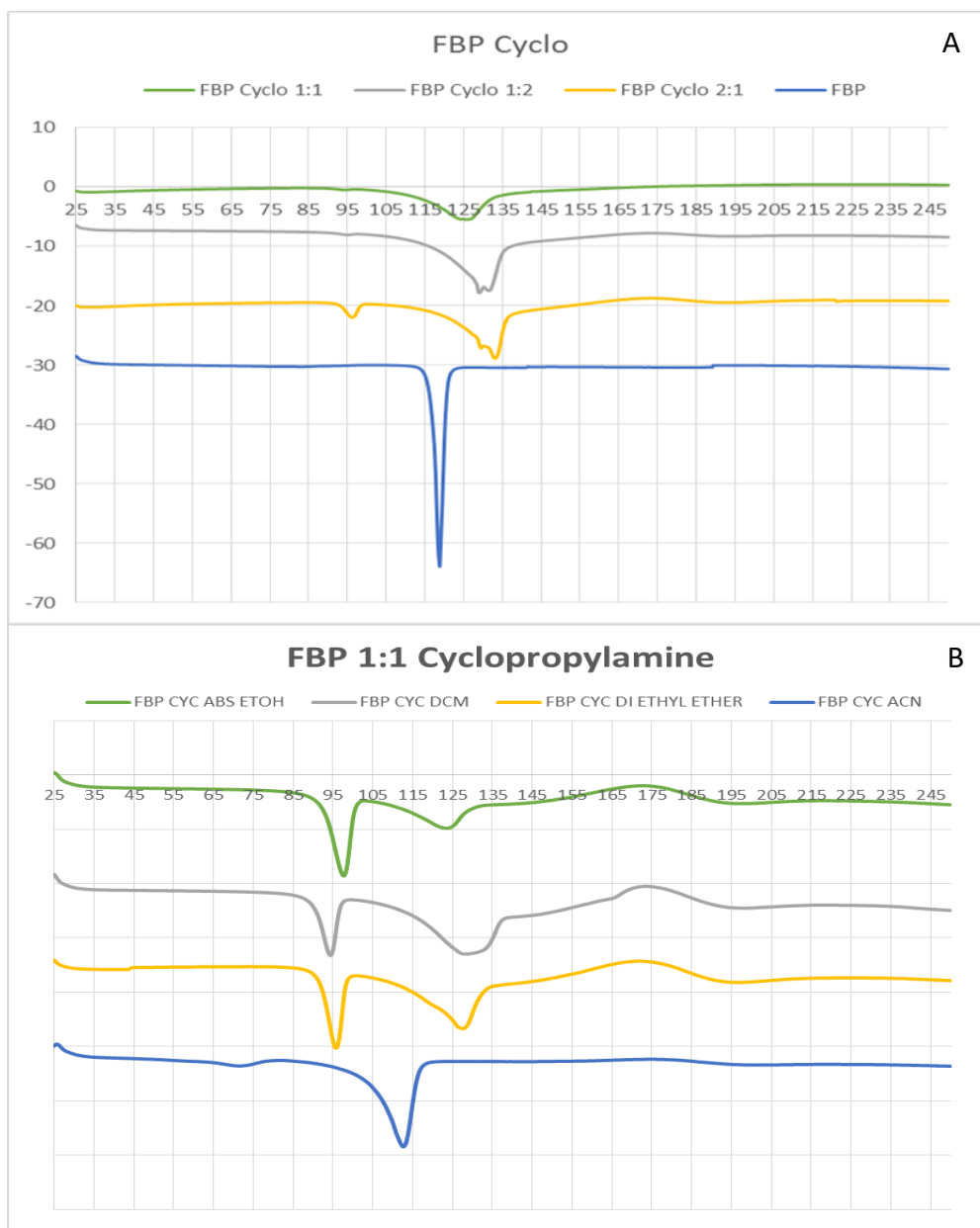


Figure 5.3: DSC data for FBP, FBP cyclo-propylamine 1:1, 1:2 & 2:1 (A-D)

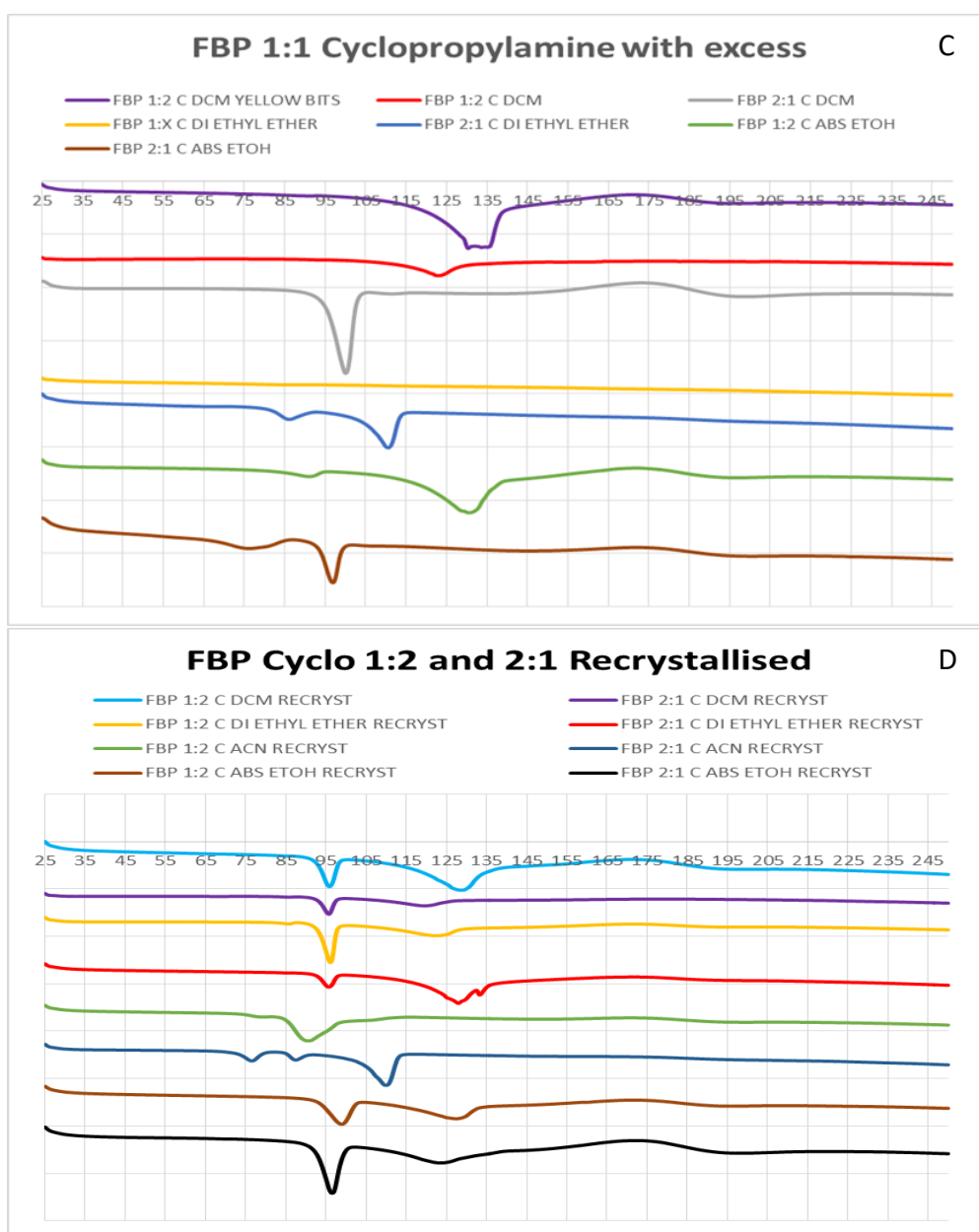


Figure 5.3: DSC data for FBP, FBP cyclo-propylamine 1:1, 1:2 & 2:1 (A-D)

Figure 5.4 illustrates the crystals at 90°C which represents the crystals prior to melting, 95°C and 104°C there is a visible onset of melting present which correlates with the DSC data, with the 95°C especially evident in the corners of the image.

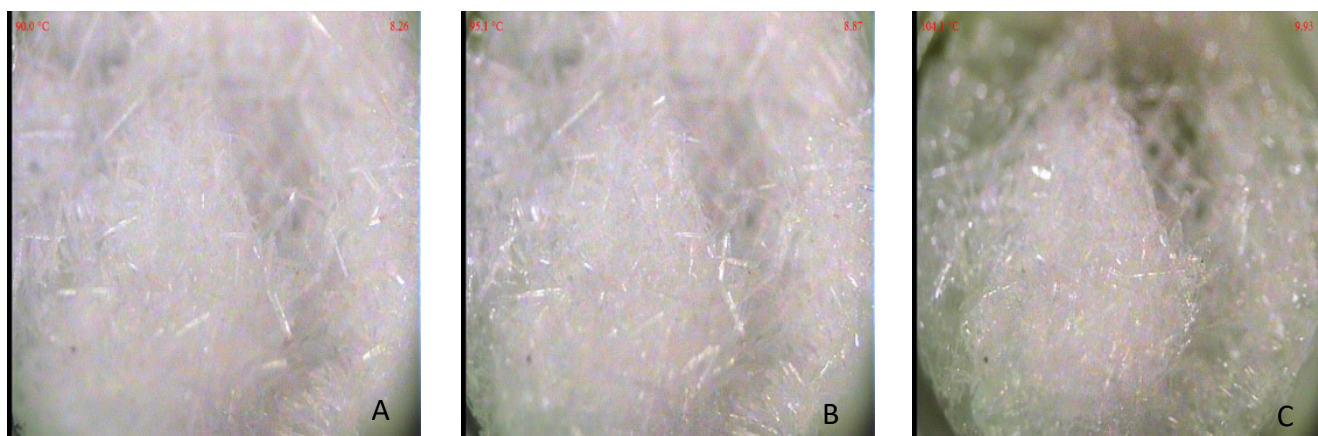


Figure 5.4: HSM for FBP 1:1 cyclo-propylamine at (A) 90°C (prior to melting), (B) 95°C and (C) 104°C

From Figure 5.5 it is observable that at 86.5°C which represents the crystals prior to melting, 95°C and 110°C there is an endothermic event present which correlates with the DSC data

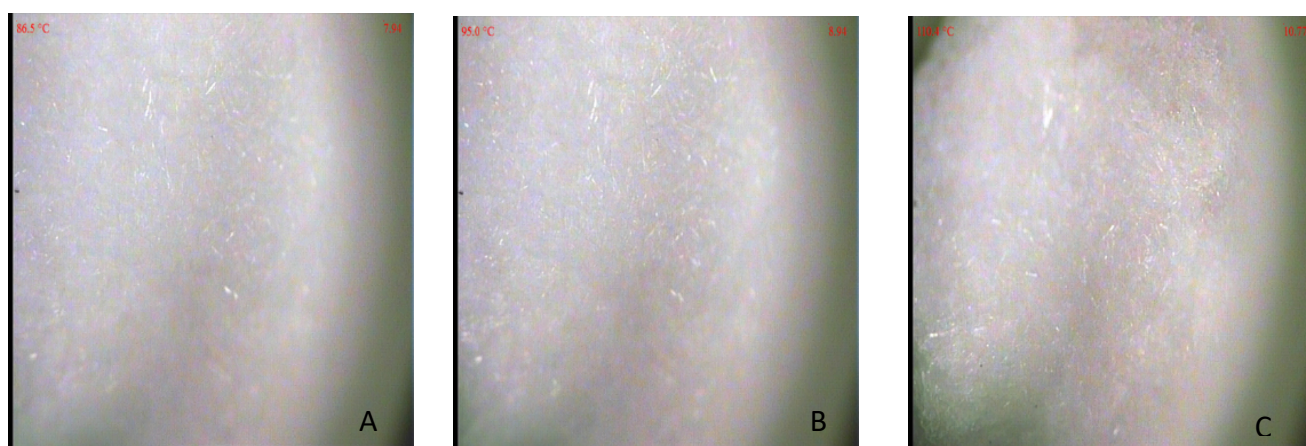


Figure 5.5: HSM for FBP 1:2 cyclo-propylamine at (A) 86.5°C (prior to melting), (B) 95°C and (C) 110°C

Figure 5.6 shows the crystals at 83.5°C which represents the crystals prior to melting; 95°C and 108°C illustrate two separate melting endotherm which correlates with the DSC data.

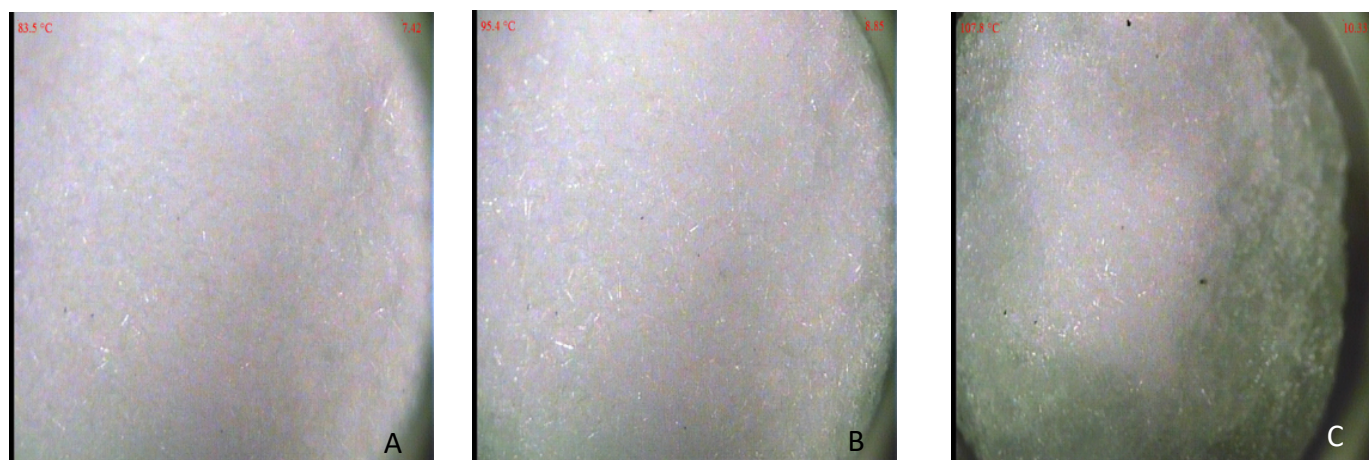


Figure 5.6: HSM for FBP 2:1 cyclo-propylamine at (A) 83.5°C (prior to melting), (B) 95°C and (C) 108°C

5.1.4 Scanning Electron Microscopy (SEM)

SEM was used to evaluate the particle size and shape morphology following salt formation from varying ratios and exploiting a range of solvent for crystallisation of the material. It is well known that the particle shape can be influenced by the solvent. Figure 5.7 displays the particle shape as a result of the salt formation process where needle shaped particles had developed. However, for the 1:2 and 2:1 ratio the particles were smaller in length and breadth. These differences are potentially the result of the drug to counter-ion interactions, as a surplus of either component can result in a quicker formation of the salt form, influencing the particle shape.

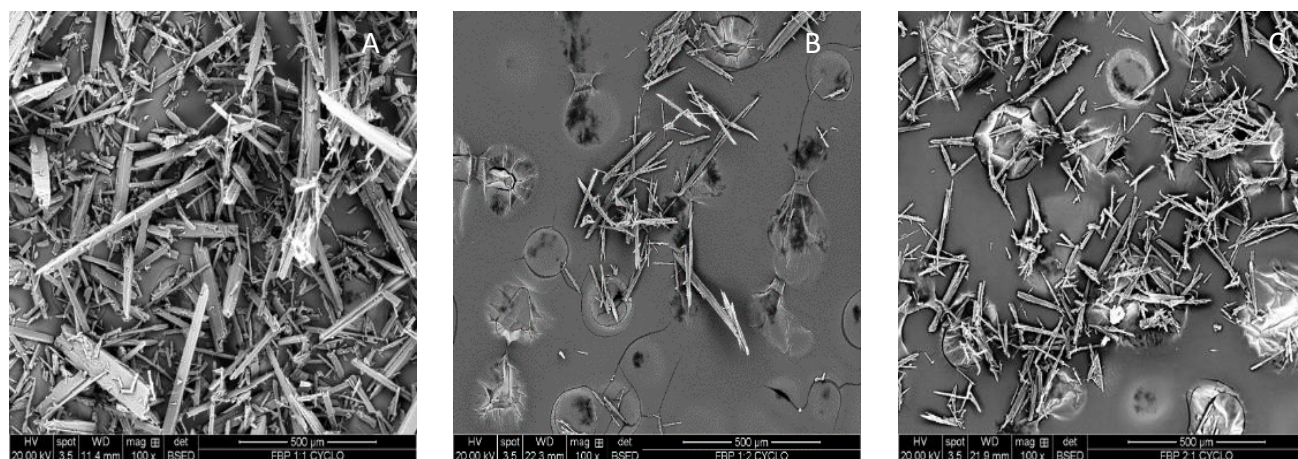
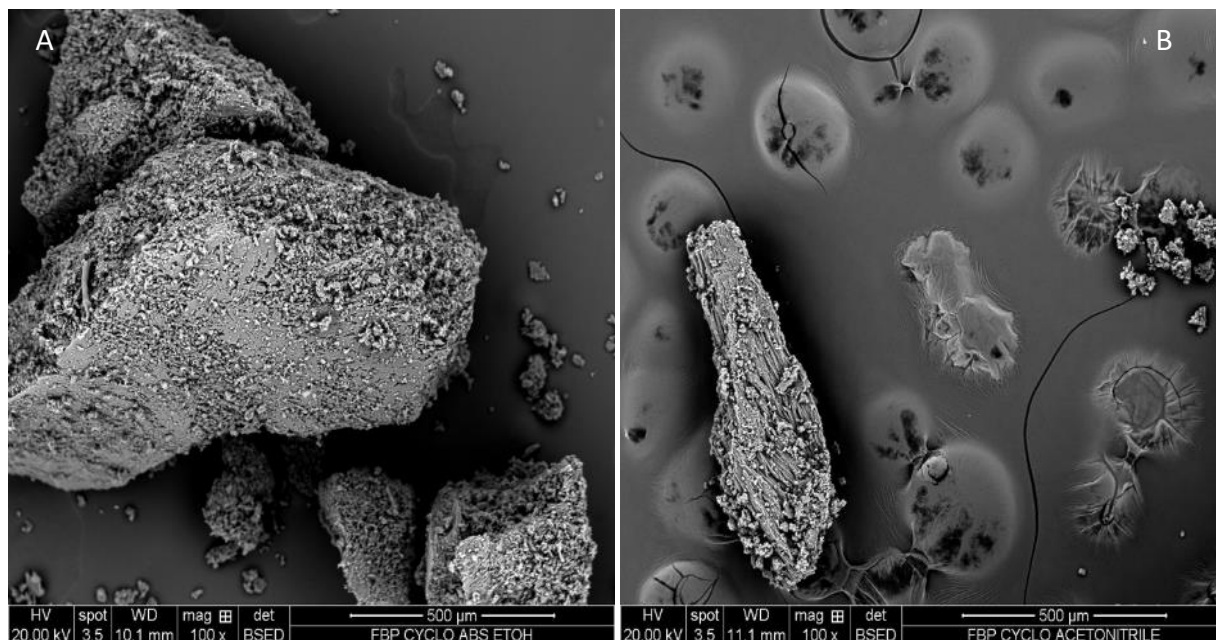


Figure 5.7: SEM Images of FBP cyclo-propylamine (A) 1:1, (B) 1:2 & (C) 2:1 AT X100 magnification

In the pharmaceutical industry, particle shape and size is particularly important, as a common technique utilised in improving bioavailability of APIs is milling. However, this may result in cohesiveness of the material, causing manufacturing difficulties. Furthermore, particle shape has shown to influence the tensile strength of a powder bed as well as the inter-particle cohesive forces [142].

Research by Debord *et al* has indicated that the particle shape has a rather substantial effect upon the compressibility of the material. They discovered that granulated powder holds improved behaviour than the native crystal form, for the same particle size [143].

Presented in figure 5.8, the recrystallisation of 1:1 FBP cyclo-propylamine form, in four individual solvents had developed an array of particle shapes and sizes. According to the ICH classification of particle shapes [144], the material presented in figure 5.8A is of an Equant shape, in contrast to B which is columnar in morphology. Figure 5.8C displayed the particles in a plate form, compared to D which is of an acicular arrangement, similar to the original form



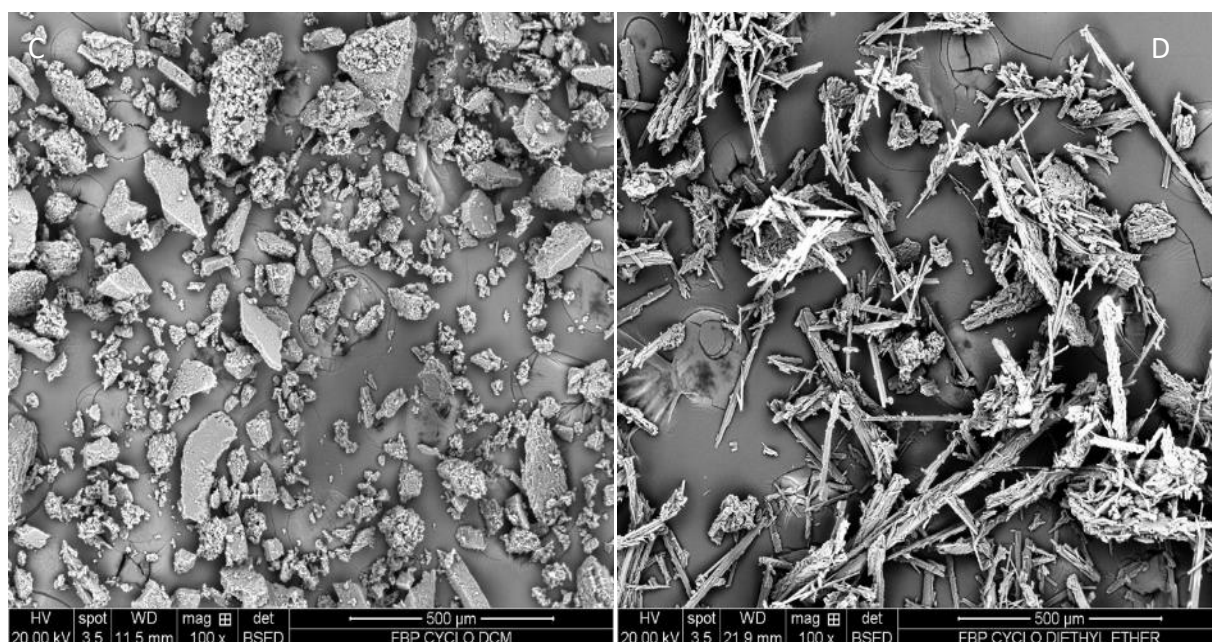


Figure 5.8: SEM Images of the resulting crystals of FBP cyclo-propylamine using various solvents, (A) Absolute Ethanol, (B) Acetonitrile, (C) DCM, (D) Diethyl Ether

Figure 5.9 illustrates the effects of modifying the drug to counter-ion ratio upon the final form. It is apparent that the proportions had a considerable effect upon the particle size as well as shape, as the crystallisation occurred in the same solvent. With the 1:2 ratio displaying a flake shape with a smooth surface, in contrast to the plate shaped particles of the 2:1 version with a rough surface.

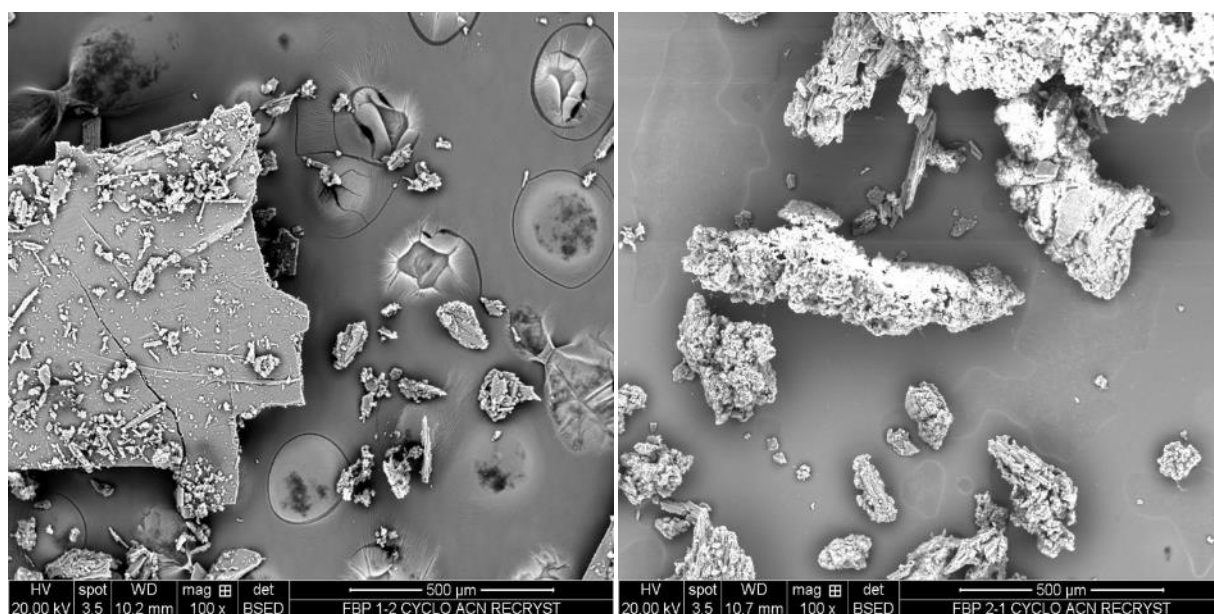


Figure 5.9: SEM Images of the resulting crystals of FBP cyclo-propylamine when adjusting the ratio

5.1.5 Tribo-electrification

Flurbiprofen in its raw form is extremely cohesive and possesses a maximum charge to mass ratio of -293 nC/g. The charge of the original salt form of the various ratios were characterised at 2, 5 and 10 minutes. The produced charge levels at each time point are depicted in figure 5.10. It is clear that the salts have a greater propensity to charge negatively, however the 1:1 and 1:2, salt charged positively when subjected in the shaker for a lower quantity of time. However, the data obtained for the 1:1 salt is noteworthy, as the time in shaker increased, the polarity of the induced charge reversed. The reasoning to this could be, from figure 5.10 it is evident that the percentage adhesion for FBP Cyclo 1:1 at 5 minutes is on average 40%, hence this would change the particle to walls contact dynamic of the system. It is anticipated that the adhered material to the shaker walls would result in a larger probability of the free material being exposed to particle to particle contacts. This may have resulted in a positive charge being produced upon the adhered particles as well as the freely moving particles, which could justify the reversal in polarity. Also, the reduced percentage adhesion at 10 mins, which may have occurred as a result of the change in polarity leading to some adhered particles becoming free. For all three materials, the polarity at 10 minutes is opposite to the parent drug. The charge to mass ratio is less than 10% in comparison to the pure material, which is likely to reduce the probability of material handling problems. The average percentage adhesion data displays that the 2:1 salt had the least affinity to adhere to the walls, with the 1:1 salt exhibiting a higher tendency to stick to the stainless steel walls of the shaker. The adhesion of particles can have an influence on the charge generation, due to particle-wall interactions being replaced by particle-particle contacts and in turn changing the polarity of the resulting charge.

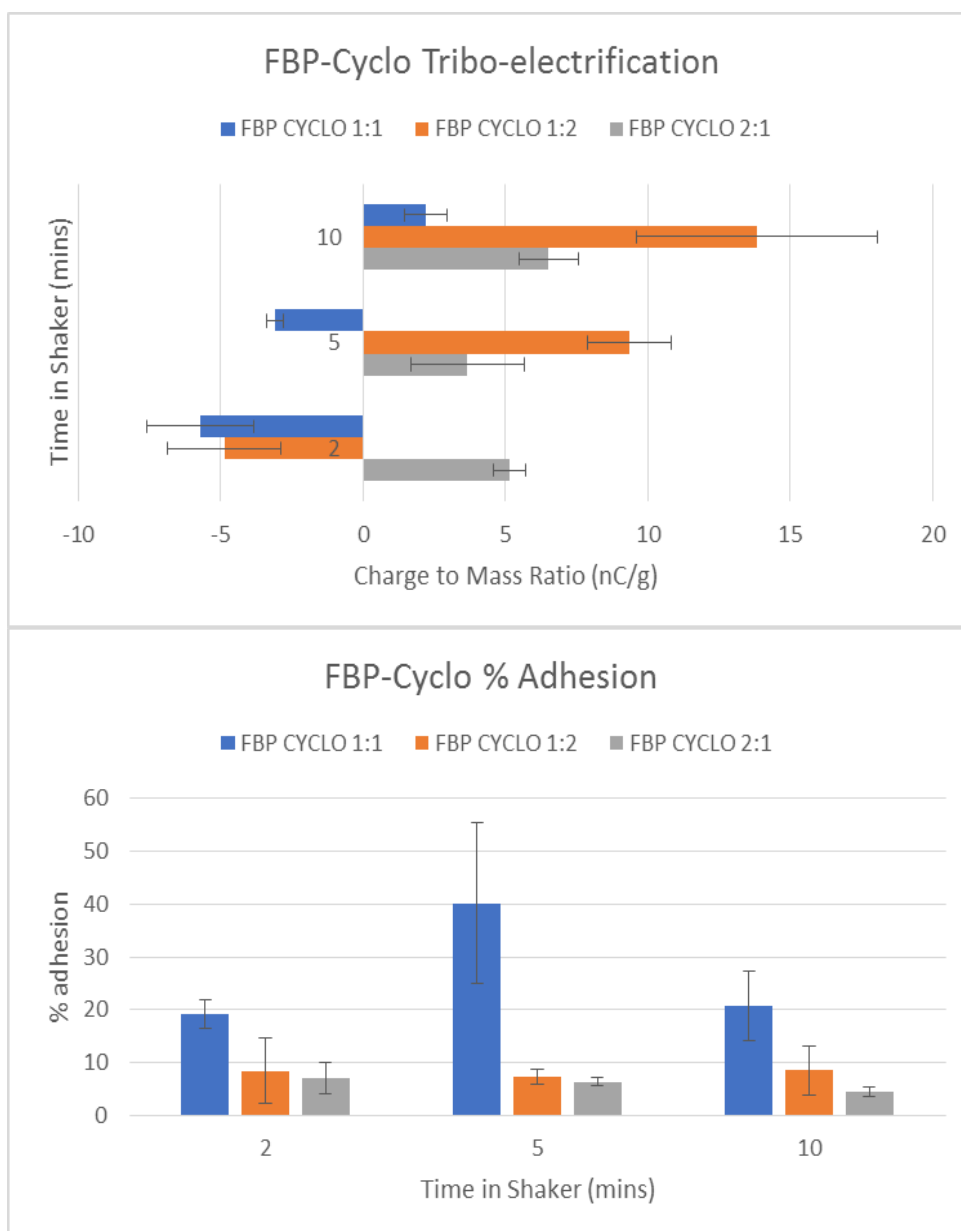


Figure 5.10: Tribo-electrification and percentage adhesion of the original salt form ratios

The following data was obtained from samples which were induced to shaking for 2 minutes only, because of limitations in sample size. For the data obtained for the recrystallised material (Figure 5.11), like the original salt forms, a vast decline in percentage adhesion, as well as the level of charge induced upon the powder in comparison to the pure drug is evident. It is clear that the original salt form has a reasonably low charging tendency at approximately 7 nC/g in either polarity, in contrast to the recrystallised material in the vast majority of cases demonstrated a much larger capability to develop a charge, yet still far lesser than the cohesive flurbiprofen's charging tendency. This may be down to the fact that the original salts

were of a crystal form, though the recrystallised material were in small powdery clusters. However, from comparing the effect of solvent selection for recrystallisation upon the charging tendency of the material, it is evident that the exception is FC Abs EtOH as it has a vastly reduced percentage adhesion in comparison to other solvents, as well as the charging propensity of the material is greatly reduced also. Hence demonstrating that counter ion selection is an important consideration, when considering salt formation, as well as the solvent selection; being pivotal in the crystal habit of a material, which in turn relates to the surface properties which relate to the tribo-electrification propensity.

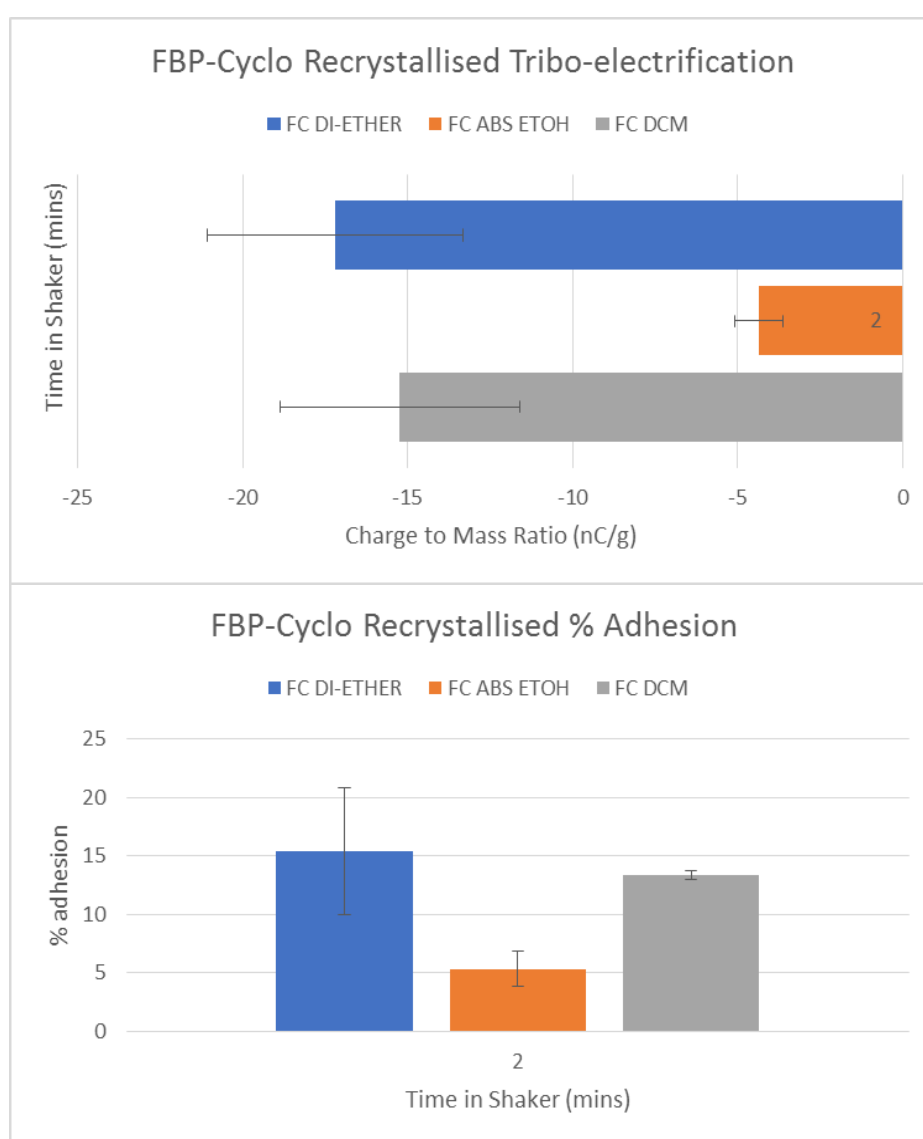


Figure 5.11: Tribo-electrification and percentage adhesion for recrystallised salts

Figure 5.12 and 5.13 exhibit the charging propensity of materials when recrystallised from varying ratios. It is evident that the starting material does affect the final recrystallised form, as in figure 5.12 when the two ratios, 1:2 and 2:1 are recrystallised from the same solvent; diethyl ether, the charging tendency as well as the percentage adhesion data is extremely different. Such high percentage adhesion levels for a material, could result in further complications during processing. From figure 5.11, 5.12 and 5.13 the data for absolute ethanol as a recrystallisation solvent shows its capability to make materials with a low propensity for charging and adhering to the shaker walls, on three occasions for the cyclopropylamine salt; absolute ethanol recrystallised material was one of the lowest charging substance. Illustrating the importance of solvent selection in relation to tribo-electrification of drug salts.

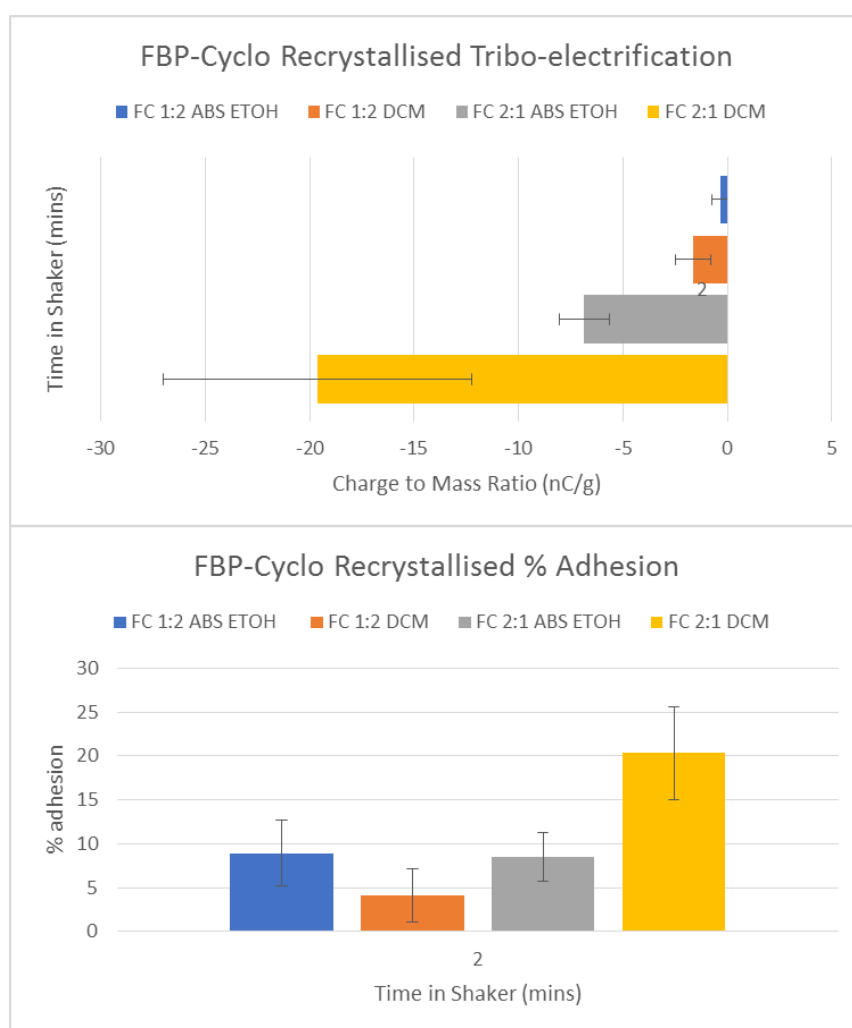


Figure 5.12: Tribo-electrification and percentage adhesion for recrystallised salts at varying ratios

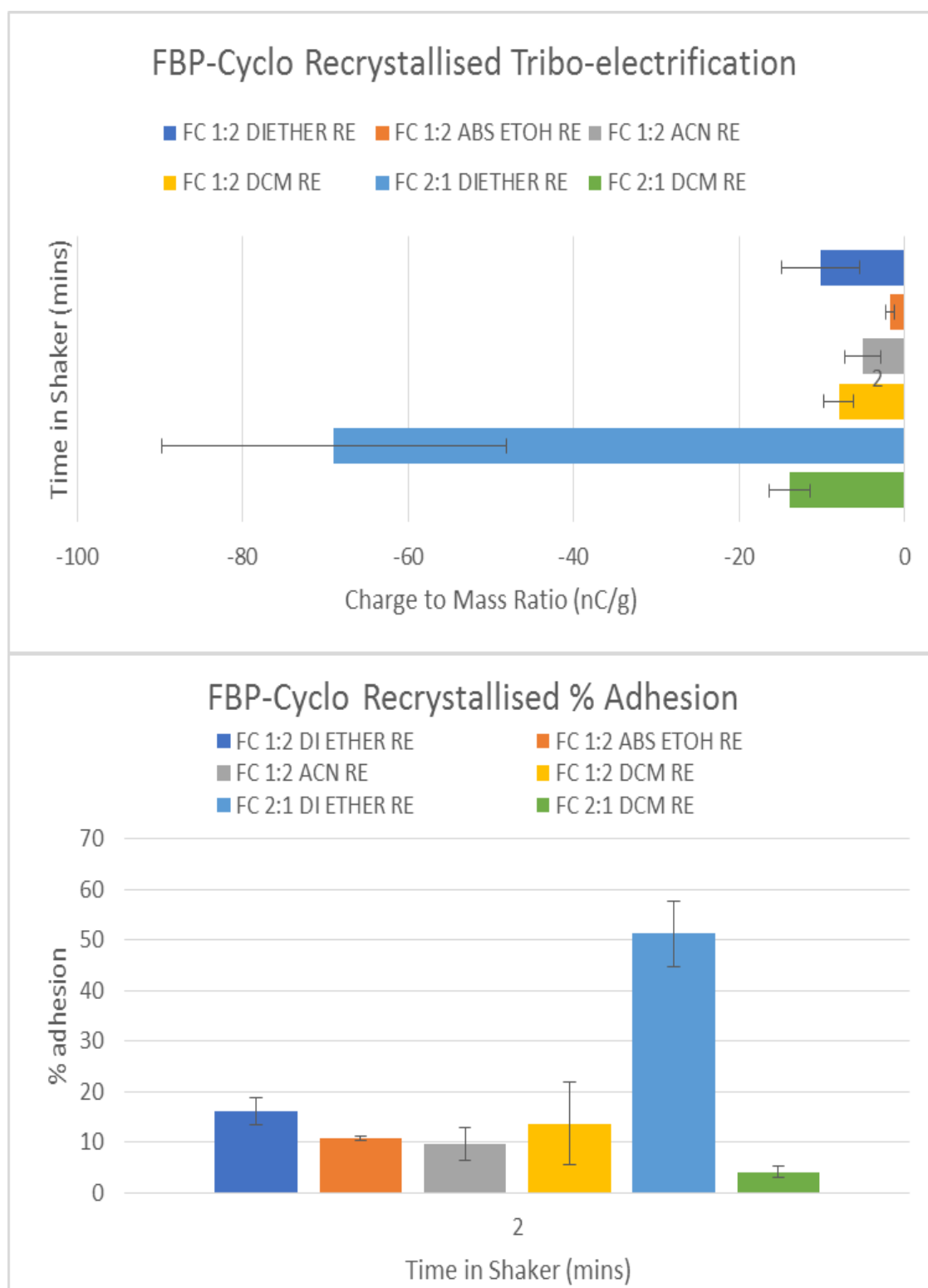


Figure 5.13: Tribo-electrification and percentage adhesion for recrystallised salts made from original salt of varying ratios

5.2 Conclusion

In conclusion, from particle shape, size and morphology to crystallinity and thermal analysis, the solvent selection has shown to influence the crystal habit, variations in the crystal habit have shown to modify the electrostatic behaviour of a material, due to variations in the arrangement of the structure. The solvent selection has an instrumental influence as the polarity of the solvent is one of the most significant aspects in influencing the crystal growth habit, which alters the surface properties of the material and in turn the tribo-electrification propensity.

The DSC and HSM data shows the changes in melting endotherms as a result of solvent selection as the recrystallisation process favoured a majority of the 93°C form, as this is prevalent when there is an excess of flurbiprofen. It could be speculated that the interaction from the extra flurbiprofen molecule with the salt form resulted in this peak formation. The original 1:1 and 1:2 possess an extremely small quantity of the material responsible for the 93°C peak.

The electrostatic charge production of the original salt forms was greatly reduced, in comparison to the parent drug, with the recrystallised material charging slightly higher than the original salt form. It is clear that both solvent selection and ratio of drug to counter-ion play a role in the tribo-electrification propensity of a material. The material produced by recrystallisation from absolute ethanol demonstrated a lower adhesion and charging propensity even when the ratio was changed. Figure 5.12 displays that altering the ratio of drug to counter-ion can play a role in the tribo-electrification tendency of a material as FC 1:2 Di-ether Re possessed an average charge of -10nC/g, in contrast to FC 2:1 Di-Ether Re which possessed an average charge level of -70nC/g. From the results it is evident that the recrystallisation process results in a number of changes to the physio-chemical properties of the drug salt and in turn leading to materials with varying propensity to charge.

6 Properties comparison of flurbiprofen cyclopropyl-ammonium salt with the salt cocrystal and flurbiprofen active ingredient

Background

Salt formation is an effective technique which can be employed during drug development in order to improve the physiochemical and pharmaceutical properties of acidic and basic drugs. Many new chemical entities tend to be poorly soluble and as such are ascribed to class II of the Biopharmaceutical Classification System (BCS). These drugs have high permeability/poor solubility profile [145]. The salt formation process entails careful evaluation of counterion selection due to their ability to alter a number of drug characteristics such as aqueous solubility, degree of crystallinity, hygroscopicity, solid state stability and the capability for producing polymorphs [146]. These properties are important during salt screening due to their influence on bioavailability, toxicity, ease of processing and therapeutic efficacy. Solubility is one of the key aspects of salt screening as an increase in solubility is likely to increase the rate and extent to which the drug can be absorbed in the gastrointestinal tract [145]. It is therefore important to identify a salt form most suitable for development [147]. Although salt formation has been widely applied to improve the aqueous solubility of ionisable drugs [117, 148-150], this research chapter has explored salt formation as a strategy to modify physico-mechanical properties important to pharmaceutical processing including compaction and tribo-electrification properties, as well as aiming to enhance drug absorption through improved aqueous solubility [6, 56, 134, 135, 151, 152]. There has been an increasing interest in engineering the morphology of pharmaceutical materials in order to form the desirable size, shape and surface properties. The internal packing dictates whether the material is crystalline, or amorphous, polymorphic or includes solvent molecules within the crystal structure (hydrates/solvates). These variations in the internal packing result in alterations to the bulk properties such as mechanical and physico-chemical characteristics [58]. A study undertaken by Murtomaa *et al*/ investigated the effect of crystallinity and particle morphology upon the tribo-electrification of dry powders in inhalers, concluding the crystallinity of the material influenced the resulting specific charge [153].

An alternative to salt formation to improve the properties of the drug to aid material handling as well as physicochemical properties is pharmaceutical cocrystals; cocrystals are multicomponent structures consisting of at least two molecules, consisting of a drug (API), and a co-former; held by hydrogen bonding, the coformer can be another active pharmaceutical ingredient (API) or an excipient [9, 10]. The formation of cocrystals has gained substantial interest due their ability to often exhibit better physicochemical properties for the API by altering the structure without affecting the pharmacological properties of the drug [11-14]. The impact of cocrystal formation is not limited to absorption and has the ability to drastically alter the drug's pharmacokinetics and solubility [15]. It can be used as an alternative to salt formation to amend the undesirable properties possessed by APIs. This was investigated by forming a cyclopropylamine salt of Flurbiprofen as well as a Flurbiprofen cyclopropylamine co-crystal which comprised of two Flurbiprofen molecules and one cyclopropylamine molecule, held together by hydrogen bonding. The pharmaceutical and physicochemical properties of the salt and cocrystal were investigated, and a direct comparison was made to establish if cocrystals do provide improved properties over the salt form.

6.1 Results and Discussion

Salt formation was confirmed by DSC, Single Crystal X-ray Diffraction, PXRD and FT-IR presenting the loss of a signature C=O stretch of the carboxylic acid group, present at 1695 cm^{-1} (Figure A4). The salt cocrystal was confirmed by Single Crystal X-ray Crystallography.

6.1.1 Single Crystal X-ray Crystallography

Crystallographic data for the flurbiprofen cyclopropylammonium salt (CCDC 1903341)

and the flurbiprofen: cyclopropylamine 2:1 salt cocrystal (CCDC 1903342) are given in table 6.1, along with data on flurbiprofen from the literature. Flurbiprofen can occur in one of three monotropically related polymorphs as well as a hydrate form, although crystallographic data is only available for form I and form III polymorphs [154-157]. Flurbiprofen utilised in this work was form I based on powder X-ray data and melting point, by reference to published data.

Table 6-1 Crystallographic data for flurbiprofen, flurbiprofen cyclopropylamine (1:1) salt and flurbiprofen cyclopropylamine (2:1) salt cocrystal

	Flurbiprofen form I*	Flurbiprofen form III**	Flurbiprofen cyclopropylamine (1:1) salt	Flurbiprofen cyclopropylamine (2:1) salt cocrystal
empirical formula	C ₁₅ H ₁₃ FO ₂	C ₁₅ H ₁₃ FO ₂	C ₁₈ H ₂₀ FNO ₂	C ₃₃ H ₃₂ F ₂ NO ₄
molecular weight	244.25	244.25	301.35	545.63
temperature (°K)	100	123	100	150
wavelength (Å)	0.71073	0.71073	0.71073	0.71073
crystal system	triclinic	monoclinic	monoclinic	orthorhombic
space group	<i>P</i> - 1	<i>P</i> 2 ₁ /n	<i>P</i> 2 ₁ /n	<i>P</i> 2 ₁ 2 ₁ 2 ₁
<i>a</i> (Å)	9.2003 (18)	5.7214(9)	6.1055 (3)	6.1716 (4)
<i>b</i> (Å)	12.683 (3)	38.715(6)	15.9502 (14)	15.4751 (11)
<i>c</i> (Å)	5.7271 (11)	5.9808(10)	16.3340 (14)	29.551 (2)
α (degrees)	83.16 (4)	90	90	90
β (degrees)	106.87 (3)	111.655(2)	97.666 (5)	90
γ (degrees)	106.90 (3)	90	90	90
<i>V</i> (Å³)	611.4(3)	1231.3(3)	1576.5 (2)	2822.3 (3)
<i>Z</i>	2	4	4	4
D_x (g cm⁻³)	1.327	1.318	1.270	1.2840
μ (mm⁻¹)	0.097	0.097	0.090	0.092
<i>F</i>(000)	256	512	640.0	1152.664
GOF	1.099	1.080	1.187	1.0541
Reflections/data/parameters	2430/170	3061/175	3581/222	7738/365
<i>R</i>_{int}	0.0168	0.0520	0.0243	0.0559
<i>R</i>₁	0.0429	0.0669	0.0553	0.0609
<i>wR</i>₂	0.1264	0.1597	0.1269	0.1125

*from Hachula B. (2018) Spectrochim. Acta Part A 188 189 – 196

**from Grzesiak, A.L., Matzger A.J. (2007) J. Pharm. Sci. 96 2978-298

The intervening CH group has alternative sites labelled C21 and C22, bearing pendant methyl groups C31 and C32. The variation in direction of approach imposes disorder on the bonded atom of the fluorophenyl ring, C4 and C4P, which can still be discerned in the adjacent atom sites C5, C5P and C9, C9P. The distances between alternative sites are 0.822, 1.048, 0.571, 0.500 and 0.533 Å, respectively. After that, the diminution in distances allows both alternatives to be covered by anisotropic displacement around a compromise position. The occupancy factor for the major sites, named first, is 0.763(5).

Flurbiprofen free acid is arranged within form I crystals as infinite 1D chains of dimers, hydrogen bonded via O-H ... O of the two carboxylic acids. As previously described for gemfibrozil organic amine salts [135], [152] formation of the salt transforms the packing arrangement; in the case of the flurbiprofen cyclopropylammonium salt crystal to a hydrogen bonded supramolecular structure of the Type III ladder-like chains as previously described [158], [159]. The ladder is made of hydrogen bonded alternating hydrophobic and hydrophilic domains of cation and anion, involving N-H...O hydrogen bonds, forming the “rails (stiles)” of the ladder, with between-chain N-H...O hydrogen bonds forming the “rungs”. The two chains of the ladder and the adjacent pair of hydrogen bonds form a hydrogen bonded ring defined as $R_4^2(8)$ and $R_4^4(12)$ rings (Type III) in the case of the cyclopropylammonium salt (Figure 6.1).

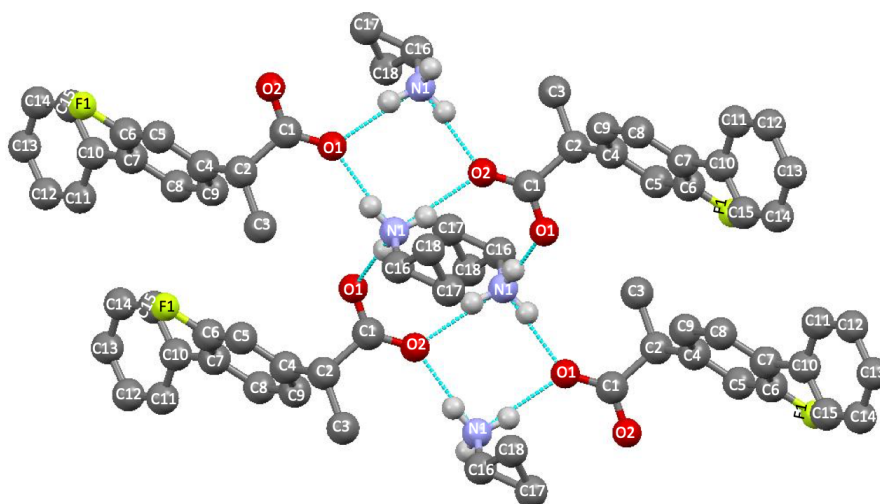


Figure 6.1 Hydrogen bonded ladders built from alternating $R_4^2(8)$ and $R_4^4(12)$ rings in the cyclopropylammonium salt of flurbiprofen with atom labelling. Hydrogen atoms not involved in hydrogen bonding and disordered alternative sites with lower occupancy have been omitted for clarity.

For the flurbiprofen cyclopropylamine 2:1 salt cocrystal, the asymmetric unit contains a molecule of the free acid, the flurbiprofen anion and the protonated cyclopropylamine (Figure 6.2).

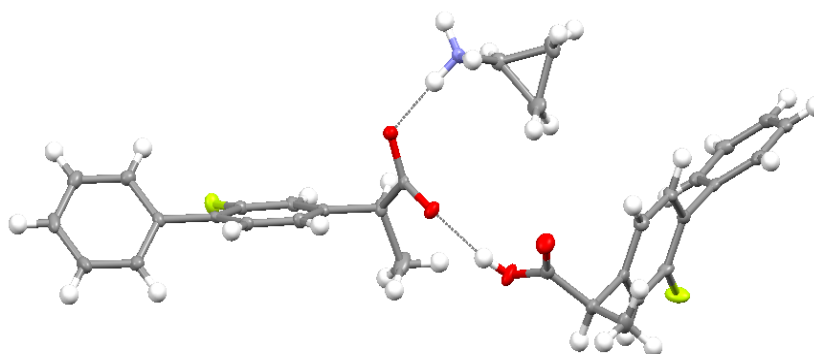


Figure 6.2: CABP arrangement within asymmetric unit for flurbiprofen cyclopropylamine 2:1 salt cocrystal

This is a conjugate acid-base pair (CABP) interaction structure as described for other pharmaceutical and pharmaceutical-like materials, [160-163] with charge-assisted hydrogen bonds. Chains of hydrogen bonded anion-cation interactions are observed, supplemented by hydrogen bonding from the free acid to the anion. A different hydrogen bond arrangement to that of the salt is enabled by the presence of the second flurbiprofen in the unit cell, yielding Type II ladders and based on R_4^3 (10) rings (Figure 6.3). Hydrogen bonds are shown in blue and hydrogen atoms not involved in hydrogen bonding have been suppressed for clarity. On the left side, the second (unionised) flurbiprofen of the unit cell is omitted to show the supramolecular ladder structure of R_4^3 (10) rings. On the right side, only one upright of the next ladder is shown, so that the acceptance of an additional hydrogen bond from an unionised flurbiprofen molecule in the unit cell shows up clearly. In the centre, there is a zone of layered, overlapping aromatic rings from flurbiprofen anions and unionised flurbiprofen molecules.

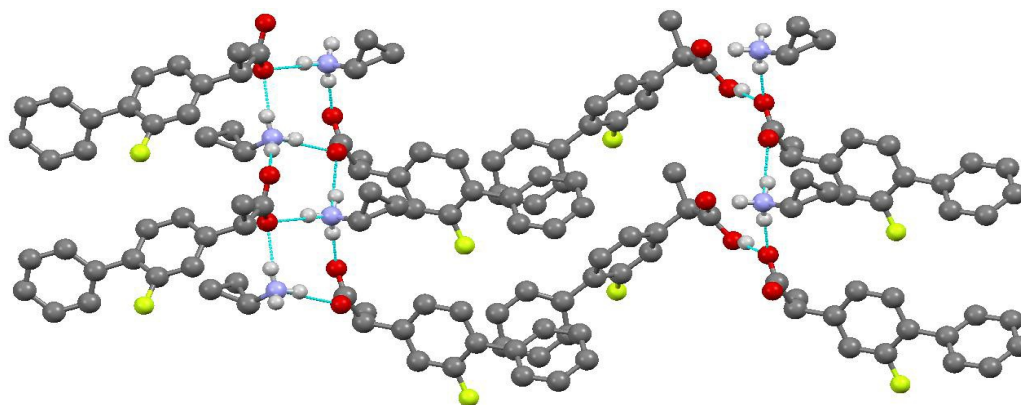


Figure 6.3: Partial structure of arrangement of flurbiprofen and cyclopropylamine within the 2:1 co-crystal to show the three different sorts of intermolecular interaction.

Two of the three-unit cell axial lengths are very similar: the change from salt to salt cocrystal is +1 % for a , -3 % for b and +81 % for c . (Table 6.1). The similarity is attributable to the presence of hydrogen-bonded ladders in both structures, and similar geometry of the hydrogen bonds. While in both structures O1 accepts two hydrogen bonds, in the salt O2 accepts only one, leaving its other lone pair unoccupied. In the salt cocrystal the carboxylic acid group donates another hydrogen bond to this atom, forming a CABP with surprisingly little disturbance to the existing hydrogen bonds. Between the hydrogen bonded ladders, the co-crystal has regions of overlapping aromatic rings (Figure 6.3).

Geometric parameters of the hydrogen bonds in the salt and salt cocrystal are listed in Table 6.2. In their analysis of sodium hydrogen bis(naproxate) methanol solvate, Peramulla and Sun [160] demonstrated the key structural importance of the CABP, linking one unionised naproxen molecule to an adjacent naproxen anion with its short O-H...O distance of only 2.48 Å puts it into the category of low barrier strong hydrogen bonds. In contrast, the corresponding O-H...O hydrogen bond in the flurbiprofen CABP is straight but not particularly short (2.643 Å). The difference may be attributable to the differences in the steric effects of the counter ions. The naproxen CABP is accompanied by a single atom, Na⁺; in the present

flurbiprofen structure the RNH_3^+ ion makes three charge-assisted hydrogen bonds with steric demands of their own that resist deformation.

Table 6-2: Selected hydrogen bond geometries for flurbiprofen, flurbiprofen cyclopropylamine (1:1) salt and flurbiprofen cyclopropylamine (2:1) salt cocrystal

	Atoms D-H...A	Distance D..A (Å)	Distance H...A (Å)	Angle D-H...A (degrees)
	N1-H1A...O1	2.775	1.88	167
Salt	N1-H1B...O2	2.689	1.79	168
	N1-H1C...O1	2.745	1.86	166
	N1-H1A...O1	2.753	1.87	164
Co-crystal	N1-H1B...O2	2.773	1.86	178
	N1-H1C...O1	2.765	1.87	167
	O4-H4...O2	2.643	1.81	168

There is a significant difference in the crystal symmetry. The salt is necessarily racemic, being in space group $P2_1/n$ with an inversion centre. The salt cocrystal in space group $P2_12_12_1$ lacks one: as determined, all copies of the flurbiprofen anion have chirality S at its asymmetric carbon atom while all copies of the free acid have R.

The salt cocrystal exhibits less disorder compared to the salt and has a density of 1.282 g cm^{-3} , compared with 1.270 g cm^{-3} for the salt. Improved packing in the salt cocrystal may be a reason for the success of the facile preparative method despite its similarity to the method used to recrystallize the salt: a sample of the salt was dissolved in methanol, producing a solution that had the “wrong” stoichiometry for the co-crystal. Since it was 2.5 times more dilute than the solution used for the salt and it was warmed, any small seed crystals of the salt would have been eliminated. The slow process of solvent evaporation and crystal growth have allowed the co-crystal with its smaller molar solubility in water (Table 6.3), and presumably also in methanol, to form preferentially.

*Table 6-3: Physical properties for flurbiprofen, flurbiprofen cyclopropylamine (1:1) salt and flurbiprofen cyclopropylamine (2:1) salt cocrystal**

	Flurbiprofen	Flurbiprofen cyclopropylamine salt	Flurbiprofen: cyclopropylamine 2:1 salt cocrystal
Melting point (onset, °C)	114.2 ± 0.26	130.0 ± 0.66	137.4 ± 0.40
Melting peak (°C)	115.8 ± 0.24	134.7 ± 0.32	142.65 ± 0.45
Melting enthalpy (J/g)	-104.6 ± 1.25	-128.7 ± 3.71	-160.6 ± 3.44
Aqueous solubility (mg/mL, 37 °C)	0.013 ± 0.003	7.911 ± 0.476	11.567 ± 0.445
pH of saturated solution	4.84 ± 0.042	7.135 ± 0.177	7.485 ± 0.021

*mean ±s.d., n = 3

6.1.2 Solid state characterisation

Powder X-ray diffraction patterns are shown in figure 6.4. Changes to the crystallographic structure consequent to salt formation result in differences in the X-ray diffraction patterns between 5°-60° at angle 2θ° concerning the drug, salt and the salt cocrystal. Notable differences in the PXRD data pattern can be observed. Some identifiable peaks in flurbiprofen such as 2θ angles 7.1, 16.4 and 29.7 are either absent or of different intensity indicating a

change in the crystal structure of the material as a result of salt/salt cocrystal formation, also the addition of a small peak at 40.5 2θ angle differentiates between the materials.

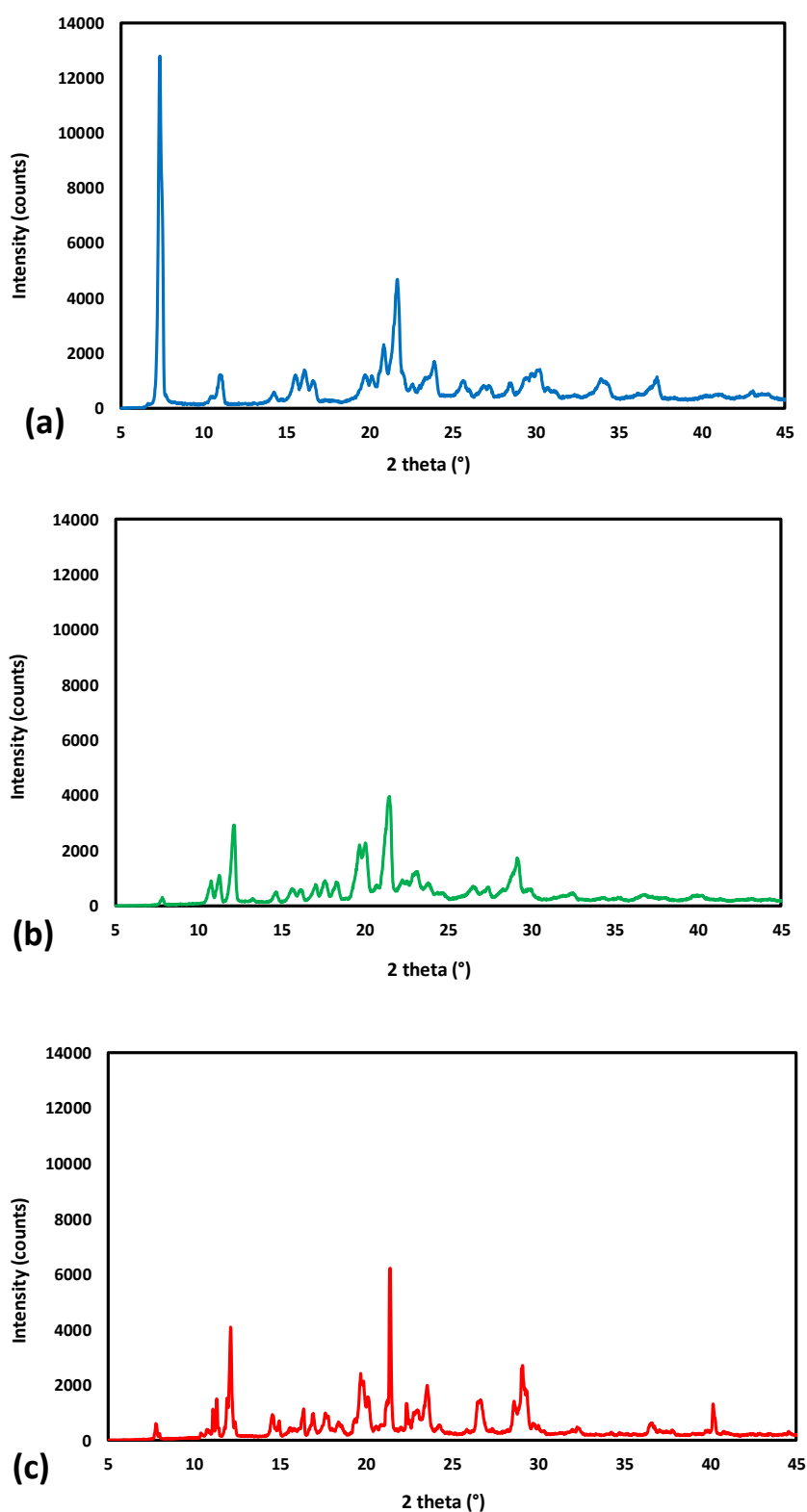


Figure 6.4: Powder XRD data for flurbiprofen (a), flurbiprofen cyclopropylamine (1:1) salt (b) and flurbiprofen: cyclopropylamine (2:1) co-crystal (c)

Table 6.3 indicates the onset and the melting peak for the salt and salt cocrystal compared to flurbiprofen. The salt cocrystal and salt show an onset of melting at a higher temperature than the parent drug, an increased melting point indicated that the newly formed material is thermodynamically stable [164]. The relative magnitudes of the melting enthalpies were salt cocrystal > salt > parent flurbiprofen, which may be associated with the more complex arrangement of hydrogen bonding in moving from the parent acid to the salt and the salt cocrystal. Flurbiprofen exhibited a plate-like in morphology (Figure 6.5a) while the salt is acicular in shape (Figure 6.5b). The salt cocrystals however produced prism and cube-like morphologies (Figure 6.5c). It was interesting to note the differences between the salt and salt cocrystal morphologies as this may well have an effect on the handling and compatibility of the material formed.

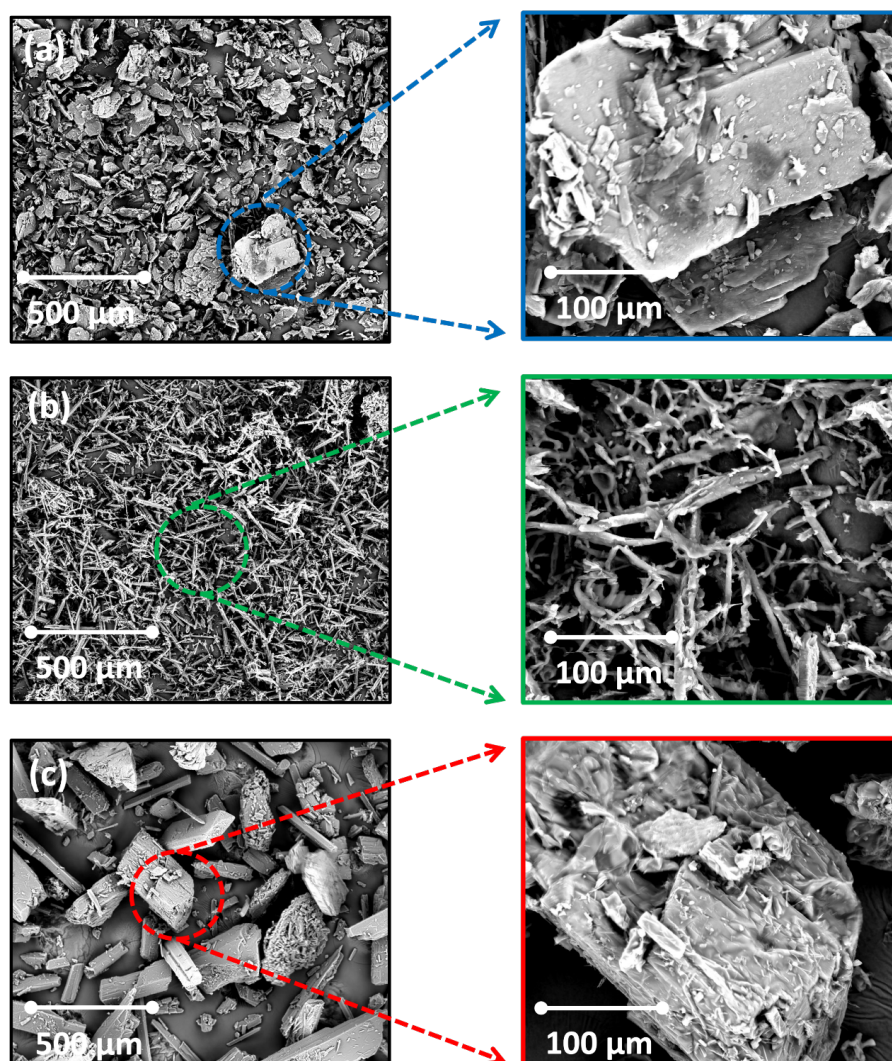


Figure 6.5: SEM images of (a) flurbiprofen (b) salt of flurbiprofen using cyclopropylamine (c) flurbiprofen cyclopropylamine salt cocrystal 2:1 ratio, Depicted at x100 and x500 magnifications.

6.1.3 Solubility

The saturated solubilities for the drug, salt and salt cocrystal are presented in table 6.3. The solubility data for FBP is in line with literature, 0.0051 mg/mL [165] and 0.024 mg/ml [166]. Table 6.3 shows the impact of the counterion in significantly improving the solubility. The solubility of the salt was increased by 600-fold whereas the salt cocrystal solubility increased by nearly 900-fold in comparison to the acidic drug. This may well have significant effects on the bioavailability of the drug and as such gives a formulator as choice into considering the other physicochemical properties of either form (i.e. salt or salt cocrystal) with regards to making an appropriate formulation. The apparent solubility benefit of the salt or salt cocrystal is likely simply an effect of the pH of the solution created by dissolving these compounds. Typically, weak acid-weak base salts would be expected to dissolve to form a buffered solution with resultant solution pH given by the mean of the pKa of the acid and the amine. Indeed, the solubility found is of the same order of magnitude as that found in the range pH 7 – 8 when a pH-solubility profile is determined for flurbiprofen at room temperature, by adjustment of solution pH with sodium hydroxide, or by use of phosphate buffers [6, 167]. The pH observed here for the saturated solutions is also a consequence of salt and salt cocrystal disproportionation. It has been found for organic amine and ammonia salts of flurbiprofen that disproportionation occurs resulting in precipitation of free acid and consequently the excess amine produces a solution pH higher than theoretical pH.

6.1.4 Mechanical Properties

Flurbiprofen, flurbiprofen cyclopropylamine salt and flurbiprofen cyclopropylamine salt cocrystal have a yield pressure in the region of 39-55 MPa (Table 6.4), similar to that reported for microcrystalline cellulose and indicating that the materials are all plastically deforming [168]. Elasticity was observed during the investigation [169]. The elastic recovery is the ability of the material to return back to its original shape when the load is removed. Yield pressure was also investigated, defined as the stress at which the material begins to deform plastically. Additionally, the solid fraction is the ability of a material to withstand a longitudinal stress. All three forms were challenging in terms of producing a well formed compact, with the most challenging being the flurbiprofen cyclopropylamine salt cocrystal, where splitting of the

compact laterally occurred as it emerged from the die. This was followed by flurbiprofen, where severe lamination was observed, flurbiprofen has a density of $1.2854 \pm 0.01 \text{ g/cm}^3$. The flurbiprofen cyclopropylamine salt was able to form a complete compact, although the tensile strength of the salt compact was low (0.82 MPa), severe sticking to the punches occurred. The challenges faced during powder compaction can be attributable to the varying powder properties of each material, such as particle shape (figure 6.5), resulting in variations in the stresses subjected to the powder bed. Nevertheless, it may be possible to produce a blend of this form of the drug with small amounts of added excipients to aid better compressibility and compactibility properties.

Table 6-4: Mechanical Properties of FBP, salt and salt cocrystal flurbiprofen, flurbiprofen cyclopropylamine (1:1) salt and flurbiprofen cyclopropylamine (2:1) salt cocrystal

Material	Compaction Pressure (MPa)	Tensile Strength (MPa) at target 85% Solid Fraction	Solid Fraction Obtained (%)	Yield Pressure (MPa)	Elastic Recovery (%)
Flurbiprofen	50	0.09 ± 0.05	81	51	7
FBP C-prop Salt	62	0.82 ± 0.15	83	55	5
FBP C-prop Co-crystal	37	-	83	39	10

The potential relationship between arrangement of molecules within the crystal and compaction properties has been explored [134, 136, 170-182] with a view that improved pharmaceutical processing may be achieved by appropriate selection of a crystal form. In particular the presence of well-defined slip planes within the crystal structure may enable plastic deformation under applied shear stress [183]. The slip planes occur where there are close-packed molecules arranged, often through hydrogen bonding, within parallel planes, within the crystal lattice, along with weak interplanar interactions between those parallel planes of molecules. Visual examination of the arrangement of molecules in packing diagrams suggested the possible presence of putative slip planes in flurbiprofen cyclopropylamine salt where the presence of flurbiprofen and the counterion arranged in layers of alternating $R_4^2(8)$ and $R_4^4(12)$ hydrogen-bonded rings with no inter-layer hydrogen bonding were noted (Figure 6.6A/ Figure A5). Slip planes were much well less defined in the case of the salt cocrystal even though layers of hydrogen bonded flurbiprofen anion, protonated flurbiprofen and the

counterion were present, arranged in a supramolecular structure of $R_4^3(10)$ rings with no strong interactions between the layers. The putative slip planes in the case of the salt cocrystal were more zig-zag in nature (Figure 6.6B/ Figure A5) or challenging to observe. These differences in slip plane arrangements may be associated with the different compaction behaviours observed, the better defined slip planes in the salt crystal lattice enabling better plastic deformation and compaction compared to the salt cocrystal.

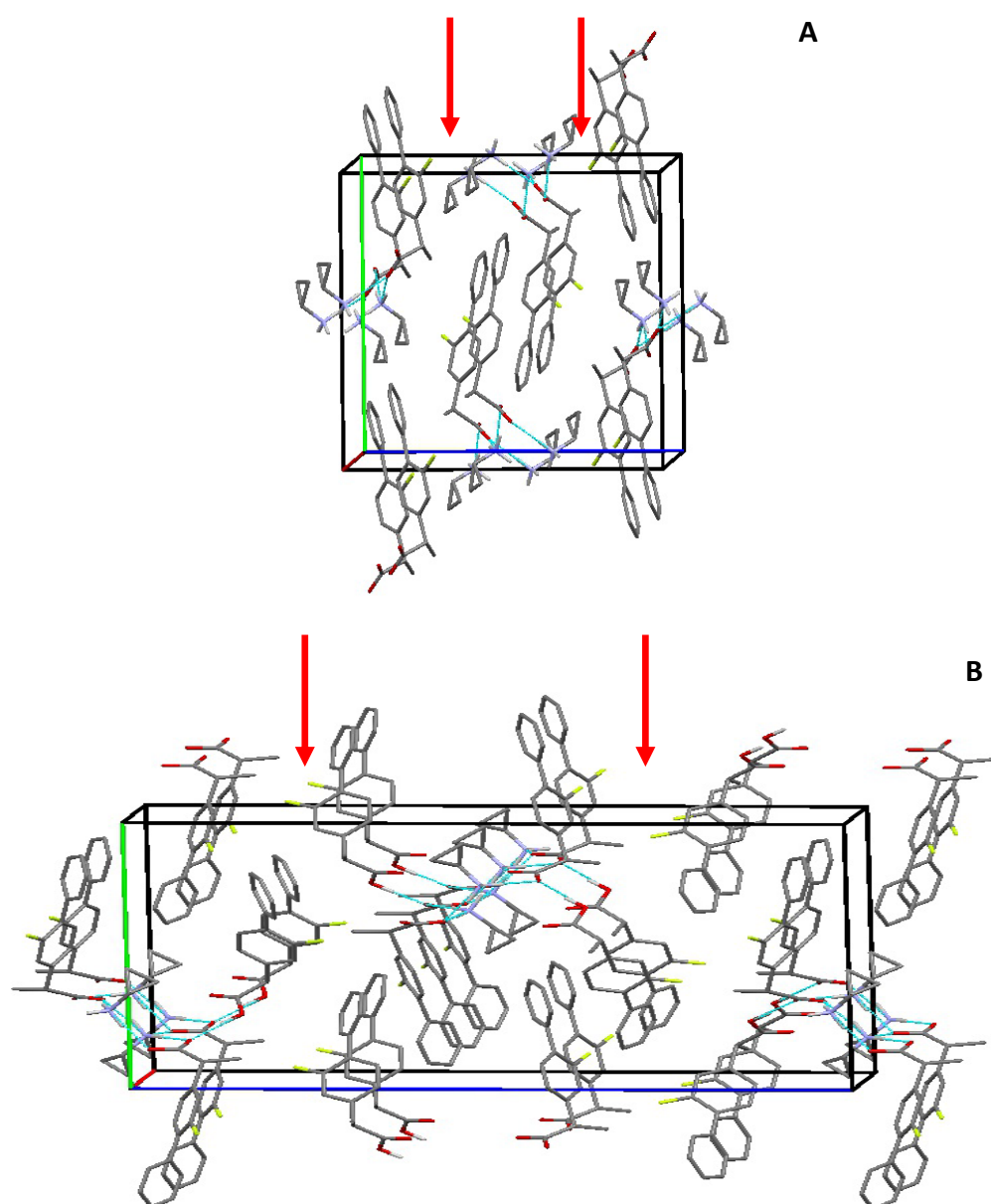


Figure 6.6: Packing diagrams for salt projecting down the *b* axis (a) and salt cocrystal projecting down the *b* axis (b). Arrows indicate position of potential slip planes.

6.1.5 Tribo-electrification and adhesion behaviour

Flurbiprofen is a commonly known cohesive material with an ability to acquire high levels of charge as well as adhering to surfaces within a relatively short period of time [76]. Due to limitations in the quantity of the salt cocrystal, a larger sieve fraction of 150-250 μm was utilised for the tribo-electrification and adhesion study for the pure drug, salt form and the salt cocrystal to maintain consistency at a time interval of 2 minutes. The drug, salt and salt cocrystal charged negatively (figure 6.7A). Flurbiprofen had a significant charge to mass ratio of -72 nC g^{-1} in comparison to the salt which possessed a much lower charging ability (-15 nC g^{-1}). Salt formation has previously been shown to modify the charging propensity of a material [56]. It was also interesting to note here also that the tribo-electrification propensity of the salt cocrystal was less than half the charge of the salt (-6 nC g^{-1}). This implies that the salt cocrystal formed had improved handling properties as compared to the salt and drug.

The charging propensity links to the tendency of the material to adhere to the walls of the shaker [184]. Flurbiprofen showed approximately 53 % adhesion to the stainless-steel shaker walls in contrast to the salt form which had 19 % of adhered material (Figure 6.7B). An increase in adhesion suggests an increase in the probability of the particle to particle interaction due to the lateral motion of the shaker. The salt cocrystal exhibited a considerably reduced adhesion tendency with just 5.6 % loss, a decrease by nearly 10-fold in relation to drug. This may have implications with regards to segregation and uniformity with the powder handling/mixing process in the formulation process.

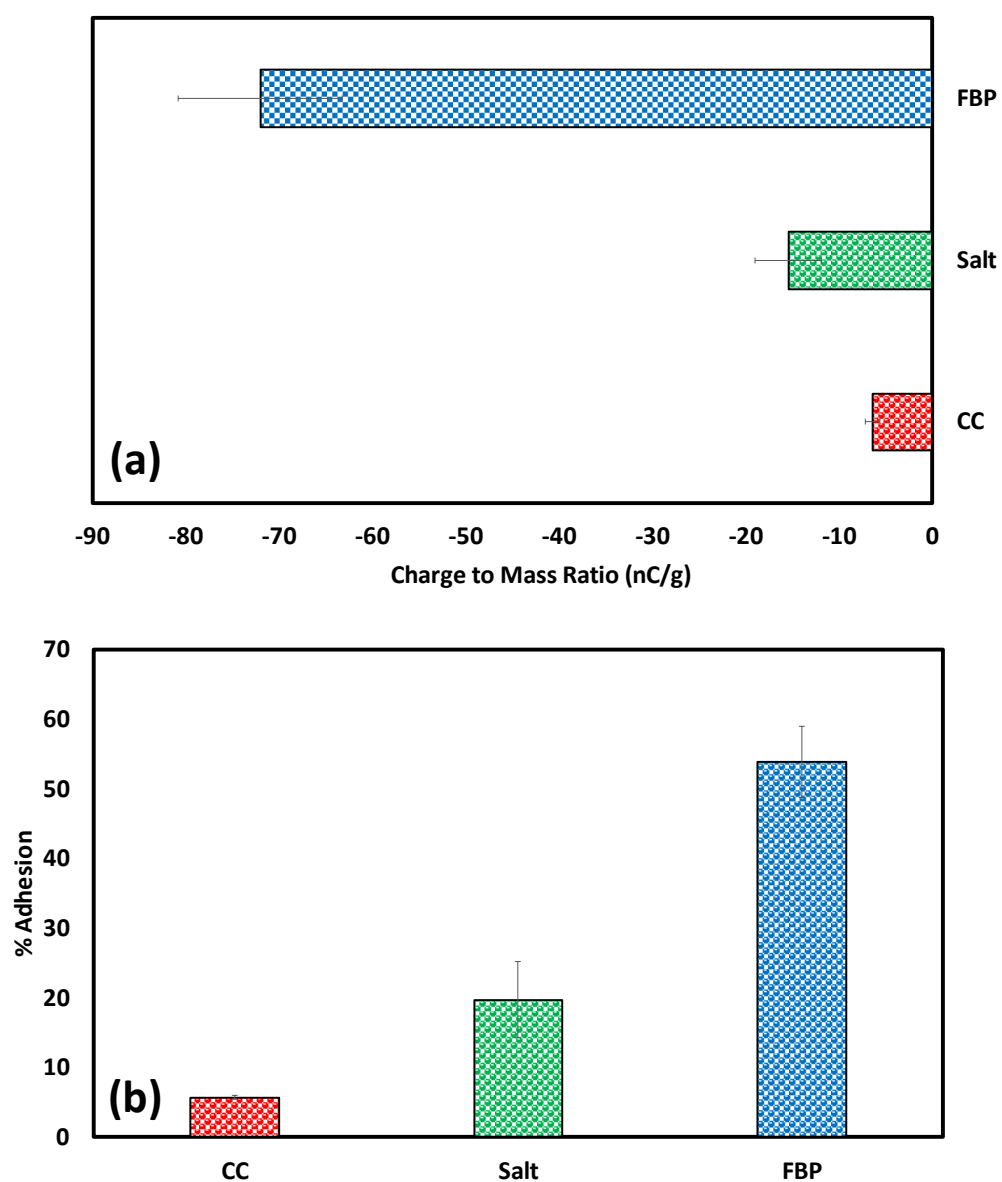


Figure 6.7: Tribo-electrification (a) and adhesion data (b) of flurbiprofen, flurbiprofen cyclopropylamine (1:1) salt and flurbiprofen: cyclopropylamine (2:1) salt co-crystal

6.2 Conclusion

In the present work, a salt and salt cocrystal of flurbiprofen and cyclopropylamine were successfully prepared. The chapter reported for the first time the crystal structure of the salt cocrystal in a 2:1 ratio (drug: counterion). The asymmetric unit of the salt cocrystal contained a molecule of the free acid, the flurbiprofen anion and the protonated cyclopropylamine. A different hydrogen bond arrangement to that of the salt was enabled by the presence of the second flurbiprofen in the unit cell, yielding Type II ladders and based on R_4^3 (10) rings. The salt is necessarily racemic, being in space group $P2_1/n$ with an inversion centre. The salt cocrystal in space group $P2_12_12_1$ lacks one: as determined, all copies of the flurbiprofen anion have chirality S at its asymmetric carbon atom while all copies of the free acid have R. The salt exhibited superior compressional and mechanical properties as compared to the salt cocrystal. However, the salt cocrystal displayed an improvement in the solubility in contrast to FBP and the salt form. This may be associated with improved plastic deformation of the salt under stress relative to the salt cocrystal enabled by a more clearly defined slip plane arrangement in the salt crystal lattice. The flurbiprofen cyclopropylamine salt cocrystal showed a substantial reduction in charging propensity and ability to adhere to the shaker walls in comparison to the parent drug with approximately 10-fold reduction. Furthermore, a large reduction of 2.5-fold was observed when compared to the salt form. Our present work depicts that both strategies have their merits and could be considered on a case by case basis. However, the salt cocrystal provides an alternative approach for the improvement of a number of pharmaceutical and physicochemical properties in comparison to the salt, those predominantly being the material handling and solubility.

7 The influence of counterion selection on physico-chemical and electrostatic properties of analogous carboxylic acid salts

Background

Physico-chemical properties of pharmaceutical materials often require to be modified in order to achieve a material with optimal processing characteristics for formulation [34]. A number of strategies have been utilised in the past to improve the physical properties to overcome material handling problems during scale-up. An example of one such strategy is salt formation of acidic or basic drugs which is a common technique used in the pharmaceutical industry to overcome some of the undesirable characteristics of the parent drug, whilst enhancing the solubility. Previous research has shown salt formation to vastly improve the solubility of a drug as well as the dissolution profile [117], resulting in an increase in absorption rate [185]. Approximately half of the drugs administered for medicinal therapy are in the salt form [23]. Attraction via intermolecular Coulombic forces between the charged groups of the parent drug and counterion allows for a salt to be formed, ensuring the required conditions are met to reduce impurities that may otherwise alter the final crystal habit resulting in the formation of polymorphs or hydrates possessing undesirable physicochemical properties [186].

In order to achieve the optimal salt form, the selection process involving an API form and a counterion is critical for both pharmaceutical and chemical processing, to avoid development issues early on [133]. The optimal formulation does not necessarily equate to the salt form with the greatest dissolution rate and solubility [133]. A number of factors need to be taken into account, such as thermal stability, degree of crystallinity, bulk physical properties, hygroscopicity and physical stability [187]. An aspect of material handling regularly overlooked in the early stages of drug development is the electrostatic charge affinity of a material, commonly referred to as tribo-electrification phenomena. Particle electrification is a common occurrence in many industries, including the pharmaceutical industry, affecting material handling properties. Tribo-electrification is brought about by physical contact between material and the processing equipment as well as contacts with other particles

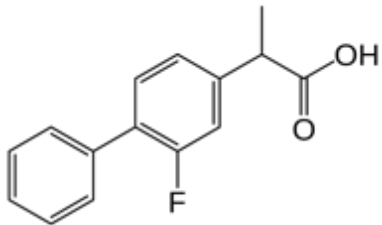
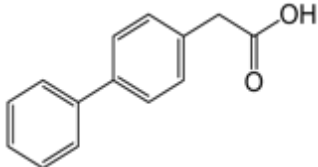
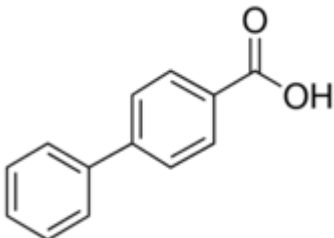
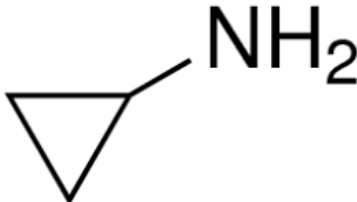
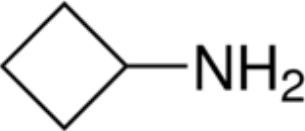
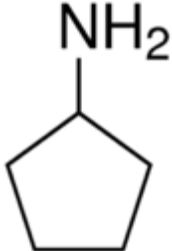
[188]. Salt formation is known to alter the particle morphology, resulting in changes in the charge transfer process [56]. The key previous study in this field by Šupuk et al [56] investigated the influence of salt formation on electrostatic properties of Flurbiprofen salts using a selection of counterions based on differences in their mechanical properties. In this study the main focus was to investigate salt formation from linear series counterions which differentiated on the number of hydrocarbons in the chain length of the cyclic group of the counterion. This is the first time a study has investigated the structural effects upon the triboelectrification propensity of a material, this also allowed for the influences upon the physicochemical properties to be studied as a result of the structural properties. The counterions were combined with Flurbiprofen (FBP) and two additional APIs of similar structure namely Felbinac (Felbi) and Biphenyl-4-carboxylic acid (B4CA) to form the salts. The aim was to enhance the understanding of the effects of the salts formed from linear series counterions on physico-chemical and tribo-electrification properties of the resulting salts. This approach allowed for the structural effects of the API and counterions to be investigated thus enhancing the current understanding of the influence of salt formation on electrostatic properties.

Powder handling involves a number of industrial operations such as sieving, mixing and conveying, enabling particles to make frequent contact with the walls of the processing equipment as well as themselves. During these contacts, a charge transfer occurs and the particles remain charged upon their separation [189]. The resulting charge of particles can cause a number of material handling problems, and in the pharmaceutical industry may lead to segregation of formulations, affecting content uniformity, blockages of pipes due to inter-particle cohesion and in extreme cases may lead to dust explosions [82].

In this study, three model API compounds were used (Table 1), namely; Flurbiprofen, Felbinac and Biphenyl-4-carboxylic acid. FBP is known for its high tribo-electrification propensity and adhesion tendency as well as poor mechanical and adhesion properties [56]. Felbinac and Biphenyl-4-carboxylic acid were selected due to their similarities in molecular structure to FBP as well as their lack of the highly electronegative Fluorine group allowed for a comparison to potentially indicate any physicochemical changes attributed to the Fluorine group. These drugs were used to form a number of salts using a linear series of counterions, namely; cyclopropylamine (C-Prop), cyclobutylamine (CBA) and cyclopentylamine (CPA) (Table 7.1). The counterions differed in the addition of an extra carbon in the cyclic group of the

counterion. A number of analytical techniques were utilised to confirm successful salt formation, solubility and intrinsic dissolution rate (IDR) were carried out for the pure APIs and salt forms. A custom built tribo-electrification device was used to measure the charge of the salt particles [101], as a function of time, with the percentage particle adhesion also being assessed by determining the recovered material post tribo-electrification. The potential impact of salification upon solubility, IDR, particle morphology, powder flow properties, surface area analysis, particle adhesion and tribo-electrification behaviour of the salts were assessed.

Table 7-1 Parent Drugs and Counter-ion Structures

		
Flurbiprofen (FBP)	Felbinac (Felbinac)	Biphenyl-4-carboxylic acid (B4CA)
		
Cyclopropylamine (C-Prop)	Cyclobutylamine (CBA)	Cyclopentylamine (CPA)

7.1 Results and Discussion

7.1.1 Solid State Characterisation

Salt formation was confirmed by undertaking FT-IR analysis (Figure 7.1/A6), whereby the patterns of the parent APIs were compared to those produced by the salt. Flurbiprofen possesses a peak at 1215 cm^{-1} which represents the C-F stretch, the three parent compounds;

FBP, Felbi and B4CA presented a characteristic broad peak at 2500-3300 cm^{-1} due to hydrogen bonding. A signature C=O stretching of the carboxylic acid group is present at 1695 cm^{-1} for Flurbiprofen, in the case of felbinac and biphenyl-4-carboxylic acid this peak is found at 1680 (Figure A6). The signature C=O peak was not present in the salts, indicating successful salt formation. Furthermore, also the presence of stretching in the 1440-1335 cm^{-1} region are characteristic to carboxylic salts.

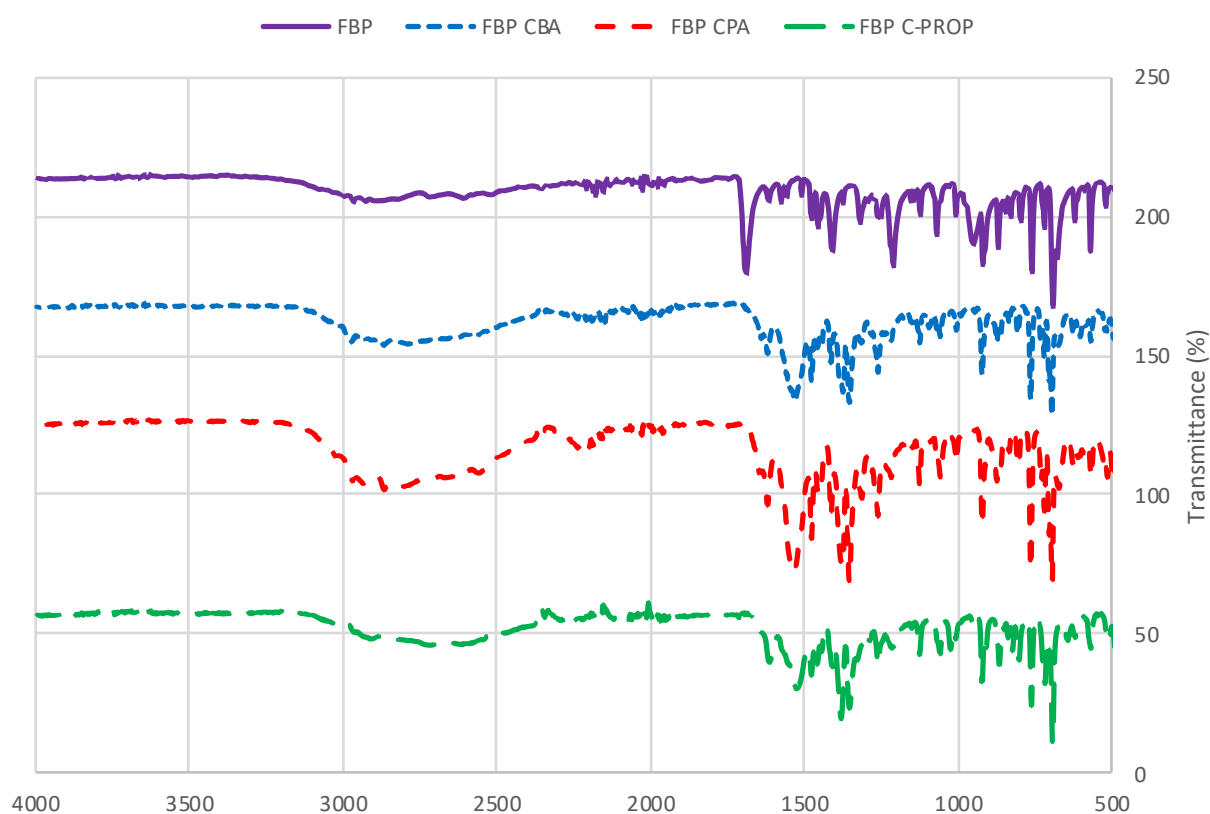


Figure 7.1 FT-IR data for FBP and its salts

Powder X-ray diffraction patterns are shown in Figure 7.2/A7. Changes to the crystallographic structure consequent to salt formation result in differences in the X-ray diffraction patterns between 5°-60° at angle 2θ concerning the pure compounds and their salt forms. Notable differences in the PXRD data pattern can be observed. Some identifiable peaks are present in the pure materials; for flurbiprofen these are present at approximately 2θ angles 7, 16 and 29, for felbinac they are found in the region of 2θ angles 11 and 18, and for biphenyl-4-carboxylic acid displays peaks at approximately 2θ angles 6, 18, and 21. These identifiable peaks are either absent or of different intensity in the salts formed indicating a change in the

crystal structure of the material as a result of the salt formation. Furthermore, due to the similarities in the counterions, the PXRD patterns produced by the salts formed using cyclobutylamine and cyclopentylamine for all the pure drugs are similar, with cyclopropylamine showing greater differences in comparison to the pure drugs (Figure 7.2/A7).

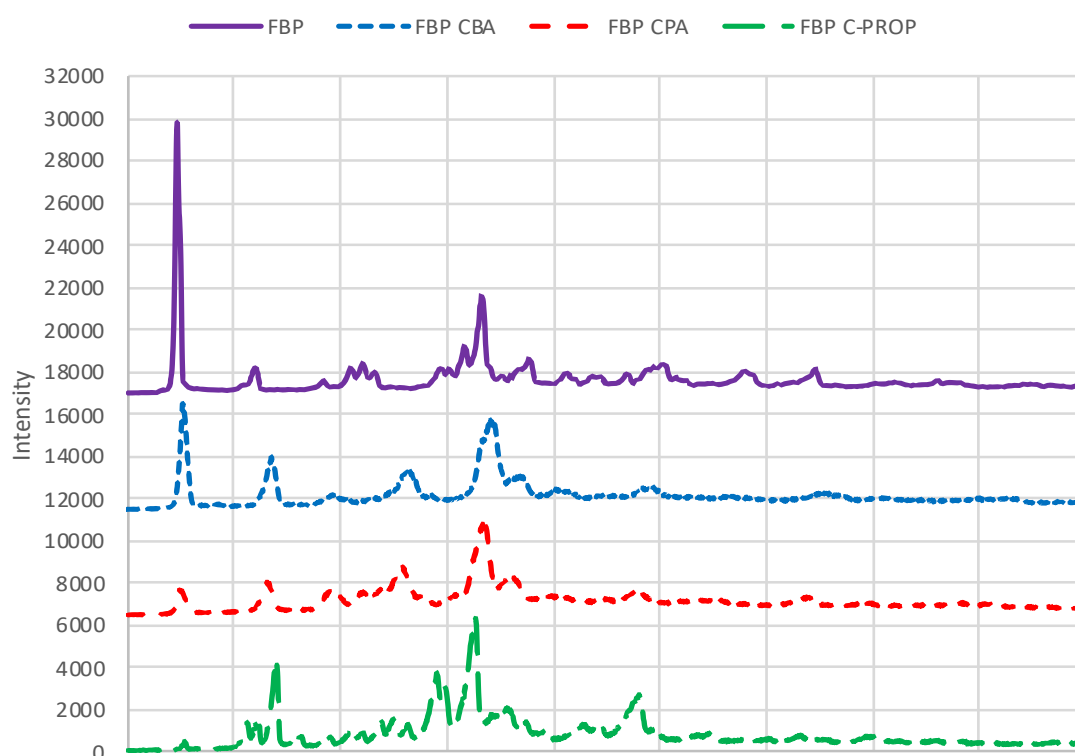


Figure 7.2 XRD data for FBP and its salts

NMR analysis was also used to confirm the salt formation. The analysis was utilised to account for each hydrogen atom in the expected molecule, NMR spectra for the parent compounds and salts are presented below, flurbiprofen (Figure 7.3), the salts of flurbiprofen (Figure 7.4), felbinac (Figure 7.5), salts of felbinac ((Figure 7.6), B4CA (Figure 7.7) and the salts of B4CA (Figure 7.8). Salt formation is strengthened by the fact that carboxylic acids present a ^1H NMR chemical shift in the region of 10-13 ppm due to the hydroxyl group, the removal of this shift and the addition of chemical shifts as a result of hydrogens present within the counter-ion are indicative of successful salt formation. As well as this a chemical shift of the proton

attached to the carbon subsequent to the COOH group is evident, for example for flurbiprofen and flurbiprofen CBA salt, the chemical shift is 3.77 ppm and 3.40 ppm, respectively.

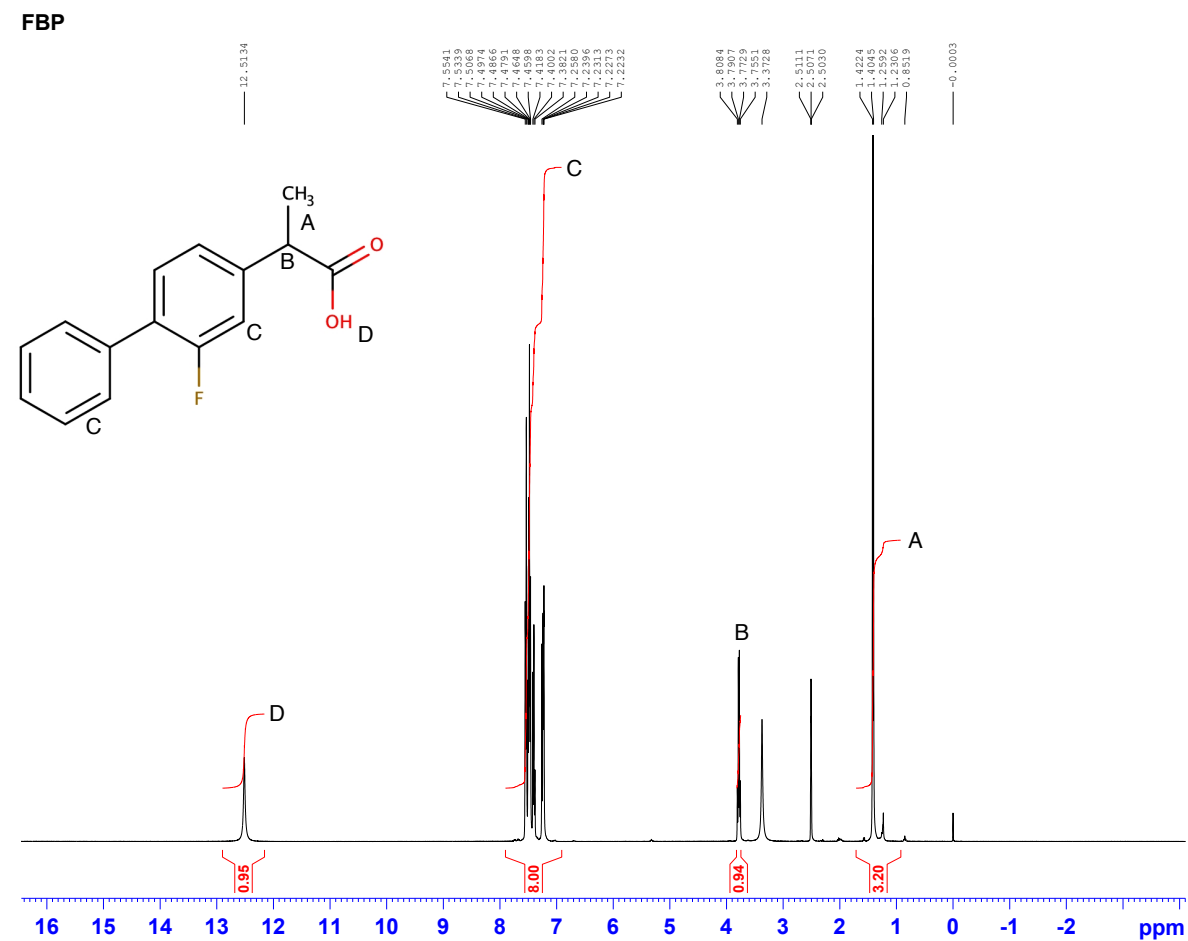


Figure 7.3: NMR Scan for Flurbiprofen

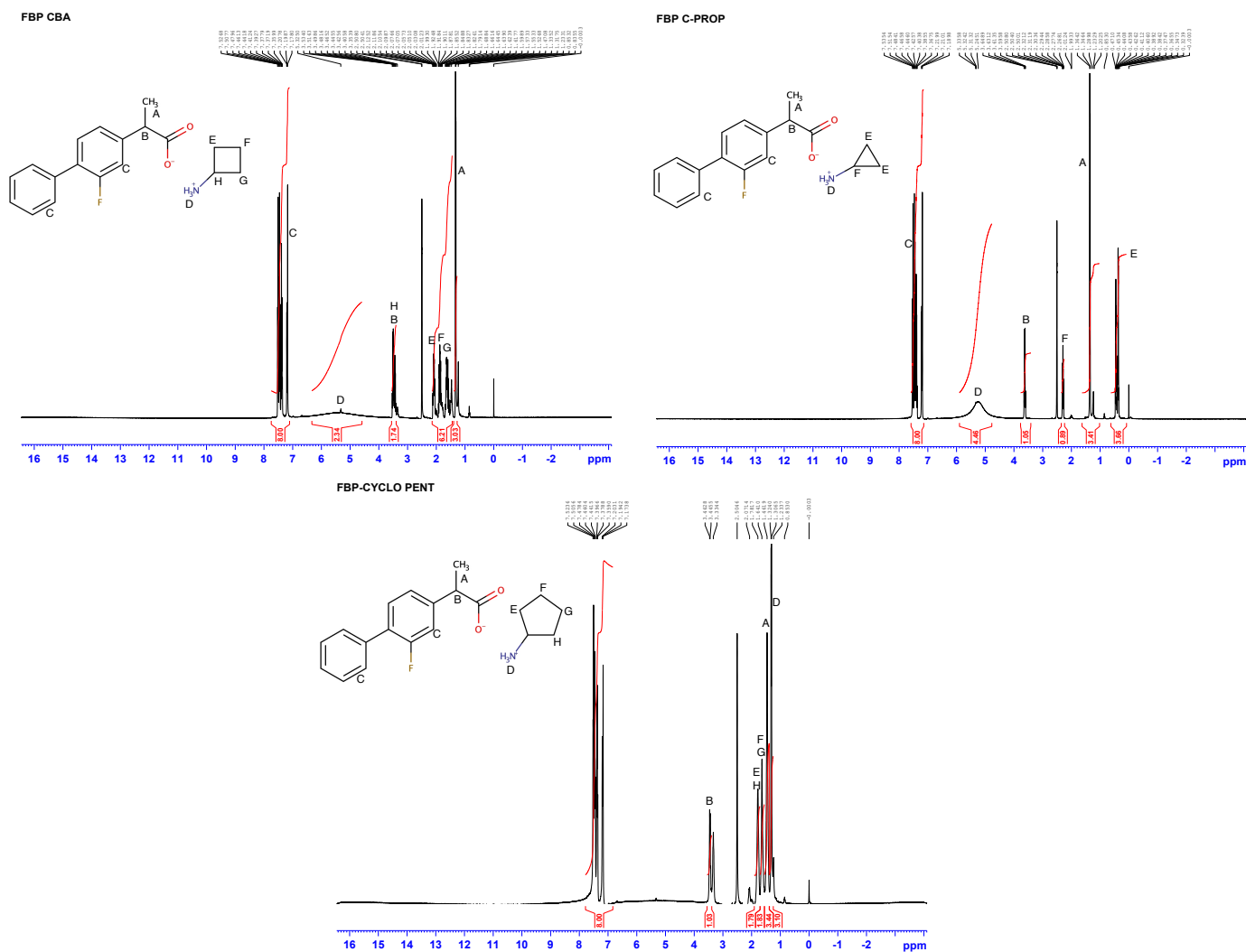


Figure 7.4: NMR Scan for the Salts of Flurbiprofen

FELBINAC

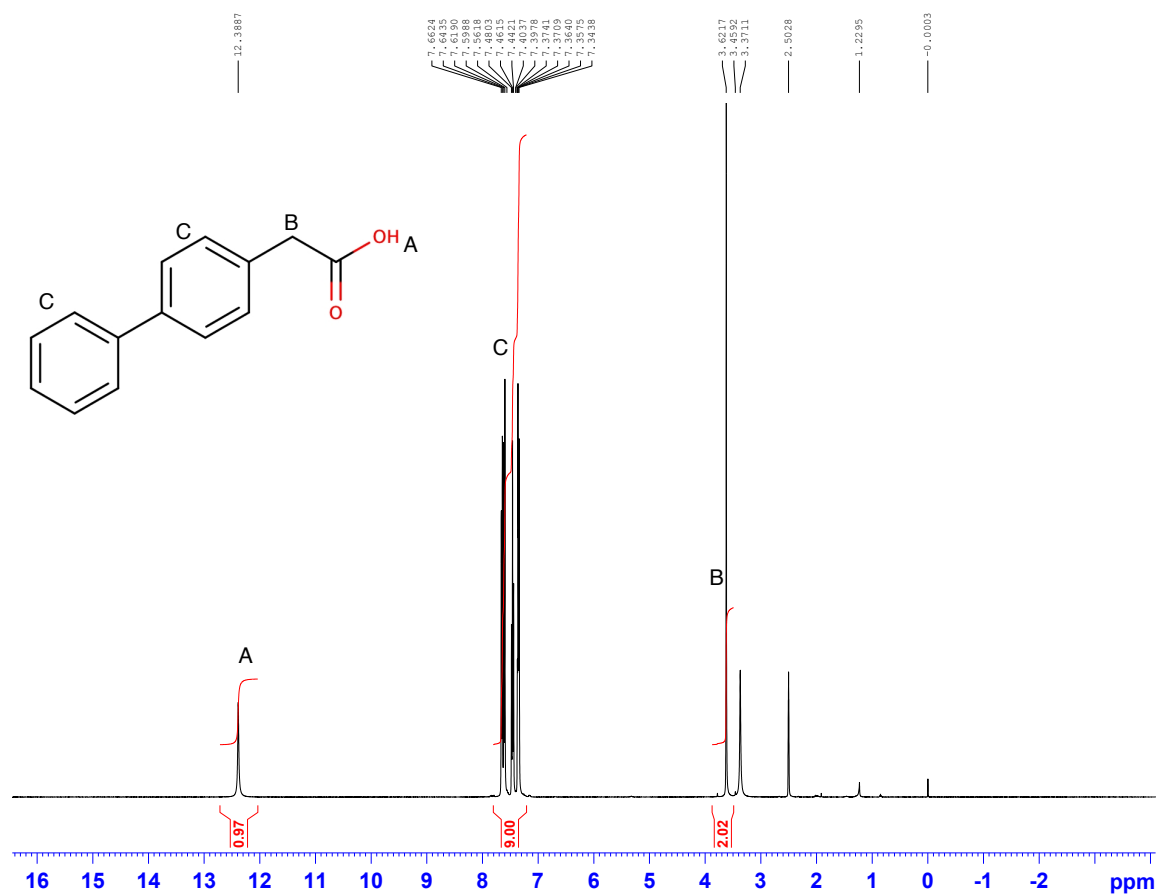


Figure 7.5: NMR Scan for Felbinac

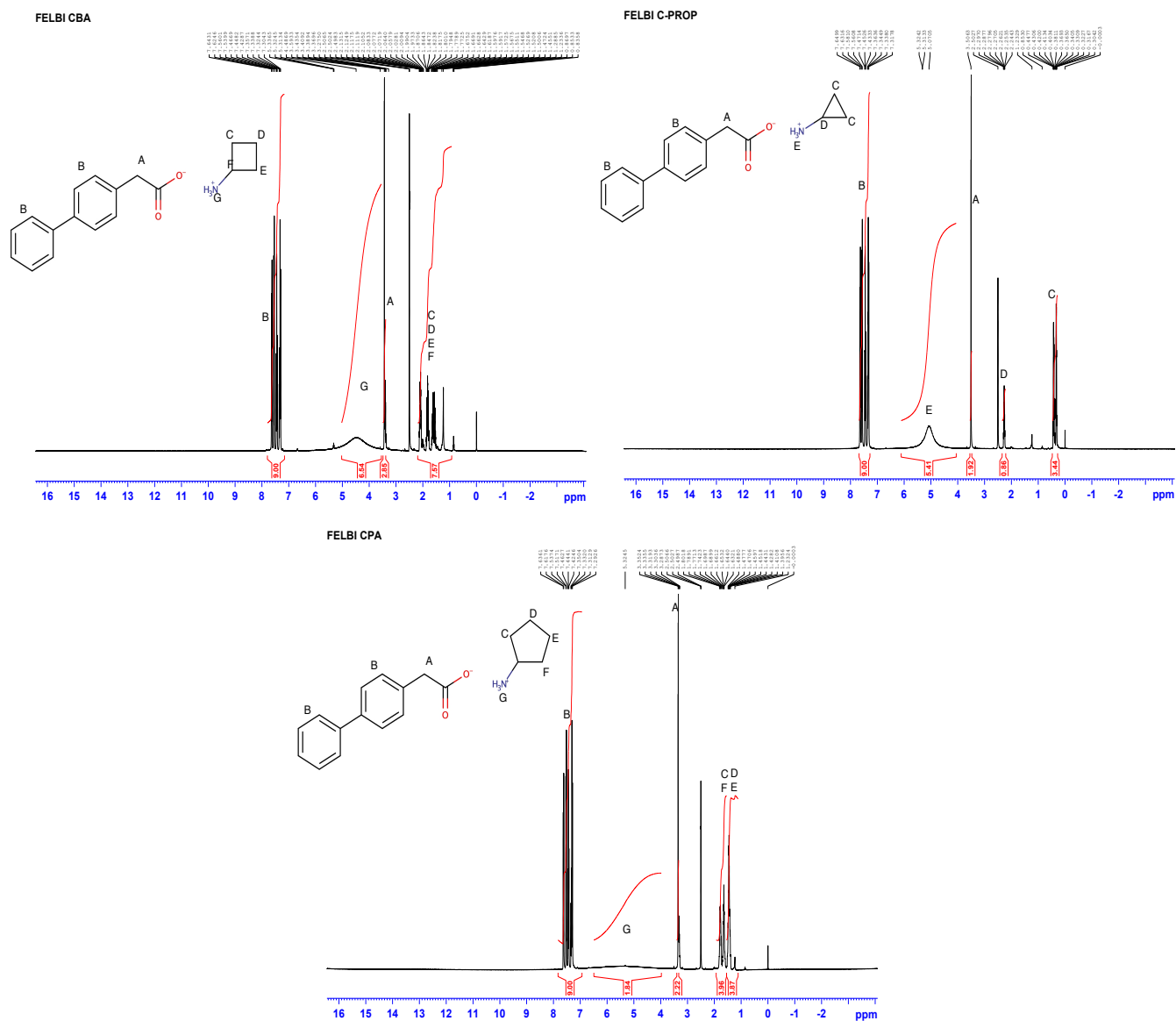


Figure 7.6: NMR Scan for the Salts of Felbinac



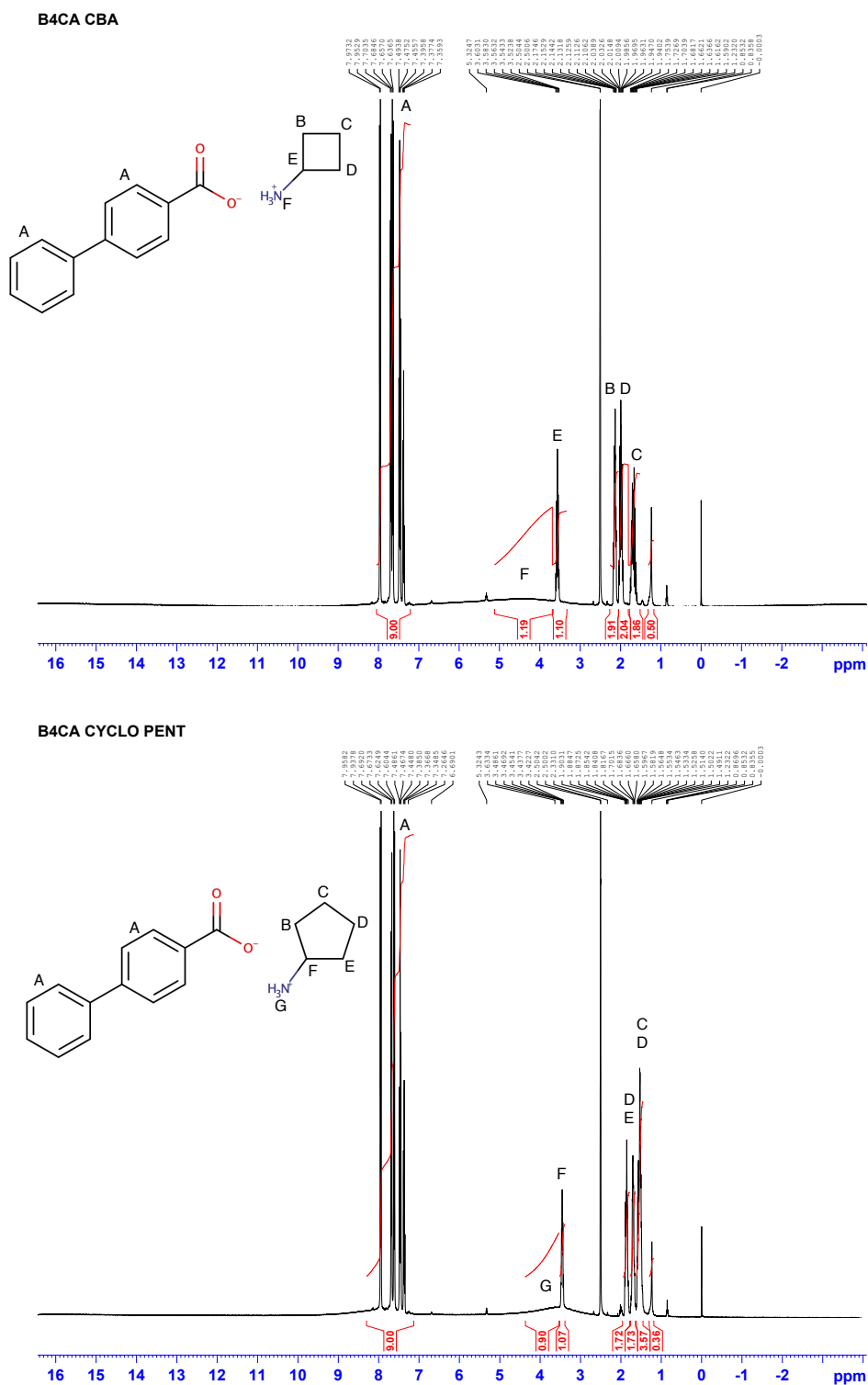


Figure 7.8: NMR Scan for the Salts of Biphenyl-4-carboxylic acid

Table 7.2 indicates the melting onset and endset for the salt forms compared to the pure drugs measured using DSC. In the case of FBP, it possessed the lowest onset of melt (114.2 ± 0.26 °C) in comparison to the other parent compounds; Felbi showed a melting onset of 160.98 ± 0.18 °C and B4CA with a greater onset of the parent drugs, present at 222.12 ± 0.24 °C. In the case of FBP the salts showed an onset of melt at a higher temperature than the parent drug, increasing as the chain length of the counterion increased. An increased melting point indicated that the newly formed material is thermodynamically stable. In the case of felbinac, although the C-Prop and CBA salt possessed a lower onset of melt than the parent compound, indicating disorder in crystallinity. The trend regarding an increase in onset of melt in relation with the counterion chain length for the salts was observed. Biphenyl-4-carboxylic acid presented a similar trend to felbinac with the two counterions showing an increase in melting enthalpy as the chain length increased, however; a lower onset of melt was present in both counterion cases in comparison to the pure drug. B4CA C-Prop presented a mixture of salt and parent compound upon salt formation hence was disregarded for further analysis to ensure that the crystallisation conditions of the salt form were consistent as these can influence particle habit. However, the CBA and CPA salts were still used for the analysis.

Table 7-2: Melting onset and endset for the parent compounds and salts

Sample	Melting point (onset, °C)	Melting endset (°C)
FBP	114.2 ± 0.26	117.64 ± 0.29
FBP C-prop	130.0 ± 0.66	134.7 ± 0.32
FBP CBA	160.85 ± 0.41	170.53 ± 0.19
FBP CPA	187.57 ± 0.55	195.79 ± 0.33
Felbi	160.98 ± 0.18	166.59 ± 0.15
Felbi C-prop	95.01 ± 0.71	104.12 ± 0.41
Felbi CBA	157.07 ± 0.32	163.56 ± 0.27
Felbi CPA	171.76 ± 0.47	183.14 ± 0.51
B4CA	222.12 ± 0.24	227.16 ± 0.29
B4CA CBA	152.46 ± 0.54	164.48 ± 0.31
B4CA CPA	170.26 ± 0.63	174.28 ± 0.48

TGA analysis was undertaken to confirm the exclusion of solvates and hydrates within the crystal lattice. The inclusion of water molecules within the crystal lattice have shown to alter the symmetry, shape and number of molecules within a unit cell [190]. From Figure 7.9/A8 it is evident that there were no weight losses indicative of solvate/hydrate formation. The initial step indicated the loss of the counterion, with the onset increasing as the carbon chain length increases. This trend was seen in the case of all the salts of the pure drugs. A second weight loss step accounted for the decomposition phase.

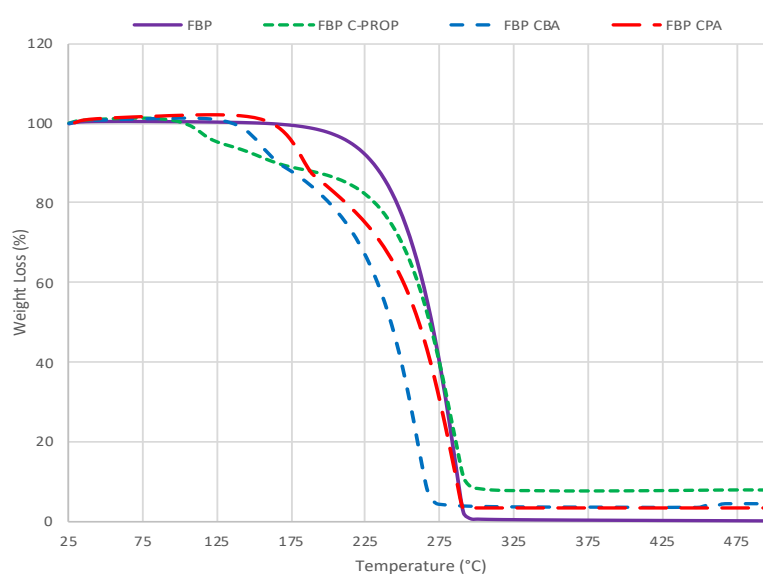


Figure 7.9 TGA data for FBP and its salts

7.2 Saturated Solubility and Intrinsic Dissolution

Solubilities of flurbiprofen was below the detection limit of 0.026 mg/ml. Values of 0.0512 mg/ml [191] and 0.0106 mg/ml [192] have been published for flurbiprofen.

The saturated solubilities improved in all cases following the salt formation (Table 7.3). All pure APIs displayed solubilities in the region of 0.1 mM, increasing from around 100-fold up to approximately 500-fold in the case of the Felbi C-Prop salt. The data suggests a trend in the solubility values with increasing chain length resulting in a decrease in aqueous solubility. This trend was observed in all cases of the salt forms of the linear series of counterion. An increase in chain length causes an increase in the lipophilicity of the counterion hence a reduction in the aqueous solubility. However, the degree of improved solubility is not similar as flurbiprofen showed an increase in solubility by around 106, 354 and 608 fold for the CPA, CBA and C-Prop salt forms respectively, in comparison with felbinac, illustrating increase of

solubility by around 142, 200 and 527 fold for the counterions CPA, CBA and C-Prop, respectively. Felbinac C-Prop salt displayed the greatest increase in solubility from all the salts. B4CA showed the least improvement in solubility of around 110 and 194 fold for the CPA and CBA sat forms, respectively. Comparing this data with the onset of melt from the DSC indicates a trend; as the melting point decreases, solubility is increased. Supporting the notion that as the melting point decreases, the solubility increases due to the reduced energy needed to break the crystal lattice.[2, 6]

Table 7-3: Solubility data for the parent compounds and the salts

Sample	Solubility (mg/ml)	Solubility (mM)	pH
FBP	0.013 ± 0.003	0.053	4.84 ± 0.042
FBP CPA	1.385 ± 0.012	4.204	7.11 ± 0.021
FBP CBA	4.609 ± 0.406	14.614	7.19 ± 0.035
FBP C-Prop	7.911 ± 0.476	14.499	7.13 ± 0.017
Felbi	0.021 ± 0.006	0.099	4.78 ± 0.028
Felbi CPA	2.997 ± 0.318	10.078	7.07 ± 0.014
Felbi CBA	4.211 ± 0.512	14.861	7.26 ± 0.019
Felbi C-Prop	11.086 ± 1.147	41.153	7.64 ± 0.005
B4CA	0.012 ± 0.005	0.061	2.84 ± 0.041
B4CA CPA	1.314 ± 0.039	4.637	7.58 ± 0.028
B4CA CBA	2.323 ± 0.078	8.625	7.75 ± 0.028

The IDR and solubility data for the pure compounds and their salts are presented in Table 7.4 for ease of comparison, the profiles were linear for all materials investigated. The IDR rank order mirrors the order of solubility, i.e. C-PROP > CBA > CPA > parent compound, and was the case for all three APIs. The salts of felbinac showed the greatest enhancement in dissolution, significantly higher for the felbinac c-prop salt in comparison to the other salts and felbinac. From the IDR experiments it can be concluded that the dissolution profiles can be associated with saturated aqueous solubility data, also a rank dissolution order can be elucidated from the solubility data.

Table 7-4: IDR data for the parent compounds and the salts

Material	IDR (mg/min/cm²)	Solubility (mg/ml)
FBP	0.171 ± 0.0093	0.013 ± 0.003
FBP CPA	0.215 ± 0.0256	1.385 ± 0.012
FBP CBA	0.548 ± 0.0074	4.609 ± 0.406
FBP C-Prop	0.741 ± 0.0178	7.911 ± 0.476
Felbi	0.212 ± 0.0146	0.021 ± 0.006
Felbi CPA	0.405 ± 0.0256	2.997 ± 0.318
Felbi CBA	0.678 ± 0.0169	4.211 ± 0.512
Felbi C-Prop	2.594 ± 0.0878	11.086 ± 1.147
B4CA	0.064 ± 0.0089	0.012 ± 0.005
B4CA CPA	0.305 ± 0.0294	1.314 ± 0.039
B4CA CBA	0.438 ± 0.0048	2.323 ± 0.078

7.3 Particle Shape Analysis

The particle shape and morphology of the APIs and the resulting salts formed using the counterions were analysed by SEM and are presented in Figures 7.10 and A9. Utilising different counterions resulted in differing particle morphologies to the parent compounds. The results show the salts to have recrystallised primarily with acicular morphologies, with the exception of FBP CPA, producing a rounded particle shape. It is evident that a number of salts show agglomerates of acicular particles producing larger particles of rounded shape. The B4CA salts produce predominantly acicular particles, with lower quantity of agglomeration. In comparison to the pure compounds, FBP and Felbinac are flake-like in morphology, and B4CA is a mixture of cubic and flake morphologies, all starting materials presented flat surfaces.

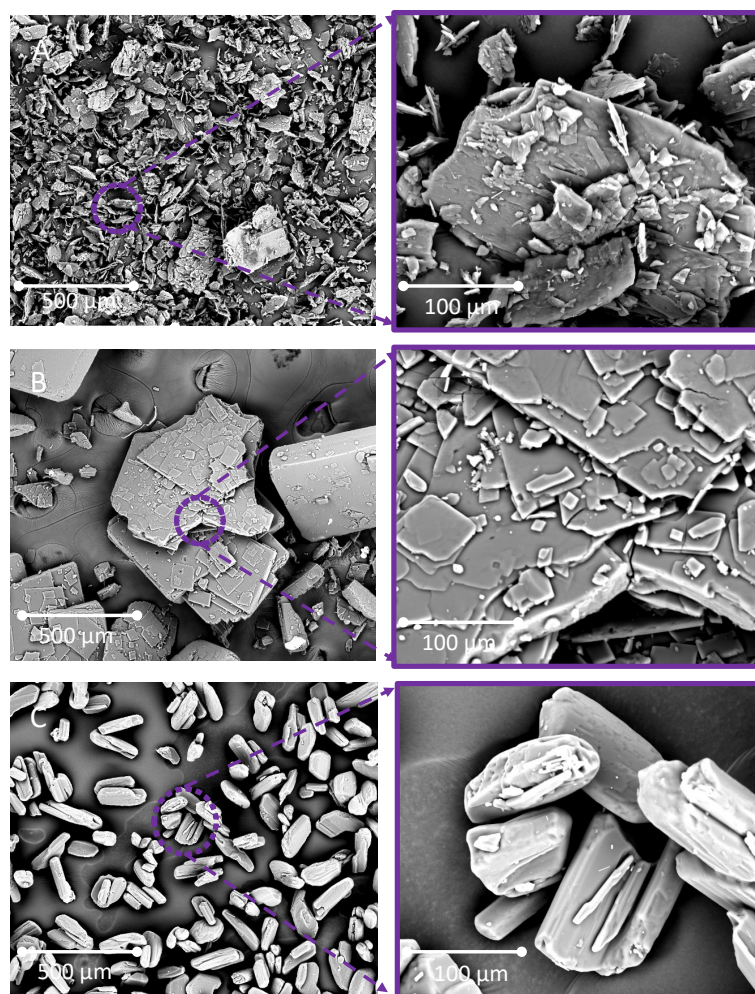


Figure 7.10: SEM images of, A) FBP, B) Felbi and C) B4CA depicted at 100x and 500x magnifications.

7.4 Powder Flow

The flow properties of the pure materials and the salt samples was measured with the Schulze shear tester at a standard pre-shear load of 10 kPa and the results are shown in Figure 7.11. The *ffc* results show that the pure compounds, FBP and B4CA presented to be easy flowing whilst felbinac showed to be free flowing. This compared with the salts of fbp which generally presented to be cohesive with a *ffc* between 3.0 and 3.9, for both sieve fractions; 180-250μm and 425-500μm, with the exception of fbp CPA at the larger sieve fraction, presenting a *ffc* of 5.4, indicating easy flow. Felbinac presented a similar trend with the majority of the salts presenting to be cohesive with the *ffc* values between 2.8 and 3.6 for both sieve fractions, excluding Felbi CBA, 425-500μm which showed to be easy flowing. In the case of B4CA, the only salt form indicating to be cohesive is B4CA CBA at the smaller sieve fraction with an *ffc*

of 2.8, and at the larger sieve fraction presented a ffc of 4.5, indicating easy flow. This is similar to B4CA CPA salt presenting an ffc of 5.3 and 6.3 for the smaller and larger sieve fractions, respectively, and was the only salt form shown to be easy flowing. Upon consideration of particle shape from the SEM images (Figure 7.10 and A9) it is evident that the easy flowing ability of the pure materials may be due to the particle shape being flake like and possessed large flat surfaces which allow for the particles to slide over one another, improving the ability to flow. However, in the case of the salts, the majority of the particles consisted of an acicular morphology as well as agglomerates of needle like particles. It is well-known that acicular materials possess poor powder flow properties due to the ability for the particles to interlock and restrict flow. [193, 194]. It was revealed that acicular particles have an increased tendency to stick to metal surfaces than plate like particles, the increased propensity to stick is associated with a higher surface polarity [195].

In the case of FBP CPA which presented to be easy flowing, this can be accounted by it possessing a more rounded particle morphology with the ability to slide over other particles and a reduced tendency for interlocking, hence presented a ffc value of 5.4. It is interesting to note that the B4CA salts also possess acicular particle morphologies however in the case of the CPA salt, displayed an easy flowing ability, even at the smaller sieve fraction. This may be due to the reduced agglomerate formation in comparison to some of the other salts, it can be seen that the agglomerates of the acicular particles are comprised of a random assortment of particles to form a larger rounded particle. This increases the probability of the particles to interlock and hinder flow, whereas the reduced agglomeration of the B4CA salts allows for an increase in likelihood of the particles laying in a similar plane to one another, hence reducing the chances of interlocking. Furthermore, the experiment was conducted with two different particle sizes to study the effect of particle size on the flow properties of the materials. It is evident that in some cases, increasing the particle size did improve powder flow, however the improvements seen were minimal, due to the powder ffc value remaining within the cohesive banding with the exception of FBP CPA, Felbi CBA and B4CA CBA which presented a relatively substantial increase in ffc as a result of an increase in the particle size.

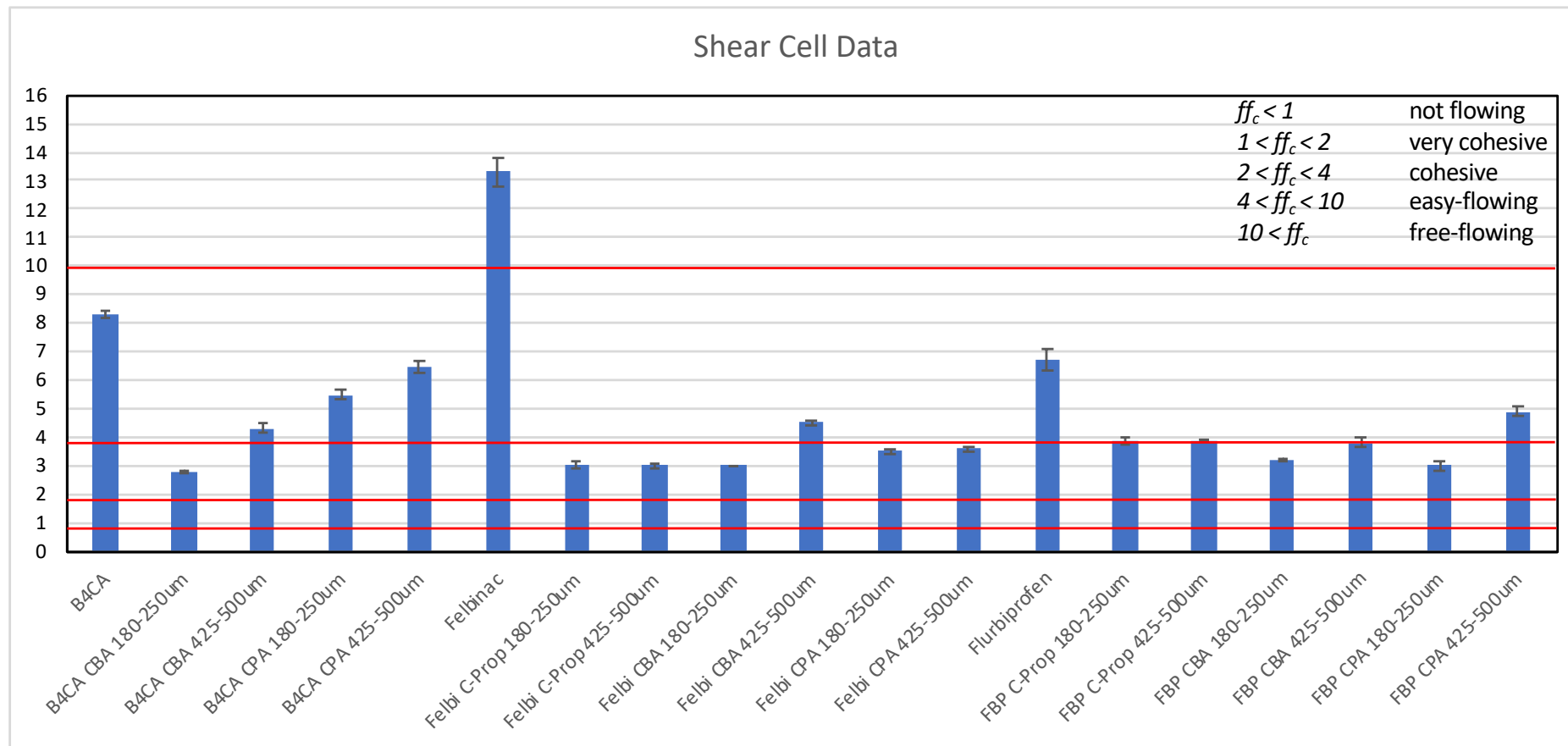


Figure 7.11: Shear cell data for parent compounds and salt forms

7.5 Brunauer–Emmett–Teller (BET) analysis

The surface area of the pure compounds and subsequent salts were determined by nitrogen adsorption at 77 K and resulted are summarised in Table 7.5. The specific surface area of pure FBP was found to be $0.2984 \text{ m}^2/\text{g}^{-1}$, in comparison to felbinac which presented $0.0372 \text{ m}^2/\text{g}^{-1}$ and B4CA showed a surface area of $0.0760 \text{ m}^2/\text{g}^{-1}$. In the case of the salts there appeared to be a trend whereby all salt forms appear to have a slightly larger surface area than the pure compound as well as an increase in surface area as the counterion chain length increased. FBP C-Prop presents a surface area value of $0.8851 \text{ m}^2/\text{g}^{-1}$, the CBA salt form showed a small increase to $2.6583 \text{ m}^2/\text{g}^{-1}$, and FBP CPA increased further to $6.0748 \text{ m}^2/\text{g}^{-1}$. Felbinac showed similar data with the C-Prop salt possessing a surface area of $1.0632 \text{ m}^2/\text{g}^{-1}$, in comparison to Felbi CBA which presented $2.1479 \text{ m}^2/\text{g}^{-1}$, and the CPA salt showing a surface area of $3.9901 \text{ m}^2/\text{g}^{-1}$. The B4CA salts also followed the same trend whereby B4CA CBA had a surface area of $1.0341 \text{ m}^2/\text{g}^{-1}$, and B4CA CPA presented $1.1618 \text{ m}^2/\text{g}^{-1}$. Although the surface area of the pure compounds and the salts are different, the values are not hugely dissimilar from one another especially when comparing the pure compounds to each other and the salts to one another, indicating that the physical properties of the materials are comparable. When compared with Section 7.3 it is evident that the salts produced needle shaped particles or agglomerates of needle particles which explains the increase in surface area in comparison to the parent material.

Table 7-5 BET surface area data for parent compounds and salts

Sample	BET Surface Area/m² g⁻¹
FBP	0.2984
FBP CPA	6.0748
FBP CBA	2.6583
FBP C-Prop	0.8851
Felbi	0.0372
Felbi CPA	3.9901
Felbi CBA	2.1479
Felbi C-Prop	1.0632
B4CA	0.0760
B4CA CPA	1.1618
B4CA CBA	1.0341

7.6 Tribo-electrification and adhesion behaviour

Tribo-electrification of the pure APIs and the salts was undertaken at time points 0.5, 2, 5 and 10 mins, these timepoints were chosen as they allowed for the material's saturated charge level to be established, i.e. the amount of charge generated as a result of particle impacts at which no further charge would occur. Presented in Figure 7.12 is the charging propensity data for the pure materials; FBP, Felbi and B4CA, the data displays that all the parent drugs charge with a negative polarity, hence are accepting electrons from the shaking motion with the stainless steel walls. It is evident that the charging behaviour of Felbi and FBP, presented extremely highly charging propensities, (-366 and -293 nC/g), respectively; at 10 mins, with a large tendency to adhere to the shaker walls. The adhesion values measured were between 60-70% at the same time interval, in comparison to B4CA which exhibited particularly low charging propensity (-3 nC/g) after being induced to the shaking motion for 10 mins as well as a maximum percentage adhesion value below 12%. From the BET data it is evident that the parent compounds and subsequent salt forms presented not too dissimilar specific surface area, hence it can be stated that the differences in charging propensity are not solely related to surface area of the resulting salts, as well as particle size. Large differences in surface area would have resulted in completely different particle interactions to the shaker walls as well

as other particles. However, differences in charging propensity can be attributed to the counterion selection as well as starting material.

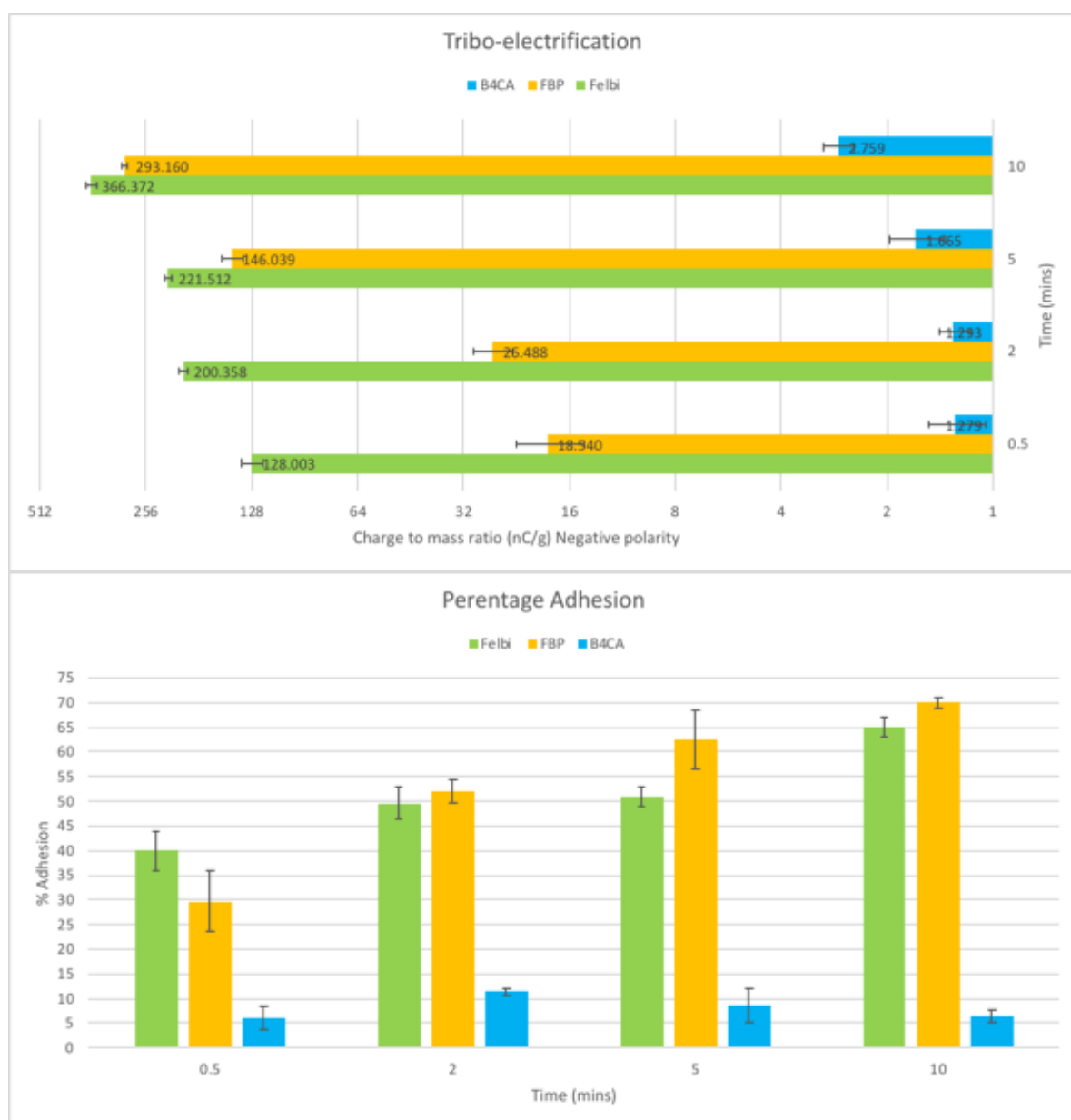
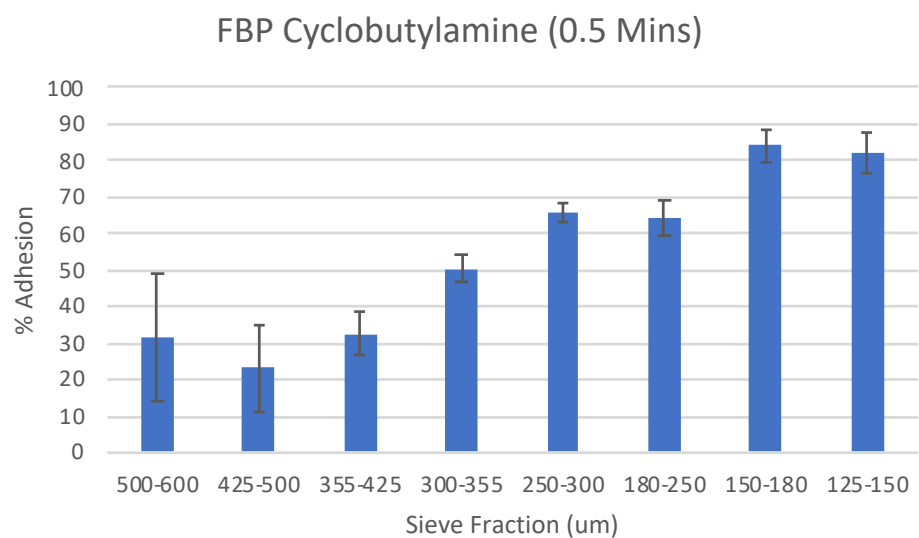
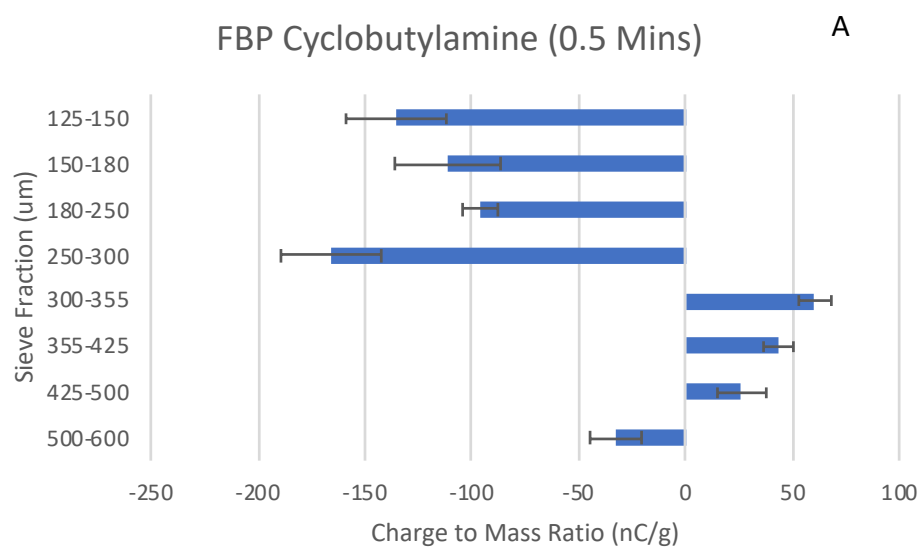


Figure 7.12: Tribo-electrification and adhesion data for the parent compounds

The salts exhibited interesting charge values, on initial observation it appears that the propensity for charge of the salt form has reduced in contrast to the starting material. However in the case of FBP CBA (Figure 7.13/A10) a charge value of -165 nC/g was produced at 0.5 mins, and as the time interval increased the charge value did not increase above this value. This may be due to the fact that at 0.5 mins the probability for particle to wall contacts

are greater than particle to particle interactions as the short time interval limits the time available for particles to adhere and for particle to particle interactions to occur.



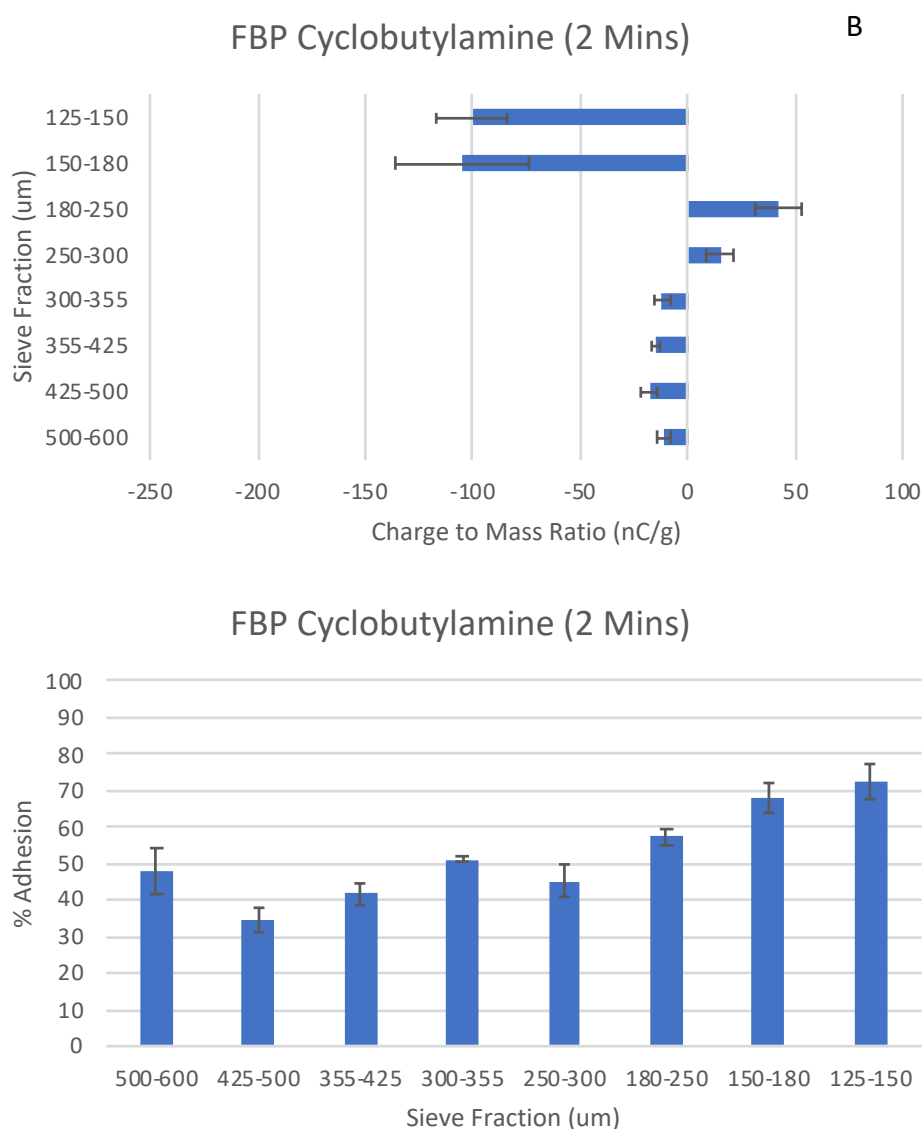
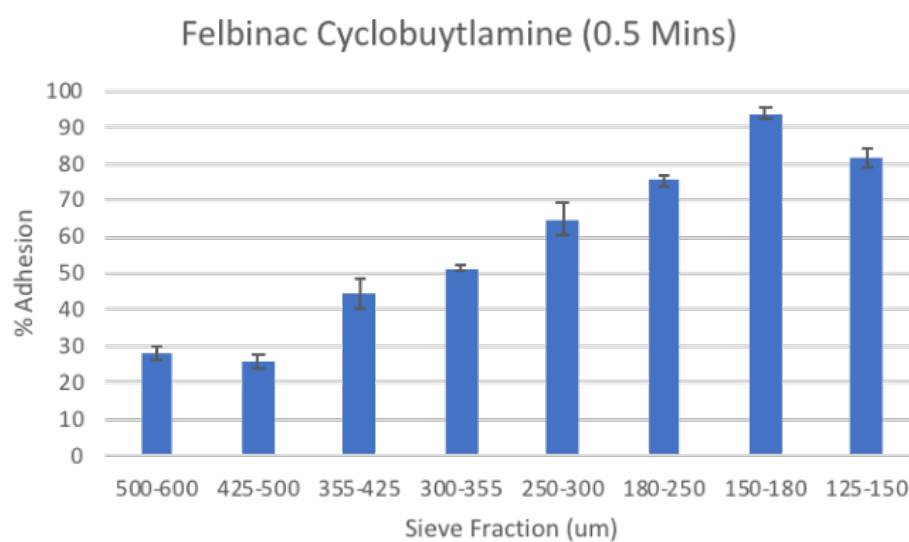
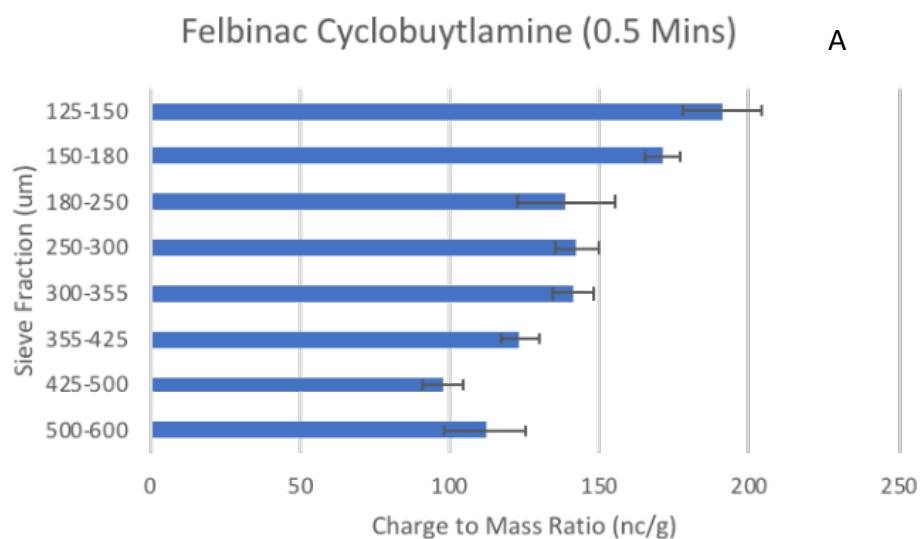


Figure 7.13: Tribo-electrification and adhesion data for FBP CBA at (A) 0.5 and (B) 2 mins

A similar trend is seen for Felbi CBA (Figure 7.14/A11), the polarity had reversed in comparison to the pure materials, and however a high charging propensity of at least 100 nC/g is present, and reaching approximately 250 nC/g at 5 mins. The percentage adhesion is up to 90% resulting in a small quantity of material resulting in such a high charge value, hence any adhered material having a potentially higher propensity to charge. In comparison to the shear cell data which showed both sieve fractions to be cohesive for FBP CBA, resulting in high levels of % adhesion and the smaller fraction for Felbi CBA which showed to be extremely cohesive, by presenting large amount of adhered materials (70-90%) whereas the larger sieve fraction showed only (25-44%).



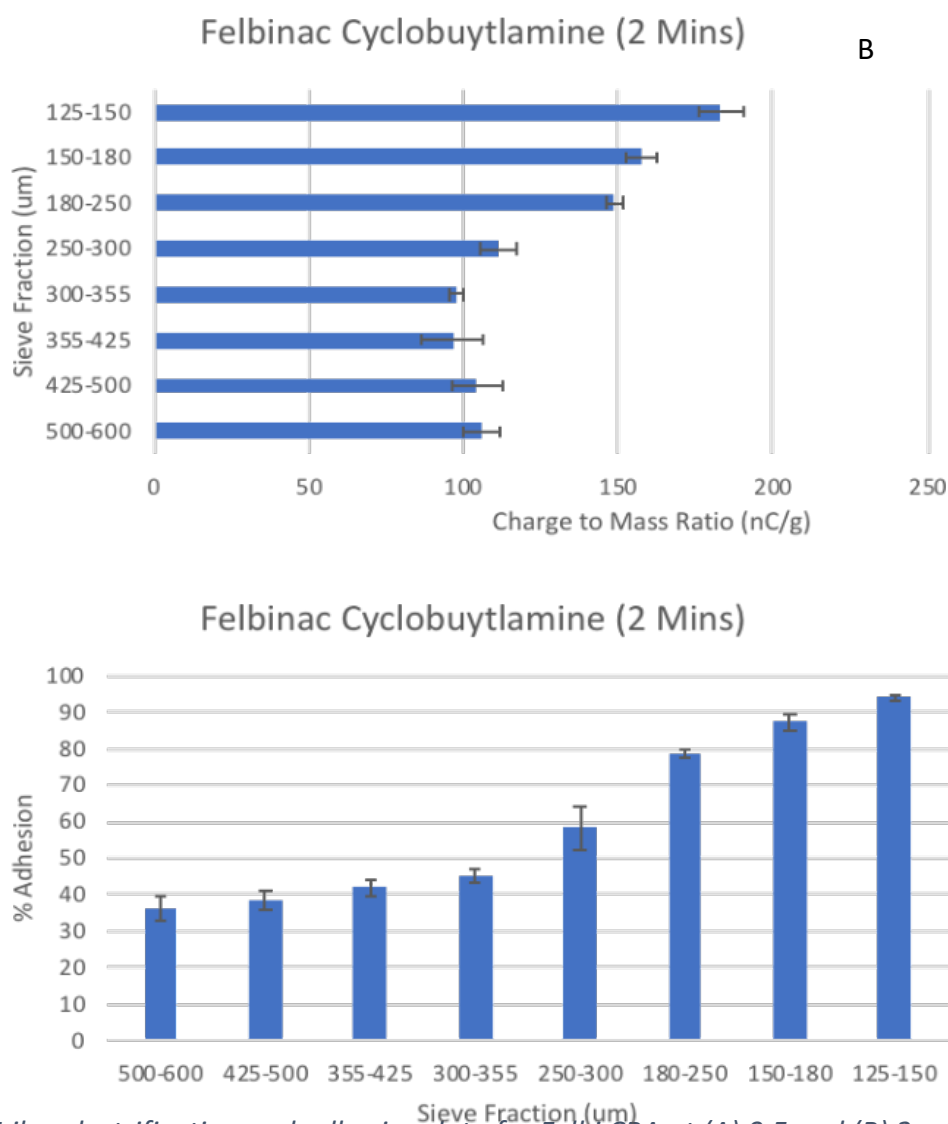
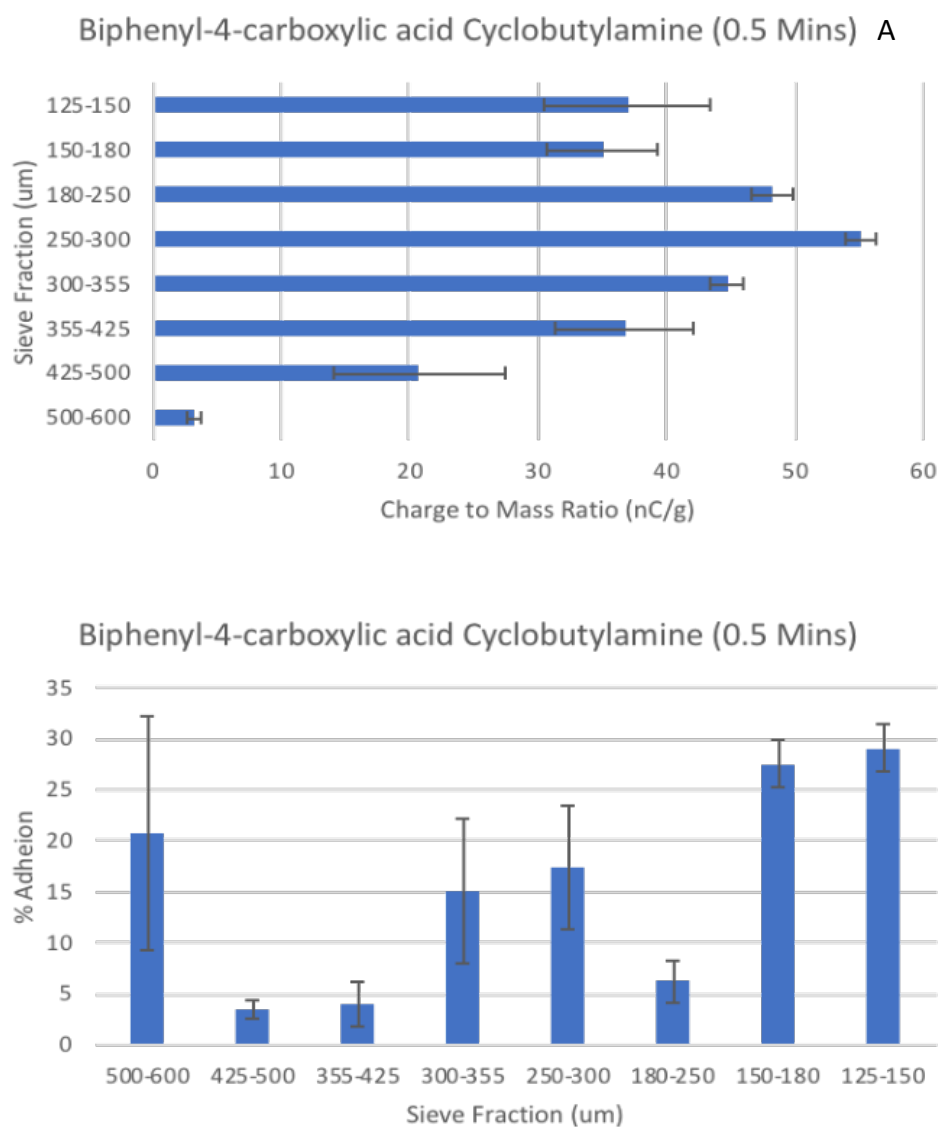


Figure 7.14: Tribo-electrification and adhesion data for Felbi CBA at (A) 0.5 and (B) 2 mins

In contrast to B4CA CBA (Figure 7.15/A12), which displayed noteworthy data, it is evident that the starting material is extremely low charging, however it appears that the low charging characteristics have also presented in the salt form. At time intervals 0.5, 2 and 5 mins the maximum charge value was below 60 nC/g and at 10 mins the polarity has reversed. However, the charge value does not exceed -60 nC/g, the cause for the polarity reversal is potentially an increase in particle to particle interactions hence altering the charge behaviour of the material in contrast to the shorter time intervals which would have potentially had greater particle to wall interactions. Furthermore, the B4CA salt exhibited a very low percentage

adhesion value of around 30% in contrast to the FBP CBA (Figure 7.13/A10) and Felbi CBA (Figure 7.14/A11) salt form, allowing for a greater quantity of material to be accounted for in the charge measurement. As well as indicating a lesser cohesive material, which is evident from the shear cell data as the larger sieve fraction presented to be easy flowing. Exhibiting less than 10% of adhered material in contrast to the 180-250 μ m fraction with a maximum of around 20% at 2 mins.



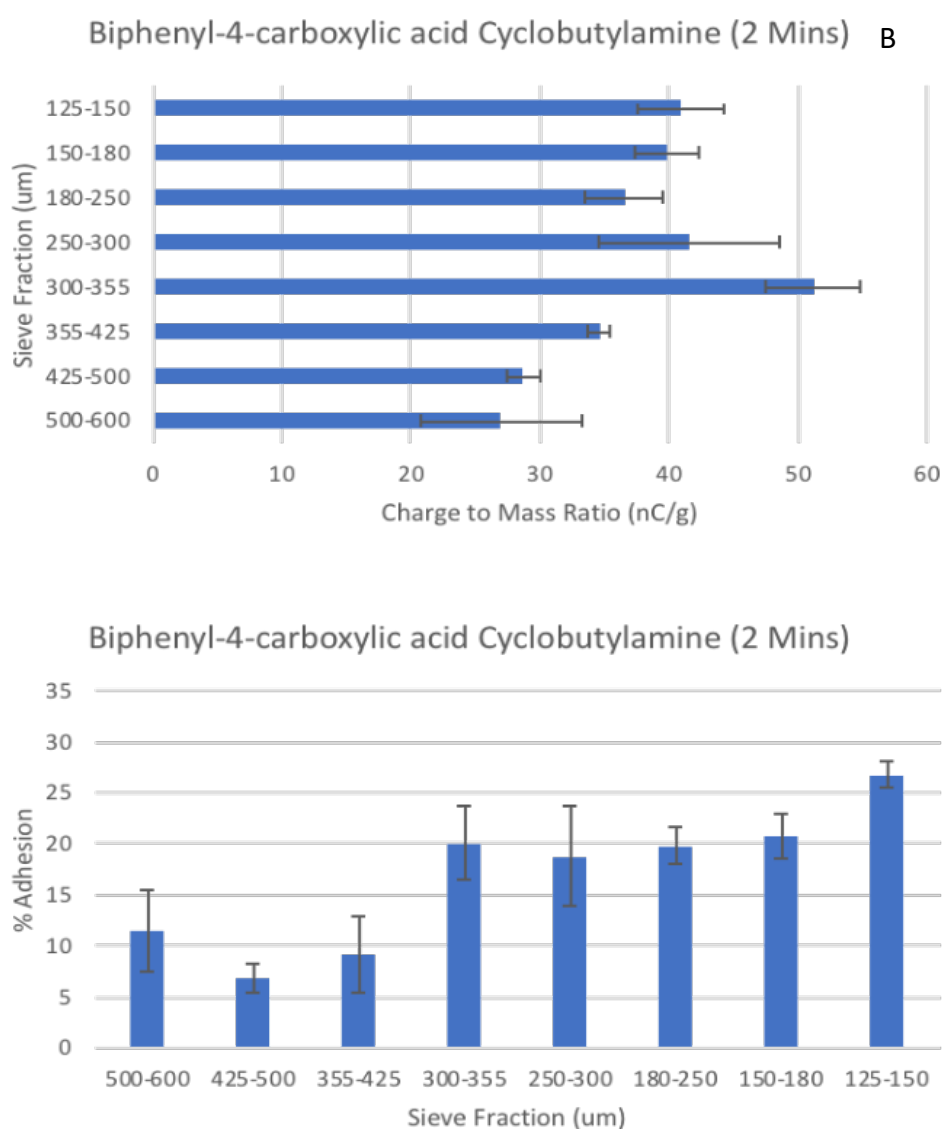
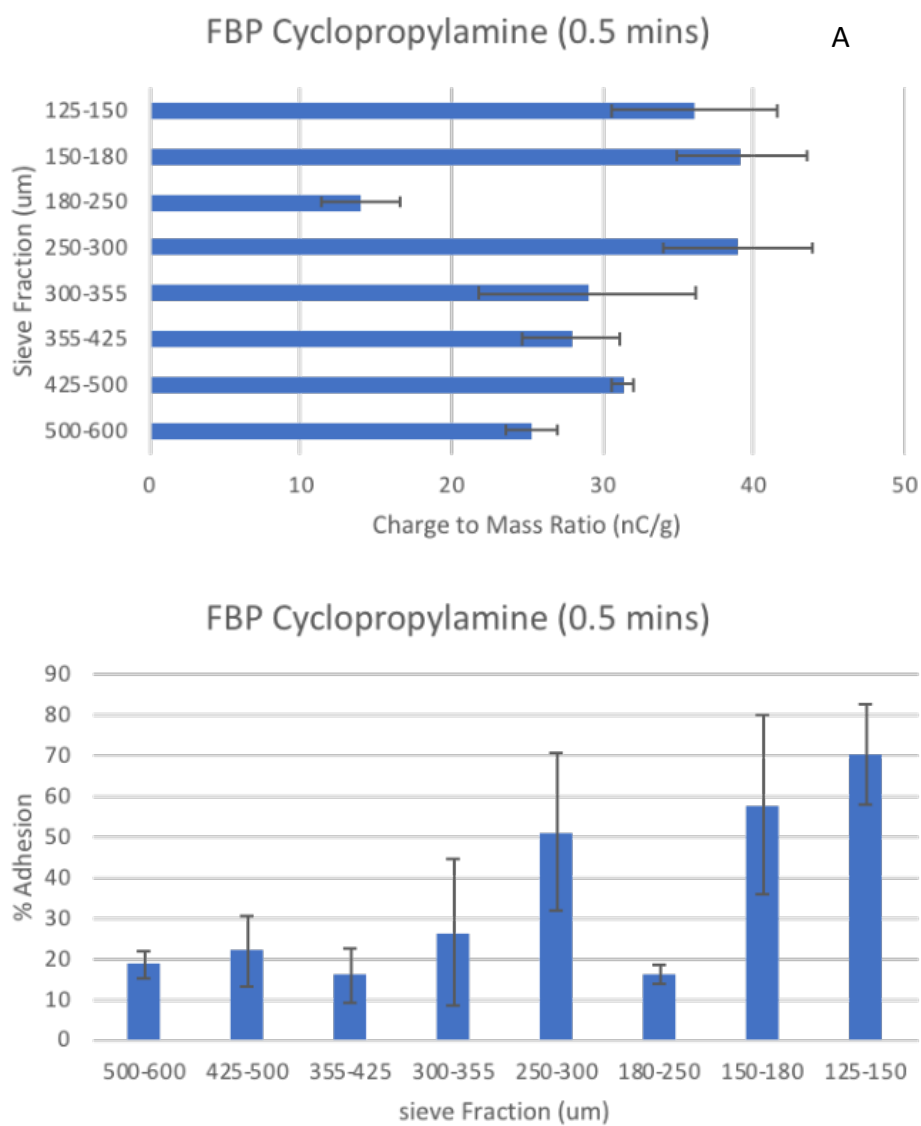


Figure 7.15: Tribo-electrification and adhesion data for B4CA CBA at (A) 0.5 and (B) 2 mins

From Figure 7.16/A13, the charging data for FBP C-Prop is interesting as the salt form showed a considerable reduction in charging propensity, at time points 0.5 and 2 min the maximum charge value was below 50 nC/g. The percentage adhesion at 0.5 mins was considerable, up to 80%, however at 2 mins a vast reduction is evident, with approximately 40% adhering. This trend continues at 5 and 10 mins indicating that the material has a lower propensity to charge as well as adhere to the shaker walls, in relation to the shear cell data this correlates as

although the material has a reduction in adhesion. A cohesive behaviour is still present due to considerable levels of materials adhering to the shaker walls are evident.



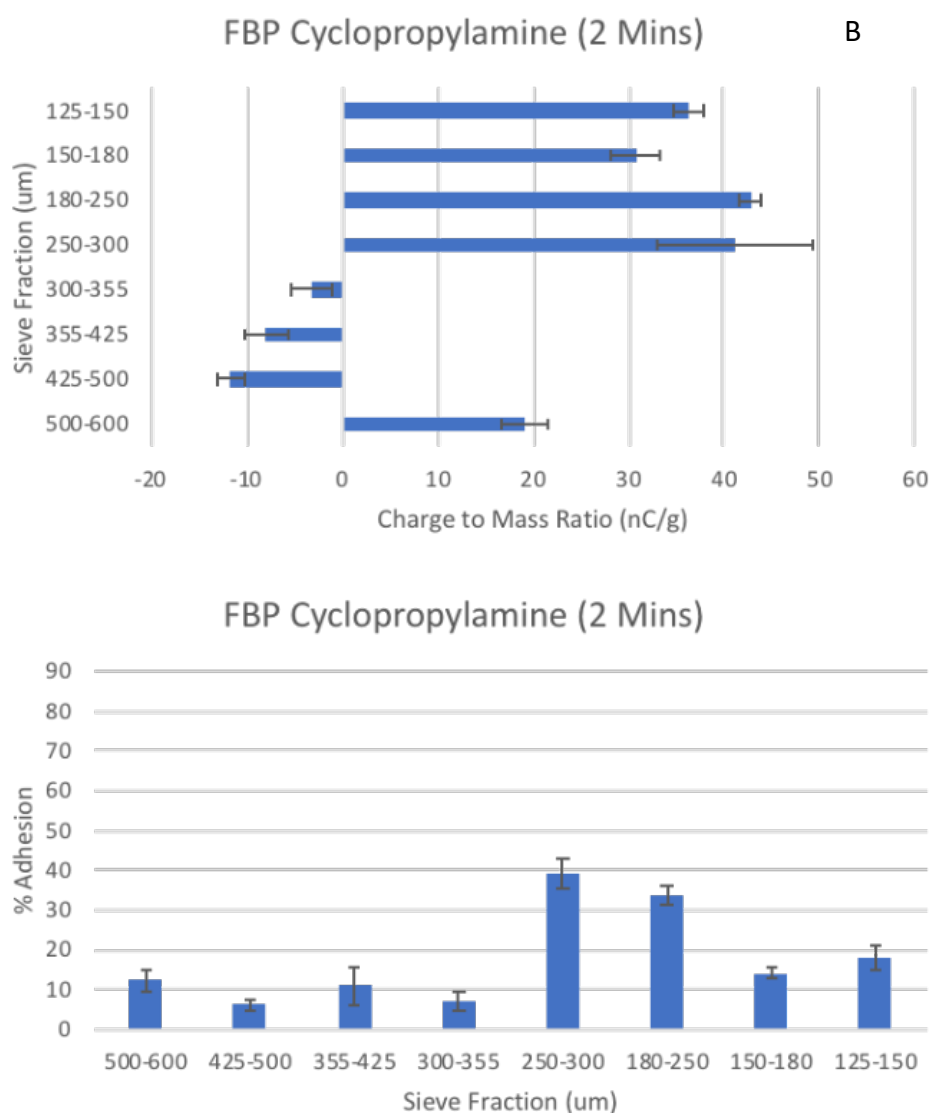
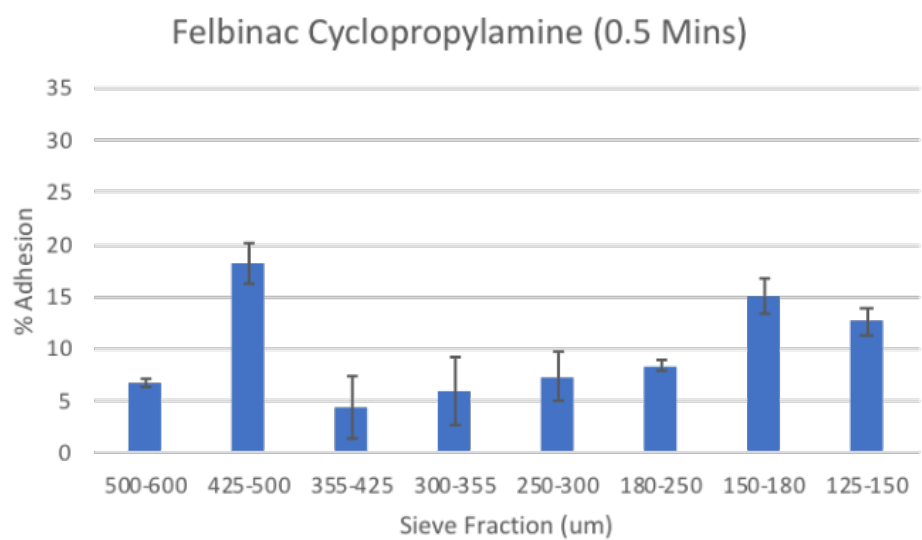
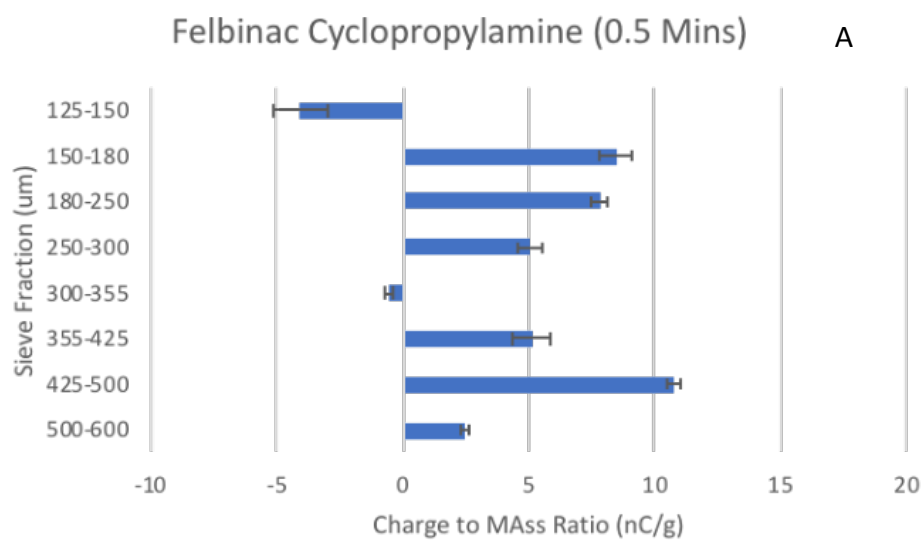


Figure 7.16: Tribo-electrification and adhesion data for FBP C-prop at (A) 0.5 and (B) 2 mins

A similar trend is apparent when compared with Felbi C-Prop (Figure 7.17/A14), producing a relatively low charge value of below 20 nC/g at time 0.5 and 2 mins, as well as a small percentage adhesion of below 30% for these time points, in contrast to the CBA salt which presented as high as 80-90%. This trend continues for 5 and 10 mins as the material charged no greater than 70 nC/g and the tendency of adhesion was below 60%, indicating that although the C-Prop salt presents cohesive tendencies on the shear cell, its charging propensity and adhesion affinity to the shaker walls are greatly reduced in contrast to the other salts such as FBP CBA which presented to be cohesive on the shear cell.



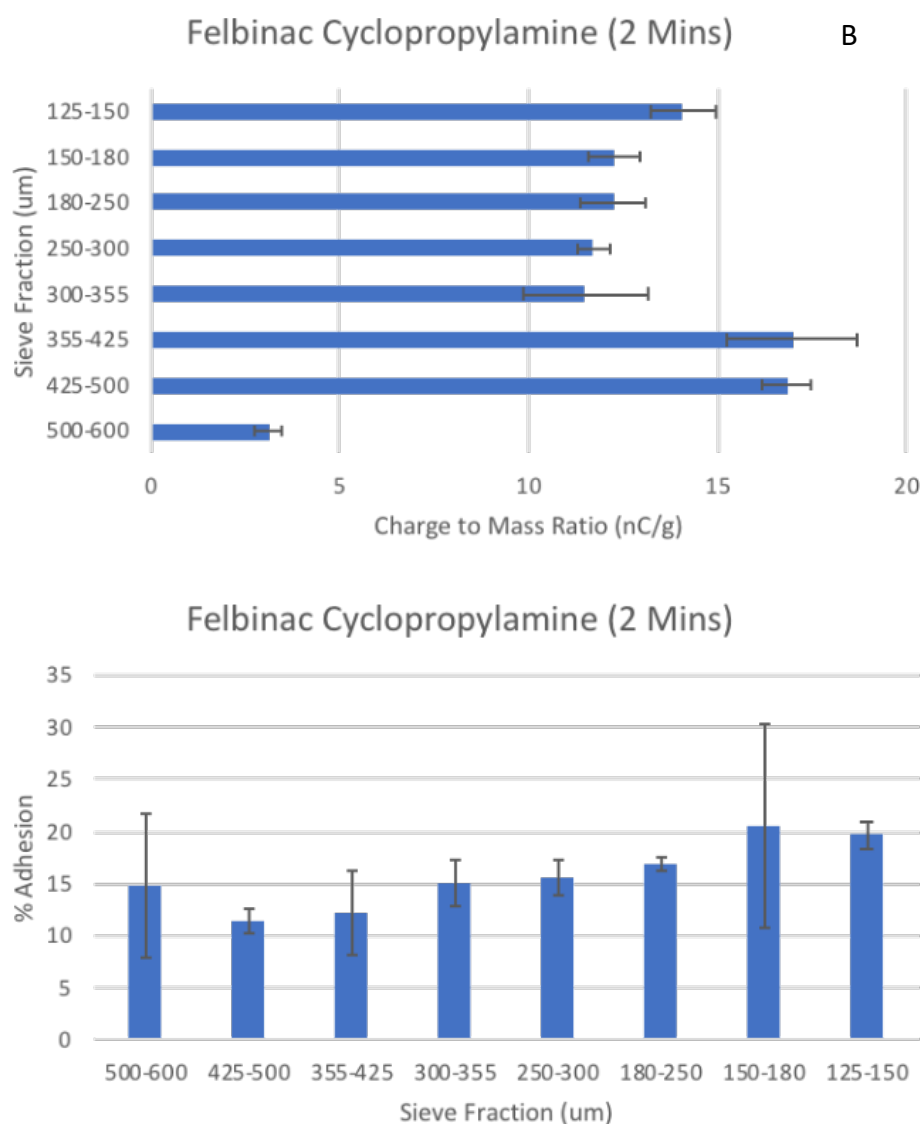
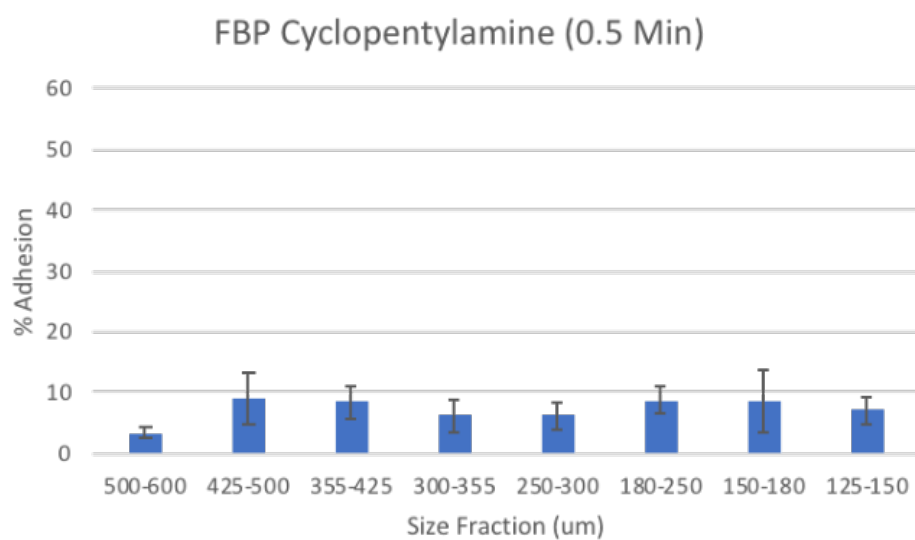
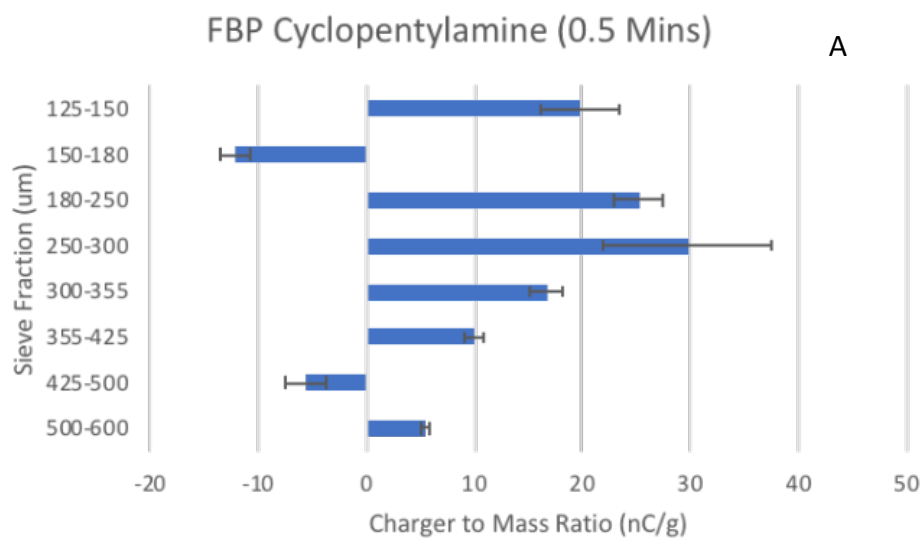


Figure 7.17: Tribo-electrification and adhesion data for Felbi C-prop at (A) 0.5 and (B) 2 mins

The charging propensity and adhesion tendency for FBP CPA is presented in Figure 7.18/A15. It is evident that the salt form is highly charging as well as it had a high affinity to adhere to the shaker walls. This is especially apparent at 2 mins as the smaller sieve fractions produced charge values of ~190 nC/g and adhesion value of over ~40%, this trend is also present at 5 and 10 mins with the charge value exceeding 200 nC/g and the adhesion tendency reaching 90% for the smaller sieve fractions.



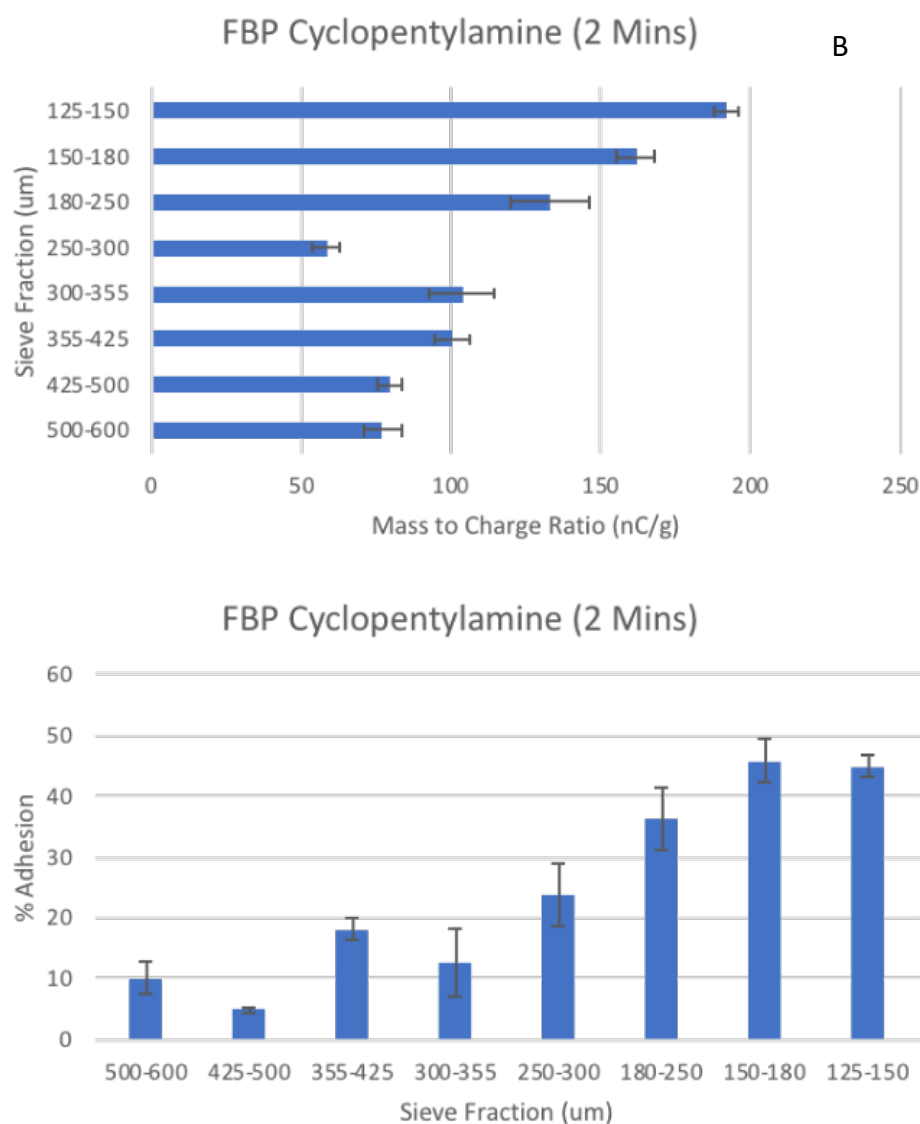
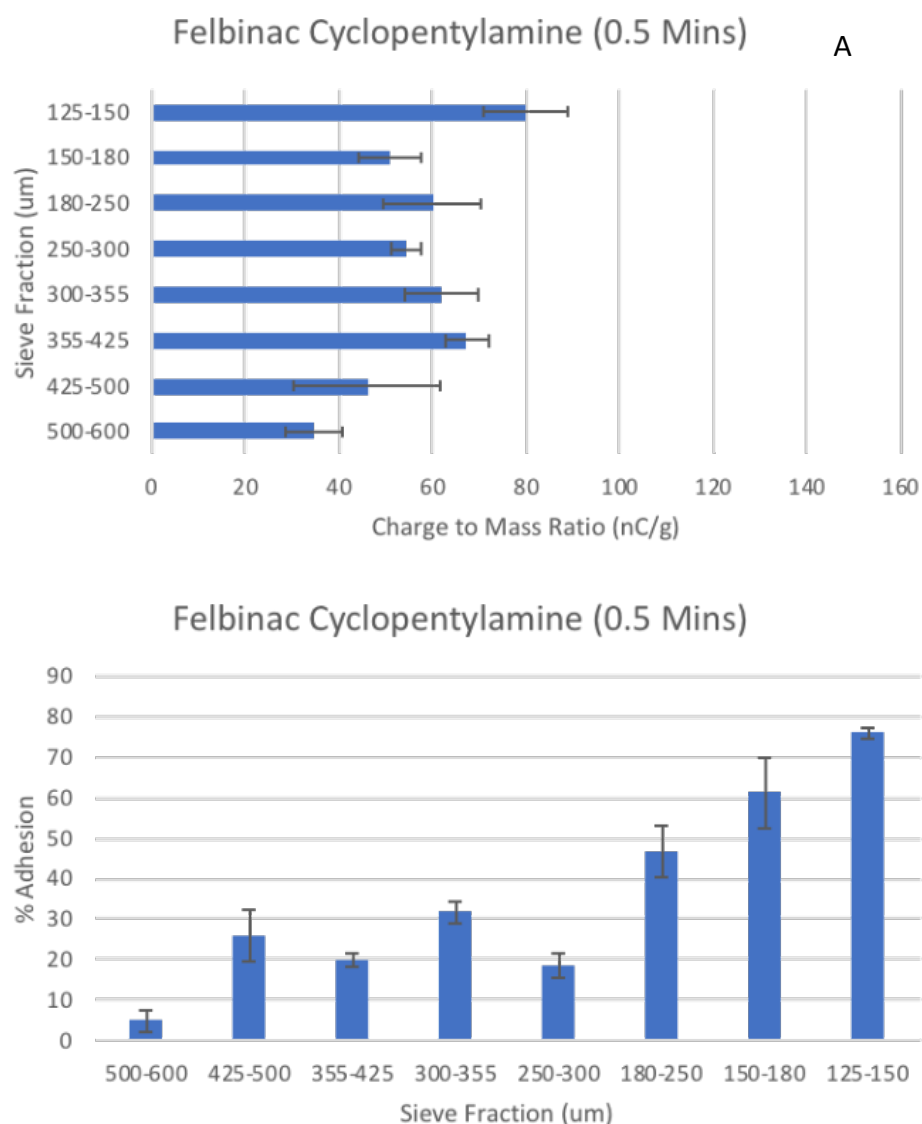


Figure 7.18: Tribo-electrification and adhesion data for FBP CPA at (A) 0.5 and (B) 2 mins

A similar trend is found for the Felbinac CPA salt form (Figure 7.19/A16), whereas when comparing with the B4CA CPA (Figure 7.20/A17) salt an interesting trend is evident, like the B4CA CBA salt; the CPA salt is also a low charging material with a maximum charge of below ~40 nC/g and a small adhesion tendency to the shaker walls, presenting less than 40% for all time intervals. This relates extremely well to the shear cell data as it showed to be easy flowing and the percentage adhesion was relatively low in comparison to the FBP and Felbi CBA/CPA salts. This is interesting as from the trends it is evident that for flurbiprofen and felbinac, which are highly charging with large levels of adhesion tendencies produced CBA

and CPA salts of similar behaviour, with C-Prop showing slight improvements. Whereas pure B4CA (Figure 7.12) showed to be an extremely low charging and sticking material and produced salts of similar characteristics, although charging slightly higher than the starting material itself. Yet considerably lower when compared with the salts of the same counterion for FBP and Felbi. Further work is required to determine if the trend of low charging starting material producing low charging salt forms.



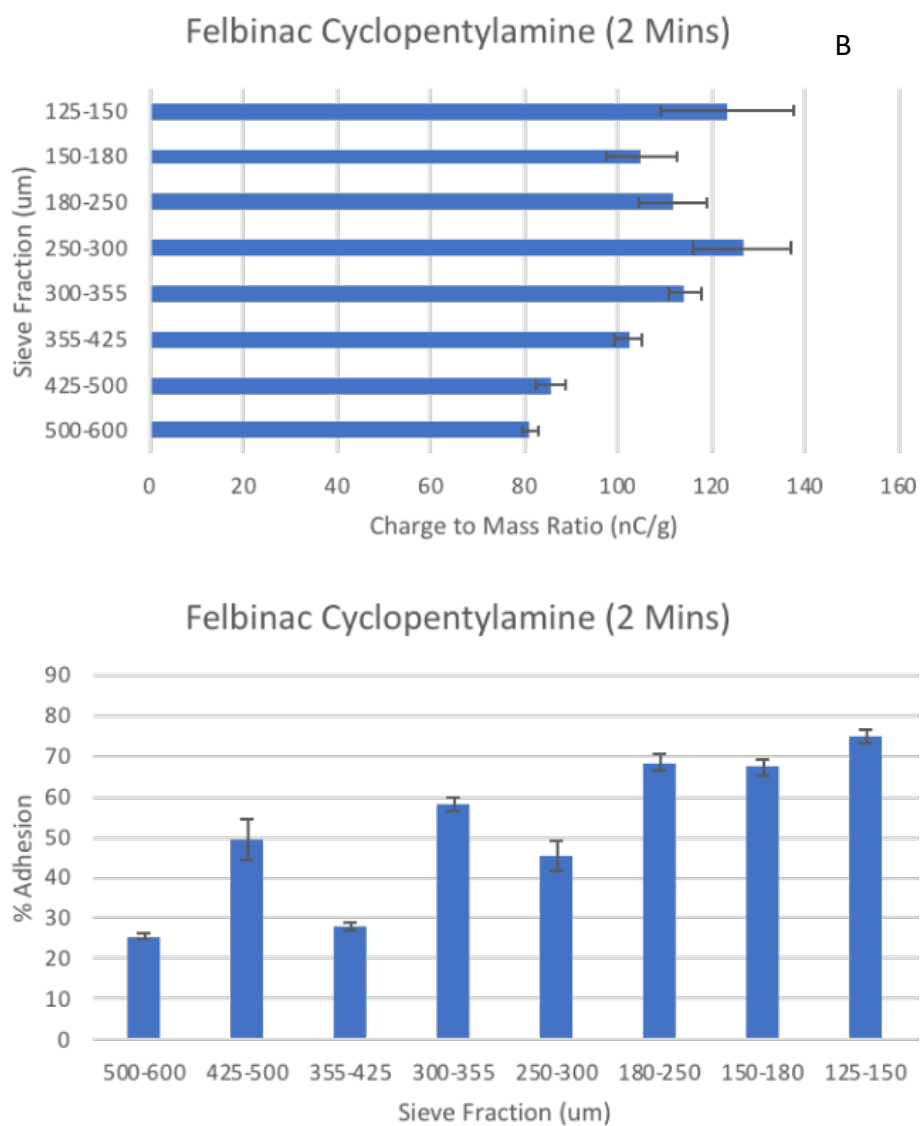
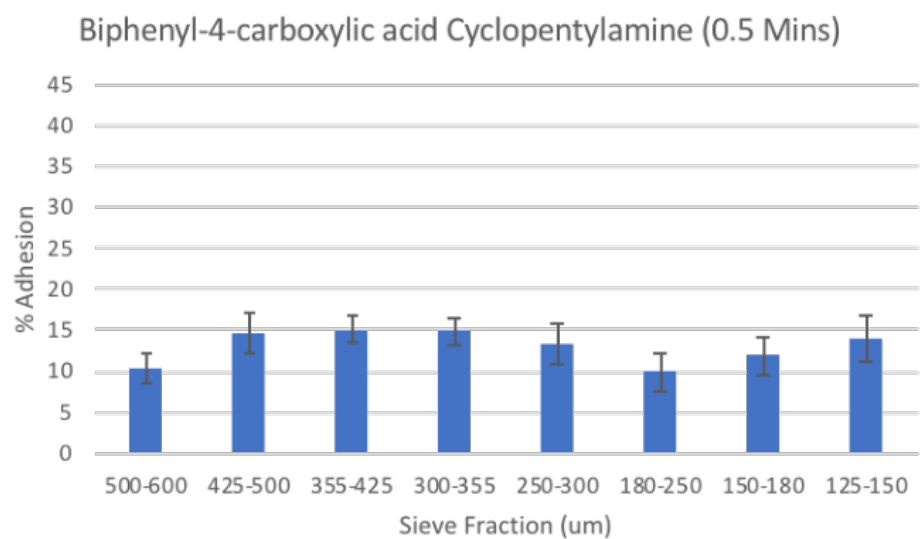
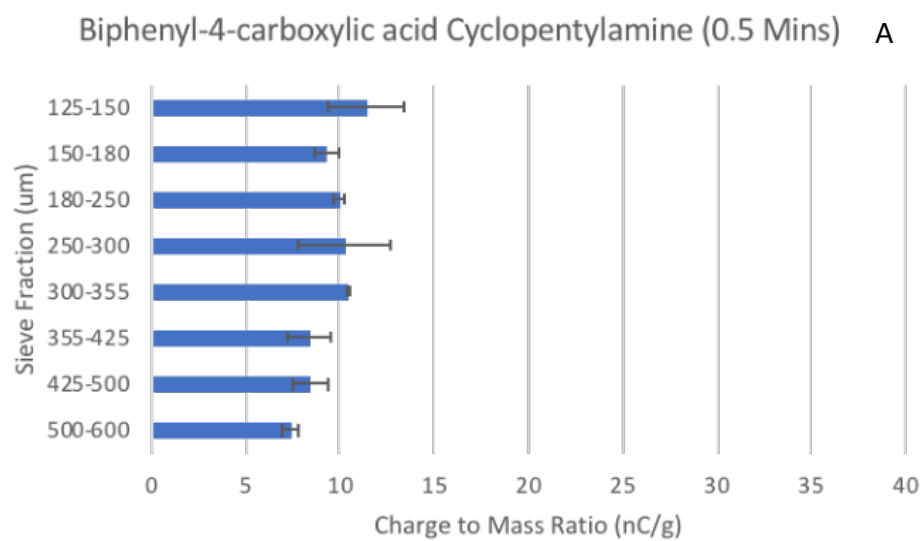


Figure 7.19: Tribo-electrification and adhesion data for Felbi CPA at (A) 0.5 and (B) 2 mins



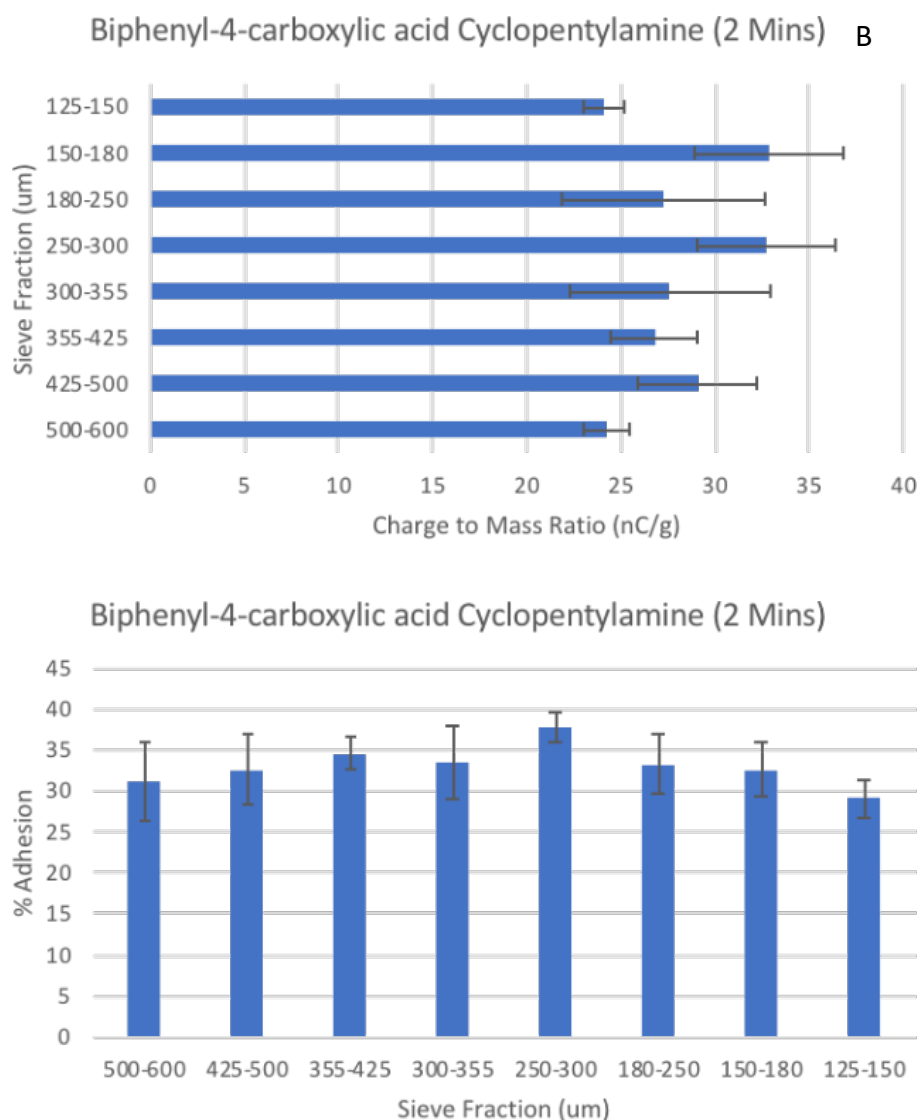


Figure 7.20: Tribo-electrification and adhesion data for B4CA CPA at (A) 0.5 and (B) 2 mins

7.7 Conclusion

The results show that the choice of parent compound as well as counterion are especially important due to significant differences in the physicochemical properties of the resulting material. The results indicate that the salt forms presented greater solubility in comparison to the parent compound, with an apparent trend whereby the solubility decreased as the carbon chain of the counterion increased, and felbinac C-Prop presenting the greatest solubility in comparison to the other salts and APIs. The same trend was seen for the IDR data and once again Felbi C-prop presented the greatest IDR. SEM images show that the salt forms presented vastly different particle morphologies to their parent compound which were flake

like with flat surfaces in comparison to acicular material and in some cases agglomerates of the needle like particles. This reflected to hinder the powder flowability, as the flake like particles exhibited to be either easy flowing or free flowing in comparison to the majority of the salt forms which were cohesive. The BET data did indicate that the pure compounds presented the smallest surface area in comparison to the salts, this may be due to an increase in porosity of the resulting salt form, indicating a larger surface area, however; the differences between the salt forms were not overly considerable. Furthermore, the FBP and Felbinac parent drugs had a great propensity for triboelectric charging and adhesion tendency, whereas the B4CA starting material was extremely low in both cases. The parent compounds charged negatively against the stainless steel surface. Therefore it can be anticipated that electrons are being transferred from the stainless steel surface to the powder particles (charging them negatively). The salts show to have a lower net charge in comparison to the parent drug however the CBA and CPA salt for both felbinac and FBP present high adhesion tendencies resulting in a considerable quantity of potentially highly charging material going unaccounted for with regards to charging propensity, also the small amount of material under measurement is highly charging. The C-Prop salts for both felbinac and FBP did present lower charging propensity as well as adhesion tendency, therefore aiding material handling properties, although the salt did display cohesive flow properties, the improved solubility and IDR are extremely beneficial. The salts of B4CA seem to exhibit the parent compound's low charging propensity and adhesion tendency, as well as displaying easy flow in most cases. Therefore proving to be the material with the greatest handling properties. The parent materials with high charging propensity; Flurbiprofen and Felbinac, structurally both have a larger chain length connecting the carboxylic acid group to the benzene ring. Also in the case of Flurbiprofen, the electronegative fluorine may influence the resulting charge. In comparison to the Biphenyl-4-carboxylic acid which presented a low charging propensity and structurally differs in a shorter chain between the benzene ring and the carboxylic acid group. In the case of Flurbiprofen and Felbinac the C-Prop salt did charge the least, in comparison to the C-but and C-Pent salts. However a strong and apparent trend was not observed whereby the charging increased as the carbon chain length of the counterion increased. The charging propensity of the starting material influenced the charging material of the salt, as Biphenyl-4-carboxylic acid salts, were low charging for both C-But and C-Pent counterions.

8 Conclusions

The work undertaken in this research project has investigated the influence of salt formation on physicochemical properties and tribo-electric charging of carboxylic acid drugs. Flurbiprofen, Felbinac and Biphenyl-4-carboxylic acid have been used as model materials for salt formation with the following amine counterions; cyclopropylamine, cyclobutylamine and cyclopentylamine. As well as scrutinised counterion selection for salt formation in the North American in comparison to European territories.

The key conclusions which may be drawn from this research are summarised as follows:

8.1 Analogous Carboxylic Acid Salts

- From the DSC data it is apparent that as the size of the counterion increased, the melting onset also increased, for flurbiprofen and felbinac parent compounds, the salt form had a greater melting onset however for biphenyl-4-carboxylic acid the salts exhibited a lower onset of melt in comparison to the parent drug.
- The solubility study demonstrated an opposite trend to the melting onset, as the size of the counterion increased, the solubility decreased, with felbinac cyclopropylamine presenting the greatest solubility from the parent drugs and salt forms.
- The trend for intrinsic dissolution was similar to the solubility trend, as it presented an increase in intrinsic dissolution as the size of counterion decreased.
- From the SEM images it is evident that the salt forms presented vastly different particle morphologies in comparison to their parent compound which were flake-like with flat surfaces, whereas the salts were acicular material and in some cases agglomerates of the needle like particles.
- FBP and Felbinac parent drugs had a great propensity for triboelectric charging and adhesion tendency, whereas the B4CA starting material was extremely low in both cases, the parent compounds charged negatively against the stainless steel surface.
- The salts show to have a lower net charge in comparison to the parent drug however the CBA and CPA salt for both felbinac and FBP present high adhesion tendencies.
- The C-Prop salts for both felbinac and FBP did present lower charging propensity as well as adhesion tendency.

- The salts of B4CA seem to exhibit the parent compounds low charging propensity and adhesion tendency, as well as displaying easy flow in most cases. Therefore proving to be the material with the greatest handling properties.

8.2 Flurbiprofen, Flurbiprofen Cyclopropyl-ammonium Salt and Salt Cocrystal

- The salt and salt cocrystal were successfully prepared, with the first time reporting of the salt cocrystal in a 2:1 ratio (drug: counterion).
- A different hydrogen bond arrangement to that of the salt was enabled by the presence of the second flurbiprofen in the unit cell.
- The salt exhibited an elevated melting onset (130.0 ± 0.66 °C) in comparison to the parent compound (114.2 ± 0.26 °C) whereas the salt cocrystal demonstrated a further elevated onset in comparison to the salt (137.4 ± 0.40 °C), as a result of the hydrogen bonding present within the structure.
- The salt exhibited better compressional and mechanical properties as compared to the salt cocrystal, This may be associated with improved plastic deformation of the salt under stress relative to the salt cocrystal enabled by a more clearly defined slip plane arrangement in the salt crystal lattice.
- The salt cocrystal displayed an improvement in the solubility in contrast to FBP and the salt form.
- The salt cocrystal exhibited the least charging propensity when compared with the salt and parent drug, as well as its reduced tendency to adhere to the shaker walls. In total there appears to be approximately a 10-fold reduction in the tribo-electrification and adhesion tendencies.
- From the data it is evident that both the salt and salt cocrystal provide enhanced physicochemical properties and reduced tribo-electric charging propensity in comparison to the parent compound, however the salt cocrystal provides an alternative with improved physicochemical properties in comparison to the salt, predominantly the solubility and material handling.

8.3 Salt Former Ratios

- From the DSC and HSM data it is evident that the recrystallisation process favoured the 93°C form, this was especially evident when an excess of flurbiprofen was used, indicating that an interaction between the flurbiprofen and recrystallised salt resulted in a change in form.
- From the SEM data it is apparent that altering just the ratio of drug to counterion influenced the particle size greatly, however the particle shape (needle) remained consistent. However the differences in particle shape are more evident as a result of solvent selection due to different crystallisation conditions.
- The tribo-electrification propensities were influenced by the both the ratio of drug to counterion and solvent selection. As the material produced by recrystallisation from absolute ethanol demonstrated a lower adhesion and charging propensity, indicating the potential ability to not only form lower charging material as a result of salt formation, to further enhance that by solvent selection.
- It is evident that the fbp cyclo 1:1 had the lowest charging propensity in comparison to the fbp cyclo 1:2 and fbp cyclo 2:1 salts.
- From the results it is evident that the recrystallisation process results in a number of changes to the physio-chemical properties of the drug salt and in turn leading to materials with varying propensity to charge.

8.4 Salt Trends

- The commonly reported statistic stating that approximately 50% of drugs are administered in a salt form stands true, as 45.4% of drugs were found to be a salt form from the orange book database.
- It is evident that the most popular anion used for salt formation is Chloride, with a percentage incidence of 49.7%, its popularity stems from its simplicity, cost, availability and significant experience of use in the past.
- The most popular cation is sodium, presenting a percentage incidence of 67.5%.
- Mesylate salt showed an interesting trend, a communication in the Pharmeuropa surfaced resulted in a reduction in its popularity, however table 4.7 indicates its

growing approval, accounting for the second most popular anion utilised for NCE's, with 4 and 6 incidences during 2007-2012 and 2013-2018.

- 899 APIs were classified for use in the oral drug delivery. From these, the salts of bases accounted for 333 (37.1%) and 74 (8.2%) of them were salts from acidic molecules.
- 236 approved APIs were used in injectable form, consisted of 80 (33.9%) non-salts, 106 (45.0%) API salts from basic entities and 50 (21.1%) were salts from acidic molecules.
- For the trends in new chemical entities, Chloride and sodium continued to dominate with percentage incidences of 36.7% and 55.6% respectively. The oral route was the most popular for both anion and cation NCE.
- A total of 1596 products are listed in the BNF, with similar trends to the orange book, presenting Sodium and Chloride as the most popular cation and anion respectively.
- An increase towards diversifying counterion selection is emerging, with some NCE presenting incidences for a range of anions and cations, although low in percentage in comparison to Chloride and Sodium, yet still demonstrating diversity in drug discovery

9 Future Work

The work carried out in this thesis has resulted in numerous possible lines of research worthy of further exploration. These are summarised below:

It would be beneficial for the continuous update of the salt trends to establish the popularity of certain counterions and the emergence of new chemical entities, as well as the effects of a potentially more diversified counterion selection on future trends.

An in-depth analysis of the form produced at 93°C as a result of altering the drug: counterion ratio as well as changing the solvent would be beneficial as it would provide a greater understanding of the resulting material and any potential benefits in comparison to the original salt form and parent drug.

Further research into the lower charging propensity of salts formed or recrystallised from absolute ethanol to establish if this is a trend which presents a similar trait for other active ingredients and counterions.

The low charging propensity of biphenyl-4-carboxylic acid and its subsequent salts would benefit from further studies to ascertain if this trend continues for other low charging materials in order to better predict materials with a low charging propensity for better material handling properties.

Due to a large adhesion tendency of some of the salts, it would be of benefit for a shaking machine to incorporate a faraday cup so a live measurement of charge-to-mass ratio can be obtained

References

1. Serajuddin, A.T.M., *Salt formation to improve drug solubility*. Advanced Drug Delivery Reviews, 2007. **59**(7): p. 603-616.
2. Gould, P.L., *Salt selection for basic drugs*. International Journal of Pharmaceutics, 1986. **33**(1): p. 201-217.
3. Huang, L.-F. and W.-Q. Tong, *Impact of solid state properties on developability assessment of drug candidates*. Advanced Drug Delivery Reviews, 2004. **56**(3): p. 321-334.
4. Davies, G., *Changing the salt, changing the drug*. Pharmaceutical Journal, 2001. **266**(7138): p. 322-323.
5. Bighley, L., S. Berge, and D. Monkhouse, *Salt forms of drugs and absorption*. Encyclopedia of Pharmaceutical Technology, 1996. **13**: p. 453-499.
6. David, S.E., P. Timmins, and B.R. Conway, *Impact of the counterion on the solubility and physicochemical properties of salts of carboxylic acid drugs*. Drug Development and Industrial Pharmacy, 2012. **38**(1): p. 93-103.
7. Nidhi, K., et al., *Hydrotropy: A promising tool for solubility enhancement: A review*. International Journal of Drug Development and Research, 2011. **3**: p. 26-33.
8. Cruz-Cabeza, A.J., *Acid–base crystalline complexes and the pKa rule*. CrystEngComm, 2012. **14**(20): p. 6362-6365.
9. Douroumis, D., S.A. Ross, and A. Nokhodchi, *Advanced methodologies for cocrystal synthesis*. Advanced Drug Delivery Reviews, 2017. **117**: p. 178-195.
10. Childs, S.L., G.P. Stahly, and A. Park, *The Salt–Cocrystal Continuum: The Influence of Crystal Structure on Ionization State*. Molecular Pharmaceutics, 2007. **4**(3): p. 323-338.
11. Cheney, M.L., et al., *Coformer Selection in Pharmaceutical Cocrystal Development: a Case Study of a Meloxicam Aspirin Cocrystal That Exhibits Enhanced Solubility and Pharmacokinetics*. Journal of Pharmaceutical Sciences, 2011. **100**(6): p. 2172-2181.
12. Maeno, Y., et al., *Novel pharmaceutical cocrystal consisting of paracetamol and trimethylglycine, a new promising cocrystal former*. International Journal of Pharmaceutics, 2014. **473**(1): p. 179-186.
13. Hong, C., et al., *A Novel Strategy for Pharmaceutical Cocrystal Generation Without Knowledge of Stoichiometric Ratio: Myricetin Cocrystals and a Ternary Phase Diagram*. Pharmaceutical Research, 2015. **32**(1): p. 47-60.
14. Stainton, P., et al., *First Comparative Study of the Three Polymorphs of Bis(isonicotinamide) Citric Acid Cocrystals and the Concomitant Salt 4-Carbamoylpyridinium Citrate Isonicotinamide*. Crystal Growth & Design, 2018. **18**(7): p. 4150-4159.
15. Shan, N., et al., *Impact of pharmaceutical cocrystals: the effects on drug pharmacokinetics*. Expert Opinion on Drug Metabolism & Toxicology, 2014. **10**(9): p. 1255-1271.
16. Jones, T.B., *13 - Electrostatics and Dust Explosions in Powder Handling A2 - Yang, Wen-Ching*, in *Fluidization, Solids Handling, and Processing*. 1999, William Andrew Publishing: Westwood, NJ. p. 817-871.
17. Engers, D.A., et al., *Triboelectrification of pharmaceutically relevant powders during low-shear tumble blending*. Journal of Electrostatics, 2006. **64**(12): p. 826-835.

18. Karner, S. and N. Anne Urbanetz, *The impact of electrostatic charge in pharmaceutical powders with specific focus on inhalation-powders*. Journal of Aerosol Science, 2011. **42**(6): p. 428-445.
19. Pina, A.S., A. Hussain, and A.C.A. Roque, *An Historical Overview of Drug Discovery*, in *Ligand-Macromolecular Interactions in Drug Discovery: Methods and Protocols*, A.C.A. Roque, Editor. 2010, Humana Press: Totowa, NJ. p. 3-12.
20. Prasad, V. and S. Mailankody, *Research and Development Spending to Bring a Single Cancer Drug to Market and Revenues After Approval* *Cost of Developing a Single Cancer Drug*. JAMA Internal Medicine, 2017. **177**(11): p. 1569-1575.
21. Mullard, A., *New drugs cost US\$2.6 billion to develop*. Nature Reviews Drug Discovery, 2014. **13**: p. 877.
22. Viswanathan, P., Y. Muralidaran, and G. Ragavan, *Chapter 7 - Challenges in oral drug delivery: a nano-based strategy to overcome*, in *Nanostructures for Oral Medicine*, E. Andronesco and A.M. Grumezescu, Editors. 2017, Elsevier. p. 173-201.
23. Paulekuhn, G.S., J.B. Dressman, and C. Saal, *Trends in Active Pharmaceutical Ingredient Salt Selection based on Analysis of the Orange Book Database*. Journal of Medicinal Chemistry, 2007. **50**(26): p. 6665-6672.
24. Zorec, B. and N. Pavselj, *Active enhancement methods for intra- and transdermal drug delivery: a review*. Zdravniški vestnik, 2013. **82**: p. 339-356.
25. Takagi, T., et al., *A Provisional Biopharmaceutical Classification of the Top 200 Oral Drug Products in the United States, Great Britain, Spain, and Japan*. Molecular Pharmaceutics, 2006. **3**(6): p. 631-643.
26. Li, S., et al., *IV-IVC considerations in the development of immediate-release oral dosage form*. Journal of Pharmaceutical Sciences, 2005. **94**(7): p. 1396-1417.
27. Bergström, C.A.S. and P. Larsson, *Computational prediction of drug solubility in water-based systems: Qualitative and quantitative approaches used in the current drug discovery and development setting*. International Journal of Pharmaceutics, 2018. **540**(1): p. 185-193.
28. Niederquell, A. and M. Kuentz, *Biorelevant Drug Solubility Enhancement Modeled by a Linear Solvation Energy Relationship*. Journal of Pharmaceutical Sciences, 2018. **107**(1): p. 503-506.
29. Kesisoglou, F., M. Vertzoni, and C. Reppas, *Physiologically Based Absorption Modeling of Salts of Weak Bases Based on Data in Hypochlorhydric and Achlorhydric Biorelevant Media*. AAPS PharmSciTech, 2018. **19**(7): p. 2851-2858.
30. Savjani, K.T., A.K. Gajjar, and J.K. Savjani, *Drug solubility: importance and enhancement techniques*. ISRN pharmaceutics, 2012. **2012**: p. 195727-195727.
31. Stahl, P.H. and C.G. Wermuth, *Handbook of pharmaceutical salts: properties, selection and use*. Chem. Int, 2002. **24**: p. 21.
32. Williams, H.D., et al., *Strategies to Address Low Drug Solubility in Discovery and Development*. Pharmacological Reviews, 2013. **65**(1): p. 315.
33. Rasenack, N. and B.W. Müller, *Micron-Size Drug Particles: Common and Novel Micronization Techniques*. Pharmaceutical Development and Technology, 2004. **9**(1): p. 1-13.
34. Khadka, P., et al., *Pharmaceutical particle technologies: An approach to improve drug solubility, dissolution and bioavailability*. Asian Journal of Pharmaceutical Sciences, 2014. **9**(6): p. 304-316.

35. Friščić, T. and W. Jones, *Benefits of cocrystallisation in pharmaceutical materials science: an update*. Journal of Pharmacy and Pharmacology, 2010. **62**(11): p. 1547-1559.
36. Sopyan, I., et al., *Co-crystallization: A Tool to Enhance Solubility and Dissolution Rate of Simvastatin*. Journal of Young Pharmacists, 2017. **9**: p. 183-186.
37. Amin, K., et al., *Lyophilization of polyethylene glycol mixtures*. Journal of Pharmaceutical Sciences, 2004. **93**(9): p. 2244-2249.
38. Yalkowsky, S.H. and T.J. Roseman, *Solubilization of drugs by cosolvents*. Techniques of solubilization of drugs, 1981. **12**: p. 91-134.
39. Millard, J.W., F.A. Alvarez-Nunez, and S.H. Yalkowsky, *Solubilization by cosolvents: Establishing useful constants for the log-linear model*. International Journal of Pharmaceutics, 2002. **245**(1-2): p. 153-166.
40. Yeh, M.-K., L.-C. Chang, and A.H.-J. Chiou, *Improving tenoxicam solubility and bioavailability by cosolvent system*. AAPS PharmSciTech, 2009. **10**(1): p. 166-171.
41. Rubino, J.T. and S.H. Yalkowsky, *Cosolvency and deviations from log-linear solubilization*. Pharmaceutical research, 1987. **4**(3): p. 231-236.
42. Babu, P.R.S., et al., *Solubility enhancement of cox-II inhibitors by cosolvency approach*. Dhaka University Journal of Pharmaceutical Sciences, 2008. **7**(2): p. 119-126.
43. Pan, L., et al., *Comparison of chromatographic and spectroscopic methods used to rank compounds for aqueous solubility*. Journal of Pharmaceutical sciences, 2001. **90**(4): p. 521-529.
44. Yalkowsky, S.H. and J.T. Rubino, *Solubilization by cosolvents I: organic solutes in propylene glycol-water mixtures*. Journal of pharmaceutical sciences, 1985. **74**(4): p. 416-421.
45. Nema, S., R.J. Washkuhn, and R.J. Brendel, *Excipients and their use in injectable products*. PDA Journal of Pharmaceutical Science and Technology, 1997. **51**(4): p. 166-171.
46. Raj Vemula, V., V. Lagishetty, and S. Lingala, *Solubility Enhancement Techniques*. International Journal of Pharmaceutical Sciences Review and Research, 2010. **5**: p. 41-51.
47. Loftsson, T. and M.E. Brewster, *Pharmaceutical applications of cyclodextrins: effects on drug permeation through biological membranes*. Journal of Pharmacy and Pharmacology, 2011. **63**(9): p. 1119-1135.
48. Singh, A., Z.A. Worku, and G. Van den Mooter, *Oral formulation strategies to improve solubility of poorly water-soluble drugs*. Expert opinion on drug delivery, 2011. **8**(10): p. 1361-1378.
49. Wang, E., G. Chen, and H. Liu, *Crystal Structure of β -Cyclodextrin-Felbinac Inclusion Complex*. Chinese Journal of Chemistry, 2009. **27**(10): p. 2097-2101.
50. Chaudhary, V.B. and J.K. Patel, *Cyclodextrin inclusion complex to enhance solubility of poorly water soluble drugs: A review*. International Journal of Pharmaceutical Sciences and Research, 2013. **4**(1): p. 68.
51. L. Amidon, G., et al., *A Theoretical Basis for a Biopharmaceutic Drug Classification: The Correlation of In Vitro Drug Product Dissolution and In Vivo Bioavailability*. Pharmaceutical research, 1995. **12**: p. 413-20.
52. Ku, M.S., *Use of the Biopharmaceutical Classification System in Early Drug Development*. The AAPS Journal, 2008. **10**(1): p. 208-212.

53. Food and A. Drug, *Guidance for industry: waiver of in vivo bioavailability and bioequivalence studies for immediate-release solid oral dosage forms based on a biopharmaceutics classification system*. Food and Drug Administration, Rockville, MD, 2000.
54. Yasir, M., et al., *Biopharmaceutical Classification System :An Account*. International Journal of PharmTech Research, 2010. **2**.
55. Sachan, N.K., et al., *Biopharmaceutical classification system: A strategic tool for oral drug delivery technology*. Asian Journal of Pharmaceutics (AJP): Free full text articles from Asian J Pharm, 2014. **3**(2).
56. Šupuk, E., et al., *The influence of salt formation on electrostatic and compression properties of flurbiprofen salts*. International Journal of Pharmaceutics, 2013. **458**(1): p. 118-127.
57. S. Mahanty, J.S., Niranjan Patra Ch, *Particle design of drugs by spherical crystallization techniques*. Int J Pharm Sci Nanotech, 2010. **3**(2): p. 912–918.
58. Vippagunta, S.R., H.G. Brittain, and D.J.W. Grant, *Crystalline solids*. Advanced Drug Delivery Reviews, 2001. **48**(1): p. 3-26.
59. Buckton, G., *Solid-state properties, Aulton's pharmaceutics, The science of dosage form design, Aulton M.E.* 3rd ed. 2007, London: Churchill Livingstone.
60. Garside, J., *Industrial crystallization from solution*. Chemical Engineering Science, 1985. **40**(1): p. 3-26.
61. Dirksen, J.A. and T.A. Ring, *Fundamentals of crystallization: Kinetic effects on particle size distributions and morphology*. Chemical Engineering Science, 1991. **46**(10): p. 2389-2427.
62. El-Zhry El-Yafi, A.K. and H. El-Zein, *Technical crystallization for application in pharmaceutical material engineering: Review article*. Asian Journal of Pharmaceutical Sciences, 2015. **10**(4): p. 283-291.
63. Jaradzadeh, Y.M., A. Khoei, N.S., *Improvement of physicomachanical properties of carbamazepine by recrystallization at diggerent pH values*. Acta Pharm, 2009. **59**(2): p. 187-197.
64. Karimi-Jafari, M., et al., *Creating Cocystals: A Review of Pharmaceutical Cocystal Preparation Routes and Applications*. Crystal Growth & Design, 2018. **18**(10): p. 6370-6387.
65. aimah Barikah, K.Z., *Traditional and Novel Methods for Cocystal Formation: A Mini Review*. Systematic Reviews in Pharmacy, 2018. **9**: p. 79-82.
66. Fernandes, G.J., M. Rathnanand, and V. Kulkarni, *Mechanochemical Synthesis of Carvedilol Cocystals Utilizing Hot Melt Extrusion Technology*. Journal of Pharmaceutical Innovation, 2018.
67. Pando, C., A. Cabañas, and I.A. Cuadra, *Preparation of pharmaceutical co-crystals through sustainable processes using supercritical carbon dioxide: a review*. RSC Advances, 2016. **6**(75): p. 71134-71150.
68. Titapiwatanakun, V., A.W. Basit, and S. Gaisford, *A New Method for Producing Pharmaceutical Co-crystals: Laser Irradiation of Powder Blends*. Crystal Growth & Design, 2016. **16**(6): p. 3307-3312.
69. Hart, A., *Effect of particle size on detergent powders flowability and tabletability*. J. Chem. Eng. Process Technol, 2015. **6**(1): p. 215-218.
70. Schulze, D., *Flow properties of powders and bulk solids*. Braunschweig/Wolfenbu ttel, Germany: University of Applied Sciences, 2006.

71. Matsusaka, S., et al., *Triboelectric charging of powders: A review*. Chemical Engineering Science, 2010. **65**(22): p. 5781-5807.
72. Harper, W.R., *Contact and frictional electrification*. 1967.
73. Engers, D.A., et al., *Triboelectric charging and dielectric properties of pharmaceutically relevant mixtures*. Journal of Electrostatics, 2007. **65**(9): p. 571-581.
74. *Work Function*. In Oxford Dictionary; Available from: https://www.lexico.com/en/definition/work_function.
75. Jachowicz, J., M. Garcia, and G. Wis-Surel, *Relationship Between Triboelectric Charging and Surface Modification of Human Hair: Polymeric Versus Monomeric Long Alkyl Chain Quaternary Ammonium Salts*. Textile Research Journal, 1987. **57**(9): p. 543-548.
76. Ghorl, M.U., E. Šupuk, and B.R. Conway, *Tribo-electric charging and adhesion of cellulose ethers and their mixtures with flurbiprofen*. European Journal of Pharmaceutical Sciences, 2014. **65**: p. 1-8.
77. Horn, R.G., D.T. Smith, and A. Grabbe, *Contact electrification induced by monolayer modification of a surface and relation to acid-base interactions*. Nature, 1993. **366**(6454): p. 442-443.
78. Molerus, O. and M. Nywlt, *The influence of the fine particle content of the flow behaviour of bulk materials*. Powder Technology, 1984. **37**(1): p. 145-154.
79. Pai, D.M. and B.E. Springett, *Physics of electrophotography*. Reviews of Modern Physics, 1993. **65**(1): p. 163-211.
80. Menéndez, F., et al., *Porcelain insulators in electrostatic precipitator*. Journal of Electrostatics, 2015. **76**: p. 188-193.
81. Domnick, J., A. Scheibe, and Q. Ye, *The Simulation of the Electrostatic Spray Painting Process with High-Speed Rotary Bell Atomizers. Part I: Direct Charging*. Particle & Particle Systems Characterization, 2005. **22**(2): p. 141-150.
82. Matsusaka, S. and H. Masuda, *Electrostatics of particles*. Advanced Powder Technology, 2003. **14**(2): p. 143-166.
83. Hogue, M.D., et al., *Insulator–insulator contact charging and its relationship to atmospheric pressure*. Journal of Electrostatics, 2004. **61**(3–4): p. 259-268.
84. Adams, C.K., *Nature's electricity*. 1987: Blue Ridge Summit, PA: Tab Books, 1987.
85. Greason, W.D., *Electrostatic discharge: a charge driven phenomenon*. Journal of Electrostatics, 1992. **28**(3): p. 199-218.
86. Watanabe, H., et al., *Triboelectrification of pharmaceutical powders by particle impact*. International journal of pharmaceutics, 2007. **334**(1-2): p. 149-155.
87. Matsusaka, S. and H. Masuda, *Simultaneous measurement of mass flow rate and charge-to-mass ratio of particles in gas–solids pipe flow*. Chemical Engineering Science, 2006. **61**(7): p. 2254-2261.
88. Watanabe, H., et al., *Measurement of Charge Transfer due to Single Particle Impact*. Particle & Particle Systems Characterization, 2006. **23**(2): p. 133-137.
89. Matsuyama, T. and H. Yamamoto, *Charge relaxation process dominates contact charging of a particle in atmospheric conditions*. Journal of Physics D: Applied Physics, 1995. **28**(12): p. 2418.
90. Carter, P.A., et al., *An experimental investigation of triboelectrification in cohesive and non-cohesive pharmaceutical powders*. Drug Development and Industrial Pharmacy, 1992. **18**(14): p. 1505-1526.

91. Trigwell, S., et al., *Effects of Powder Velocity and Contact Materials on Tribocharging of Polymer Powders for Powder Coating Applications*. Particulate Science and Technology, 2008. **26**(2): p. 145-157.
92. Mukherjee, R., et al., *Effects of particle size on the triboelectrification phenomenon in pharmaceutical excipients: experiments and multi-scale modeling*. Asian Journal of Pharmaceutical Sciences.
93. Rowley, G., *Quantifying electrostatic interactions in pharmaceutical solid systems*. International Journal of Pharmaceutics, 2001. **227**(1–2): p. 47-55.
94. Ireland, P.M., *Triboelectrification of particulate flows on surfaces: Part I — Experiments*. Powder Technology, 2010. **198**(2): p. 189-198.
95. Afzal, M.S., et al., *The effect of mesoporous silica impregnation on tribo-electrification characteristics of flurbiprofen*. International Journal of Pharmaceutics, 2018. **544**(1): p. 55-61.
96. Eilbeck, J., et al., *Effect of contamination of pharmaceutical equipment on powder triboelectrification*. International Journal of Pharmaceutics, 2000. **195**(1–2): p. 7-11.
97. Young, P.M., et al., *Influence of Humidity on the Electrostatic Charge and Aerosol Performance of Dry Powder Inhaler Carrier based Systems*. Pharmaceutical Research, 2007. **24**(5): p. 963-970.
98. Rowley, G. and L.A. Mackin, *The effect of moisture sorption on electrostatic charging of selected pharmaceutical excipient powders*. Powder Technology, 2003. **135–136**: p. 50-58.
99. Elajnaf, A., P. Carter, and G. Rowley, *Electrostatic characterisation of inhaled powders: Effect of contact surface and relative humidity*. European Journal of Pharmaceutical Sciences, 2006. **29**(5): p. 375-384.
100. Thomas, B., B. Roger, and K.P. James, *Flow*, in *Pharmaceutical Dosage Forms - Tablets*. 2008, CRC Press. p. 75-110.
101. Šupuk, E., C. Seiler, and M. Ghadiri, *Analysis of a Simple Test Device for Tribo-Electric Charging of Bulk Powders*. Particle & Particle Systems Characterization, 2009. **26**(1-2): p. 7-16.
102. Matsuyama, T., et al., *Tribo-Electrification and Associated Segregation of Pharmaceutical Bulk Powders*. Powder and particle, 2011. **29**: p. 208-223.
103. Peart, J., *Powder Electrostatics: Theory, Techniques and Applications*. KONA Powder and Particle Journal, 2001. **19**: p. 34-45.
104. Ghorl, U.M., E. Šupuk, and R.B. Conway, *Tribo-electrification and Powder Adhesion Studies in the Development of Polymeric Hydrophilic Drug Matrices*. Materials, 2015. **8**(4).
105. Sheldrick, G.M., *SADABS. Program for Empirical Absorption Correction*. University of Gottingen. Germany, 1996.
106. Sheldrick, G.M., *Crystal structure refinement with SHELXL*. Acta Crystallographica Section C, 2015. **71**(1): p. 3-8.
107. Maddineni, S., et al., *Dissolution research-A predictive tool for conventional and novel dosage forms*. Asian Journal of Pharmacy and Life Science ISSN, 2012. **2231**: p. 4423.
108. Callahan, J.C., et al., *Equilibrium Moisture Content of Pharmaceutical Excipients*. Drug Development and Industrial Pharmacy, 1982. **8**(3): p. 355-369.

109. Bastin, R.J., M.J. Bowker, and B.J. Slater, *Salt Selection and Optimisation Procedures for Pharmaceutical New Chemical Entities*. Organic Process Research & Development, 2000. **4**(5): p. 427-435.
110. Gupta, D., et al., *Salts of Therapeutic Agents: Chemical, Physicochemical, and Biological Considerations*. LID - E1719 [pii] LID - 10.3390/molecules23071719 [doi]. (1420-3049 (Electronic)).
111. Acharya, P.C., et al., *Chapter 13 - Role of Salt Selection in Drug Discovery and Development*, in *Dosage Form Design Considerations*, R.K. Tekade, Editor. 2018, Academic Press. p. 435-472.
112. Elder, D.P., R. Holm, and H.L.d. Diego, *Use of pharmaceutical salts and cocrystals to address the issue of poor solubility*. International Journal of Pharmaceutics, 2013. **453**(1): p. 88-100.
113. Savjani, K.T., A.K. Gajjar, and J.K. Savjani, *Drug Solubility: Importance and Enhancement Techniques*. ISRN Pharmaceutics, 2012. **2012**: p. 10.
114. Hughes, D.L., *Patent Review of Manufacturing Routes to Recently Approved PARP Inhibitors: Olaparib, Rucaparib, and Niraparib*. Organic Process Research & Development, 2017. **21**(9): p. 1227-1244.
115. Morris, K.R., et al., *An integrated approach to the selection of optimal salt form for a new drug candidate*. International Journal of Pharmaceutics, 1994. **105**(3): p. 209-217.
116. Trask, A.V., et al., *Screening for crystalline salts via mechanochemistry*. Chemical Communications, 2006(1): p. 51-53.
117. Serajuddin, A.T., *Salt formation to improve drug solubility*. Advanced drug delivery reviews, 2007. **59**(7): p. 603-616.
118. Berge, S.M., L.D. Bighley, and D.C. Monkhouse, *Pharmaceutical Salts*. Journal of Pharmaceutical Sciences, 1977. **66**(1): p. 1-19.
119. *U.S. Food and Drug Administration*. Orange Book: Approved drug products with therapeutic equivalence evaluations; Available from: <http://www.fda.gov/cder/ob/>
120. *Joint Formulary Committee*. British National Formulary; Available from: <https://bnf.nice.org.uk>.
121. *BNF 66*. Joint Formulary Committee 2013: London: Pharmaceutical Press.
122. Makary, P., *Principles of Salt Formation*. Vol. 2. 2014. 1.
123. McDougall, D.J., et al., *Inclusion of salt form on prescription medication labeling as a source of patient confusion: a pilot study*. Pharmacy practice, 2016. **14**(1): p. 677-677.
124. Kinch, M.S., *An overview of FDA-approved biologics medicines*. Drug Discovery Today, 2015. **20**(4): p. 393-398.
125. Saal, C. and A. Becker, *Pharmaceutical salts: A summary on doses of salt formers from the Orange Book*. European Journal of Pharmaceutical Sciences, 2013. **49**(4): p. 614-623.
126. Europe, C., *Enquiry: alkyl mesilates (methanesulphonates) impurities in mesilates salts*. Pharmeuropa, 2000. **12**: p. 27.
127. Snodin, D. and A. Teasdale, *Mutagenic Alkyl-Sulfonate Impurities in Sulfonic Acid Salts: Reviewing the Evidence and Challenging Regulatory Perceptions*. Organic Process Research & Development, 2015. **19**(11): p. 1465-1485.
128. Balaji, N. and S. Sultana, *GC and GC-MS Detection of Alkyl Mesylates in Active Pharmaceutical Ingredients*. Vol. 46. 2017. 88-92.

129. Sitaram, C., et al., *Determination of Alkyl Methanesulfonates in Doxazosin Mesylate by Gas Chromatography-mass Spectrometer*. Indian journal of pharmaceutical sciences, 2011. **73**(1): p. 107-110.
130. Kakadiya, P.R., et al., *Low level determinations of methyl methanesulfonate and ethyl methanesulfonate impurities in emtricitabine active pharmaceutical ingredient by LC/MS/MS using electrospray ionization*. Analytical chemistry insights, 2011. **6**: p. 21-28.
131. U.S. Food and Drug Administration. Available from: <https://www.fda.gov>.
132. Wong, J., et al., *Major Degradation Product Identified in Several Pharmaceutical Formulations against the Common Cold*. Analytical Chemistry, 2006. **78**(22): p. 7891-7895.
133. Gupta, D., et al., *Salts of Therapeutic Agents: Chemical, Physicochemical, and Biological Considerations*. Molecules, 2018. **23**(7).
134. David, S.E., et al., *Comparative physical, mechanical and crystallographic properties of a series of gemfibrozil salts*. Journal of Pharmacy and Pharmacology, 2010. **62**(11): p. 1519-1525.
135. Ramirez, M., et al., *Crystal Packing Arrangement, Chain Conformation, and Physicochemical Properties of Gemfibrozil Amine Salts*. Crystal Growth & Design, 2017. **17**(7): p. 3743-3750.
136. Wang, C., et al., *Relationships among Crystal Structures, Mechanical Properties, and Tableting Performance Probed Using Four Salts of Diphenhydramine*. Crystal Growth & Design, 2017. **17**(11): p. 6030-6040.
137. Wang, C., S. Hu, and C.C. Sun, *Expedited development of a high dose orally disintegrating metformin tablet enabled by sweet salt formation with acesulfame*. International Journal of Pharmaceutics, 2017. **532**(1): p. 435-443.
138. Paul, S., et al., *Reduced Punch Sticking Propensity of Acesulfame by Salt Formation: Role of Crystal Mechanical Property and Surface Chemistry*. Molecular Pharmaceutics, 2019. **16**(6): p. 2700-2707.
139. Landis, M.S., et al., *Commentary: Why Pharmaceutical Scientists in Early Drug Discovery Are Critical for Influencing the Design and Selection of Optimal Drug Candidates*. AAPS PharmSciTech, 2018. **19**(1): p. 1-10.
140. Hatcher, L.E., et al., *Tuning Morphology in Active Pharmaceutical Ingredients: Controlling the Crystal Habit of Lovastatin through Solvent Choice and Non-Size-Matched Polymer Additives*. Crystal Growth & Design, 2020. **20**(9): p. 5854-5862.
141. Chen, J., et al., *Effect of Solvent on the Crystal Structure and Habit of Hydrocortisone*. Crystal Growth & Design, 2008. **8**(5): p. 1490-1494.
142. Fukunaka, T., et al., *Effect of Particle Shape of Active Pharmaceutical Ingredients Prepared by Fluidized-Bed Jet-Milling on Cohesiveness*. Journal of Pharmaceutical Sciences, 2005. **94**(5): p. 1004-1012.
143. Debord, B., et al., *Study of Different Crystalline forms of Mannitol: Comparative Behaviour under Compression*. Drug Development and Industrial Pharmacy, 1987. **13**(9-11): p. 1533-1546.
144. Bauer, J., *Pharmaceutical Solids: Size, Shape, and Surface Area*. Journal of Validation Technology, 2009. **15**.
145. Amidon, G.L., et al., *A Theoretical Basis for a Biopharmaceutic Drug Classification: The Correlation of in Vitro Drug Product Dissolution and in Vivo Bioavailability*. Pharmaceutical Research, 1995. **12**(3): p. 413-420.

146. Giron, D., *Characterisation of salts of drug substances*. Journal of Thermal Analysis and Calorimetry, 2003. **73**(2): p. 441-457.
147. Guerrieri, P., et al., *Analysis of Relationships Between Solid-State Properties, Counterion, and Developability of Pharmaceutical Salts*. AAPS PharmSciTech, 2010. **11**(3): p. 1212-1222.
148. Stahl, P.H., et al., *Handbook of pharmaceutical salts : properties, selection, and use*. 2002, Weinheim; New York: VHCA : Wiley-VCH.
149. Agharkar, S., S. Lindenbaum, and T. Higuchi, *Enhancement of solubility of drug salts by hydrophilic counterions: Properties of organic salts of an antimalarial drug*. Journal of Pharmaceutical Sciences, 1976. **65**(5): p. 747-749.
150. Jones, P.H., et al., *Insoluble erythromycin salts*. Journal of Pharmaceutical Sciences, 1969. **58**(3): p. 337-339.
151. Asare-Addo, K., et al., *Direct imaging of the dissolution of salt forms of a carboxylic acid drug*. Vol. 551. 2018.
152. Cheung, E.Y., et al., *Structural properties of a family of hydrogen-bonded co-crystals formed between gemfibrozil and hydroxy derivatives of t-butylamine, determined directly from powder X-ray diffraction data*. Journal of Solid State Chemistry, 2007. **180**(3): p. 1068-1075.
153. Murtomaa, M., et al., *Effect of particle morphology on the triboelectrification in dry powder inhalers*. International Journal of Pharmaceutics, 2004. **282**(1): p. 107-114.
154. Flippen, J.L. and R.D. Gilardi, *(+)-2-(2-Fluoro-4-biphenyl)propionic acid (flurbiprofen)*. Acta Crystallographica Section B, 1975. **31**(3): p. 926-928.
155. Henck, J.O. and M. Kuhnert-Brandstatter, *Demonstration of the Terms Enantiotropy and Monotropy in Polymorphism Research Exemplified by Flurbiprofen*. Journal of Pharmaceutical Sciences, 1999. **88**(1): p. 103-108.
156. Plass, K.E., A.L. Grzesiak, and A.J. Matzger, *Molecular Packing and Symmetry of Two-Dimensional Crystals*. Accounts of Chemical Research, 2007. **40**(4): p. 287-293.
157. Hachuła, B., et al., *Polymorphs of oxindole as the core structures in bioactive compounds*. CrystEngComm, 2018. **20**(12): p. 1739-1745.
158. Kinbara, K., et al., *Crystal Structures of the Salts of Chiral Primary Amines with Achiral Carboxylic Acids: Recognition of the Commonly-Occurring Supramolecular Assemblies of Hydrogen-Bond Networks and Their Role in the Formation of Conglomerates*. Journal of the American Chemical Society, 1996. **118**(14): p. 3441-3449.
159. Billing, D.G. and A. Lemmerer, *Synthesis, characterization and phase transitions of the inorganic–organic layered perovskite-type hybrids [(C_nH_{2n+1}NH₃)₂PbI₄](n= 12, 14, 16 and 18)*. New Journal of Chemistry, 2008. **32**(10): p. 1736-1746.
160. Perumalla, S.R. and C.C. Sun, *Design and synthesis of solid state structures with conjugate acid–base pair interactions*. CrystEngComm, 2012. **14**(11): p. 3851-3853.
161. Perumalla, S.R. and C.C. Sun, *Improved solid-state stability of salts by cocrystallization between conjugate acid–base pairs*. CrystEngComm, 2013. **15**(29): p. 5756-5759.
162. Perumalla, S.R., S. Paul, and C.C. Sun, *Enabling the Tablet Product Development of 5-Fluorocytosine by Conjugate Acid Base Cocrystals*. Journal of Pharmaceutical Sciences, 2016. **105**(6): p. 1960-1966.

163. Lou, B., S.R. Perumalla, and C.C. Sun, *Significant Expansion of the Solid State Landscape of Salicylic Acid Based on Charge-Assisted Hydrogen Bonding Interactions*. *Crystal Growth & Design*, 2015. **15**(1): p. 24-28.
164. Ross, S.A., D.A. Lamprou, and D. Douroumis, *Engineering and manufacturing of pharmaceutical co-crystals: a review of solvent-free manufacturing technologies*. *Chemical Communications*, 2016. **52**(57): p. 8772-8786.
165. Oh, D.H., et al., *Comparison of solid self-microemulsifying drug delivery system (solid SMEDDS) prepared with hydrophilic and hydrophobic solid carrier*. *International Journal of Pharmaceutics*, 2011. **420**(2): p. 412-418.
166. Maitre, M.M., M.R. Longhi, and G.G. Granero, *Ternary Complexes of Flurbiprofen with HP- β -CD and Ethanolamines Characterization and Transdermal Delivery*. *Drug Development and Industrial Pharmacy*, 2007. **33**(3): p. 311-326.
167. Anderson, B.D. and R.A. Conradi, *Predictive Relationships in the Water Solubility of Salts of a Nonsteroidal Anti-Inflammatory Drug*. *Journal of Pharmaceutical Sciences*, 1985. **74**(8): p. 815-820.
168. Rowe, R.C. and R.J. Roberts, *Mechanical Properties*. In: *Pharmaceutical Powder Compaction Technology*, Marcel Dekker, New York, 1996.
169. Alderborn, G. and C. Nystrom, *Pharmaceutical Powder Compaction Technology*. 1995: CRC Press.
170. Joiris, E., et al., *Compression Behavior of Orthorhombic Paracetamol*. Vol. 15. 1998. 1122-30.
171. Sun, C. and D.J.W. Grant, *Influence of Crystal Structure on the Tableting Properties of Sulfamerazine Polymorphs*. *Pharmaceutical Research*, 2001. **18**(3): p. 274-280.
172. Sun, C. and D. J W Grant, *Improved Tableting Properties of p-Hydroxybenzoic Acid by Water of Crystallization: A Molecular Insight*. Vol. 21. 2004. 382-6.
173. Feng, Y. and D.J.W. Grant, *Influence of Crystal Structure on the Compaction Properties of n-Alkyl 4-Hydroxybenzoate Esters (Parabens)*. *Pharmaceutical Research*, 2006. **23**(7): p. 1608-1616.
174. Reddy, C.M., G. Rama Krishna, and S. Ghosh, *Mechanical properties of molecular crystals—applications to crystal engineering*. *CrystEngComm*, 2010. **12**(8): p. 2296-2314.
175. Khomane, K.S., P.K. More, and A.K. Bansal, *Counterintuitive Compaction behavior of Clopidogrel Bisulfate Polymorphs*. *Journal of Pharmaceutical Sciences*, 2012. **101**(7): p. 2408-2416.
176. Khomane, K.S. and A.K. Bansal, *Weak Hydrogen Bonding Interactions Influence Slip System Activity and Compaction Behavior of Pharmaceutical Powders*. *Journal of Pharmaceutical Sciences*, 2013. **102**(12): p. 4242-4245.
177. Khomane, K.S., et al., *Molecular Understanding of the Compaction Behavior of Indomethacin Polymorphs*. *Molecular Pharmaceutics*, 2013. **10**(2): p. 631-639.
178. Upadhyay, P., et al., *Relationship between crystal structure and mechanical properties of ranitidine hydrochloride polymorphs*. *CrystEngComm*, 2013. **15**(19): p. 3959-3964.
179. Krishna, G.R., et al., *Correlation Among Crystal Structure, Mechanical Behavior, and Tabletability in the Co-Crystals of Vanillin Isomers*. *Crystal Growth & Design*, 2015. **15**(4): p. 1827-1832.
180. Chang, S.-Y. and C.C. Sun, *Superior Plasticity and Tabletability of Theophylline Monohydrate*. *Molecular Pharmaceutics*, 2017. **14**(6): p. 2047-2055.

181. Upadhyay, P.P., C.C. Sun, and A.D. Bond, *Relating the tableting behavior of piroxicam polytypes to their crystal structures using energy-vector models*. International Journal of Pharmaceutics, 2018. **543**(1): p. 46-51.
182. Wang, C. and C.C. Sun, *Identifying Slip Planes in Organic Polymorphs by Combined Energy Framework Calculations and Topology Analysis*. Crystal Growth & Design, 2018. **18**(3): p. 1909-1916.
183. Zolotarev, P.N., et al., *Searching New Crystalline Substrates for OMBE: Topological and Energetic Aspects of Cleavable Organic Crystals*. Crystal Growth & Design, 2016. **16**(3): p. 1572-1582.
184. Ghorri, M.U., E. Šupuk, and B.R. Conway, *Tribo-electrification and powder adhesion studies in the development of polymeric hydrophilic drug matrices*. Materials, 2015. **8**(4): p. 1482-1498.
185. *Investigation of the effect of solubility increase at the main absorption site on bioavailability of BCS class II drug (risperidone) using liquisolid technique AU - Khames, Ahmed*. Drug Delivery, 2017. **24**(1): p. 328-338.
186. Braun, D.E., P.G. Karamertzanis, and S.L. Price, *Which, if any, hydrates will crystallise? Predicting hydrate formation of two dihydroxybenzoic acids*. Chemical Communications, 2011. **47**(19): p. 5443-5445.
187. Wiedmann, T.S. and A. Naqwi, *Pharmaceutical salts: Theory, use in solid dosage forms and in situ preparation in an aerosol*. Asian Journal of Pharmaceutical Sciences, 2016. **11**(6): p. 722-734.
188. Šupuk, E., et al., *Tribo-electrification of active pharmaceutical ingredients and excipients*. Powder Technology, 2012. **217**: p. 427-434.
189. Greason, W.D., *Investigation of a test methodology for triboelectrification*. Journal of Electrostatics, 2000. **49**(3): p. 245-256.
190. Khankari, R.K. and D.J.W. Grant, *Pharmaceutical hydrates*. Thermochimica Acta, 1995. **248**: p. 61-79.
191. Baek, H.H., et al., *Enhanced solubility and bioavailability of flurbiprofen by cycloamylose*. Archives of Pharmacal Research, 2011. **34**(3): p. 391-397.
192. Avdeef, A., C.M. Berger, and C. Brownell, *pH-Metric Solubility. 2: Correlation Between the Acid-Base Titration and the Saturation Shake-Flask Solubility-pH Methods*. Pharmaceutical Research, 2000. **17**(1): p. 85-89.
193. Sowa, M., et al., *Particle Engineering of an API for Improved Powder-Flow Properties*. 2016.
194. Pudasaini, N., et al., *Downstream Processability of Crystal Habit-Modified Active Pharmaceutical Ingredient*. Organic Process Research & Development, 2017. **21**(4): p. 571-577.
195. Waknis, V., et al., *Molecular Basis of Crystal Morphology-Dependent Adhesion Behavior of Mefenamic Acid During Tableting*. Pharmaceutical Research, 2014. **31**(1): p. 160-172.

10 Appendices

Table A.1 Distribution of Cations Used in New Chemical Entities of Class 2:

	Overall %	2007-2012 %	2013-2018 %
Calcium	5.6	16.7	0.0
Ethanolamine	5.6	16.7	0.0
Magnesium	5.6	0.0	8.3
Meglumine	11.1	16.7	8.3
Potassium	11.1	33.3	0.0
Sodium	55.6	16.7	75.0
Strontium	5.6	0.0	8.3
Total number of salts	18	6	12

Table A.2 Number and Distribution of Anions Used in the Variety of Dosage Forms for New Chemical Entities:

	2007-2012 #				2013-2018 #			
	Oral	parenteral	Pulmonary	Topical ophthalmic	Oral	Parenteral	Pulmonary	Topical ophthalmic
Acetate	0	0	0	0	2	0	0	0
Benzoate	0	0	0	0	1	0	0	0
Besylate	1	0	0	0	0	0	0	0
Bromide	0	1	1	0	1	0	0	0
Camsylate	0	0	0	0	1	0	0	0
Chloride	15	2	0	1	10	5	1	0
Citrate	1	0	0	0	1	0	0	0
Esylate	0	0	0	0	1	0	0	0
Fumarate	3	0	0	0	1	0	0	0
Hippurate	0	0	0	0	1	0	0	0
Lactate	0	0	0	0	1	0	0	0
Malate	0	0	0	0	5	0	0	0
Maleate	2	0	1	0	0	0	0	0
Mesylate	3	1	0	0	5	0	0	1
Oxalate	0	0	0	0	1	0	0	0
Phosphate	1	0	0	0	2	1	0	0
Succinate	1	0	0	0	3	0	0	0
Sulfate	0	0	0	0	3	3	0	0
Tartrate	0	0	0	0	2	0	0	0
Tosylate	1	0	0	0	5	0	0	0
Total	28	4	2	1	46	9	1	1
Overall %	80.0	11.4	5.7	2.9	80.7	15.8	1.8	1.8

Table A.3 Number and Distribution of Cations Used in the Different of Dosage Forms for New Chemical Entities:

	2007-2012 #		2013-2018 #	
	Oral	Parenteral	Oral	Parenteral
Calcium	1	0	0	0
Ethanolamine	1	0	0	0
Magnesium	0	0	1	0
Meglumine	0	1	1	1
Potassium	2	0	0	0
Sodium	1	0	7	2
Strontium	0	0	1	0
Total	5	1	10	3
Overall %	83.3	16.7	76.9	23.1

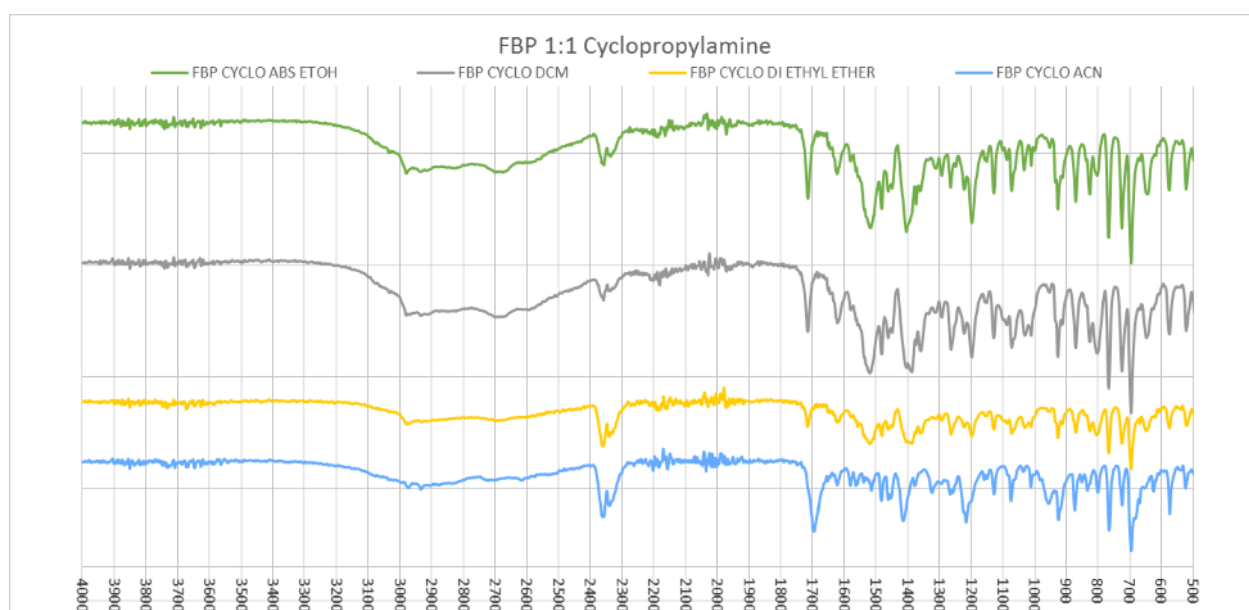


Figure A.1 FT-IR spectrum for the 1:1 salt after recrystallisation from various solvents

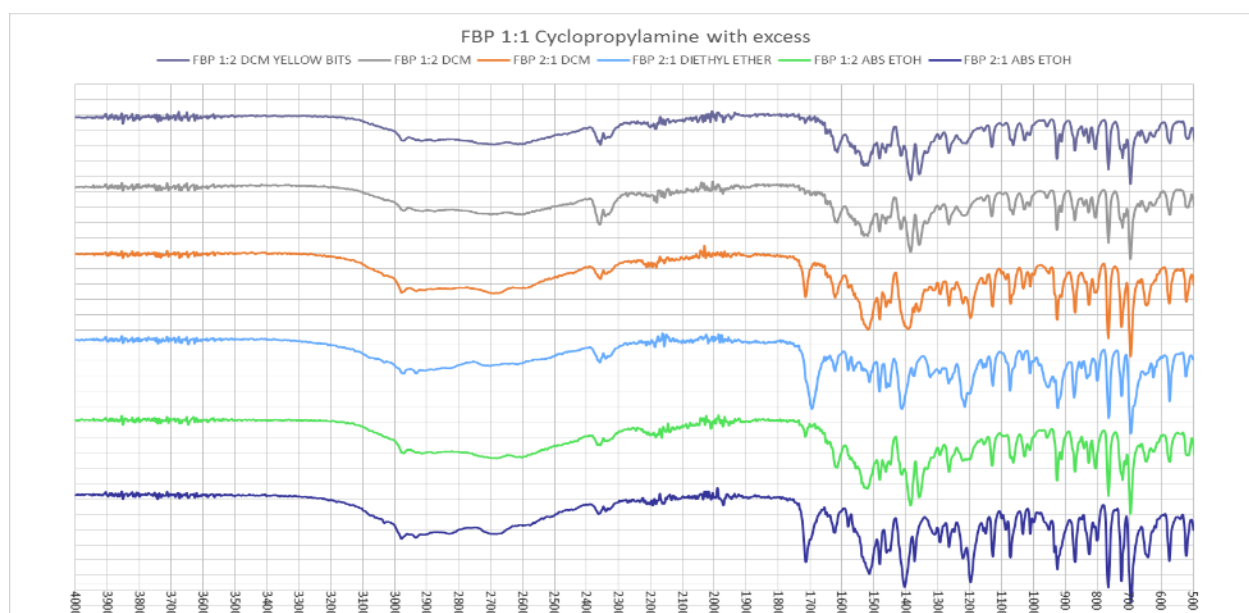


Figure A.2 FT-IR spectrum for the 1:1 salt with excess of either drug or counter-ion

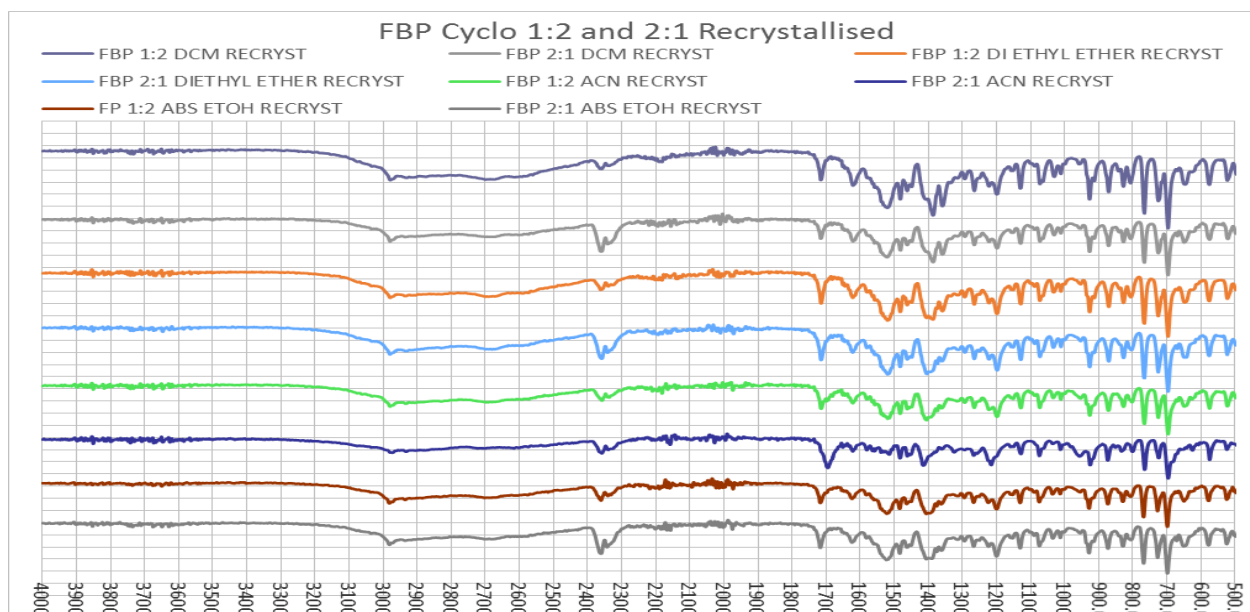


Figure A.3 FT-IR spectrum for 1:2 and 2:1 salts recrystallised from various solvents

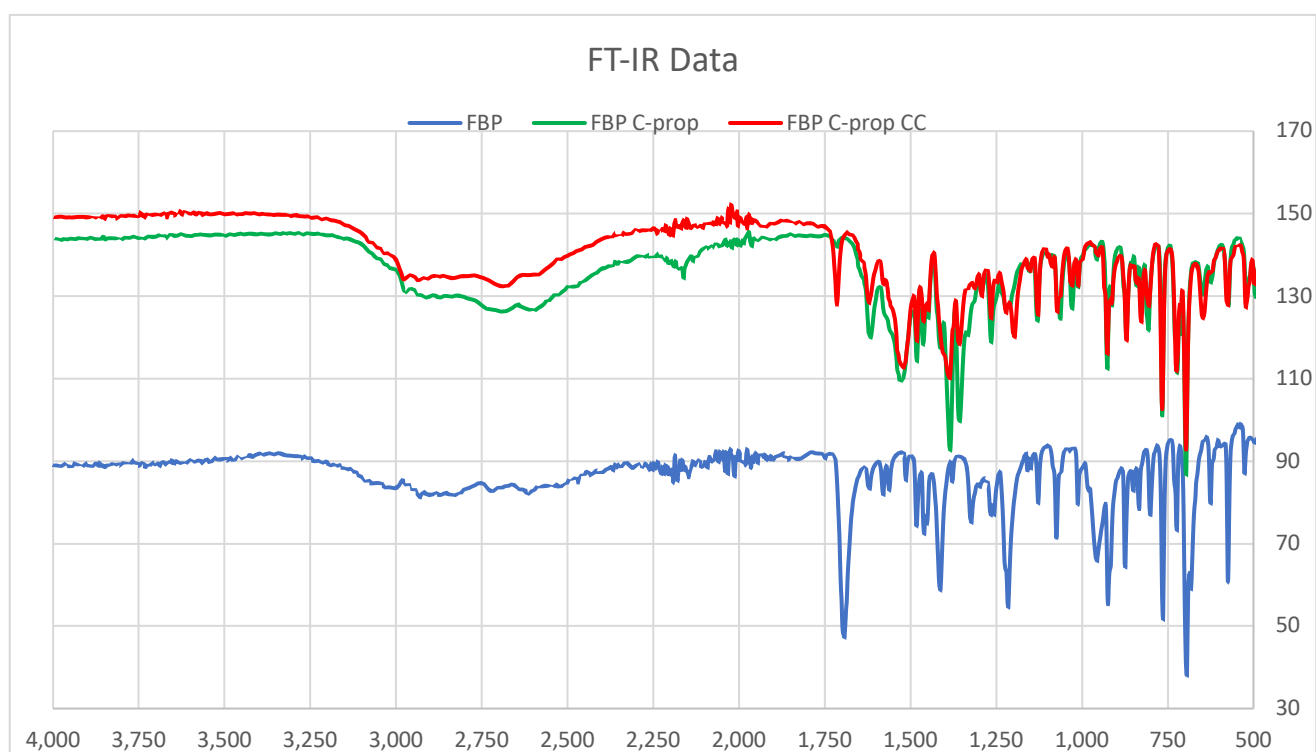


Figure A.4 FT-IR data for flurbiprofen, flurbiprofen cyclopropylamine (1:1) salt and flurbiprofen: cyclopropylamine (2:1) salt cocrystal

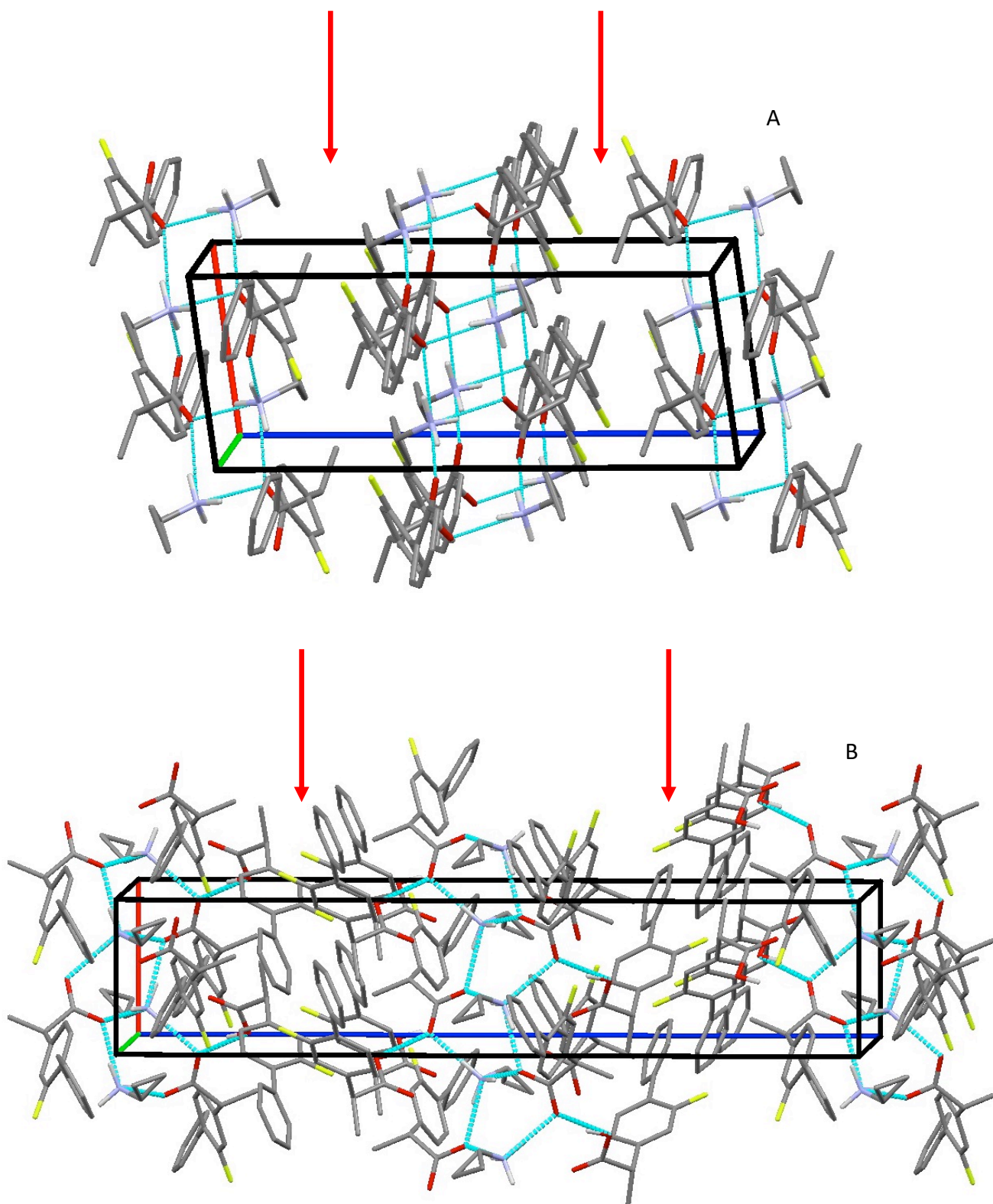


Figure A.5 Packing diagrams for salt projecting down the *b* axis (A) and salt cocrystal the *a* axis (B). Arrows indicate position of potential slip planes

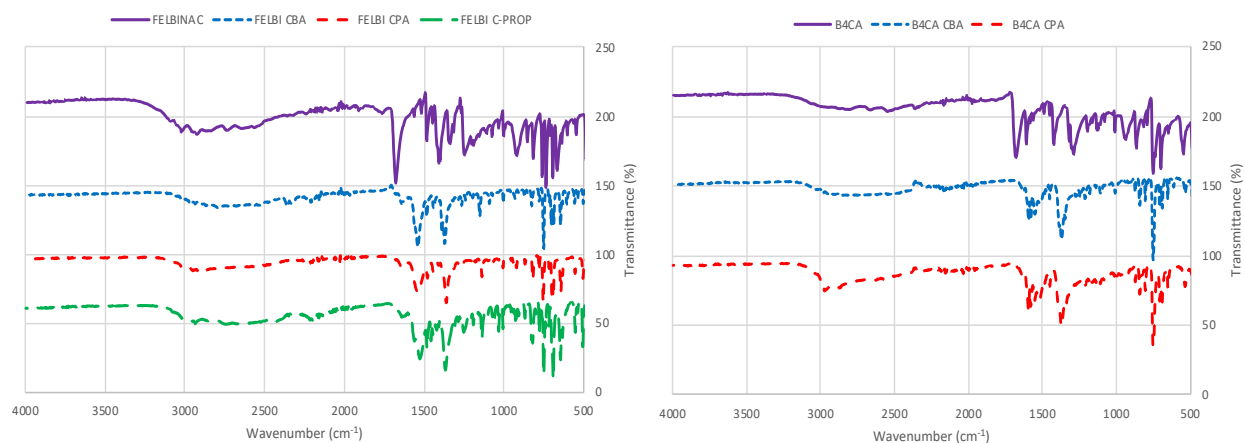


Figure A.6 FT-IR data for felbinac, B4CA and the subsequent salts

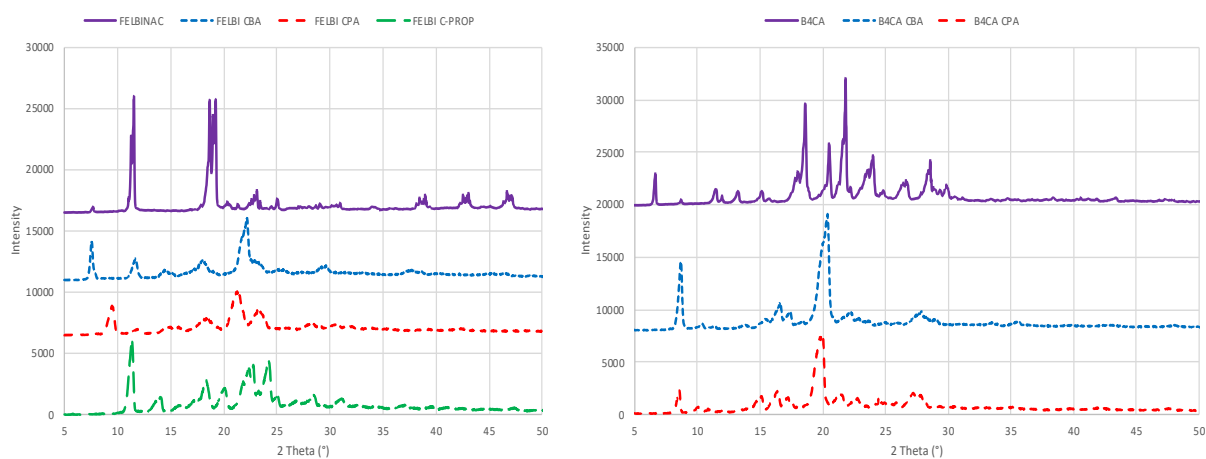


Figure A.7 XRD data for felbinac, B4CA and the salts

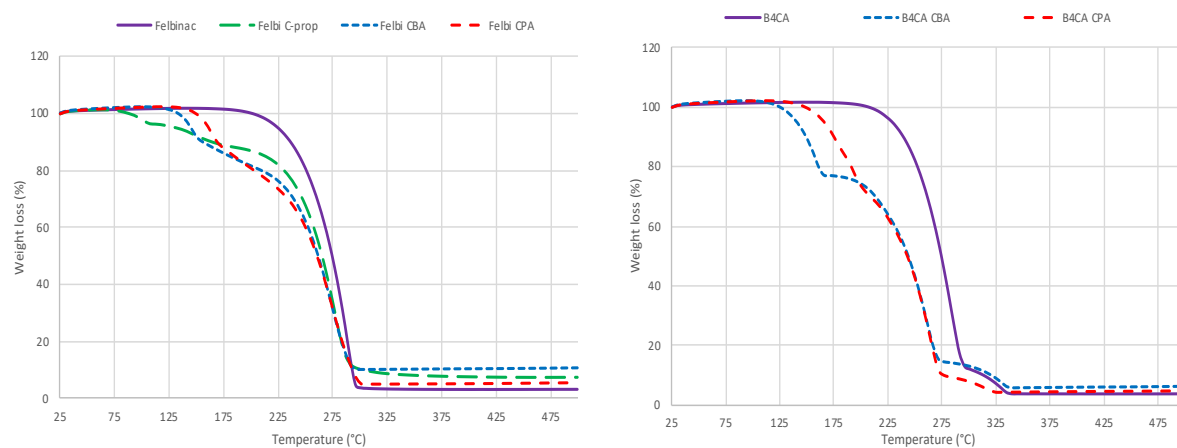


Figure A.8 TGA data for felbinac, B4CA and the subsequent salts

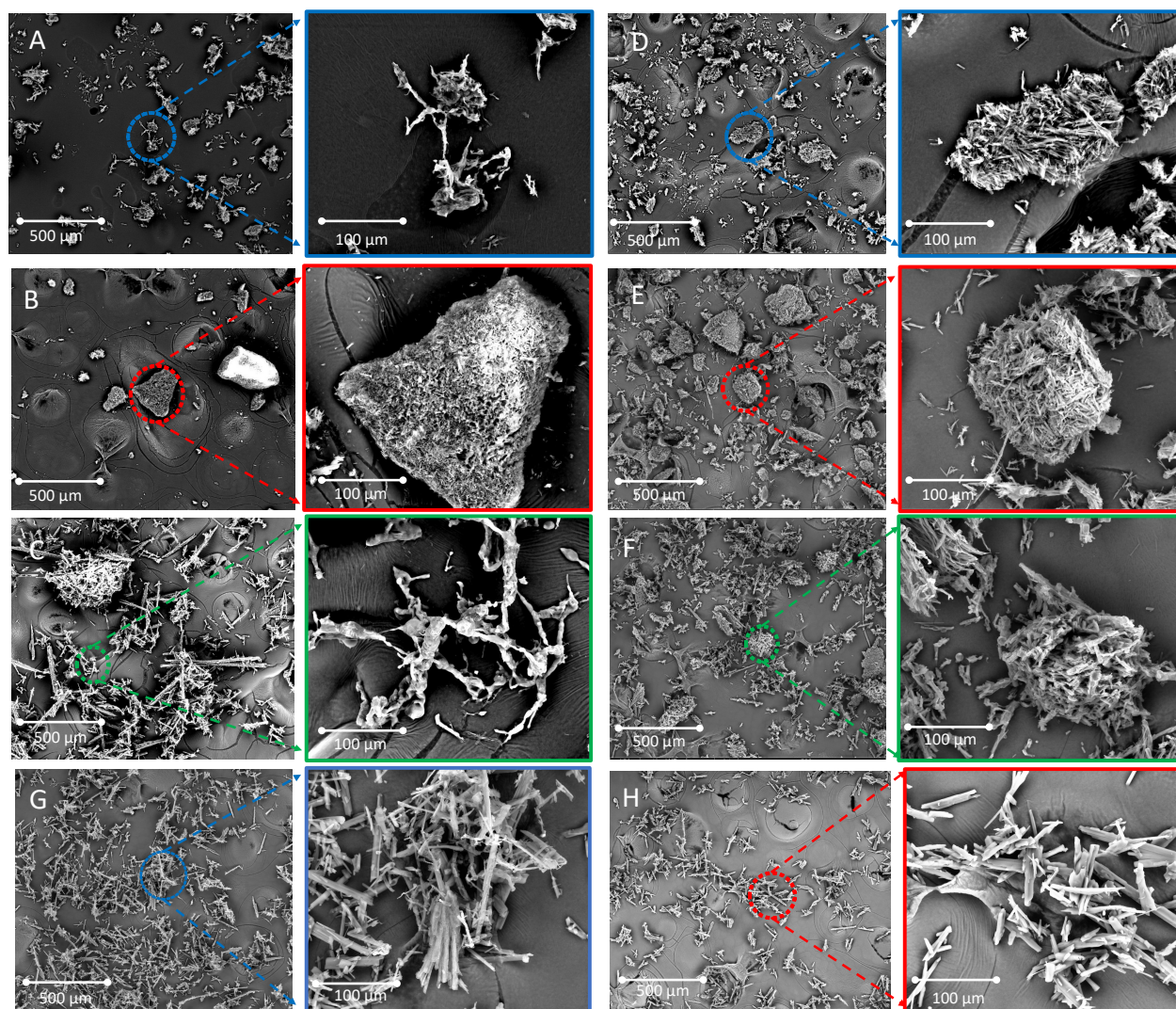


Figure A.9 SEM images of A) FBP CBA, B) FBP CPA, C) FBP C-prop, D) Felbi CBA, E) Felbi CPA, F) Felbi C-prop G) B4CA CBA and H) B4CA CPA depicted at 100x and 500x magnifications.

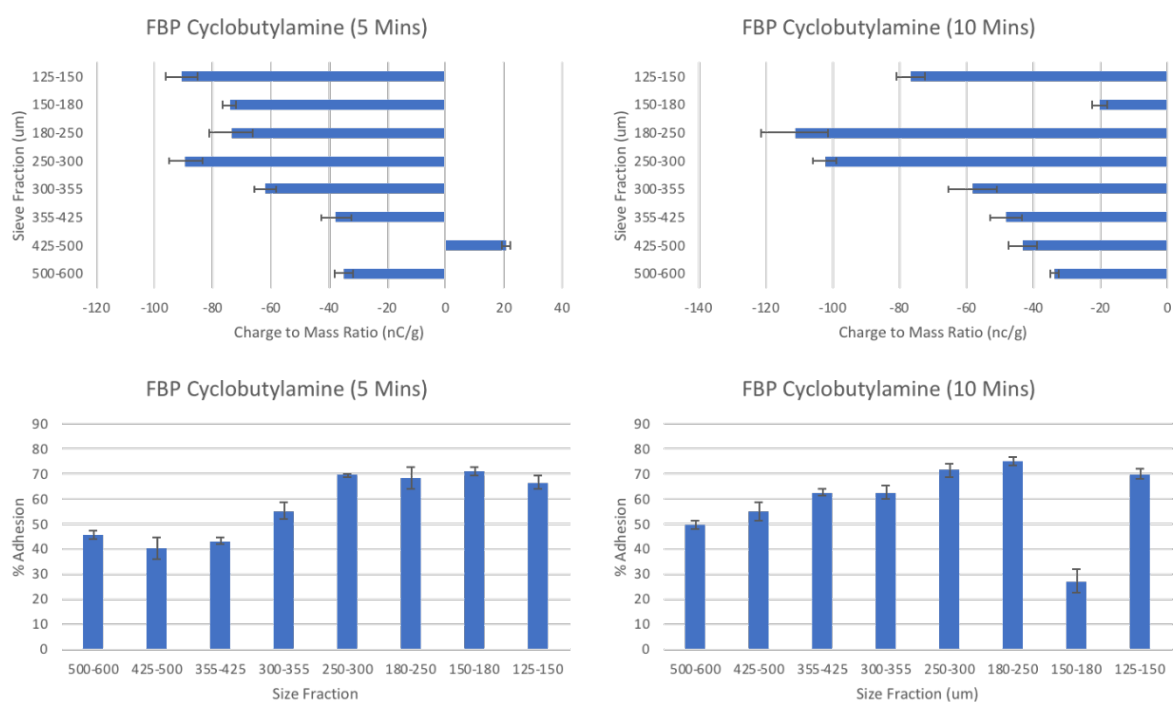


Figure A.10 Tribo-electrification and adhesion data for FBP CBA at 5 and 10 mins

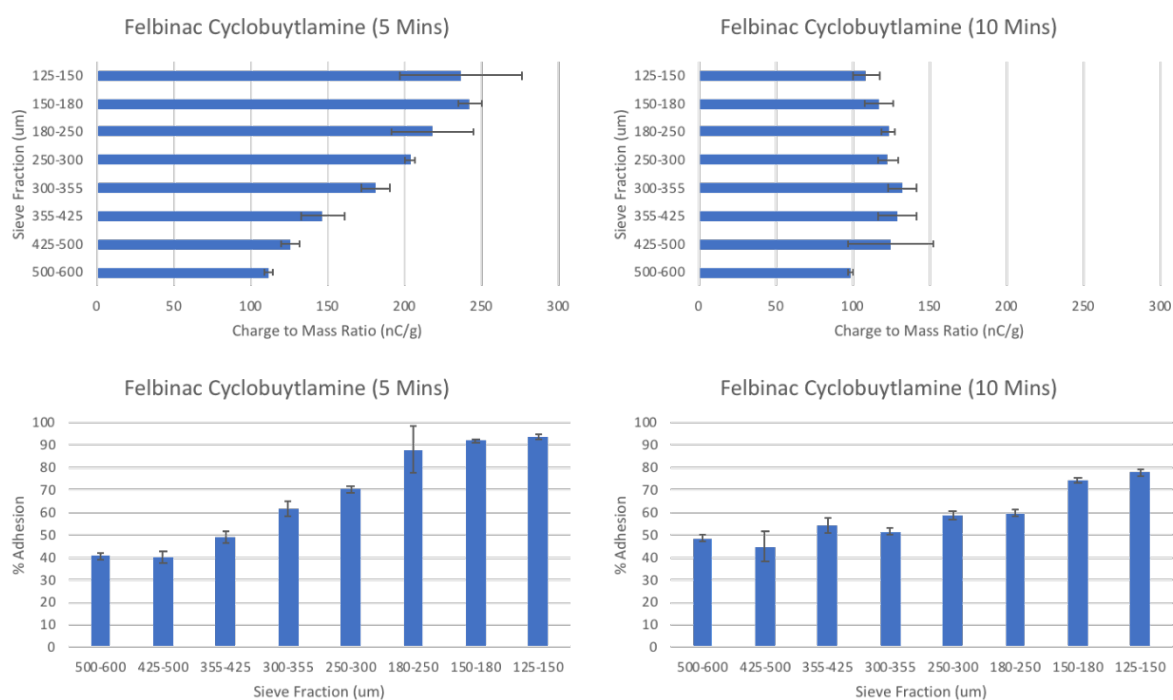


Figure A.11 Tribo-electrification and adhesion data for Felbi CBA at 5 and 10 mins

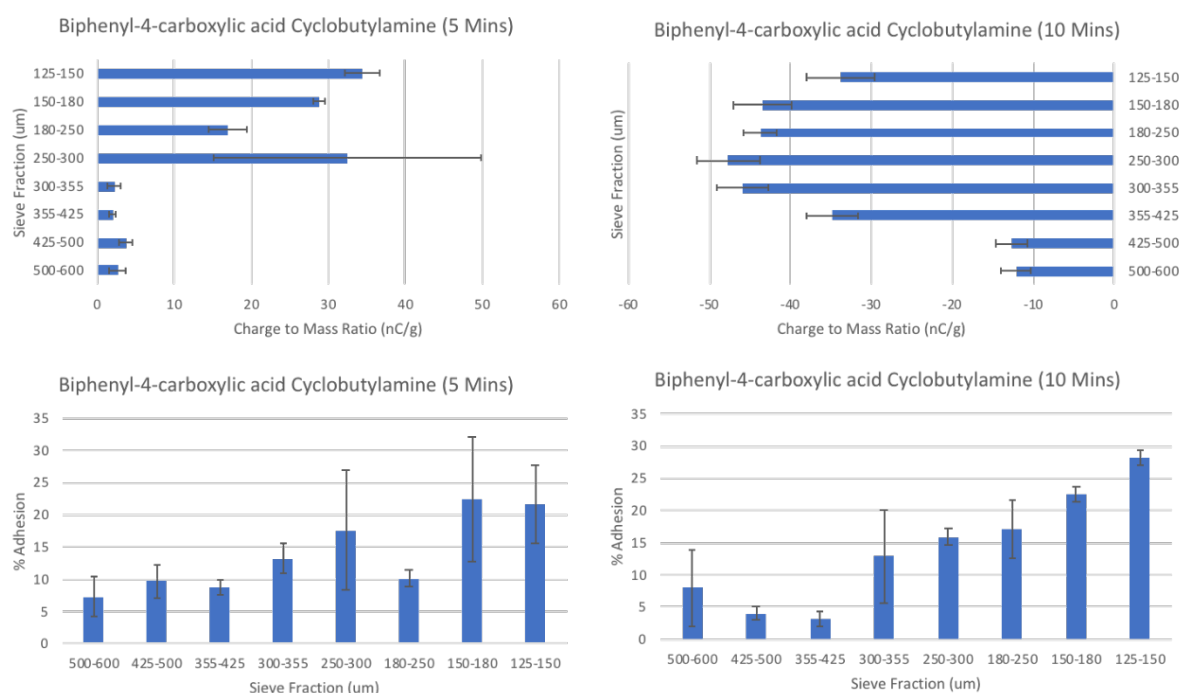


Figure A.12 Tribo-electrification and adhesion data for B4CA CBA at 5 and 10 mins

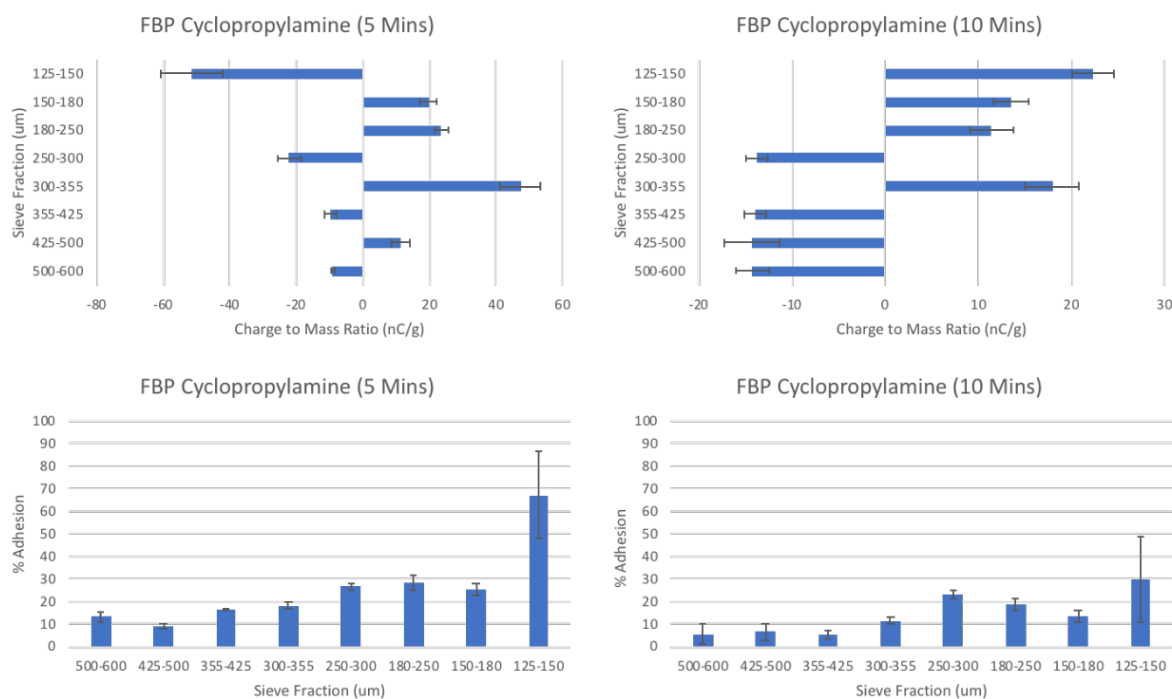


Figure A.13 Tribo-electrification and adhesion data for FBP C-Prop at 5 and 10 mins

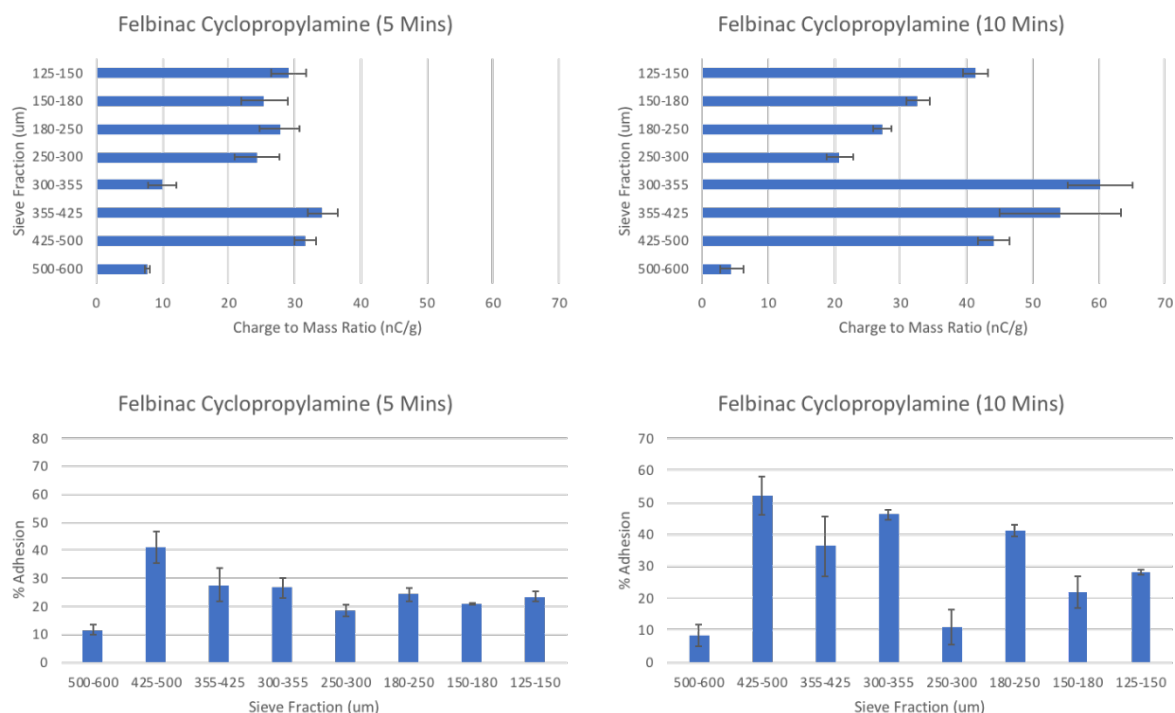


Figure A.14 Tribo-electrification and adhesion data for Felbi C-Prop at 5 and 10 mins

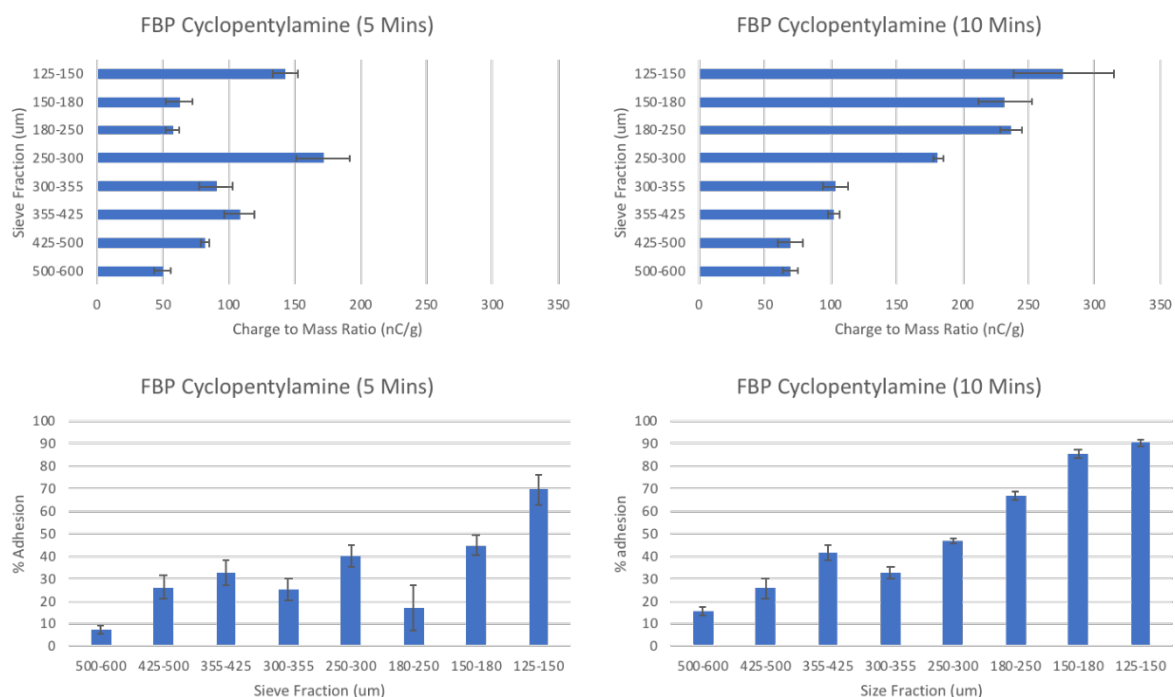


Figure A.15 Tribo-electrification and adhesion data for FBP CPA at 5 and 10 mins

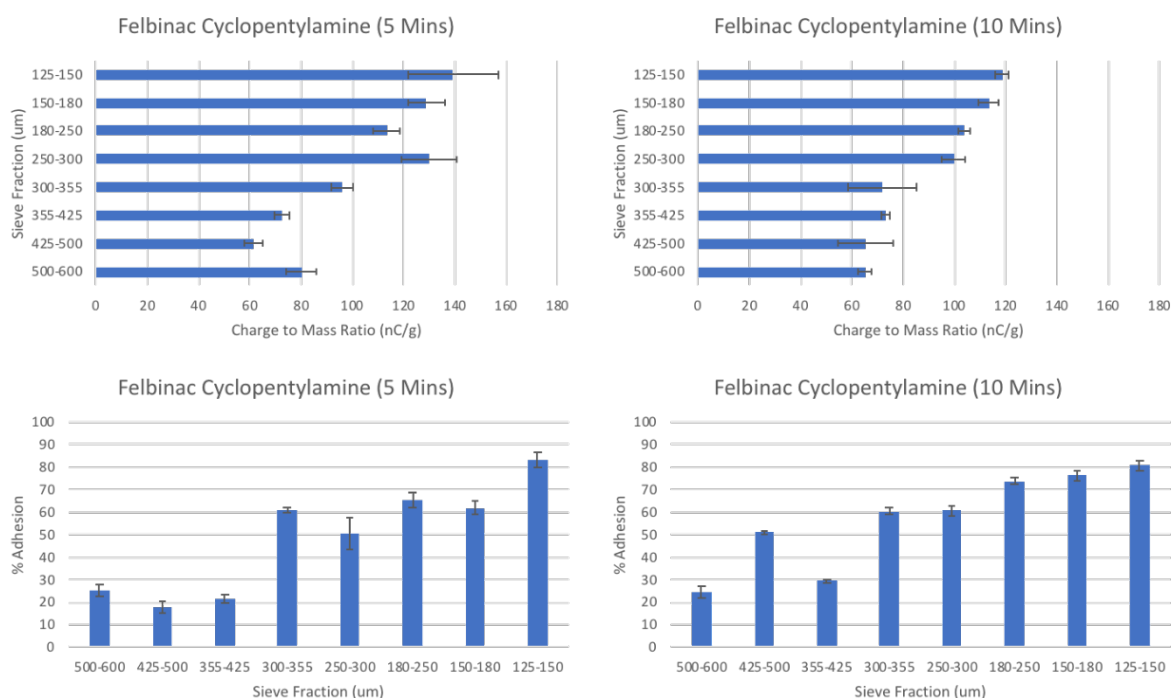


Figure A. 17 Tribo-electrification and adhesion data for Felbi CPA at 5 and 10 mins

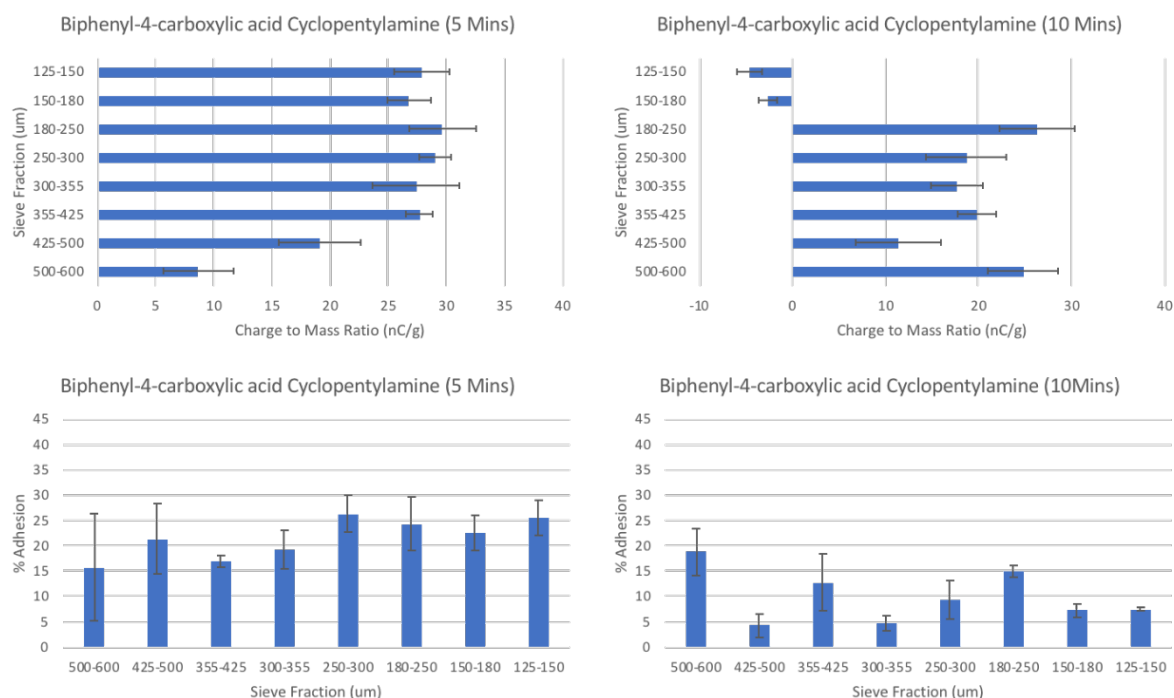


Figure A. 16 Tribo-electrification and adhesion data for B4CA CPA at 5 and 10 mins